

SUSANNA HAAPANEN

# Production, Functional Characterization and Inhibition of Carbonic Anhydrases of Parasites



SUSANNA HAAPANEN

Production, Functional Characterization and  
Inhibition of Carbonic Anhydrases of Parasites

ACADEMIC DISSERTATION

To be presented, with the permission of  
the Faculty of Medicine and Health Technology  
of Tampere University,  
for public discussion in the auditorium F114  
of the Arvo building, Arvo Ylpön katu 34, 33520, Tampere,  
on 19<sup>th</sup> January 2024 at 12 o'clock.

## ACADEMIC DISSERTATION

Tampere University, Faculty of Medicine and Health Technology  
Finland

<i>Responsible supervisor and Custos</i>	Professor Seppo Parkkila Tampere University Finland	
<i>Supervisor</i>	PhD Maarit Patrikainen Tampere University Finland	
<i>Pre-examiners</i>	Professor Thor Eysteinnsson University of Iceland Iceland	Assistant Professor María Reyes-Batlle Universidad de La Laguna Spain
<i>Opponent</i>	Assistant Professor Hanna Hartikainen University of Nottingham United Kingdom	

The originality of this thesis has been checked using the Turnitin OriginalityCheck service.

Copyright ©2023 author

Cover design: Roihu Inc.

ISBN 978-952-03-3209-9 (print)

ISBN 978-952-03-3210-5 (pdf)

ISSN 2489-9860 (print)

ISSN 2490-0028 (pdf)

<http://urn.fi/URN:ISBN:978-952-03-3210-5>



Carbon dioxide emissions from printing Tampere University dissertations have been compensated.

PunaMusta Oy – Yliopistopaino  
Joensuu 2023

To my family

*Now, this is not the end. It is not even the beginning of the end. But it is, perhaps, the end of the beginning.* – Winston Churchill



# ACKNOWLEDGMENTS

This doctoral thesis was carried out in the Anatomy research group in the Faculty of Medicine and Health Technology, Tampere University, under the supervision of Dean Professor Seppo Parkkila (MD, PhD) and Maarit Patrikainen (PhD) during the years 2017-2024.

I sincerely thank Seppo Parkkila for allowing me to work on these projects and for all the support and aid he has offered me during these years. I am grateful for the opportunity to teach medical students and see them grow into medical professionals. I am wholeheartedly thankful to my other supervisor, Maarit Patrikainen, who has been there for me from the beginning, even though it became official only during the last years of my thesis. Dear Maarit, without your pervasive support and extensive knowledge in the field of biomedicine, this thesis may have never seen the light of day. You have also helped me recover from work in my free time.

I want to thank the external reviewers of my thesis, Assistant Professor María Reyes-Battle and Professor Thor Eysteinnsson, for their valuable comments and the effort they gave to my thesis. I acknowledge the follow-up group members Docent Ashok Aspatwar (PhD) and Docent Sami Oikarinen (PhD) for their insights and fresh perspectives on my research. I thank the other former and present members of the Anatomy group: Harlan Barker (MSc), Jenny Parkkinen (MSc), Sami Purmonen (PhD), Leo Syrjänen (MD, PhD), Heimo Syväälä (PhD), Linda Urbanski (PhD), and Alma Yrjänäinen (MSc). I thank our skillful laboratory technicians, Marianne Kuuslahti and Sanna Kavén, for teaching me how to work in the laboratory and assisting me in many new trials I wanted to conduct. Without your expertise and knowledge, I would not have been able to carry out my experiments.

I thank Martti Tolvanen (PhD) for his exceptional knowledge in the field of bioinformatics and his ability to explain his analyses in an understandable form. I express my appreciation and gratitude to my other coauthors and collaborators: Reza Zolfaghari Emameh (PhD), Andrea Angeli (PhD), Silvia Bua (PhD), Fabrizio Carta (PhD) and Professor Claudiu T. Supuran (PhD) for their valuable work on the publications. Without you, this wouldn't be possible. I want to thank Juha Määttä

(PhD) and Niklas Kähkönen from the Protein Services facility for their help in recombinant protein production. I especially thank education manager Henna Mattila for knowing the answers to all my questions and managing my study plan in Sisu to meet all the requirements; your help has been invaluable. I thank all of those I've spent lunch and coffee breaks with and all the other coworkers I have forgotten to mention here.

I want to thank my friends, most of them from medical school, Tammelakeskus and Hatanpää Hospital. You provided me with other things to do and took my mind off work. I especially thank my best friend Virpi for our extended hours on the phone and for never complaining when I moan about everything that has gone wrong.

I want to give special thanks to my family: "Suuret kiitokset vanhemmilleni, Leenalle ja Hannulle, tuesta ja avusta elämässä, opinnoissa ja työssä. Äiti ja isä, te olette näyttäneet minulle, että sisulla ja kovalla työllä voi saavuttaa paljon, mutta vain jos sitä todella haluaa. Suureksi surukseni isäni ei saanut koskaan nähdä tämän kirjan valmistumista, vaikka hän sitä suuresti toivoi." I also want to thank my big sister Outi for being annoying you and challenging me in many ways. I have always been able to look up to you, and I appreciate all the help you have given me with your exceptional skills in many fields. I thank my dog Vili for your patience and tolerance to my long working hours and the pure joy you express when we are reunited after a long day.

I want to thank my spouse, Olli, who came into my life not very long ago, but it still feels like we have known each other much longer. You carried me during the hardest life situation I had ever been to and gave me love and support to live through it. Words will never be enough to describe my deep love and gratitude for you. Thank you for standing by my side.

This thesis work was financially supported by the Finnish Medical Foundation, Marjatta Melkas-Rusanen and Anneli Melkas Memorial Foundation of the Finnish Cultural Foundation Pirkanmaa Regional Fund and Doctoral Programme on the Faculty of Medicine and Health Technology, Tampere University.

Tampere, November 2023

Susanna Haapanen



# ABSTRACT

Carbonic anhydrases (CAs, EC 4.2.1.1) are metalloenzymes that can be found in almost all living organisms. They catalyze a vital chemical reaction: the reversible hydration of carbon dioxide ( $\text{CO}_2 + \text{H}_2\text{O} \rightleftharpoons \text{H}_2\text{CO}_3 \rightleftharpoons \text{HCO}_3^- + \text{H}^+$ ). It is part of multiple physiological and metabolic processes, such as pH regulation, gluconeogenesis and photosynthesis. CAs are divided into eight families, from which the human genome only involves  $\alpha$ -CAs. Many pathogens, such as bacteria and parasites, also have CA enzymes from other families.

*Schistosoma mansoni* is a parasitic blood fluke that causes intestinal infection in many tropical and subtropical areas. *Entamoeba histolytica* and *Acanthamoeba castellanii* are amoebae that cause different infections in humans. *E. histolytica* causes intestinal infection, and *A. castellanii* mainly infects the cornea but also causes invasive infections in immunocompromised people. The infections of these parasites are common globally, and unfortunately, the diagnosis and treatment are often delayed. The infections can be lethal, and at their mildest, they cause a significant reduction in the quality of life. My study aims to find a faster and more effective way to detect *A. castellanii* from a biological sample and discover new potential drug candidates to treat these parasitic infections.

In my thesis, I produced the  $\beta$ -CAs of *E. histolytica* and *S. mansoni* using *Escherichia coli* as a protein production organism. We studied the inhibitory effects of many known CA inhibitors and identified several promising candidates or potential leads for further development. In addition, we developed a novel rapid diagnostic method to detect *A. castellanii* from a biological sample. The novel method could replace the current gold standard, sample culture, which is slow in clinical diagnostics. We established a new method to investigate potential drug candidates for treating *A. castellanii*, as the current treatment options are only moderately effective and have many adverse side effects. By this method, we tested several clinically used CA inhibitors with interesting outcomes.

Dorzolamide and acetazolamide were found to be new promising options for treating *Acanthamoeba* keratitis. The advantage of these drugs is also the long use

history with human patients in treating other conditions, which has made the side effects and risks very familiar to medical staff. Unfortunately, acetazolamide was only moderately effective against the  $\beta$ -CAs of *S. mansoni* and *E. histolytica*, as was dorzolamide against the  $\beta$ -CA of *E. histolytica*. In contrast, dorzolamide was an effective inhibitor against the  $\beta$ -CA of *S. mansoni*. We also found many other effective inhibitors against the  $\beta$ -CAs of *E. histolytica* and *S. mansoni*.

This thesis increases the knowledge and options to use the CAs of parasites to diagnose and treat infections caused by parasites.

# TIIVISTELMÄ

Hiilihappoanhydraasit (carbonic anhydrase, CA) ovat metalloentsyymejä, joita esiintyy kaikkialla elollisessa luonnossa. Niiden tehtävä on katalysoida elintärkeää käänteistä reaktiota: hiilidioksidin hydraatiota hiilihapoksi ( $\text{CO}_2 + \text{H}_2\text{O} \rightleftharpoons \text{H}_2\text{CO}_3 \rightleftharpoons \text{HCO}_3^- + \text{H}^+$ ). Reaktio on osana monissa fysiologisissa ja metabolisissa prosesseissa, kuten happo-emästasapainon säätelyssä, glukoneogeenisissa ja yhteyttämisissä. Hiilihappoanhydraasit jaetaan yhteensä kahdeksaan perheeseen, joista ihmisillä esiintyy vain ensimmäisenä löydettyä  $\alpha$ -entsyymiperhettä. Monilla taudinaiheuttajilla, kuten bakteereilla ja loisilla, on myös muiden hiilihappoanhydraasiperheiden proteiineja.

*Schistosoma mansoni* on suolistotulehdusta aiheuttava halkiomato, jota esiintyy endeemisenä monilla trooppisilla ja subtrooppisilla seuduilla. *Entamoeba histolytica* ja *Acanthamoeba castellanii* ovat ihmisille infektioita aiheuttavia ameboja. *E. histolytica* aiheuttaa suolistotulehdusta ja *A. castellanii* pääasiassa sarveiskalvon tulehdusta, sekä immuunipuutteisille henkilöille myös syviä infektioita. Yhteistä näille loisille on, että niiden diagnostiikassa tai hoidossa on puutteita, ja ne ovat globaalisti erittäin yleisiä. Niiden aiheuttamat sairaudet voivat olla tappavia, ja aiheuttavat lievimmilläänkin merkittävää elämänlaadullista haittaa. Väitöskirjatutkimukseni tavoitteena on löytää nopeampi menetelmä tunnistaa *A. castellanii* biologisesta näytteestä sekä löytää uusia potentiaalisia lääkeainemolekyylejä näiden kolmen loisen aiheuttamien sairauksien tehokkaammaksi hoitamiseksi.

Väitöstutkimuksessani tuotin *E. histolytica*n ja *S. mansoni*n  $\beta$ -hiilihappoanhydraasit *Escherichia coli* -bakteereissa. Tutkimme hiilihappoanhydraasin inhibiittorien vaikutusta tuotettuihin entsyymeihin, ja löysimme useita lupaavia inhibiittoreita. Lisäksi kehitimme uuden nopean diagnostisen menetelmän *A. castellanii*n havaitsemiseksi näytteestä, sillä nykyinen ameban viljelyyn perustuva menetelmä on kliiniseen diagnostiikkaan liian hidaskäyttöinen. Nykyiset *A. castellanii*n aiheuttamien infektioiden hoitoon käytetyt lääkkeet ovat vain kohtalaisen tehokkaita ja niihin liittyy useita haittavaikutuksia, joten kehitimme uuden menetelmän uusien lääkeaineiden etsimistä varten ja testasimme useita, jo klinisessä käytössä olevia hiilihappoanhydraasin estäjiä menetelmällämme.

Havaitsimme, että dorsolamidi ja asetatsoliamidi ovat lupaavia uusia vaihtoehtoja akantamebakeratiitin hoitamiseksi. Niiden etuna on pitkään jatkunut käyttö ihmispotilaiden muiden sairauksien hoidossa, joten niiden haitta- ja sivuvaikutukset ovat tunnettuja. Valitettavasti asetatsoliamidi on vain kohtalaisen tehokas inhiboimaan *E. histolytica*n ja *S. mansoni*n  $\beta$ -hiilihappoanhydraaseja. Dorsolamidi on tehokas inhibiittori *S. mansoni*n  $\beta$ -hiilihappoanhydraasia vastaan, toisin kuin *E. histolytica*n  $\beta$ -hiilihappoanhydraasia se inhiboi huonosti. Onneksi moni muu inhibiittori on tehokas estämään niiden molempien toimintaa.

Tämä väitöskirja lisää tietoa ja mahdollisuuksia hyödyntää hiilihappoanhydraaseja loisinfektioiden diagnostikassa ja hoidossa.

# CONTENTS

1	Introduction.....	21
2	Review of literature .....	23
2.1	General aspects of CA enzymes.....	23
2.1.1	Families .....	24
2.1.2	Structures .....	26
2.1.3	Carbonic anhydrase inhibitors .....	28
2.2	Parasites.....	29
2.2.1	<i>Schistosoma mansoni</i> .....	30
2.2.2	<i>Entamoeba histolytica</i> .....	34
2.2.3	<i>Acanthamoeba castellanii</i> .....	36
2.3	Polymerase chain reaction as a diagnostic method .....	41
2.4	Drug development .....	42
2.4.1	Previous drug discovery methods for <i>A. castellanii</i> .....	43
2.4.2	Medication for eye.....	44
3	Aims of the study.....	45
4	Materials and methods.....	46
4.1	Recombinant CA enzyme production (I, II, III).....	46
4.1.1	Vector construction.....	46
4.1.2	Production of recombinant protein.....	48
4.1.3	Purification of recombinant protein.....	49
4.2	CA kinetics and inhibition measurements (I, II, III) .....	50

4.3	<i>Acanthamoeba castellanii</i> culture (IV, V).....	53
4.4	Inhibition of <i>Acanthamoeba castellanii</i> (V).....	54
4.5	Cell sample preparation (IV).....	56
4.6	Development of traditional PCR method (IV).....	57
4.7	Development of qRT–PCR method (IV).....	60
4.8	Data analysis.....	61
4.8.1	Statistical analyses (V).....	61
4.8.2	Bioinformatic analyses (I, II, V).....	63
4.9	Ethics (I–V).....	64
5	Results.....	66
5.1	Recombinant CA enzymes.....	66
5.2	Inhibition of <i>Acanthamoeba castellanii</i> .....	71
5.3	Diagnostic method for detecting <i>Acanthamoeba castellanii</i> .....	76
5.4	Bioinformatic analyses.....	78
5.4.1	3D-modeling of SmaBCA.....	78
5.4.2	Sequence similarities of different protozoans.....	79
5.4.3	Expression of CAs of <i>A. castellanii</i> .....	81
6	Discussion.....	83
6.1	Fight against diarrhea.....	83
6.2	Carbonic anhydrase inhibitors – the answer to antimicrobial resistance?.....	84
6.3	Novel prospects for the diagnosis of <i>Acanthamoeba keratitis</i> .....	87
7	Summary and conclusions.....	89
8	References.....	91

## List of Figures

- Figure 1. Catalytic mechanism of an  $\alpha$ -class carbonic anhydrase.
- Figure 2.  $\alpha$ -CAs and  $\eta$ -CAs have a similar 3D-structure.
- Figure 3. Representation of the general active site structure of a CA using the  $\eta$ -CA of *Plasmodium falciparum* as a model.
- Figure 4. Taxonomic classification of *Schistosoma mansoni*, *Entamoeba histolytica* and *Acanthamoeba castellanii*.
- Figure 5. The life cycle of *Schistosoma mansoni*.
- Figure 6. The life cycle of *Entamoeba histolytica*.
- Figure 7. The life cycle of *Acanthamoeba castellanii*.
- Figure 8. Light microscope view showing trophozoites and cysts of *A. castellanii* together.
- Figure 9. Plasmid map of pBVboost according to Airenne et al.
- Figure 10. Chemical structures, names and numbers of sulfonamide and anion inhibitors.
- Figure 11. 96-well plate from inhibitor assay stained with crystal violet and ready for colorimetric analysis.
- Figure 12. SDS-PAGE images presenting SmaBCA and EhiCA.
- Figure 13. The first phase of the inhibitor assay represents the inhibition of growth of *A. castellanii* with six different inhibitors.
- Figure 14. The second phase of the inhibitor assay illustrates cyst survival after the inhibitor effect, hence modeling the infectious capacity of the cysts after treatment.
- Figure 15. The excystation assay illustrates the capacity of cysts to excystate in the presence of six different CA inhibitors.
- Figure 16. Pipeline of both traditional PCR and qRT-PCR methods designed for diagnostics of *A. castellanii*.
- Figure 17. The results from traditional PCR are represented in agarose gel with a 1 kb standard marker.
- Figure 18. The 3D model of SmaBCA predicts the enzyme to be a dimer.

Figure 19. Multiple sequence alignment shows the similarities of the sequences of  $\beta$ -CAs of different *Schistosoma* species.

Figure 20. Sequence logo of 162 metazoan  $\beta$ -CA sequences.

Figure 21. Expression of CAs of *A. castellanii* compared to the mean expression of all genes.

### *List of Tables*

Table 1. Composition of PYG medium with additives.

Table 2. The initial primer pairs for the development of the PCR-based diagnostic method.

Table 3. The final PCR mix composition.

Table 4. Primers used in qRT-PCR.

Table 5. The reaction mix composition used in qRT-PCR.

Table 6. Kinetic properties of SmaBCA and EhiCA.

Table 7. Inhibition of SmaBCA and EhiCA with sulfonamides, anions and clinically used drugs.



# ABBREVIATIONS

3D	Three-dimensional
AK	Acanthamoeba keratitis
AMR	Antimicrobial resistance
Asp	Aspartic acid
BSL	Biosafety level
CA	Carbonic anhydrase
CAI	Carbonic anhydrase inhibitor
cpBCA	Cytoplasmic $\beta$ -CA of <i>Acanthamoeba castellanii</i>
Cys	Cysteine
DNA	Deoxyribonucleic acid
EhiCA	$\beta$ -CA of <i>Entamoeba histolytica</i>
<i>EhiCA</i>	Gene of the $\beta$ -CA of <i>Entamoeba histolytica</i>
EMA	European Medicines Agency
FDA	Food and Drug Administration
GAE	Granulomatous amoebic encephalitis
Gln	Glutamine
His	Histidine
His-tag	Polyhistidine-tag, hexa histidine-tag
Ile	Isoleucine
IPTG	Isopropyl- $\beta$ -D-thiogalactopyranoside
LB	Luria-Bertani medium, Luria broth

Lys	Lysine
Met	Methionine
mRNA	Messenger ribonucleic acid
MSA	Multiple sequence alignment
MW	Molecular weight
NCBI	The National Center for Biotechnology Information
NM	Not measured
NTDs	Neglected tropical diseases
OD	Optical density
Ori	Origin of plasmid replication
PBS	Phosphate-buffered saline
PCR	Polymerase chain reaction
Pro	Proline
qRT-PCR	Quantitative real-time polymerase chain reaction
RG	Reference gene
RNA	Ribonucleic acid
RPKM	Reads per kilobase million
rpm	Rounds per minute
rRNA	Ribosomal ribonucleic acid
RT	Room temperature
SDS-PAGE	Sodium dodecyl sulfate-polyacrylamide gel electrophoresis
Ser	Serine
SmaBCA	$\beta$ -CA of <i>Schistosoma mansoni</i>
<i>SmaBCA</i>	Gene of the $\beta$ -CA of <i>Schistosoma mansoni</i>
Thr	Threonine
TPM	Transcripts per million

Tyr

Tyrosine

Val

Valine

WHO

World Health Organization



# ORIGINAL COMMUNICATIONS

This thesis is based on the following original communications, which are referred to in the text by their Roman numerals (I-V):

- I            **Haapanen S**, Bua S, Kuuslahti M, Parkkila S, Supuran CT. Cloning, characterization and anion inhibition studies of a  $\beta$ -carbonic anhydrase from the pathogenic protozoan *Entamoeba histolytica*. *Molecules*. 2018 Nov 28;23(12):3112
- II            Bua S, **Haapanen S**, Kuuslahti M, Parkkila S, Supuran CT. Sulfonamide inhibition studies of a new  $\beta$ -carbonic anhydrase from the pathogenic protozoan *Entamoeba histolytica*. *Int J Mol Sci*. 2018 Dec 8;19(12):3946
- III           **Haapanen S\***, Angeli A\*, Tolvanen M, Emameh RZ, Supuran CT, Parkkila S. Cloning, characterization and inhibition of the novel  $\beta$ -carbonic anhydrase from the parasitic blood fluke *Schistosoma mansoni*. *J Enzyme Inhib Med Chem*. 2023 Mar 1;38(1):2184299
- IV           **Haapanen S**, Patrikainen MS, Parkkila S. Ultrasensitive and rapid diagnostic tool for detection of *Acanthamoeba castellanii*. *Diagn Microbiol Infect Dis*. 2023 Jul 26;107(2):116014
- V            **Haapanen S**, Barker H, Carta F, Supuran CT, Parkkila S. A novel drug screening assay for *Acanthamoeba castellanii* and the anti-amoebic effect of carbonic anhydrase inhibitors (submitted)

\*equal contribution

# AUTHOR'S CONTRIBUTION

- I            Designed and performed recombinant protein production, created figures, analyzed the results, revised and accepted the final manuscript.
- II            Designed and performed recombinant protein production, created figures excluding the molecular structure figure, analyzed the results, revised and accepted the final manuscript.
- III            Designed and performed recombinant protein production, created the protein fractions figure, analyzed the inhibition results, contributed to the creation of multiple sequence alignment, 3D model figure and sequence logo, wrote the first draft of the manuscript, revised and accepted the final manuscript.
- IV            Designed and performed the PCR, contributed to designing and performing quantitative real-time PCR, analyzed the results, created the figures, wrote the first draft of the manuscript, revised and accepted the final manuscript.
- V            Designed and performed the drug screening assay, analyzed the results, created the figures except phylogenetic trees, wrote the first draft of the manuscript, revised and accepted the final manuscript.

# 1 INTRODUCTION

Carbonic anhydrases (CAs, EC 4.2.1.1) are metalloenzymes indispensable for life. They are ubiquitously found in most living organisms from single-celled plankton to humans. They catalyze the reversible hydration of carbon dioxide:  $\text{CO}_2 + \text{H}_2\text{O} \rightleftharpoons \text{HCO}_3^- + \text{H}^+$  (Chegwidden and Carter 2000).

CAs are classically divided into eight families:  $\alpha$ -,  $\beta$ -,  $\gamma$ -,  $\delta$ -,  $\zeta$ -,  $\eta$ -,  $\theta$ - and  $\iota$ -CAs, of which the human genome involves enzymes from the  $\alpha$ -family only. All CAs have a highly conserved active site, containing two-valent metal ions, such as zinc ( $\text{Zn}^{2+}$ ), iron ( $\text{Fe}^{2+}$ ), or cobalt ( $\text{Co}^{2+}$ ), hence the name metalloenzyme (Akocak and Supuran 2019). CAs take part in many physiological processes, for example maintaining the pH in cells (Supuran 2018). They are under intense research for use as targets for antimicrobial agents to treat infectious diseases because of the threat of rising antimicrobial resistance. Novel carbonic anhydrase inhibitors (CAIs) have been synthesized and tested to create compounds targeting only a specific CA-family to minimize potential adverse side effects (Pastorekova et al. 2004; Nocentini, Capasso, and Supuran 2023). Disease-causing parasites have CAs from other families than the  $\alpha$ -CAs present in humans. Therefore, the CAs of different parasites are under investigation to be used as drug targets to treat the diseases.

Parasitic diseases are a major global health threat, but their disease burden is mostly concentrated in developing countries. The World Health Organization (WHO) has listed 20 diseases caused by bacteria, viruses and parasites into a heterogeneous group of neglected tropical diseases (NTDs). NTDs are prevalent mostly in rural areas, low-income countries and conflict zones. They are neglected as they are often not included in global health agendas. Even the second most lethal parasitic disease in the world, schistosomiasis, is on the list of NTDs (Gundamaraju 2014; Siqueira et al. 2017). Access to treatment with praziquantel or oxamniquine (da Silva et al. 2017) is low, as only 15% of children in need of treatment receive it (Siqueira et al. 2017). On the contrary, malaria, the most lethal parasitic disease, is not on the list of NTDs and is far better known and treated (WHO).

Endemic to the same areas as schistosomiasis, amebiasis is an intestinal infection is caused by *Entamoeba histolytica*, a pathogenic amoeba. It affects millions of people annually and is a huge cause of morbidity (Shirley et al. 2018). Amebiasis is treatable, but the treatment is two-phasic, which increases the risk of treatment failure (Rashidul Haque et al. 2003).

Another amoeba, *Acanthamoeba castellanii*, is an opportunistic pathogen mainly causing sight-threatening keratitis, an infection of the cornea (Maycock and Jayaswal 2016). Although the infection is only rarely invasive, it is a significant cause of monocular blindness and thus, causes loss of quality-adjusted life years. Keratitis is difficult to diagnose as its clinical manifestation resembles bacterial and viral eye infections, and the gold standard diagnostic method is culturing of the sample, which is very time-consuming (Chew et al. 2011). Even with thorough treatment involving different eye drops for several weeks, the eye sight may still be lost as a result of keratitis.

This thesis aims to develop tools and methods which could improve the diagnosis and treatment of different parasitic infections. We produced the selected CAs as recombinant proteins which were further characterized using biochemical methods. We also established an amoeba culture in our facilities and developed a novel PCR-based diagnostic method and drug screening assay for *A. castellanii*.



## 2 REVIEW OF LITERATURE

### 2.1 General aspects of CA enzymes

The presence of a carbonic acid dehydrating enzyme in blood was first suggested in the 1920s when it was observed that the theoretical reaction speed of uncatalyzed hydration of carbon dioxide seemed too slow for physiological purposes (Baird Hastings et al. 1927). However, it took roughly ten years before the first carbonic anhydrase (CA, EC 4.2.1.1) was discovered in the red blood cells of human in 1932 (Meldrum and Roughton 1933a; 1933b). Almost at the same time, the first two human CAs, named CA I and CA II, were discovered in human erythrocytes (Meldrum and Roughton 1933b). These two CAs belong to the alfa-CA family. Only a few years later, in 1939, a CA from a plant was found, which, decades later, was discovered to belong to a new family of CAs,  $\beta$ -CAs (Neish 1939). Since then, the discovery of new carbonic anhydrases has been extensive, because CAs are ubiquitous in nature. They have an important role in the reversible hydration of carbon dioxide ( $\text{CO}_2$ ) (Figure 1):



CAs are central to many processes in cells, especially in gluconeogenesis, urea synthesis, lipogenesis, and photosynthesis in autotrophs, because they provide bicarbonate to reactions and/or maintain the optimal pH value for the cell reactions (Supuran 2018). CAs also play a significant role in transforming  $\text{CO}_2$  into a soluble form to prevent cell damage, the reaction they were initially discovered from (Gilmour 2010). However, the functions of CAs are not always beneficial for the organism, as CAs also contribute to maintaining optimal pH value for tumor growth (Mboge et al. 2018) and to enhancing vascular calcification, thus promoting the development of atherosclerosis (Adeva-Andany et al. 2015; Yuan et al. 2019). Because of the multiple roles of CAs, many drugs targeting them have been developed to treat a variety of conditions, for example glaucoma and epilepsy (Supuran 2018).

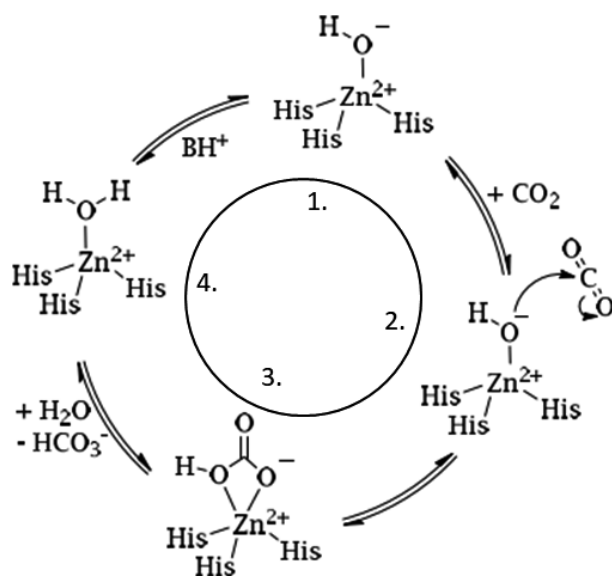


**Figure 1.** Catalytic mechanism of an  $\alpha$ -class carbonic anhydrase. Three amino acids coordinate the metal ion ( $\text{Zn}^{2+}$ ). In step 1  $\text{Zn}^{2+}$  disintegrates the proton ( $\text{H}^+$ ) from the water molecule ( $\text{H}_2\text{O}$ ) producing a  $\text{Zn}^{2+}$ -coordinated hydroxide ion ( $\text{OH}^-$ ). Then  $\text{OH}^-$  performs a nucleophilic attack on the oxygen molecule of carbon dioxide ( $\text{CO}_2$ ) (step 2) resulting in bicarbonate ions ( $\text{HCO}_3^-$ ).  $\text{HCO}_3^-$  is released from  $\text{Zn}^{2+}$  regenerating the active site (step 3) and a new water molecule is attached (step 4) to have its proton released in the buffer (B). Figure modified from (Nocentini, Capasso, and Supuran 2023).

## 2.1.1 Families

CAs are divided into eight families:  $\alpha$ -,  $\beta$ -,  $\gamma$ -,  $\delta$ -,  $\zeta$ -,  $\eta$ -,  $\theta$ - and  $t$ -CAs. Detailed structural analyses have shown that some of the novel CAs are only new members of an existing family instead of forming an entire new family as had initially been thought. For example,  $\epsilon$ -CAs were found to be  $\beta$ -CA-like enzymes and thus, are no longer considered their own family but a subgroup of  $\beta$ -CAs, carboxysomal CAs (Cannon, Heinhorst, and Kerfeld 2010). Additionally,  $\theta$ - and possibly  $\zeta$ -CAs are  $\beta$ -CA-like enzymes (M. Tolvanen, unpublished observations). Another structural resemblance is found between  $\eta$ -CAs and  $\alpha$ -CAs.  $\eta$ -CAs are folded similarly to  $\alpha$ -CAs (Figure 2), but a conserved histidine residue in the active site (H119) in  $\alpha$ -CAs is changed in  $\eta$ -CAs (H119Q) (De Simone et al. 2015).  $\delta$ -CAs also structurally resemble  $\alpha$ -CAs; however, they are still considered separate families (Del Prete et al. 2014). On the contrary,  $\gamma$ -CAs are structurally and evolutionally distinct from the

other CA-classes, as are  $\iota$ -CAs, which were found in 2019 in marine phytoplankton (Jensen et al. 2019).

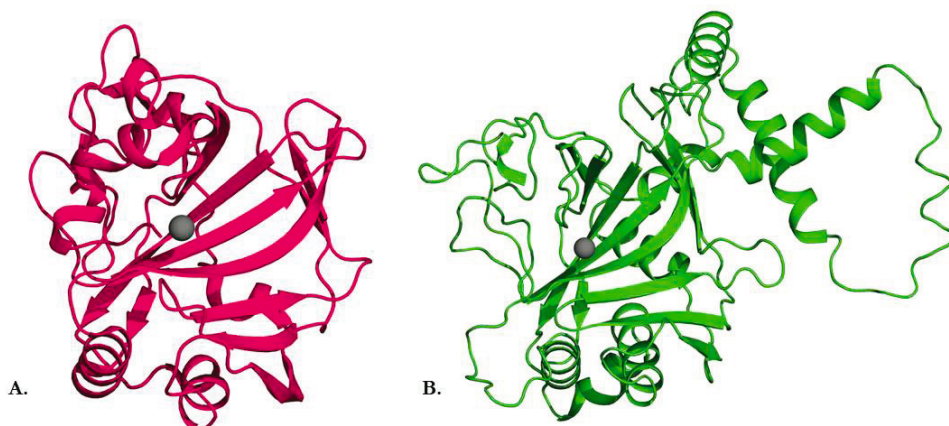


**Figure 2.**  $\alpha$ -CAs and  $\eta$ -CAs have a similar 3D-structure. The predicted structure of  $\alpha$ -CA of *Persephonella marina* [A. (Kim et al. 2019)] and the  $\eta$ -CA of *Plasmodium falciparum* [B. (De Simone et al. 2015)] demonstrate the similarity well. Models created with The PyMOL Molecular Graphic System (version 2.5.0).

$\alpha$ -CAs are not only found in the genomes of eukaryotes but also in many prokaryotes (Capasso and Supuran 2015).  $\beta$ -CAs are even more widespread and are present in photosynthetic organisms, archaea, bacteria, and yeasts (Liljas and Laurberg 2000; Rowlett 2010; Zolfaghari Emameh et al. 2016; Zolfaghari Emameh et al. 2020). They also present in higher organisms, such as insects, nematodes and protozoans, but not in chordates (Liljas and Laurberg 2000; Rowlett 2010; Zolfaghari Emameh et al. 2016; Zolfaghari Emameh et al. 2020).  $\gamma$ -CAs are found in fungi, plants, bacteria, archaea and yeasts (Ferry 2010; Zolfaghari Emameh et al. 2020).  $\delta$ -CAs are widely present in marine phytoplankton (Lane et al. 2005; Park, Song, and Morel 2007; Alterio et al. 2012).  $\zeta$ -CAs have been found in a diatom, in *Conticribra weisflogii* (previously *Thalassiosira weisflogii*) (Alterio et al. 2012), acting in close relation with the  $\delta$ -CA of the organism (Lane et al. 2005; Park, Song, and Morel 2007; Alterio et al. 2012).  $\eta$ -CAs have been found in the malaria-causing *Plasmodium* genus and the toxoplasmosis-causing *Toxoplasma gondii* (De Simone et al. 2015; Chasen et al. 2017).  $\theta$ -CAs were first discovered in 2016 in the lumen of thylakoids in the chloroplast and were later found in bacteria, marine diatoms and green algae (Kikutani et al. 2016).  $\iota$ -CAs are the most recently discovered CAs, as they were found in 2019. They are widely present in single-celled organisms and have been discovered in bacteria,

diatoms, green algae and cyanobacteria (Jensen et al. 2019; Akocak and Supuran 2019).

## 2.1.2 Structures

The three-dimensional (3D) structures of numerous CAs have been reported and are available in PDB database (<https://www.rcsb.org/>). The most reported ones are  $\alpha$ -,  $\beta$ -, and  $\gamma$ -CAs, for which multiple crystallographic structures have been resolved.  $\alpha$ -CAs are most commonly in a monomeric state. The monomers are composed of a  $\beta$ -sheet core with  $\alpha$ -helices around it (see Figure 2) (Lomelino, Andring, and McKenna 2018). The fundamental oligomeric state of  $\beta$ -CAs is dimeric, but they can also form multimers, for example tetramers, octamers and so on. Crystallographic studies show  $\beta$ -CA monomers to have four- to fivefold  $\beta$ -sheets as a core surrounded by  $\alpha$ -helices, which interact to form dimers (Rowlett 2010). This will be further discussed in the results section. In contrast to  $\alpha$ - and  $\beta$ -CAs,  $\gamma$ -CAs are trimers. The only  $\zeta$ -CA structure is from *Conticribra weissflogii* and appears to be largely similar to  $\beta$ -CAs with a dimeric structure (Xu et al. 2008).

CAs are metalloenzymes, e.g., they have a metal ion in their active site. Most commonly, the metal ion is zinc ( $Zn^{2+}$ ), which in some CA-families in some cases may be replaced by another metal ion (Akocak and Supuran 2019). For example,  $\gamma$ -CAs use iron ( $Fe^{2+}$ ) but are also in active form with  $Zn^{2+}$  or cobalt ( $Co^{2+}$ ) (Akocak and Supuran 2019).  $\zeta$ -CAs may contain cadmium ( $Cd^{2+}$ ) instead of  $Zn^{2+}$  (Alterio et al. 2015), and  $\iota$ -CAs usually have manganese ( $Mn^{2+}$ ) in their active site (Jensen et al. 2019; Del Prete et al. 2020; Petreni et al. 2021). However,  $\iota$ -CAs have a distinct feature from other CA classes; they do not necessarily possess a metal ion in the active site at all (Hirakawa et al. 2021).

The overall structure of the active site of CAs is conserved between the families (Figure 3). Three active site residues and a water molecule are positioned in tetrahedral formation to the metal ion (Lomelino, Andring, and McKenna 2018). The amino acid composition of the active site of  $\alpha$ -CAs includes three histidines in positions  $x$ ,  $x+2$ ,  $x+25$  ( $x=94$  in human CA II) coordinating the metal ion (Lomelino, Andring, and McKenna 2018). Similarly,  $\gamma$ -CAs have coordinating amino acid positions  $x$ ,  $x+36$ ,  $x+41$ , one from each monomer ( $x=81$  in  $\gamma$ -CA of *Methanosarcina thermophila*) (Zimmerman, Tomb, and Ferry 2010).  $\delta$ -CAs have the same coordination ( $x$ ,  $x+3$ ,  $x+112$ ,  $x+114$  in  $\delta$ -CA of *Conticribra weissflogii*) (Cox et al. 2000).  $\beta$ -CAs and  $\zeta$ -CAs have only one histidine, and the other two residues are

cysteine. For  $\beta$ -CAs, the residues are x (Cys), x+56 (His), x+59 (Cys) (x= 42 in  $\beta$ -CA of *Vibrio cholerae* and *Pseudomonas aeruginosa*) (Rowlett 2010; Ferraroni et al. 2015; Pinard et al. 2015), and the corresponding residues for  $\zeta$ -CAs are x (Cys), x+52 (His), x+62 (Cys) (x=263 in the  $\zeta$ -CA of *Conticribra weissflogii*) (Amata et al. 2011). Although having a high structural resemblance to  $\alpha$ -CAs,  $\eta$ -CAs have a different active site: one of the histidines is replaced with glutamine with the result of amino acids in positions x (His), x+2 (His), x+19 (Gln) (x=299 in the  $\eta$ -CA of *Plasmodium falciparum*) (De Simone et al. 2015). The active site structure of  $\theta$ -CAs is not yet well established (Lomelino, Andring, and McKenna 2018); however, there are preliminary observations that the active site might have amino acid residues from two different chains (M. Tolvanen, unpublished observations). The newest member of the CA family,  $\iota$ -CA, has an unknown active site composition.

CAs have different signal peptides for multiple subcellular locations. They have been found for example in mitochondria, chloroplasts, cytoplasm and membranes. Some of them are secreted, for example CA VI is secreted into saliva and milk in humans, cows, sheep and rats (Fernley et al. 1991; Karhumaa et al. 2001; Yrjänäinen, Patrikainen, Azizi et al. 2022). The location of some CAs still remain unknown.

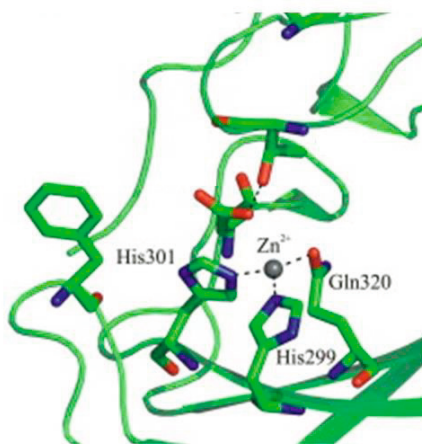


**Figure 3.** Representation of the general active site structure of a CA using the  $\eta$ -CA of *Plasmodium falciparum* as a model. Figure shows the  $Zn^{2+}$  on the center as well as the zinc coordinating amino acid residues: two histidines and one glutamine. Figure modified from De Simone et al. 2015.

### 2.1.3 Carbonic anhydrase inhibitors

CAIs are used to treat many conditions, for example glaucoma (Supuran, Altamimi, and Carta 2019), brain edema (Li, Zhang, and Zhang 2018; Wan et al. 2023), mountain sickness (Imray et al. 2010; Davis and Hackett 2017) and epilepsy (Mechrgui and Kanani 2022; Farzam and Abdullah 2022). CAIs have previously also been used in treating high blood pressure due to their diuretic effect; however, currently, more effective medication for high blood pressure is in use (Kehrenberg and Bachmann 2022). CAIs are an interesting class of drugs because human genome has 15 CAs which take part in many cellular processes. The investigation of new applications for CAI use is intensive. The role of CAs in lipogenesis has been recognized as a potential target process for antiobesity treatment (Supuran 2022), and its role in tumor environment management provides an insight for antitumor agent development (Tonissen and Poulsen 2021; Kumar et al. 2022; de Campos et al. 2022). CAIs have also been investigated as therapeutic agents in central nervous system diseases, such as Alzheimer's disease, because in long-term use, they can reduce oxidative stress, mitochondrial dysfunction and amyloid accumulation, thus preventing memory loss (Provinsi et al. 2019; Lemon et al. 2021).

Infectious diseases are a global health problem, as totally new classes of antibiotics have not entered in the clinical field in three decades which increases the risk of antimicrobial resistance (Hutchings, Truman, and Wilkinson 2019). For instance, tuberculosis, caused by *Mycobacterium tuberculosis* bacteria, is difficult to treat as it requires four different antibiotics, and multidrug resistant strains are an enormous clinical challenge. Therefore, new  $\beta$ -CA-targeting inhibitors have been developed to respond to the need for new drugs against tuberculosis and other mycobacterial diseases (Aspatwar et al. 2018). Unfortunately, these inhibitors are still in preclinical tests so it will take a long time to know whether they can be used as treatment against tuberculosis (Aspatwar et al. 2020).

The CAIs that are clinically used either topically or orally belong to the class of sulfonamides. For instance, the four CAIs used to treat glaucoma (acetazolamide, methazolamide, dorzolamide and brinzolamide) are all sulfonamides. In Finland, dorzolamide and brinzolamide are favored over acetazolamide and methazolamide as they are topically administered and thus cause fewer adverse side effects than the orally administered options (Nesher and Ticho 2003).

All clinically used CAIs have adverse side effects, these include abdominal pain, blurred vision, changes in taste, diarrhea, fatigue, headache, nausea, paresthesia,

tinnitus and vomiting (Arbabi et al. 2022). Allergy to sulfa could also be a problem in administering sulfonamide derivatives; however, serious allergic reactions, such as anaphylaxis, are rare (Lee et al. 2004).

CAIs have a three-part structure: a zinc-binding group, a linker region, and a tail region (Pinard, Mahon, and McKenna 2015). The classical inhibition mechanisms include the binding of the inhibitor to the zinc ion of the active site or the water coordinating the zinc or hydroxyl bound to zinc (McKenna and Supuran 2014). Sulfonamides and another vastly investigated group of CAIs, anions, bind straight to the zinc ion (Singh et al. 2018). Nonclassical inhibitors have other inhibition mechanisms, such as binding outside the active site or hindering access to the active site. Additionally, some mechanisms are still unknown (Singh et al. 2018).

## 2.2 Parasites

A parasite is an organism that exploits another organism, the host (Worms, Thomson et al. 1856). Parasitizing is common and it occurs everywhere in nature. Usually, it is beneficial for the parasite not to kill the host, although the host may experience a disadvantage compared to its nonparasitic stage. Specializing in certain host species is typical for parasites (Starkey and Blagburn 2022).

Human parasites are divided into endoparasites and ectoparasites, where the former live within the body and the latter superficially in the skin (Adekiya et al. 2021; Anderson and Paterek 2022). Almost every organ system can harbor parasites, for instance, amoebas in the central nervous system, different worms in the intestines, and mites on the skin. While some parasites are harmless, parasitic infections can be severe and cause over one million deaths yearly (Naghavi et al. 2015), of which almost 80% are caused by malaria. Another dangerous parasite type are the diarrhea-causing parasites, which are especially lethal for children under the age of five in developing countries where access to sanitation and clean water may be compromised (Hart and Umar 2000).

While tropical and subtropical countries have the highest incidence of parasitic infections, travel has spread them worldwide (Ogbera and Anaba 2000). Very common parasites include for example *Schistosoma mansoni* and *Entamoeba histolytica*, which cause intestinal infections and are endemic in tropical and subtropical countries (Colley et al. 2014; Shirley et al. 2018). On the other hand, *Acanthamoeba castellanii* inhabits soil and water globally, but it is an opportunistic pathogen.

Interestingly, *E. histolytica* and *A. castellanii* are quite close relatives, as they belong to the same order (Figure 4).

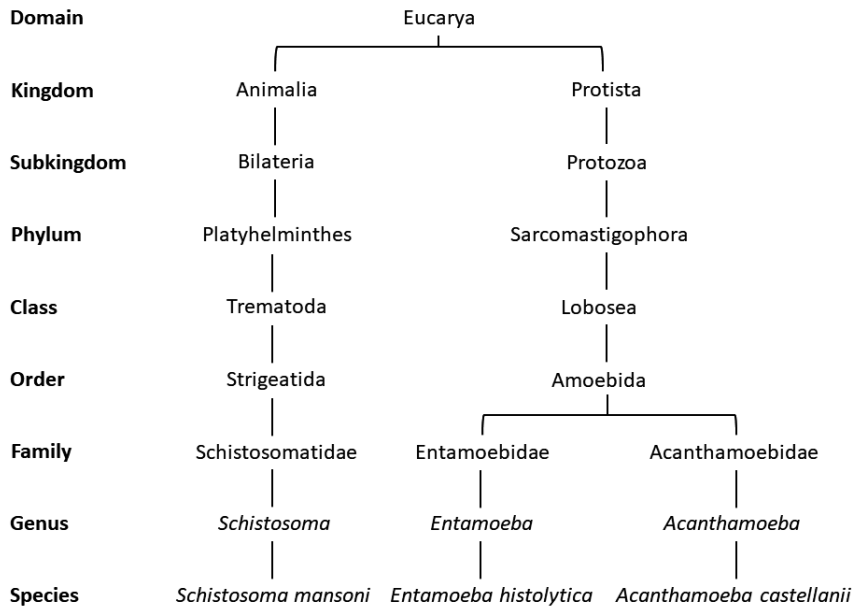


**Figure 4.** Taxonomic classification of *Schistosoma mansoni*, *Entamoeba histolytica* and *Acanthamoeba castellanii*. They are all eucaryotic organisms, and *E. histolytica* and *A. castellanii* are rather close relatives, both belonging to the order Amoebida. Classification information was retrieved from the Integrated Taxonomic Information System (ITIS, [https://www.itis.gov/servlet/SingleRpt/SingleRpt?search\\_topic=TSN&search\\_value=55320#null](https://www.itis.gov/servlet/SingleRpt/SingleRpt?search_topic=TSN&search_value=55320#null)) and Khan 2006.

## 2.2.1 *Schistosoma mansoni*

*Schistosoma mansoni* is a parasitic blood fluke belonging to the genus *Schistosoma* (Gryseels 2012; Colley et al. 2014) with approximately 20 other species (Agatsuma 2003), of which *Schistosoma japonicum* (Agatsuma 2003; McManus et al. 2018) and *Schistosoma hematobium* (Khiani and King 2009; McManus et al. 2018) are also significant parasitic disease causative pathogens. *S. mansoni* and *S. japonicum* cause an intestinal infection commonly called schistosomiasis, sometimes also called bilharzia, and *S. hematobium* causes a urogenital infection (McManus et al. 2018).

Approximately 250 million people get infected by *S. mansoni* every year (Khiani and King 2009; Colley et al. 2014; LoVerde 2019), which makes schistosomiasis the



second most harmful parasitic infection after malaria (LoVerde 2019). *S. mansoni* is endemic in Africa, the Caribbean, the Middle East and South America (Gryseels 2012; McManus et al. 2018), in contrast to *S. japonicum* which is mainly found in South and East Asia (Agatsuma 2003).

The life cycle of *S. mansoni* requires fresh water, humans as the definitive host, and fresh water snails of *Biomphalaria* species as the intermediate host. Thus, they have an indirect (heteroxenous) life cycle (Colley et al. 2014; Nation et al. 2020) (Figure 5). *S. mansoni* uses humans as the definitive host, but other *Schistosoma* species may also use other mammals; for instance *S. japonicum* may use dogs, cats, horses, pigs and water buffaloes (Llanwarne and Helmbly 2020). Cercariae, one of the life forms of *S. mansoni*, are infective and can be contracted only from water contact; the other forms are not able to infect humans (Gryseels 2012; Colley et al. 2014).

Schistosomiasis can be divided into two phases depending on the duration of the disease: acute and chronic phase (Elbaz and Esmat 2013; McManus et al. 2018). The first sign of schistosomiasis can be cercarial dermatitis with the symptom of itching rash. This occurs for the first hours to days before schistosomulae enter venous circulation (Gryseels et al. 2006; McManus et al. 2018; Hambrook and Hanington 2021). Acute symptoms of intestinal infection start a few weeks after contracting the blood fluke and include diarrhea (Elbaz and Esmat 2013), abdominal pain (Elbaz and Esmat 2013) and fever (Nelwan 2019), which usually ease by themselves within 2-10 weeks (Gryseels et al. 2006). People born and living in endemic areas may have an asymptomatic or minorly symptomatic acute phase suspected to be due to *in utero* desensitization from the previously infected mother or repeatedly occurring penetration of cercariae through the skin, leading to adaptation of the immune system (McManus et al. 2018). However, the human immune system is not capable of overcoming the parasite; thus, the infection turns into a chronic, less symptomatic version after the acute phase (Siqueira et al. 2017).

Chronic schistosomiasis affects many organs, such as the liver, lungs, spleen, and intestine (Gryseels et al. 2006; McManus et al. 2018). Adult worms incorporate host antigens on their surface, successfully escaping the host immune response, but the eggs are highly antigenic, evoking multiple immune responses (Llanwarne and Helmbly 2020; Hambrook and Hanington 2021). The main function of the egg is to migrate through the host's intestine wall to enter the lumen and eventually the environment (Gryseels et al. 2006). Typically, some eggs are trapped in different organs, where they induce the immune system to form granulomas (Llanwarne and Helmbly 2020; Hambrook and Hanington 2021), which interfere with the normal

function of the organ. As mature worms can live in veins for decades, they gradually generate the main effects to organs of chronic schistosomiasis, which can be fatal (Gryseels 2012; McManus et al. 2018). Typically, the affected organs are the intestines and liver, leading to ulcers, polyps and even cancer development in the intestines and cirrhosis and its complications in the liver (Elbaz and Esmat 2013).

Parasitic infections are not the only disease prevalent in the incidence areas of the parasites. In the endemic areas of *S. mansoni*, chronic viral hepatitis prevalence is high, and coinfections with schistosomiasis are common, inducing even faster development of fibrotic changes in the liver (Gasim, Bella, and Adam 2015) and therefore faster occurrence of complications, such as esophageal varices, portal hypertension and hepatocellular cancer (Elbaz and Esmat 2013). Additionally, extragastrointestinal changes have been reported in the kidney (Barsoum 2004; Neves et al. 2020), central nervous system (De Abreu Ferrari 2004) and lung (De Abreu Ferrari 2004; Bamefleh and Al-Hussain 2021).

Diagnosis of intestinal schistosomiasis is made with a microscopic examination to detect the eggs in stool (Grzegorek et al. 2023). Usually, serological samples are used as completing tests. However, travelers, who often spend a short time in the incidence area, have a low egg count, which emphasizes the importance of antibodies in diagnosis (Grzegorek et al. 2023). With extraintestinal infections, imaging also plays a significant role in diagnosing the infection. While the diagnosis itself is relatively easy to make, the access to health care in the typical incidence areas is often restricted, which delays the treatment.

The currently used treatment against schistosomiasis is praziquantel (Siqueira et al. 2017). Another medicine, oxamniquine, has also been found to be effective against *S. mansoni* but not against *S. japonicum* and *S. hematobium* (Cioli, Pica-Mattoccia, and Archer 1995; Rugel et al. 2020). Previously, oxamniquine was widely used, but praziquantel has replaced it with fewer side effects and a wider therapeutic effect on different species of the *Schistosoma* genus (Siqueira et al. 2017). Praziquantel is effective only against adult worms, not any stages of larvae, resulting in a high risk of recurring infections (Llanwarne and Helmbly 2020). Praziquantel increases the flow of  $\text{Ca}^{2+}$  across the tegument, a protective layer on the outer surface of the worm, resulting in high intracellular  $\text{Ca}^{2+}$  concentration and contraction of the parasite (Vale et al. 2017). Praziquantel is also used as preventive medication for people in high-risk areas without collecting diagnostic samples (Cioli et al. 2014; Llanwarne and Helmbly 2020) resulting in even more extensive use of praziquantel and thereby rising resistance issues (Doenhoff et al. 2002; Botros and Bennett 2007).

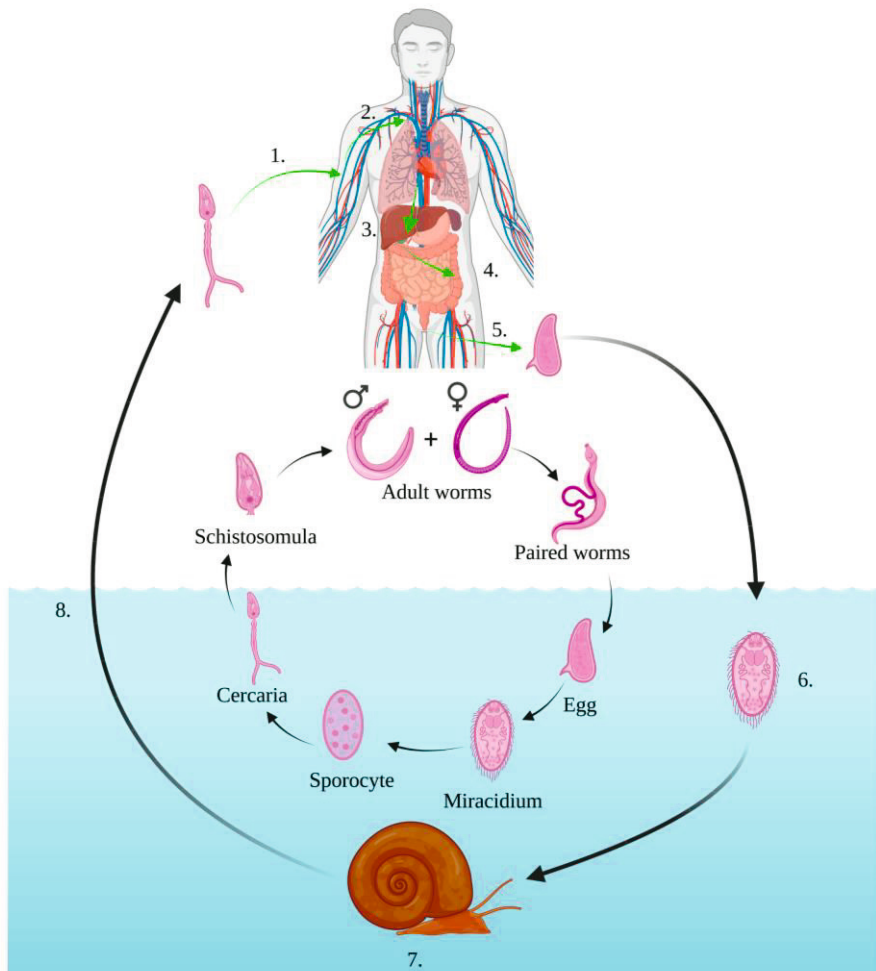


**Figure 5.** The life cycle of *Schistosoma mansoni*. The figure was constructed according to McManus et al. 2018, LoVerde 2019 and Nation et al. 2020. 1. Cercariae penetrate healthy skin and lose their tail, becoming schistosomulae. 2. Schistosomulae enter venous circulation and travel through the lungs and heart. 3. Schistosomulae enter the portal vein system of the liver where they mature and pair. 4. Paired worms seek mesenteric veins to lay eggs. 5. Eggs are excreted in feces to the environment. 6. Eggs, that reach fresh water, hatch and miracidia are released. 7. Miracidia enter fresh water snails (*Biomphalaria* spp.) and form sporocysts which are means for asexual reproduction. 8. Sporocysts release cercariae that exit the snail and wait to encounter the host in water. Figure created with BioRender.com.

No commercially distributed vaccines are available against schistosomiasis; however, three recombinant protein-based vaccines are already in clinical trials (Eyayu, Zeleke, and Worku 2020). Other mechanisms of action, such as helper T-cell-based immunizing, have also been studied to find the most effective and safe vaccine

(Rahmani et al. 2019). Vaccines are expected to be the most successful way to reduce the global disease burden and long-term complications of schistosomiasis.

*Schistosoma mansoni* has six  $\alpha$ -CAs and one  $\beta$ -CA (SmaBCA); however, UniProt (<https://www.uniprot.org/>) (Apweiler et al. 2004) shows two competing sequences for  $\beta$ -CA. These are 241 (UniProt ID G4V6B2) and 266 (UniProt ID A0A3Q0KBP5) amino acids long. It is presumed that the short version is falsely predicted and the newer, longer sequence from transcriptomic data is the correct one (M. Tolvanen, observations in publication III). One of the  $\alpha$ -CAs has already been recombinantly produced and tested against different CAIs (Angeli et al. 2020; 2022).

### 2.2.2 *Entamoeba histolytica*

*Entamoeba histolytica* is a protozoan parasite that causes an intestinal infection called amebiasis in human hosts (Hashmey, Genta, and White 1997; Shirley et al. 2018). It is a close relative to *Entamoeba dispar* which is currently considered a harmless intestine-colonizing amoeba. *E. dispar* was previously presumed asymptomatic *E. histolytica* infection but later turned out to be intestinal colonization of *E. dispar* (Stauffer, William; Ravdin 2003; Stanley 2003). *E. histolytica* is also quite a close relative of *Acanthamoeba castellanii*, as they belong to the same order (Figure 4). *A. castellanii* will be discussed later.

Amoebiasis affects approximately 500 million people annually and is thus considered the third most harmful parasitic infection after malaria and schistosomiasis (Sardar et al. 2023; Vasconcelos et al. 2023). Approximately 3.1% of deaths due to diarrhea are caused by amebiasis (Troeger et al. 2017). It is endemic in Africa, Central and South America, southern parts of Asia and Pacific countries (Center for Discovery and Innovation in Parasitic Diseases 2020). Increasing travel has spread the infection outside of its endemic region, too (Shirley et al. 2018).

The symptoms of amebiasis usually begin two to four weeks after the contraction. The infection has three main forms: intraluminal infections with no evident symptoms, colitis including the symptoms of abdominal pain, fever and watery or bloody diarrhea, (Showler and Boggild 2013), and disseminated infection to other organs, such as to the liver causing an abscess (R. Haque et al. 2000), bowel perforation and peritonitis (Shirley et al. 2018). The symptoms of amoebiasis may vary from extremely mild to life-threatening.

People are infected by *E. histolytica* via the fecal-oral route, usually from cyst-contaminated food or drink (Figure 6). After ingestion of the cysts, they travel through the intestines to the end of the small bowel or the beginning of the large bowel, where one cyst expels four trophozoites. They ingest gut bacteria and food and multiply by dividing. Some trophozoites encyst and are excreted in feces to be ingested by another host. Some trophozoites invade and ulcerate the wall of the bowel with multiple mechanisms, degrading the host's extracellular matrix, killing immune effector cells and causing cytolysis, causing bloody diarrhea and occasionally invading other organs (Cornick and Chadee 2017). Cysts are extremely resistant to environmental factors and survive, for instance, gastric acid, contrary to trophozoites.

The diagnosis of amebiasis is preferred to be confirmed with polymerase chain reaction (PCR) to differentiate *E. histolytica* infection from nonpathogenic *Entamoeba* species, such as the earlier mentioned *E. dispar*. The benefits of PCR also include the possibility of testing many intestinal pathogens in the same assay (Van Lieshout and Verweij 2010; Verweij and Rune Stensvold 2014). Previously, the diagnosis was based on microscopy examination of stool samples and detection of cysts. However, it is impossible to recognize different *Entamoeba* species from one another by microscopy only (Paulos et al. 2019).

Treatment of amebiasis consists of two consequent phases: tissue and intraluminal amebicides. Tissue amebicides are used for symptomatic patients to treat intestinal and extraintestinal infections (Haque et al. 2003). The preferred drug choice is metronidazole or tinidazole, usually with oral administration, as they have excellent bioavailability (approximately 80% for metronidazole). For asymptomatic patients and symptomatic ones after the tissue amebicide course, intraluminal amebicide is administered to exile cysts from the gut as tissue amebicides are inefficient against cysts (Freeman, Klutman, and Lamp 1997). Clinically used intraluminal amebicides are paromomycin, diloxanide furoate and iodoquinol. Combination therapy with tissue amebicide followed by intraluminal amebicide is recommended to prevent relapses (Freeman, Klutman, and Lamp 1997; Kikuchi et al. 2013). The resistance of *E. histolytica* against metronidazole is rare in clinical use (Samarawickrema et al. 1997; Wassmann et al. 1999). Since, the treatment is two-phasic it may be challenging to complete in the incidence area of *E. histolytica*.

*E. histolytica* uses only human and nonhuman primates as hosts, thus eradication of *E. histolytica* is possible. Extensive research in developing a vaccine against *E. histolytica* has been conducted, but none of the presently developed vaccines have

reached clinical trials (Quach, St-Pierre, and Chadee 2014; Kantor et al. 2018; Nagaraja and Ankri 2019).

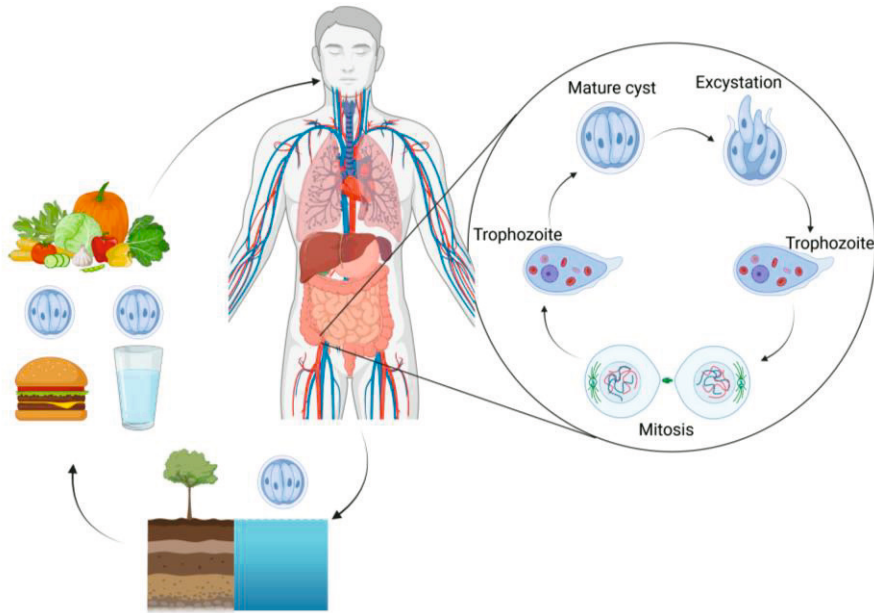


**Figure 6.** The life cycle of *Entamoeba histolytica*. Cysts survive in the environment as infectious and are transferred through the fecal-oral route to the human host. Excystation takes place in the bowel and trophozoites multiply and encystate in the large intestine. Cysts are excreted in feces into the environment to be ready to infect the next host. Figure created with Biorender.com.

In the genome of *E. histolytica*, only one CA is recognized, belonging to the  $\beta$ -family (Agarwal et al. 2020). Six entries are found in UniProt (<https://www.uniprot.org/>) (Apweiler et al. 2004), all having the same sequence except one (M7WM51\_ENTHI) which differs by one amino acid (E36Q) from the five others. The  $\beta$ -CA of *Entamoeba histolytica* (EhiCA) has not been previously produced *in vitro*, which is addressed in this thesis. Since, *E. histolytica* has only one CA, it is potential target to prevent and treat amoebiasis.

### 2.2.3 *Acanthamoeba castellanii*

*A. castellanii* is an opportunistic pathogen and usually causes keratitis, an infection of the cornea (Maycock and Jayaswal 2016; Fu, Ophth, and Gomaa 2019; Niederkorn 2021). *Acanthamoeba keratitis* (AK) is sight-threatening, but fortunately, loss of eye

sight requires predisposing conditions or risk factors, such as contact lens usage, corticosteroid eye drop usage or eye trauma, for example, due to ocular operations. Immunocompromised people are at risk of contracting an invasive infection, usually in the brain, causing granulomatous amoebic encephalitis (GAE) (Marciano-Cabral and Cabral 2003; de Lacerda and Lira 2021). Skin lesions and invasion of other organs are also possible for severely immunocompromised people, such as organ transplant patients (Bronfield et al. 2017).

*A. castellanii* is ubiquitously present in the environment in two life forms: metabolically active trophozoites and dormant cysts (Figures 7 and 8). It belongs to the genus *Acanthamoeba* and has close relatives of free-living amoebae in the genera *Entamoeba*, *Naegleria*, *Balamuthia* and *Hartmannella*, which are also able to cause infections in humans (Khan 2006). *A. castellanii* was discovered in 1930, but it took over four decades before the first infection was confirmed (Khan 2006). The genus *Acanthamoeba* is divided into 23 genotypes, T1-T23, based on the sequence of 18S rRNA (Fuerst, Booton, and Crary 2015; Mirahmadi et al. 2019; Putaporntip et al. 2021). Most of the genotypes are nonpathogenic, but *A. castellanii* belongs to the highly pathogenic T4 genotype, which is further divided into seven subtypes, T4A-T4F and T4-Neff, with *A. castellanii* being classified into T4A, T4B and T4-Neff depending on the isolated strain (Stothard et al. 1998; Fuerst 2014).

The *Acanthamoeba* genus can also be classified into three groups (I-III) based on cyst morphology (Putaporntip et al. 2021). The most abundant is group II with 86.9% of 130 isolates, while group I and group III only have 7.7% and 5.4%, respectively (Putaporntip et al. 2021). Cysts are highly resistant to environmental factors, and the reaction of trophozoites to unfavorable conditions is encystation (Figure 5) (Chávez-Munguía et al. 2005). Cysts are also infectious, and the change in surroundings induces excystation into active trophozoites (Lakhundi, Khan, and Siddiqui 2014).

The diagnosis of AK has traditionally been made by culturing cornea samples for two weeks (Chew et al. 2011). The diagnostic delay is tremendous not only due to the diagnostic method but also due to the lack of suspicion in emergency rooms. Approximately two-thirds of the patients have been treated with anti-viral medication and the same number with antibiotics before the correct diagnosis (Chew et al. 2011). Many PCR-based diagnostic methods have been developed; however, they have not reached widespread clinical use (Maycock and Jayaswal 2016). Additionally, confocal microscopy is a very accurate way of diagnosing AK, but it

requires special equipment and a skilled microscopist, which restricts its broad use (Alantary, Heaselgrave, and Hau 2022).

*A. castellanii* is the most abundant pathogen found in AK patients (Horn et al. 2000); however, one-off cases have been reported involving *A. polyphaga*, *A. hatchetti*, *A. culbertsoni*, *A. rhyssodes*, *A. lugdunensis*, *A. quina* and *A. griffini* (Ishibashi 1997; Schaumberg, Snow, and Dana 1998; Marciano-Cabral and Cabral 2003). Over half of the cultured AK cases also harbor other pathogens, called endosymbionts (Bacon et al. 1993; Iovieno et al. 2010; Rayamajhee et al. 2022) (Figure 7). Endosymbionts are bacteria, most commonly belonging to the phyla Actinobacteria or Proteobacteria (Horn and Wagner 2004; Iovieno et al. 2010; Gu et al. 2022); viruses, usually belonging to Pandoraviridae or Mimiviridae (Rayamajhee et al. 2021); or fungi, which are the rarest endosymbiont (Rayamajhee et al. 2021). The virulence of *A. castellanii* may increase because of the effect of endosymbionts, possibly through horizontal gene transfer (Purssell, Lau, and Boggild 2017; Gu et al. 2022). In addition, many of the endosymbionts are pathogens themselves which leads to coinfections. For instance, *Pseudomonas aeruginosa* is a typical endosymbiont of *A. castellanii*, and their coinfection is more difficult to treat than a single infection of either pathogen (Gu et al. 2022).

Treatment of AK is time-consuming and includes many harmful side effects with possibly unsatisfying results. There is no consensus on the best choice of treatment, and it is always decided individually for every patient. Medication is administered as topical eye drops, most commonly biguanide derivatives, polyhexamethylene biguanide hydrochloride and chlorhexidine gluconate (Sangkanu et al. 2021), or diamidine derivatives, propamidine and hexamidine isethionate (Lorenzo-Morales, Khan, and Walochnik 2015; Carrijo-Carvalho et al. 2017). They are used in mono- or combination therapy (Bagga et al. 2021). There is slight evidence that combination therapy produces better treatment outcomes than monotherapy (Duguid et al. 1997). They are administered hourly at the beginning, and the courses of treatment last for weeks, generally at least 3-4 weeks (Maycock and Jayaswal 2016). In addition to the damage of AK to the cornea and vision, medications can cause loss of corneal tissue regeneration, corneal ulceration, scleritis, iris atrophy and glaucoma, especially if the response to treatment is inadequate and the course needs to be extended (Carrijo-Carvalho et al. 2017). Evidence of rising resistance in clinical samples against conventional treatment options, such as polyhexamethylene biguanide hydrochloride, emphasizes the need for new treatment options (Huang et al. 2017).



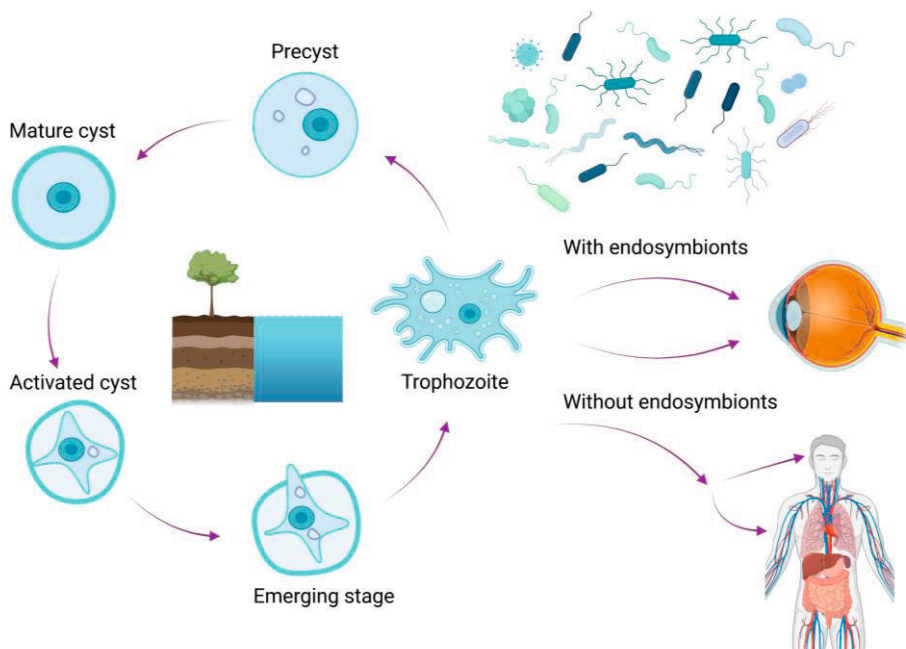


**Figure 7.** The life cycle of *Acanthamoeba castellanii*. *A. castellanii* lives in soil and water, and the cysts are extremely resilient to environmental factors. Trophozoites may harbor other microorganisms ('Trojan horses') (Mirabedini et al. 2022), and coinfections occur. Contact with contaminated water (or soil) to the eye, wounded skin or lower respiratory tract can lead to infections: keratitis in the first case and invasive or skin infection in the case of the last two options. Figure created with Biorender.com and modified from article V by Susanna Haapanen.

The search for new treatment options against AK is intensive (Anwar, Numan, et al. 2019; Abdul Mannan Baig et al. 2019; Shahbaz et al. 2020; Rice et al. 2020). A new treatment choice with 3-aryl-6,7-dimethoxyquinazoline-4-(3H)-one -library drug candidates has been discovered; however, the compounds are not in clinical use, so we do not know their effects on humans (Shahbaz et al. 2020).

Quinazolinones include three clinically used drugs: prazosin hydrochloride, doxazosin mesylate and terazosin hydrochloride (Jafari et al. 2016). Nevertheless, Shahbaz et al. used only synthetically composed derivatives and not clinically used derivatives in their inhibitor assay so the effect of clinical compounds remains unknown (Shahbaz et al. 2020). Other compounds have been developed, such as cobalt nanoparticles, which have been shown to be effective; however, they have the same limitation as quinazolinone assays: there is no clinical data with patients in other

conditions (Anwar, Numan, et al. 2019). Clinically approved drugs, diazepam, phenobarbitone and phenytoin, and their silver nanoparticles showed amoebicidal and cysticidal effects against *A. castellanii* *in vitro*, suggesting potential treatment options for GAE, as the tested drugs readily cross the blood–brain barrier (Anwar, Rajendran, et al. 2019). However, a lack of clinical testing remains.

The size of the genome of *Acanthamoeba castellanii* is debated. From Neff-strain, it has been suggested to be 42.02 Mb (used as the reference genome in NCBI) (Hasni et al. 2020), 43.83 Mb or 46.71 Mb (NCBI). The largest size of the genome has been reported for strain ATCC 50370 with 115.3 Mb (NCBI) or 121.2 Mb (Chelkha et al. 2018), although NCBI states the genome to be too large.

*A. castellanii* has eight CAs: three  $\alpha$ -, three  $\beta$ - and two  $\gamma$ -CAs (Baig et al. 2018; Baig et al. 2019). All  $\alpha$ -CAs are predicted to be membrane-associated. The  $\beta$ -CAs are predicted to have mitochondrial, cytoplasmic and transmembrane isoforms, one of each. Knowledge of the subcellular location of  $\gamma$ -CAs in mitochondria is more extensive than that of the other CA families in *A. castellanii*.  $\gamma$ -CAs have been found to be part of the mitochondrial electron transport chain, indicating that they have a role in the utilization of energy in the cell (Gawryluk and Gray 2010; Gawryluk et al. 2012).  $\gamma$ -CAs were previously found to be present in the chloroplasts of photosynthesizing organisms forming  $\text{HCO}_3^-$  by hydration of  $\text{CO}_2$ , and some indications suggest that  $\text{HCO}_3^-$  may also be transported across the inner mitochondrial membrane (Braun and Zabaleta 2007). However, the presence of  $\gamma$ -CAs in the genus *Acanthamoebae*, which have no chloroplasts, suggests a specific function for  $\gamma$ -CAs in the action of mitochondrial complex I, although the specific role is still unknown (Gawryluk and Gray 2010). The presence of  $\gamma$ -CAs as a part of mitochondrial complex I is not unique to *A. castellanii* as they are present in diatoms as well (Cainzos et al. 2021).

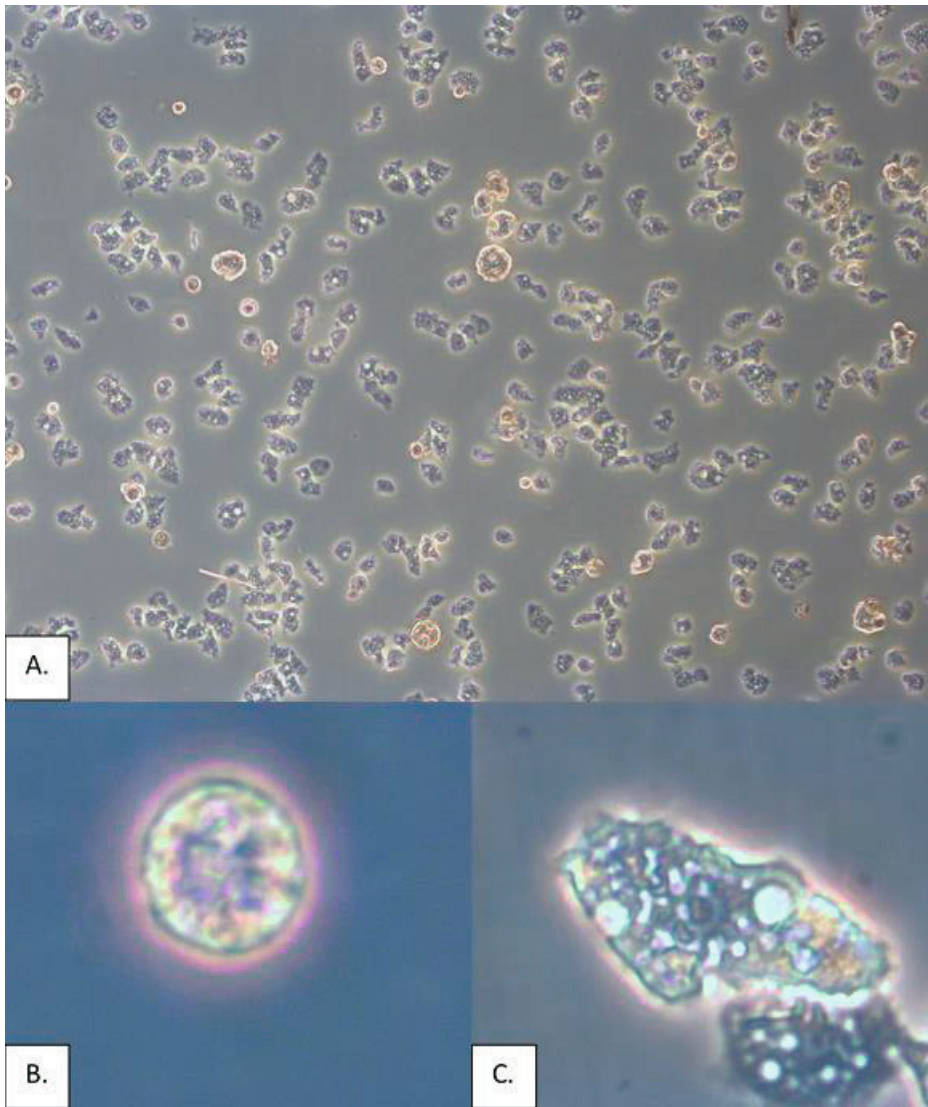


**Figure 8.** A. Light microscope view showing trophozoites and cysts of *A. castellanii* together (10x objective). B. Cyst (40x objective) C. Trophozoite (40x objective). The diameter of a trophozoite is 12-35  $\mu\text{m}$  and the one of a cyst is 5-20  $\mu\text{m}$  (Khan 2006).

### 2.3 Polymerase chain reaction as a diagnostic method

The first DNA-detection based methods for the recognition of pathogens were introduced in the 1980s when the enterotoxin genes of *Escherichia coli* were detected

from bacterial colonies (Moseley et al. 1980). In the beginning, short, labeled DNA fragments, called DNA probes, were used to hybridize with the corresponding sequences from the sample (Yang and Rothman 2004). Amplification of DNA fragments *in vitro* using prior known oligonucleotides, polymerase chain reaction (PCR), was developed by a team in Cetus Corporation in 1983 (Eisenstein 1990), although the original idea was already presented in 1971 (Kleppe et al. 1971).

The development of faster and more accurate techniques is ongoing, and many new advantages to the primary PCR method have been presented. Currently, the standard in clinical laboratories is quantitative real-time PCR (qRT-PCR), a PCR method monitoring DNA amplification during the reaction with the aid of fluorescent marking. It is used in genotyping tumors, surveillance of water quality, and confirming safety in the food industry, for instance (Wong and Medrano 2005). A modification of quantitative PCR, reverse transcription PCR is used in the diagnostics of many infections, with the newest example being the diagnostics of SARS-CoV-2 infection (Rong et al. 2022). For diagnostic purposes, panels including many different pathogens or genomic mutations tested simultaneously have become increasingly common, thus, accelerating diagnostics even further. New methods, for example, isothermal techniques, are under development to provide PCR-based accuracy and sensitivity to bed-side diagnostic tools (Y. Zhao et al. 2015).

## 2.4 Drug development

Drug discovery and development is a multiyear, if not multidecade, process. Traditionally, it is divided into two main phases, the preclinical and clinical phase. When a new compound, or new chemical entity, has been discovered, a vast number of tests are performed to determine the characteristics of the compound, toxicity, effects on different organ systems and suitability of different administration forms (Kaitin 2010). Many compounds are stated as unfit for medical use in the preclinical phase and do not continue to the next level. However, if the drug candidate survives through preclinical tests, it is further processed in the clinical phase. The clinical phase has trials from I to IV where the drug is first administered to healthy volunteers and eventually through patient test groups to phase IV trial where the drug has already an approval for market and the use is monitored in population-based use (Powers 2004).

The development of a new treatment does not always have to be as long and complicated as described above. After the approval of the European Medicines

Agency (EMA), Food and Drug Administration (FDA), or national pharmaceutical agent monitoring agencies, the drug usually has permission to be used in the treatment of one medical condition. Nevertheless, it is very common that later new indications are discovered. For instance, sodium-glucose transport protein 2 inhibitors were initially indicated for the treatment of type 2 diabetes; however, currently, they have an official indication in chronic kidney disease and heart failure despite the blood glucose status of the patient. Since the drug was approved for patient use, the permission to be use in the treatment of other conditions was fast.

The WHO has stated antimicrobial resistance (AMR) as one of the top ten global public health threats. New antimicrobial agents with a novel mechanism of action were introduced in the 1990s (Terreni, Taccani, and Pregnotato 2021), but after that, only derivatives with the currently known mechanisms have been developed, leading to a rising problem of antimicrobial resistance. This is highly noticeable in bacterial infections, as many, especially gram-negative bacteria, have rising resistance against traditional antibiotics, and new ones are still in clinical trials (Luther et al. 2019). However, the resistance of parasites against anti-parasitic medication is also rising, even though slower than the antibiotic resistance of bacteria (Capela, Moreira, and Lopes 2019). Rising AMR is not only a problem for human health, as agriculture and livestock rearing are highly dependent on the use of antimicrobial medication as well (Hennessey et al. 2020; Yu et al. 2023). Hence, the need for drugs with new mechanisms of action is immense (Spellberg et al. 2004).

### 2.4.1 Previous drug discovery methods for *A. castellanii*

The need for new treatment against AK and invasive *A. castellanii* infections has evoked not only drug development but also investigation of new methods to test drugs against *A. castellanii*. The most commonly used screening method is based on detecting the viability of the amoeba with Trypan blue and counting the live cells with a hemocytometer (Anwar, Numan, et al. 2019; Shahbaz et al. 2020). In addition, newer techniques have been invented: staining the cells with sulforhodamine B and measuring optical density (OD) (Ortega-Rivas et al. 2016), measuring alamarBlue reduction in the culture (McBride et al. 2005), and combining computational methods to build new compounds and preliminarily test them before using alamarBlue to determine viability (Sebastián-Pérez et al. 2021). Similar techniques have also been used in the testing of compounds used clinically in other conditions (Anwar, Rajendran, et al. 2019).

## 2.4.2 Medication for eye

Medications used for eye diseases can be divided into systemic, intraocular injections, and topical drugs (Nayak et al. 2020). Due to the unique location of the eye and the straight access to its surface, topical drugs have become popular for treating conditions on the surface of the eye. Topical administration reduces the systemic side effects and thus improves the suitability to a larger variety of patients in comparison to systemic administration. However, topical drugs can lead to local disadvantageous effects, such as allergic reactions, blurring of the vision and irritation (Loftsson, Jansook, and Stefánsson 2012). It also poses challenges for the characteristics of the drug, as the eye has mechanisms, such as blinking and baseline and reflex lacrimation for removing foreign objects from the eye, including the drug (Gholizadeh et al. 2021). Many drugs have overcome these by frequent administration of medication, but new mechanisms for better adherence have also been developed, for instance, different nanotechnology-based methods which are also investigated for the possibility of penetrating deeper into the eye structures than just the surface (Akhter et al. 2022).

### 3 AIMS OF THE STUDY

The aims of this study were to enhance our knowledge of the diagnosis and treatment options of three clinically relevant parasitic infections: *Acanthamoeba keratitis*, schistosomiasis and amebiasis. My research had four specified goals:

1. Determining effective CAIs among readily known and clinically used inhibitors against *Acanthamoeba castellanii*
2. Designing a novel ultrasensitive PCR-based diagnostic method for detecting *Acanthamoeba castellanii* infections
3. Producing and characterizing recombinant  $\beta$ -CA of *Schistosoma mansoni* and studying its inhibition using CAIs
4. Producing and characterizing recombinant  $\beta$ -CA of *Entamoeba histolytica* and studying its inhibition using CAIs

All three parasites of interest are common worldwide and cause vast loss of quality-adjusted life-years, especially in areas where access to health care, clean water and sanitation is limited.

## 4 MATERIALS AND METHODS

### 4.1 Recombinant CA enzyme production (I, II, III)

CAs of the chosen parasites introduced in chapter 2 were produced recombinantly in specific *Escherichia coli* cells and purified in a nickel resin column. The accuracy of the retrieved protein was confirmed with gel electrophoresis and mass spectrometry.

#### 4.1.1 Vector construction

The DNA sequences of the desired CAs were retrieved from the UniProt database ([www.uniprot.org](http://www.uniprot.org)) (Apweiler et al. 2004) and modified for protein production in *E. coli*. The coding sequence of *SmaBCA* was, however, incorrectly predicted in the databases, initially hindering recombinant protein production. Therefore, Dr. Reza Zolfaghari Emameh (PhD) and Dr. Martti Tolvanen (PhD) predicted a new sequence to enable the protein production presented in detail in publication III. Plasmid vectors were constructed in GeneArt (Invitrogen, Regensburg, Germany) with Gateway cloning using a specific plasmid vector, pBVboostFG (Laitinen et al. 2005). pBVboostFG is a plasmid vector modified from pBVboost for a wide range of expression studies on bacterial, insect and mammalian proteins. Airene et al. constructed pBVboost using the pFastbac1 donor vector as the backbone (Invitrogen, Carlsbad, CA, USA) and replaced ampicillin with the *Bacillus subtilis* levansucrase gene (*SacB*) from the pDNR-LIB vector (BD Biosciences Clontech Palo Alto, CA, USA) (Airene et al. 2003). Further modifications to the plasmid vector were applied by Laitinen et al. to enable recombinational cloning (Figure 9). The bacteriophage lambda-derived recombination cassette was cloned into pBVboost to create the pbVboostFG plasmid vector (Laitinen et al. 2005).



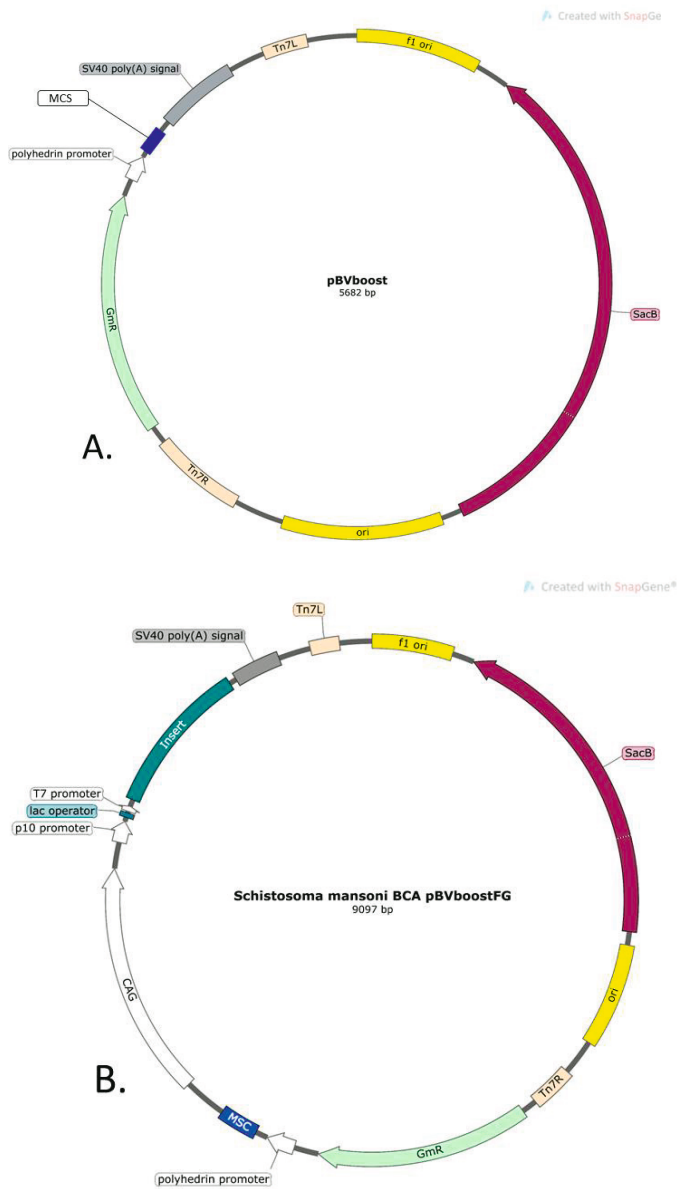


**Figure 9.** A. Plasmid map of pBVboost according to Airenne et al. 2003 B. Plasmid map of pBVboostFG with the insert containing *SmaBCA* (Urbanski et al. 2020). The plasmid for the production of EhiCA was constructed similarly, with the difference in the CA sequence. GmR, gentamycin resistance gene; ori, origin of replication; SacB, *Bacillus subtilis* levansucrase gene. Plasmid figures were created with SnapGene 5.3.1 software (www.snapgene.com).

The implemented DNA insert was specifically designed for ligation to the pBVboostFG backbone by Professor Vesa Hytönen and Dr. Linda Urbanski (Urbanski et al. 2020). The insert consists of 5' – attL1 – Shine-Dalgarno – Kozak – Met-Ser-Tyr-Tyr – 6 × His – Asp-Tyr-Asp-Ile-Pro-Thr-Thr – Thrombin cleavage site – *Sma*BCA / *Ebi*CA – 2 × stop codon – attL2 – 3', as described in Urbanski et al. 2020. Shine-Dalgarno is a prokaryotic and Kozak is a eukaryotic protein translation initiation site, and their purpose is to enhance and maximize the probability of producing the recombinant amino acid chain in bacterial cells. Histidine (His-tag) is used in protein purification because it binds to nickel resin, allowing the efficient purification of recombinant protein in column chromatography. For the removal of the His-tag from the protein product, the thrombin cleavage site (Lys-Val) between the His-tag and the desired CA is essential.

#### 4.1.2 Production of recombinant protein

The obtained plasmid vectors were transformed into deep-frozen *E. coli* BL21 Star™ (DE3) cells (Invitrogen). The cells that were slowly thawed on ice to prevent any cell damage were combined with plasmid solution. The heat shock was started with incubation of the cell-plasmid suspension on ice for 30 min. After the incubation, the tube was submerged in +42°C water for 30 seconds and transferred on ice for two minutes. 125 µl of S.O.C. Medium (Invitrogen) was added to the suspension, and the suspension was incubated at +37°C with shaking at 200 rpm for 60 minutes. LB broth (Sigma–Aldrich, St. Louis, MO, USA) culture plates were prepared by adding 50 µl of gentamicin (Sigma–Aldrich) and spreading it evenly on the plate. The suspension was distributed equally on the plate and incubated overnight. One colony was collected from the plate and placed in 5 ml LB broth with 1:1000 gentamicin to perform preculturing. Storage stocks were prepared from this first preculture and stored in a –80°C liquid nitrogen freezer. The consequent precultures were from these storage stocks.

The preculture for recombinant *Sma*BCA was prepared differently from the above. Either 1:100 glycerol (VWR International, Radnor, PA, USA) or 1:100 glucose (Sigma–Aldrich) was added, both proven to be equally effective in reducing the number of impurities (Kopp et al. 2018). Production was performed manually in flasks in LB broth with 1:1000 gentamicin and 1:100 either glucose or glycerol at +37°C at 200 rpm. With an OD [measured with Fisher Scientific Colorimeter Model 45 (WA12173), Fisherbrand, Thermo Fisher Scientific, Waltham, MA, USA] of 0.4–

0.5, 1:1000 of 1 M isopropyl- $\beta$ -D-thiogalactopyranoside (IPTG, Thermo Fisher Scientific) was added to the culture flasks to induce recombinant protein production. IPTG binds to LacI, which normally represses the *lac operon*, but the inhibition of LacI activates the *lac operon* and promotes recombinant protein production (Marbach and Bettenbrock 2012). Culturing was continued until the next morning leading to a complete incubation and production time of 24 h. The production was terminated with centrifugation to retrieve the cell pellet at  $5,000 \times g$  for 20 min.

The production of recombinant EhiCA was conducted with a fermenter (Infors HT, Bottmingen, Switzerland) by the Tampere facility of Protein Services (PS) with the pO-stat fed-batch protocol (Määttä et al. 2011) with some alterations as described in publication I.

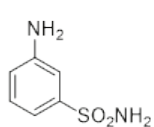
### 4.1.3 Purification of recombinant protein

The cell pellet collected from the culture flask or fermenter was diluted into a binding buffer of [50 mM  $\text{Na}_2\text{HPO}_4$  (Sigma–Aldrich), 0.5 M NaCl (VWR International), 50 mM imidazole (Sigma–Aldrich), and 10% glycerol (only for EhiCA), pH 8.0]. Then with an EmulsiFlex-C3 (AVESTIN, Ottawa, Canada) homogenizer, the suspension was homogenized to create a lysate that was centrifuged at  $13,000 \times g$  at  $+4^\circ\text{C}$  for 15 minutes to retrieve the supernatant. Nickel resin [HisPur™ Ni-NTA Resin (Thermo Fisher Scientific)] was mixed in the solution and the protein was allowed to bind to the resin at room temperature with a magnetic stirrer for 2 hours. For EhiCA, the resin was washed with binding buffer EMD Millipore™ vacuum filtering flask (Merck, Kenilworth, NJ, USA) and filter paper (pore size 2  $\mu\text{m}$ , Whatman™, Maidstone, UK) and collected into an empty column (Maxi Columns, G-Biosciences, St. Louis, MO, USA). SmaBCA was washed with a few alterations to the protocol of EhiCA: 15 x 25 ml of washing buffer [50 mM  $\text{Na}_2\text{HPO}_4$ , 0.5 M NaCl, 50 mM imidazole, and 20% glycerol, pH 8.0] and then the glycerol was washed off with 10 x 25 mL of binding buffer, both in a vacuum filtering flask. The nickel resin was collected into a column, similar to EhiCA. Elution buffer was composed of 50 mM  $\text{Na}_2\text{HPO}_4$ , 0.5 M NaCl, and 350 mM imidazole, pH 8.5 for SmaBCA and pH 7.0 for EhiCA with the addition of 10% glycerol. Both of the recombinant proteins were rewashed; SmaBCA with the same protocol as described and EhiCA with the change of resin to cobalt resin [TALON® Superflow™ cobalt resin (GE Healthcare, Chicago, IL, USA)].

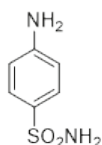
Retrieved proteins were subjected to 12% sodium dodecyl sulfate–polyacrylamide gel electrophoresis (SDS–PAGE) under reducing conditions. Precision Plus Protein™ Standards Dual Color (Bio-Rad Laboratories, Inc., Hercules, CA, USA) was used as a standard molecular weight (MW) marker. The bands and marker were visualized on the gel with PageBlue™ Protein Staining Solution (Thermo Fisher Scientific) with 30 min incubation in the stain at room temperature and removal of the excess stain with distilled water. The bands were confirmed to be the desired recombinant with mass spectrometry performed by the Tampere facility of Protein Services.

## 4.2 CA kinetics and inhibition measurements (I, II, III)

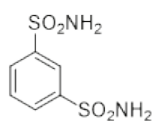
The buffer of EhiCA and SmaBCA was changed to 50 mM TRIS (VWR International), pH 8.5 with 10 kDa Vivaspin® Turbo 15 centrifugal concentrators (Sartorius™, Göttingen, Germany) prior to kinetics and inhibition measurements. The measurements were conducted with an Sx.18Mv-R Applied Photophysics stopped-flow instrument (Oxford, UK) (Khalifah 1971) at Università degli Studi di Firenze (Florence, Italy) under the supervision of Professor Claudiu Supuran with the protocol described in publication I and Berrino et al. 2017 for EhiCA and SmaBCA, respectively. The tested compounds were sulfonamide and anion derivatives (Figure 10).



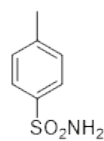
3-amino-benzenesulfonamide (1)



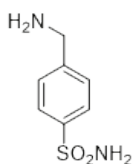
4-amino-/4-hydroxybenzenesulfonamide (2)



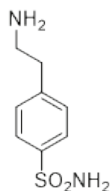
1,3-disulfamoyl benzene (3)



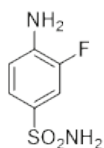
4-methyl-benzenesulfonamide (4)



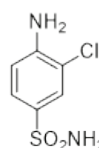
4-aminomethyl-benzenesulfonamide (5)



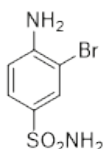
4-aminoethyl-benzenesulfonamide (6)



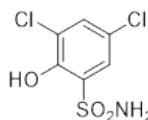
3-fluoro-4-amino-benzenesulfonamide (7)



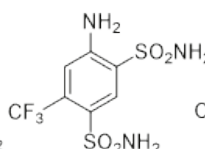
3-chloro-4-amino-benzenesulfonamide (8)



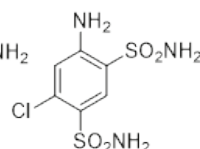
3-bromo-4-amino-benzenesulfonamide (9)



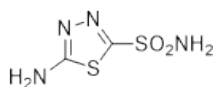
1,3-dibenzene-sulfonamide (10)



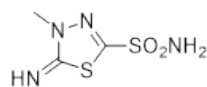
4-amino-6-trifluoromethyl-benzene-1,3-disulfonamide (11)



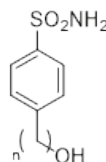
4-amino-6-chloro-benzene-1,3-disulfonamide (12)



5-amino-1,3,4-thiadiazole-2-sulfonamide (13)

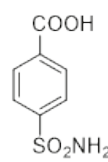


4-methyl-5-imino-1,3,4-thiadiazoline-2-sulfonamide (14)

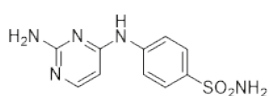


n=0, 4-amino-/4-hydroxymethyl-benzenesulfonamide (15);

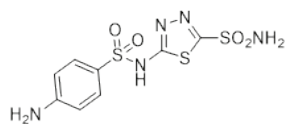
n=1, 4-hydroxymethyl-benzenesulfonamide (16);



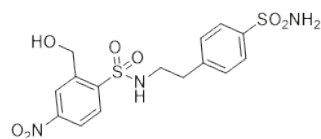
4-carboxy-benzenesulfonamide (18)



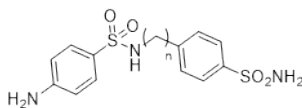
4-(2-amino-pyrimidin-4-yl)-benzenesulfonamide (19)



5-((4-aminophenyl)sulfonamido)-1,3,4-thiadiazole-2-sulfonamide (20)



4-(2-hydroxymethyl-4-nitrophenyl)sulfonamidoethyl-benzenesulfonamide (21)



n=0, 4-amino-N-(4-sulfamoylphenyl)benzenesulfonamide (22);

n=1, 4-(4-sulfanilyl-aminomethyl)-benzenesulfonamide (23);

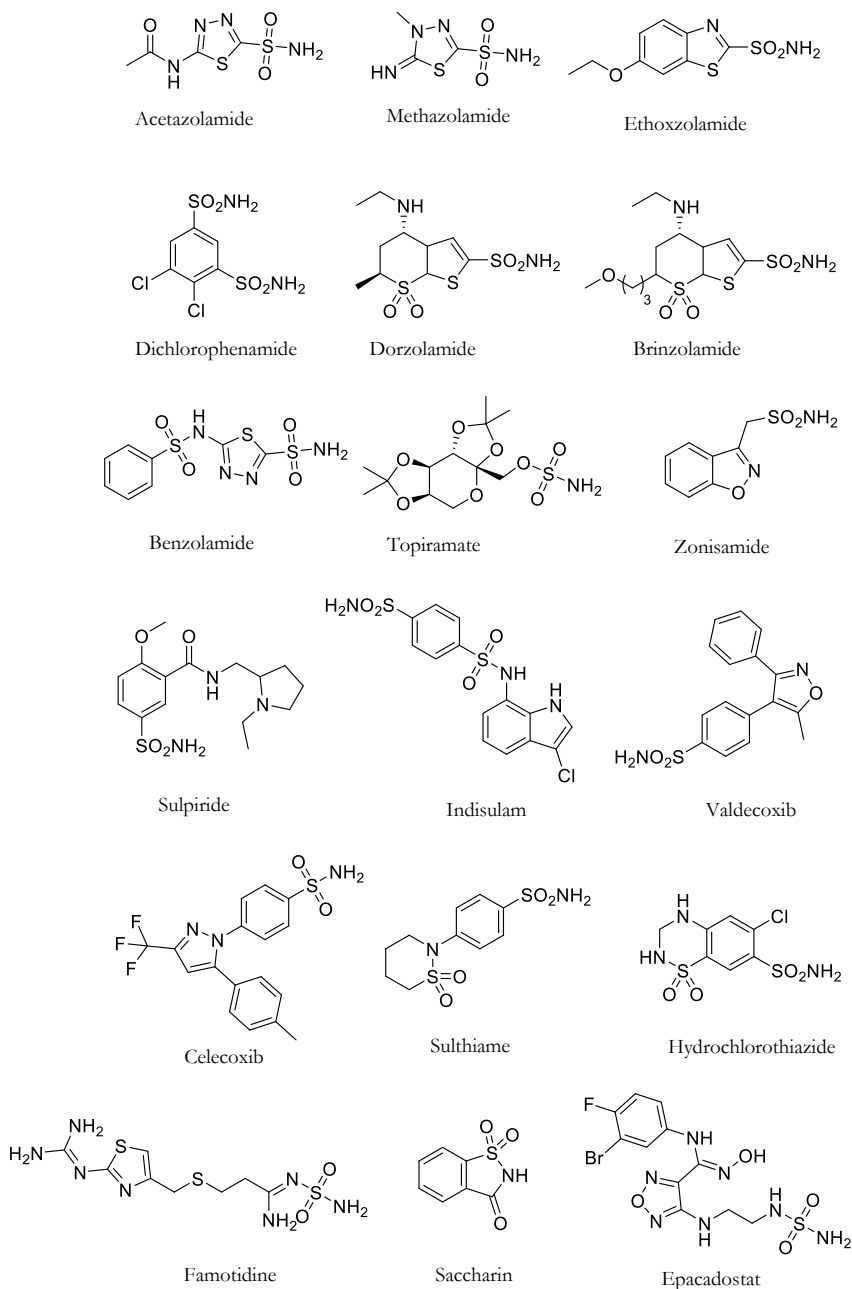


**Figure 10.** Chemical structures, names and numbers of sulfonamide and anion inhibitors. Figure modified from publication III. Figure begins already at page 51.

### 4.3 *Acanthamoeba castellanii* culture (IV, V)

We created an *Acanthamoeba castellanii* culture to be used in the development of a diagnostic method for AK and the creation of a drug screening assay. The *Acanthamoeba castellanii* (ATCC ® 30010™) strain, isolated from soil in the Pacific Grove (CA, USA) in 1957, was provided by the American Type Culture Collection (Manassas, Virginia, US).

Cells were shipped in frozen ampules, which were thawed in a water bath at +35°C for 2-3 minutes and then immediately aseptically transferred to 5 ml of peptone yeast glucose (PYG) medium with additives in T 25 tissue culture flasks (Thermo Fischer Scientific, Waltham, MA, USA) (Table 1). The axenic amoeba culture was fed with glucose. The flasks were incubated at +25°C without shaking or rotation.

**Table 1.** Composition of PYG medium with additives. The additives were added to proteose peptone-yeast solution, and the volume was set to 1000 ml and pH to 6.5. The acquired solution was autoclaved at +121°C. Glucose was filter sterilized and added to the autoclaved solution.

PYG medium	Amount (total volume 1050 ml)
Proteose peptone	20.0 g
Yeast extract	1.0 g
DI Water	900.0 ml
<u>Additives:</u>	
0.05 M CaCl <sub>2</sub>	8.0 ml
0.4 M MgSO <sub>4</sub> x 7 H <sub>2</sub> O	10.0 ml
0.25 M Na <sub>2</sub> HPO <sub>4</sub> x 7 H <sub>2</sub> O	10.0 ml
0.25 M KH <sub>2</sub> PO <sub>4</sub>	10.0 ml
Na citrate x 2 H <sub>2</sub> O	1.0 g
0.005 M Fe(NH <sub>4</sub> ) <sub>2</sub> (SO <sub>4</sub> ) <sub>2</sub> x 6 H <sub>2</sub> O	10.0 ml
2 M Glucose*	50.0 ml

\* added after autoclave

The culture was maintained twice a week by removing the old medium and replacing it with 5 ml of fresh medium. To prevent contamination, the culture was handled aseptically, and the purity of the culture was checked with a microscope (40x objective) to find any signs of contamination. To ensure the continuity of the culture

for future experiments, storage stocks were prepared according to the cell provider's instructions. The culture was multiplied by transferring 500 µl of medium from a previous culture flask to a new flask with 5 ml of fresh medium.

#### 4.4 Inhibition of *Acanthamoeba castellanii* (V)

For testing inhibitors against *A. castellanii*, we developed a drug screening assay. It is divided into two phases: inhibitor assay and excystation assay. First, we tested the viability of trophozoites in the presence of an inhibitor and the survival ability of cysts after the inhibitor in a biphasic inhibitor assay. Second, with a separate excystation assay, we tested the excystation ability of cysts in the presence of an inhibitor.

We selected six different inhibitors: five CAIs and propamidine (Brolene 0.1%, Sanofi, Paris, France), which is already in clinical use in treating AK. CAIs in this study were acetazolamide (Diamox 100 mg/ml, Mercury Pharma, Croydon, United Kingdom), brinzolamide (Azopt 10 mg/ml, Novartis, Basel, Switzerland), dorzolamide (Sigma–Aldrich), ethoxzolamide (Sigma–Aldrich) and Fc14-584B (Aspatwar et al. 2017). All, except Fc14-584B and ethoxzolamide, are in clinical use. We conducted a dilution series: 10-fold for acetazolamide, dorzolamide and brinzolamide, 2-fold for propamidine and Fc14-584B, and 2- and 5-fold for high and low concentrations of ethoxzolamide, respectively.

All assays were performed in 96-well plates (Corning Inc, Corning, NY, USA) with 1,000 cells (cysts or trophozoites) per well with a volume of cell-medium-inhibitor solution of 240 µl. For each inhibitor and each assay, there were two adjacent plates with a minimum of 3 wells (range from 3 to 8) of the same concentration of CAI in one plate.

The inhibitor assay was biphasic: inhibitor part and cyst survival part. First, trophozoites were carefully detached with a cell scraper (Sarstedt Inc., Newton, MA, USA) from the surfaces of the culture flask and mixed in the correct proportion with the inhibitor to conduct the cell-medium-inhibitor solution. It was pipetted into 96-well plates to form one plate for each desired time point (24, 48 and 72 hours). The plates were incubated at +25°C without shaking or rotation. After reaching their time points, the contents of the wells were transferred into an empty well and 50 µl of fresh medium was added to each well. These new wells constituted the cyst survival part of the assay. The emptied plates were analyzed as described later.



The cyst survival assay lasted for 5 days, after which the wells were emptied for analysis. 5 days was chosen because it takes approximately 12-36 hours for the cysts to transform back to active trophozoites (Mattar and Byers 1971; Chávez-Munguía et al. 2005) and 8-24 hours for one mitosis (Khan 2006); therefore, we wanted to assure that all infectious and viable cysts have the opportunity to excystate and start dividing.

In the excystation assay, the amoeba culture was grown above peak density to enhance cyst formation. Inhibitors and the cysts were added to 96-well plates, similar to the inhibitor assay. We incubated the plates under the same growth conditions (+25 °C, no shaking) as previously described for 72 hours. Then the plates were emptied and moved on to staining.

The empty 96-well-plates from both inhibitor and excystation assays were fixed with 100 µl of methanol (Sigma–Aldrich) per well at room temperature for 15 min. The plates were reversed to remove methanol and allowed to dry for at least 2 hours. Then, 100 µl of 0.1% crystal violet solution (Merck) was added to each well and the wells were shaken at 300 rpm for 20 minutes. Crystal violet stains the proteins and DNA of the cells (Feoktistova, Geserick, and Leverkus 2016), and the stain is diluted for absorbance measurement; thus, the more cells there are, the more bind to the stain, leading to a more intense color after dilution and higher absorbance. We diluted crystal violet with 100 µl of 10% acetic acid (Sigma–Aldrich) in each well at 300 rpm for 15 minutes (Figure 11). Absorbance was measured by analyzing the absorbance of light at 590 nm wavelength with Wallac 1420 Manager (PerkinElmer, Wallac oy, 1997-2005, version 3.00) at VICTOR3™ 1420 Multilabel Counter (PerkinElmer, Waltham, MA, USA).

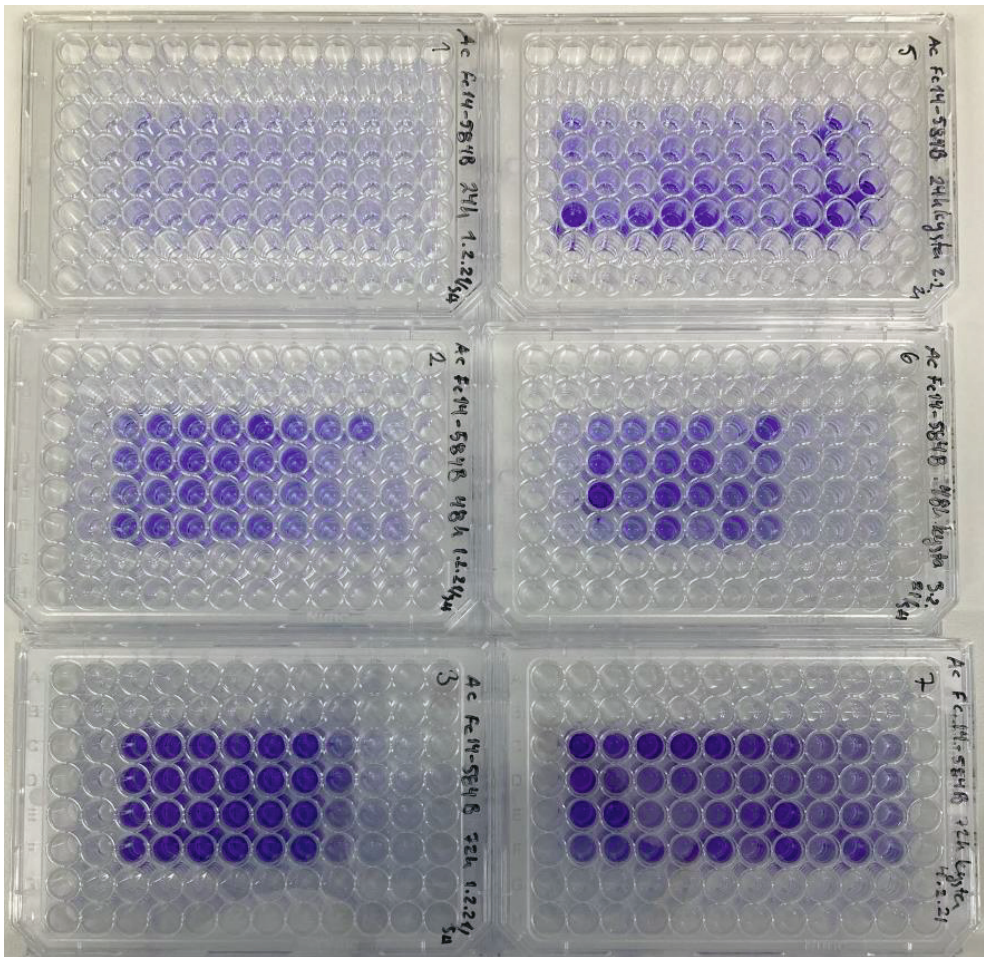


**Figure 11.** 96-well plate from inhibitor assay stained with crystal violet and ready for colorimetric analysis. The inhibitor presented as an example is Fc14-584B. The plates are 24 hours, 48 hours and 72 hours from top to bottom, inhibitor assay on the left-hand and cyst survival on the right-hand side.

#### 4.5 Cell sample preparation (IV)

In order to run PCR, cells samples were prepared with the following method. For genomic DNA isolation, amoebae were detached from the culture flask and centrifuged at  $1,500 \times g$  for 5 min. The retrieved cell pellet was handled according to the standard protocol for cultured cells by NucleoSpin Tissue (Macherey-Nagel, Düren, Germany). The concentration was determined with a NanoDrop™ One Spectrophotometer (Thermo Fisher Scientific). The concentration varied between

22.1-455.6 ng/ $\mu$ l at different isolation times, and samples were diluted into appropriate concentrations for developing traditional PCR and qRT-PCR. Human genomic DNA was used as a control to verify the absence of nonspecific binding of the primers. Furthermore, the samples are human samples, so the human genome will be present; thus, the human genome was isolated from a healthy volunteer's buccal mucosa with the same protocol as the DNA of *A. castellanii*, resulting in a concentration of 8.3 ng/ $\mu$ l.

To have faster and fewer amoebae-requiring methods, we wanted to bypass the DNA isolation step. We collected amoeba samples with different numbers of amoebae (from one cyst/trophozoite to hundreds of them) with a borosilicate needle (created with P-97 Flaming/Brown Micropipette Puller, Sutter Instruments Company, Novato, California, USA) under vision control with a microscope. The collected sample was transferred into 100  $\mu$ l DirectPCR Lysis Reagent (Tail) (Nordic BioSite, Täby, Sverige). 3  $\mu$ l Proteinase K (20 mg/ml, Macherey-Nagel) was added to the solution, and the solution was incubated at +55°C at 200 rpm for 30 minutes to produce lysate. The lysis reaction was ended using a heating block (+85°C for 50 minutes), and the lysate was ready for PCR.

## 4.6 Development of traditional PCR method (IV)

Primers were designed using the NCBI Primer-BLAST tool (<http://www.ncbi.nlm.nih.gov/tools/primer-blast/>), and the most promising 21 primer pairs were selected and manually optimized to enhance the success rate. They were tested in a multilevel process and every step ruled out nonfunctioning primers and only the best ones continued to the next phase. Initially, the primer pair count against different CA genes of *A. castellanii* ranged from one to six per gene (Table 2), but finally, only three pairs against two different genes were found to recognize only one cyst or trophozoite from the sample.

In the first phase reactions, we used isolated genomic DNA as a template and gradually lowered the concentration from 46.7 ng/reaction to 2.3 ng/reaction. The sequences were confirmed with Sanger sequencing by the Tampere Genomics Facility and the primers producing amplicons with incorrect sequences were excluded.

In the second phase, we used lysate as the template and optimized the reaction to achieve one amoeba sensitivity (Table 3). The reaction product was run on a 1.6%

agarose gel (Meridian Bioscience Inc., Cincinnati, OH, USA) at 105 V for 60 min to visualize the results with Image Lab™ Software (version 6.0, 2017, Bio-Rad Laboratories Inc., Hercules, CA, USA) with the GelGreen protocol with default settings except for inverted colors and cropped image windows.

**Table 2.** The initial primer pairs for the development of the PCR-based diagnostic method. The final three pairs functioning in the method are underlined.

Primer pair	Sequence (5' – 3')	Target gene (Entry ID)	Product length (bp)
<b>bCA_1</b>	<u>F: AAACATTGCCAACACGGTCCG</u> <u>R: GGTCAGAGATCGTACGCCAG</u>	<i>miBCA (L8GR38)</i>	326
<b>bCA_2</b>	<u>F: CTGGCGTACGATCTCTGACC</u> <u>R: AAGGGTCTCTACCTCGGAC</u>	<i>miBCA (L8GR38)</i>	332
<b>bCA_3</b>	F: TTCCTAATGACGCGGACAGG R: GCAAAGGGTCTCCTACCTCG	<i>miBCA (L8GR38)</i>	249
<b>bCA_4</b>	F: AAAGCTGGTACTCACCTGCC R: AGGTAGTACTCGGCCGTCAT	<i>cpBCA (L8GLS7)</i>	476
<b>bCA_5</b>	F: ATCTTTGACGAGGGCATGGG R: AGAAGGAGGTGTACGGACCT	<i>cpBCA (L8GLS7)</i>	623
<b>bCA_6</b>	F: TAATCTGGGTCGGTTCGTGC R: TGGGAGAAGGAGGTGTACGG	<i>cpBCA (L8GLS7)</i>	418
<b>bCA_7</b>	F: CCGGAGCTCATCTTTGACGA R: GAGAAGGAGGTGTACGGACC	<i>cpBCA (L8GLS7)</i>	633
<b>bCA_8</b>	F: CGAACCCTGTATGGGCTGT R: GAGCGAAAGCGATGAGGGAT	<i>tmBCA (L8H861)</i>	310
<b>bCA_9</b>	F: CCTCCCTGGTTGATTCCTCGG R: CCGTCTGATGAGCCACTTC	<i>tmBCA (L8H861)</i>	499
<b>bCA_10</b>	F: CGGTACCCTACATTCCTCCGA R: CACCAGAGCTGAGGCAGTAG	<i>tmBCA (L8H861)</i>	352
<b>bCA_11</b>	F: CGTCAGGTACTCCATCAGGG R: GGCAGGATCTTAGCCACGAG	<i>tmBCA (L8H861)</i>	358
<b>bCA_12</b>	F: GTGTGACGTGGAACCTGCTG R: GCGAAAGCGATGAGGGATAGA	<i>tmBCA (L8H861)</i>	395
<b>bCA_13</b>	F: CAGTGTGACGTGGAACCTGTC R: GAGCGAAAGCGATGAGGGATA	<i>tmBCA (L8H861)</i>	399
<b>aCA_1</b>	F: GTGATACCACGCAACGCATC R: CCAACCAACACACACACGAC	<i>aCA (L8GPJ9)</i>	472
<b>aCA_2</b>	F: TTGCAAGTTCATCAGCACGC R: TCTTTGGGTAGGAAAGCCCC	<i>aCA (L8H518)</i>	476
<b>aCA_3</b>	F: CACACCTCGAAGAAGCAGGT R: GAAAGGGGTGGGTACCGTG	<i>aCA (L8GXK3)</i>	440
<b>aCA_4</b>	F: CGGTACCACCCCTTTTCCTC R: CCACGAAGATCCAGCCTAGC	<i>aCA (L8GXK3)</i>	326
<b>gCA_1</b>	<u>F: TGCGACATGTAGGACGGAAC</u> <u>R: TGGGCGATGAAAAGATGGACG</u>	<i>gCA (L8HK20)</i>	671
<b>gCA_2</b>	F: GATCGTTGGCCACTGGGTTA R: TGACAAAAAGCTGCGTGTGG	<i>gCA (L8HK20)</i>	645
<b>gCA_3</b>	F: GCCTGTACGATAAGCAGCCT R: GAACGATAACAACGCGGGG	<i>gCA (L8GFM8)</i>	579
<b>gCA_4</b>	F: GTGGGCAAGAAGAGCTCCAT R: GCACACGTACGCCACTGTAT	<i>gCA (L8GFM8)</i>	419

**Table 3.** A. The final PCR mix composition. B. The final PCR protocol for the diagnostic tool.

**A.**

Reaction mix components	Volume ( $\mu$ l)
2 x Phusion Flash High Fidelity	10
Forward primer (10 $\mu$ M)	1
Reverse primer (10 $\mu$ M)	1
Nuclease-free H <sub>2</sub> O	6
Lysate	2
<b>Total</b>	<b>20</b>

**B.**

Cycle step	Temperature ( $^{\circ}$ C)	Time (s)
1. Initial denaturation	+ 98	10
2. Denaturation	+ 98	1
3. Annealing	+ 67	5
4. Extension	+ 72	15
5. Final extension	+ 72	60
38 cycles from 2. to 4.		

## 4.7 Development of qRT–PCR method (IV)

For qRT–PCR, the amplicon size of 50-150 bp is commonly recommended and by the manufacturer of PowerUp™ SYBR™ Green Master Mix (Applied Biosystems™, Thermo Fischer Scientific), which we used as a master mix in our reaction. Hence, the previously designed primers for traditional PCR produce amplicons that are too long (326 bp, 332 bp and 671 bp). Therefore, new primers were designed with the NCBI Primer-BLAST tool (<http://www.ncbi.nlm.nih.gov/tools/primer-blast/>) and the best primers against

both *mitBCA* (UniProt entry ID L8GR38) and *gCA* (UniProt entry ID L8HK20), which were the gene targets in traditional PCR, were manually selected (Table 4). Köhler et al. compared different reference genes (RGs) used in qRT-PCR with the result of showing 18 s rRNA gene and hypoxanthine-guanine phosphoribosyltransferase to have advantages compared to others in different experimental conditions (Köhler et al. 2020). Thus, we selected the primer pair 18S900 as a reference gene, according to the recommendation (table 4) (Köhler et al. 2020).

**Table 4.** Primers used in qRT-PCR.

Primer pair	Sequence (5' – 3')	Target gene (Entry ID)	Product length (bp)
<b>qgCA_1</b>	F: CAACAAGCACACTACGCTGG R: GTCATACCAGACGGAGGCAC	<i>gCA</i> (L8HK20)	130
<b>qbCA_1</b>	F: GCAGGAACCTCAAGGACGAA R: GCTTACGGCAGCAGTGTITTT	<i>mitBCA</i> (L8GR38)	128
<b>18S900 (RG)</b>	F: GCCCAGATCGTTTACCGTGA R: CATTACCCTAGTCCTCGCG	<i>18s rRNA</i> (L8GGJ8)	148

F, forward primer; R, reverse primer; RG, reference gene

We conducted qRT-PCR in a MicroAmp™ Optical 96-Well Reaction Plate with Barcode (Applied Biosystems™, Thermo Fischer Scientific) with the reaction mix shown in Table 5. Water was used as a no-template control, and human DNA isolated from the buccal mucosa of a healthy volunteer was used as a negative control. The amount of amoeba DNA varied between 0.001 ng and 100 ng per well. qRT-PCR was performed with a QuantStudio 12K Flex Real-Time PCR System (Applied Biosystems™, Thermo Fischer Scientific) with the protocol presented in Table 5.

## 4.8 Data analysis

### 4.8.1 Statistical analyses (V)

The absorbance results from the inhibitor and excystation assays were collected in Excel format and then transferred to GraphPad Prism (1992-2020 GraphPad Software, LLC, version 9.0.0). Absorbance data were collected at 24 h, 48 h and 72 h timepoints. Differences between concentration groups were evident only at the 72

h timepoint, which was the reason that statistical analysis was conducted at that point only. Unpaired t-tests were performed between the control curve (0) and the concentration under analysis, and figures were drawn with GraphPad Prism.

**Table 5.** A. The reaction mix composition used in qRT–PCR. B. The final qRT–PCR protocol used in the diagnostic tool.

**A.**

Reaction mix components	Volume (μl)
PowerUp™ SYBR™ Green Master Mix	7.5
Forward primer (10 μM)	0.5
Reverse primer (10 μM)	0.5
Nuclease-free H <sub>2</sub> O	5.5
Sample*	1
<b>Total</b>	<b>15</b>

\* isolated amoeba DNA, H<sub>2</sub>O or human DNA

**B.**

Cycle step	Temperature (°C)	Time (s)
1. Initial denaturation	+ 60	120
2. Denaturation	+ 95	120
3. Annealing	+ 95	15
4. Extension	+ 62	60
5. Infinite stage	+ 4	∞
40 cycles from 3. to 4.		



## 4.8.2 Bioinformatic analyses (I, II, V)

For the construction of plasmid for recombinant protein production, *EbiCA* required only the standard modifications executed at GeneArt (Invitrogen), but *SmaBCA* proved to require more extensive modifications. GeneArt provided the plasmid vector to produce SmaBCA as requested. However, even with extensive attempts to produce the recombinant protein, we were unsuccessful in retrieving the desired outcome. With closer analysis, Dr. Reza Zolfaghari Emameh found Rho-independent termination sites that were revealed in the mRNA sequence but not in the coding gene sequence. Consequently, he made single-nucleotide alterations to prevent immature mRNA production without any mutations to the amino acid sequence. Dr. Martti Tolvanen analyzed the sequence of SmaBCA against other *Schistosoma* species  $\beta$ -CAs, and the C-terminus was found to be incomplete. He made a prediction of the correct C-terminal sequence, which was combined with the single mutations, and we received a functioning plasmid vector from GeneArt. Later, in 2019, a new version of *SmaBCA* was updated in UniProt (UniProt ID A0A3Q0KBP5) which has only one amino acid difference from our sequence (N264D) probably due to the data retrieval method, e.g., we used genomic data while in the database, the transcriptomic data was used. A more detailed description of the alterations of the sequence is in publication III.

A 3D-model of SmaBCA was constructed with AlphaFold by Dr. Martti Tolvanen. The  $\beta$ -CA of *Pisum sativum* was used as a template for the model as described in detail in publication III. Multiple sequence alignment comparing our new sequence for SmaBCA and three homologs of other *Schistosoma* species was performed with Clustal Omega (<https://www.ebi.ac.uk/Tools/msa/clustalo/>) (Sievers et al. 2011; Madeira et al. 2022) and visualized with ESPript 3.0 (<https://esprict.ibcp.fr/ESPript/cgi-bin/ESPript.cgi>) (Robert and Gouet 2014). A total of 162 sequences of metazoan  $\beta$ -CAs were aligned and constructed as a sequence logo using Berkeley WebLogo version 3.7.12 (<https://weblogo.threeplusone.com/>) (Crooks et al. 2004) as described in detail in publication III. MSA of selected protozoan and bacterial  $\beta$ -CA sequences with SmaBCA was performed with Clustal Omega (<https://www.ebi.ac.uk/Tools/msa/clustalo/>) (Sievers et al. 2011; Madeira et al. 2022). Both the 3D-model and MSAs were constructed by Dr. Martti Tolvanen.

We were interested if *A. castellanii* even expresses its CAs, a point crucial for the inhibition studies. We obtained RNA expression data from the pre-and postinfectious state of *A. castellanii* with *Protochlamydia amoebophila* (König et al. 2017).

The data management and analyses were performed with the help of Mr. Harlan Barker. We only analyzed the preinfectious data as we were interested in the basal expression of different proteins. There was one value of expression for each gene in preinfectious state. Of the eight CAs in the genome of *A. castellanii*, five were found in the transcriptional data indicating that they are transcribed into mRNA, and possibly translated into the amino acid chain. Mr. Harlan Barker transformed the reads per kilobase million (RPKM) into transcripts per million (TPM) with the formula presented in S. Zhao, Ye, and Stanton 2020 to make the results comparable with other datasets. In the analysis of all genes, we show the mean expression value of the genes, and with an error bar the maximum expression. The analysis and graphs were created with GraphPad Prism (1992-2020 GraphPad Software, LLC, version 9.0.0).

Many databases were used in the search for information on the characteristics of the CAs of the parasites. As primary sequence databases, we used UniProt (<https://www.uniprot.org/>) for amino acid sequences and NCBI (The National Center for Biotechnology Information, <https://www.ncbi.nlm.nih.gov/>) for DNA and RNA sequences supplemented with BLAST searches with Ensembl (<https://www.ensembl.org/index.html>) and for SmaBCA also WormBase (<https://wormbase.org/#012-34-5>). Predictions of the subcellular locations of the CAs were performed with DeepTMHMM (<https://dtu.biolib.com/DeepTMHMM/>) (Hallgren et al. 2022) to aid and predict the characteristics of recombinant proteins in production.

## 4.9 Ethics (I–V)

Pathogenic organisms are graded with biosafety level (BSL) ranking according to their evaluated biohazardous potential. The ranking is four-scale, with 1 being the lowest and 4 being the highest stage. The organisms in our experiments, *E. coli* and *A. castellanii*, are graded as BSL 1 and BSL 2 –level organisms, respectively. The cell provider ranks *A. castellanii* as BSL 1 because it is not from a human sample, but the Finnish legislation grades it BSL 2 as it is potentially harmful to humans. Fundamental safety and laboratory instructions were followed when working with *E. coli*; nevertheless, working with *A. castellanii* was more constricted, containing a limited number of trained personnel and special waste handling to successfully prevent contamination to the environment as well as the infections of personnel.

The organisms we used, *E. coli* and *A. castellanii*, are not covered by test animal licenses; thus we were not obliged to apply for them for our experiments.

## 5 RESULTS

### 5.1 Recombinant CA enzymes

We produced recombinant  $\beta$ -CA enzymes of *S. mansoni* (SmaBCA) and *E. histolytica* (EhiCA) that were discovered to be doublet polypeptides with molecular weight 21/25 kDa and 25/28 kDa, respectively. SmaBCA retained the polyhistidine-tag, in contrast to EhiCA, where it was cleaved by thrombin treatment. The purified SmaBCA showed altogether six polypeptide bands in the gel electrophoresis and EhiCA four (Figure 10), all confirmed with mass spectrometry (data not shown).

The original genomic sequence of SmaBCA had inaccuracy in its predicted form in the Uniprot database. By comparing multiple sequences Dr. Martti Tolvanen made a new corrected prediction with alteration to the C-terminus of the sequence. Protein production was successful with these alterations combined with other modifications designed by Dr. Reza Zolfaghari Emameh to the coding sequence to prevent Rho-independent termination site formation in a prokaryotic cell. These protocols were described in the earlier chapter in more detail.

The kinetics of the produced recombinant SmaBCA and EhiCA were measured by our collaborators in Professor Claudiu Supuran's laboratory. The results were compared to the activity of human CA I and II (Table 6).

Multiple CAIs belonging to anion and sulfonamide groups were tested against SmaBCA and EhiCA (Table 7). The most efficient compounds were 4-(2-amino-pyrimidin-4-yl)-benzenesulfonamide (compound 19) and 4-hydroxyethyl-benzenesulfonamide (compound 17). Many CAIs were effective in the nanomolar range and most of them at micromolar or submicromolar level.

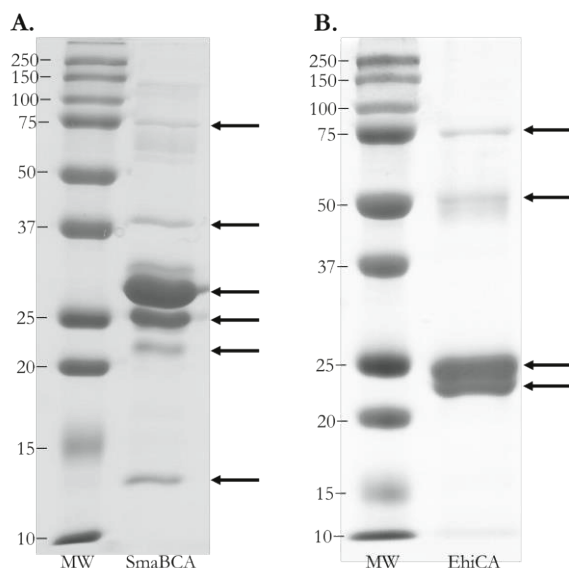


**Figure 12.** SDS-PAGE images presenting SmaBCA and EhiCA. A. SDS-PAGE of SmaBCA presenting six polypeptide bands: 13 and 22 kDa representing degraded forms, double band of 25/28 kDa as the main SmaBCA protein, and 38 and 75 kDa presumably oligomeric states. B. SDS-PAGE of EhiCA illustrating four polypeptide bands: 21/25 kDa representing the main forms and 50 and 75 kDa supposedly oligomers. Left lanes are standard molecular weight (MW) markers in kDa. All polypeptides mentioned above were isolated and confirmed to represent correct proteins by mass spectrometry (data not shown).

**Table 6.** Kinetic properties of SmaBCA and EhiCA. Human CA isoenzymes I and II were used for comparison. Classically, human CA I is considered moderately active, while human CA II is highly active. The activity of SmaBCA is lower than that of hCA I. The activity of EhiCA is between hCA I and hCA II. Table collected and built from publications I, II and III.

Enzyme	$k_{cat}$ ( $s^{-1}$ )	$K_m$ (mM)	$k_{cat}/K_m$	Family
SmaBCA	$1.38 \times 10^5$	5.9	$2.33 \times 10^7$	$\beta$
EhiCA	$(6.7 \pm 0.2) \times 10^5$	$7.5 \pm 0.08$	$(8.9 \pm 0.1) \times 10^7$	$\beta$
hCA I	$2.0 \times 10^5$	4.0	$5.0 \times 10^7$	$\alpha$
hCA II	$1.4 \times 10^6$	9.3	$1.5 \times 10^8$	$\alpha$

**Table 7.** Inhibition of SmaBCA and EhiCA with sulfonamides, anions and clinically used drugs. The inhibition of human CA I (hCA I) and CA II (hCA II) is presented for comparison. Data for the table were collected from publications I, II and III.

Compound	SmaBCA K <sub>i</sub> (μM)*	EhiCA K <sub>i</sub> (μM)*	hCA I K <sub>i</sub> (μM)*	hCA II K <sub>i</sub> (μM)*
1	1.830	2.263	28.0	0.300
2	2.516	6.011	25.0	0.240
3	1.556	0.951	0.079	0.003
4	0.776	0.833	78.5	0.320
5	0.788	0.567	25.0	0.170
6	0.327	0.798	21.0	0.160
7	0.872	>10	8.30	0.060
8	0.372	>10	9.80	0.110
9	0.960	>10	6.50	0.040
10	0.935	4.656	7.30	0.054
11	2.040	0.742	5.80	0.063
12	0.417	1.911	8.40	0.075
13	0.314	0.821	8.60	0.060
14	0.375	0.579	9.30	0.019
15	0.982	0.772	5.50	0.080
16	0.600	0.089	9.50	0.094
17	0.346	0.036	21.0	0.125
18	1.043	0.383	0.164	0.046
19	0.044	0.521	0.109	0.033
20	0.316	0.385	0.006	0.002
21	0.255	0.368	0.069	0.011
22	0.378	0.331	0.164	0.046
23	0.241	0.290	0.109	0.033
24	0.750	0.285	0.095	0.030

Sulpiride	0.254	>10	1.20	0.040
Indisulam (E7070)	0.812	0.822	0.031	0.015
Zonisamide	0.521	9.595	0.056	0.035
Celecoxib	0.092	>10	50.0	0.021
Valdecoxib	0.474	>10	54.0	0.043
Sulthiame	0.758	6.727	0.374	0.009
Saccharin	0.091	>10	18.540	5.959
Hydrochlorothiazide	0.918	3.402	0.328	0.290
Famotidine	0.096	NM	NM	NM
Dichlorphenamide	0.545	0.790	1.20	0.038
Epacadostat	0.092	NM	NM	NM
Acetazolamide	0.286	0.509	0.250	0.012
Methazolamide	0.210	0.845	0.050	0.014
Ethoxzolamide	0.246	0.746	0.025	0.014
Dorzolamide	0.090	6.444	50.0	0.009
ClO <sub>4</sub> <sup>-</sup>	NM	>100 000	>200 000	>200 000
Brinzolamide	0.083	3.051	45.0	0.003
Benzolamide	0.079	2.471	0.015	0.009
Topiramate	0.083	3.100	0.250	0.010
NO <sub>2</sub> <sup>-</sup>	>10 000	1 700	8 400	63 000
NO <sub>3</sub> <sup>-</sup>	2 270	3 600	7 000	35 000
HCO <sub>3</sub> <sup>-</sup>	7 840	280	12 000	85 000
CO <sub>3</sub> <sup>2-</sup>	740	2 400	15 000	73 000
HSO <sub>3</sub> <sup>-</sup>	4 260	11 500	18 000	89 000
SO <sub>4</sub> <sup>2-</sup>	3 720	21 600	63 000	>200 000
F <sup>-</sup>	6 280	>100 000	>300 000	>300 000
Cl <sup>-</sup>	2 850	>100 000	6 000	200 000
Br <sup>-</sup>	2 840	36 800	4 100	63 000
I <sup>-</sup>	840	7 400	300	26 000

CNO <sup>-</sup>	890	770	0.70	30.0
SCN <sup>-</sup>	930	7 900	200	1 600
HS <sup>-</sup>	820	6 900	0.60	40.0
CN <sup>-</sup>	930	>100 000	0.50	20.0
N <sub>3</sub> <sup>-</sup>	800	>100 000	1.20	1 510
Sulfamide	8	28	310	1 130
Sulfamic acid	40	>100 000	21	390
Phenylarsonic acid	20	38	31 700	49 200
Phenylboronic acid	520	47	38 600	23 100
SnO <sub>3</sub> <sup>2-</sup>	960	510	570	830
SeO <sub>4</sub> <sup>2-</sup>	3 490	6 000	118 000	112 000
TeO <sub>4</sub> <sup>2-</sup>	4 900	610	660	920
OsO <sub>5</sub> <sup>2-</sup>	580	NM	NM	NM
P <sub>2</sub> O <sub>7</sub> <sup>2-</sup>	>10 000	>100 000	25 800	48 500
V <sub>2</sub> O <sub>7</sub> <sup>2-</sup>	>10 000	>100 000	540	570
B <sub>4</sub> O <sub>7</sub> <sup>2-</sup>	4 300	290	640	950
ReO <sub>4</sub> <sup>-</sup>	9 090	7 100	110	750
RuO <sub>4</sub> <sup>-</sup>	3 650	7 000	100	690
S <sub>2</sub> O <sub>8</sub> <sup>2-</sup>	>10 000	8 400	110	84.0
SeCN <sup>-</sup>	220	870	85.0	86.0
NH(SO <sub>3</sub> ) <sub>2</sub> <sup>-</sup>	>10 000	2 200	310	760
FSO <sub>3</sub> <sup>-</sup>	>10 000	86	790	460
CS <sub>3</sub> <sup>2-</sup>	3 330	6 000	8.7	8.8
Et <sub>2</sub> NCS <sub>2</sub> <sup>-</sup>	420	510	0.79	3 100
PF <sub>6</sub> <sup>-</sup>	>10 000	>100 000	>200 000	>200 000
Triflate	>10 000	>100 000	>200 000	>200 000
BF <sub>4</sub> <sup>-</sup>	NM	>100 000	>200 000	>200 000

NM = not measured, \*Mean from 3 distinct measurements with stopped-flow, CO<sub>2</sub> hydrase assay (Khalifah 1971) with errors in the range of 5-10%.

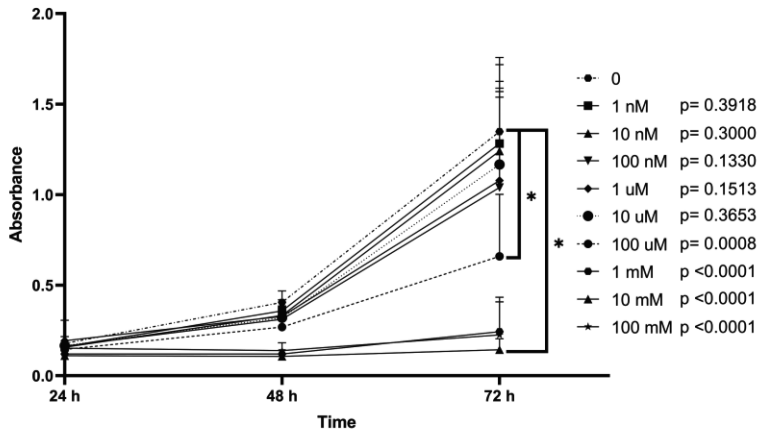


## 5.2 Inhibition of *Acanthamoeba castellanii*

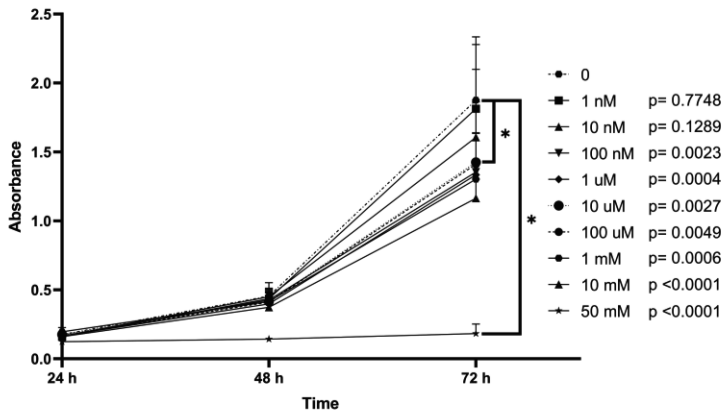
We developed a novel drug screening method for analyzing the efficiency of various drug candidates against *A. castellanii*. The method includes two assays: inhibitor assay and excystation assay, from which the former is biphasic. Our method exposes both cysts and trophozoites to the inhibitor effect and indirectly presents the infectious capacity of cysts (e.g., the ability of cysts to excystate). As a result, we found three commonly known, clinically used CAIs to be effective against *A. castellanii*: acetazolamide, dorzolamide and ethoxzolamide in both inhibitor (Figures 11 and 12) and excystation assays (Figure 13). Acetazolamide was effective against trophozoites and the excystation of cysts with the concentration of 100  $\mu\text{M}$  for both, while dorzolamide was effective with concentrations of 100 nM and 10  $\mu\text{M}$ , respectively. For ethoxzolamide the analogous concentrations were 938 nM and 188 nM. Fc14-584B was also effective with the concentrations of 15.6  $\mu\text{M}$  and 62.5  $\mu\text{M}$ , but it is not in clinical use, which makes it less compelling against the other tested CAIs. Propamidine was also tested to compare CAIs to a drug used in treating AK which was effective with all tested concentrations.

The cyst survival test represents the ability of cyst to preserve their infective capacity after the inhibitor effect. In this context, acetazolamide, dorzolamide, ethoxzolamide and Fc14-584B showed good inhibitory capacity. However, in inhibitor assay and excystation assay, brinzolamide was indicated to be relatively ineffective against *A. castellanii*. The statistical significance was calculated between different concentrations and the control (curve 0) at 72 h.

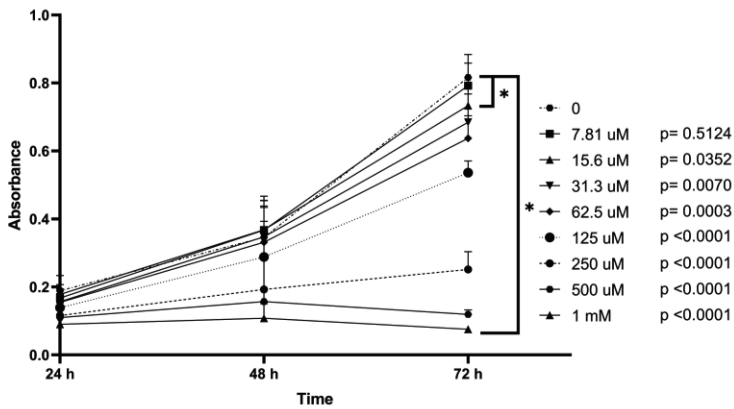
### Acetazolamide



### Dorzolamide



### Fc14-584B



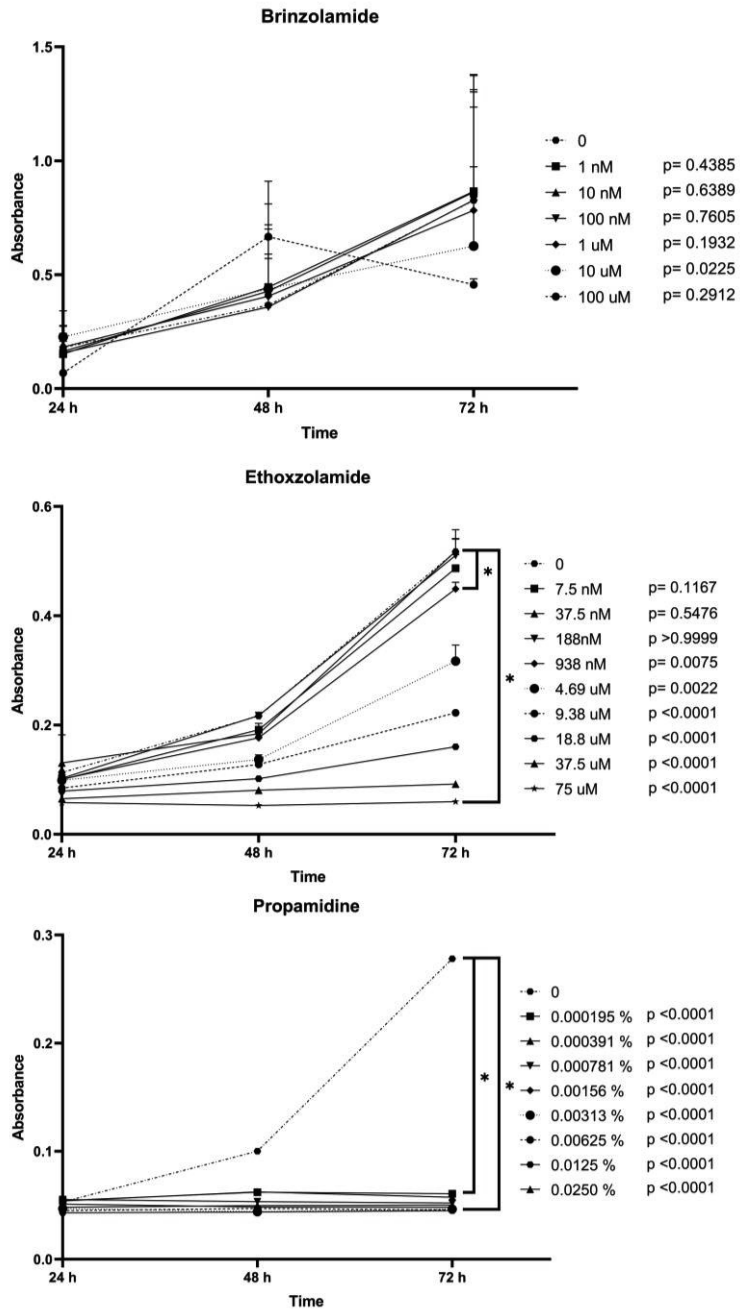
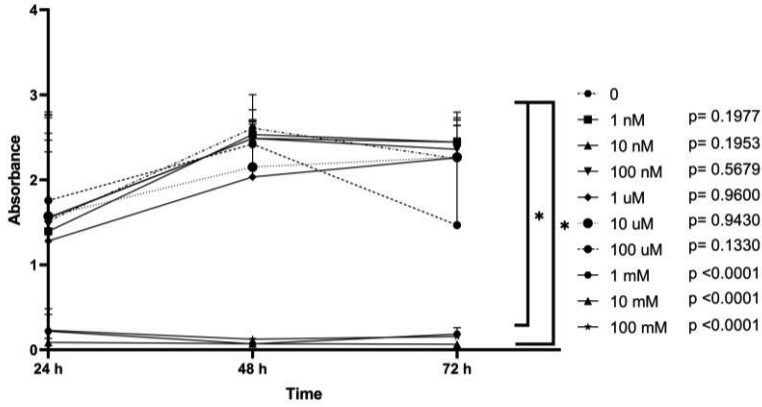
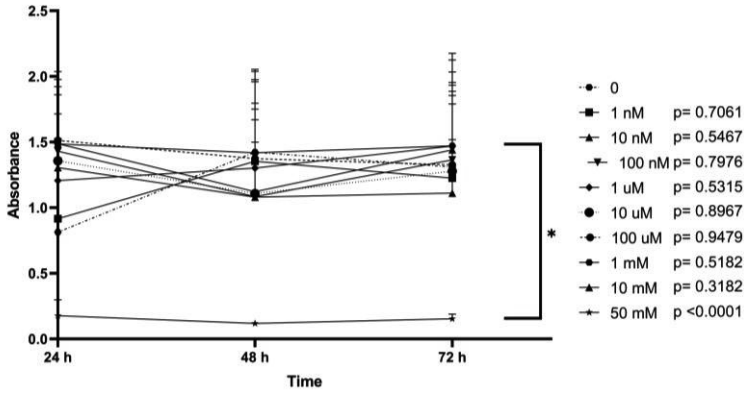


**Figure 13.** The first phase of the inhibitor assay represents the inhibition of growth of *A. castellanii* with six different inhibitors. The absorbance of different concentrations of inhibitors were compared with the control curve (0) at 72 h time point to determine the statistical significance. Figure begins already at page 72. \*=  $p < 0.05$

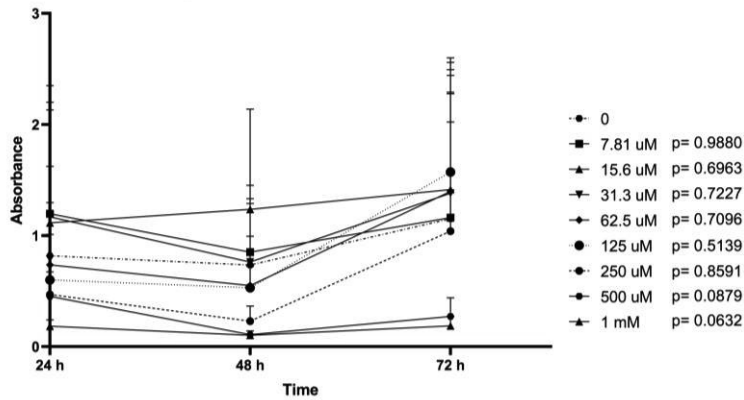
**Cyst survival after acetazolamide**



**Cyst survival after dorzolamide**



**Cyst survival after Fc14-584B**



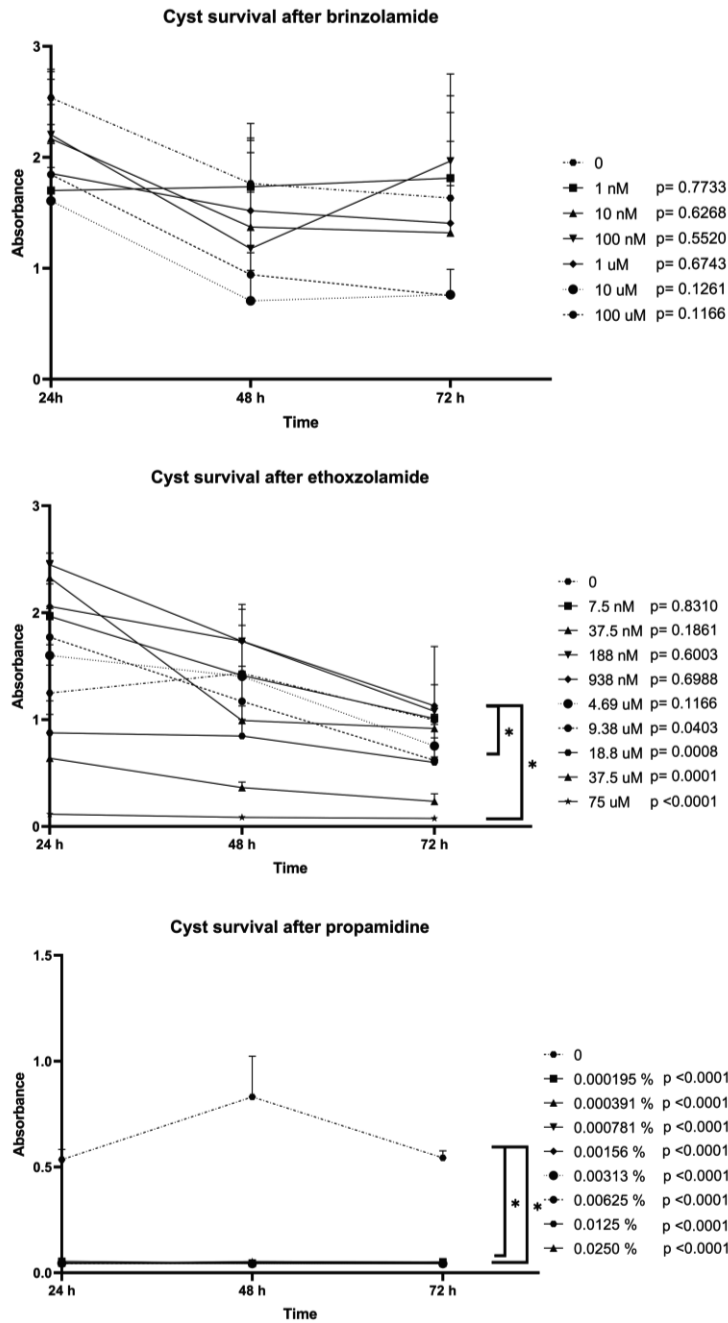


**Figure 14.** The second phase of the inhibitor assay illustrates cyst survival after the inhibitor effect, hence modeling the infectious capacity of the cysts after treatment. The same six CA inhibitors are used as in the first phase and the obtained absorbance data of different inhibitor concentrations are compared to control curve (0) at 72 h to determine statistical significance. Figure begins already at page 74. \*=  $p < 0.05$

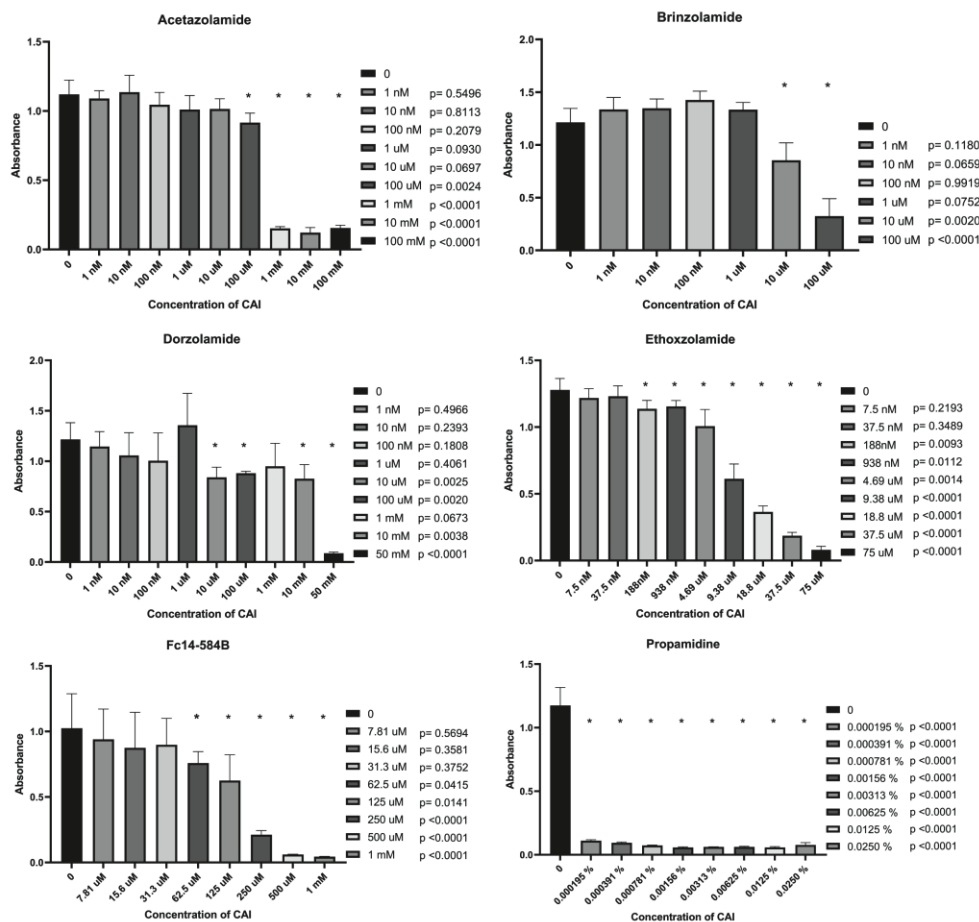


**Figure 15.** The excystation assay illustrates the capacity of cysts to excystate in the presence of six different CA inhibitors. The absorbance data of different concentrations of the inhibitors were compared to the control curve (0) at 72 h to determine the statistical significance. \* =  $p < 0.05$

### 5.3 Diagnostic method for detecting *Acanthamoeba castellanii*

We developed traditional PCR and qRT-PCR-based methods to detect *A. castellanii* from a sample (Figure 16). Traditional PCR offers a result with the sensitivity of only one cyst or trophozoite in less than three hours. Hence, the result can be obtained during the patient's emergency room visit and the correct treatment initiated almost instantly. The method does not require any expensive or special laboratory technology or equipment: a traditional thermocycler and gel electrophoresis facility are enough. Thus, it can be performed in any diagnostic laboratory. We found three

primer pairs, two detecting a  $\beta$ -CA and one detecting  $\gamma$ -CA of *A. castellanii*, to provide equally accurate results in the same amount of time (Figure 17).

We also developed a qRT-PCR method as it is nowadays more commonly used in modern diagnostic laboratories. Our method uses two alternative primer pairs: one against the same  $\beta$ -CA as in traditional PCR and the other against the same  $\gamma$ -CA. Both primer pairs can detect 0.01 ng of amoeba DNA at the minimum. The genome of *A. castellanii* is at least 1.9 ng [equal to 42.02 Mb (Hasni et al. 2020)]; therefore, with our method, a single trophozoite or cyst of *A. castellanii* can be detected.

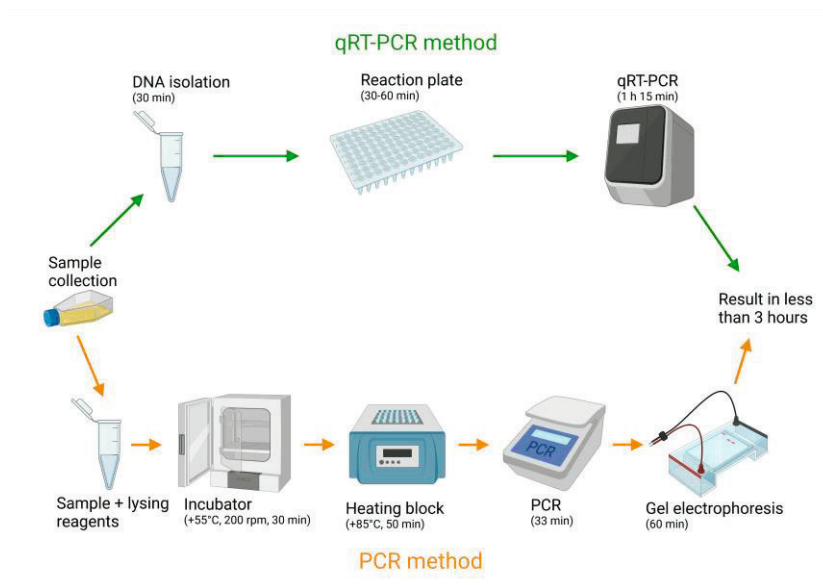


**Figure 16.** Pipeline of both traditional PCR and qRT-PCR methods designed for diagnostics of *A. castellanii*. The result is achieved in less than three hours by both methods. Figure created with Biorender.com.

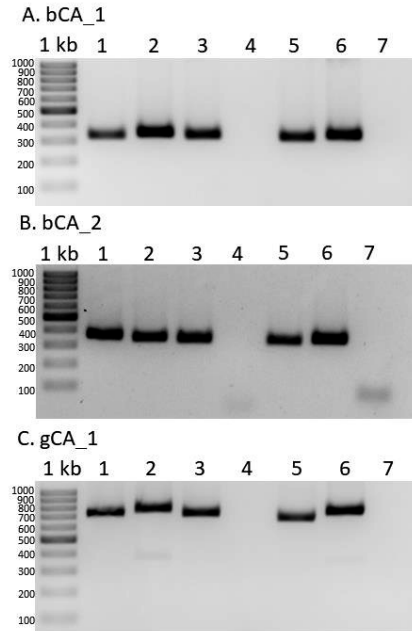


**Figure 17.** The results from traditional PCR represented in agarose gel with 1 kb standard marker. Lines: 1) one cyst, 2) one trophozoite, 3) 5 cysts and 5 trophozoites, 4) buccal mucosa, 5) amoebas with buccal mucosa, 6) hundreds of amoebas, 7) negative control

## 5.4 Bioinformatic analyses

### 5.4.1 3D-modeling of SmaBCA

The 3D model of SmaBCA was predicted with AlphaFold (Figure 18). The model predicts a dimer to be the most likely form of existence in nature, as the N-terminal  $\alpha$ -helices are positioned next to the other monomer, similar to the dimer of  $\beta$ -CA of *Pisum sativum* (Kimber 2000).



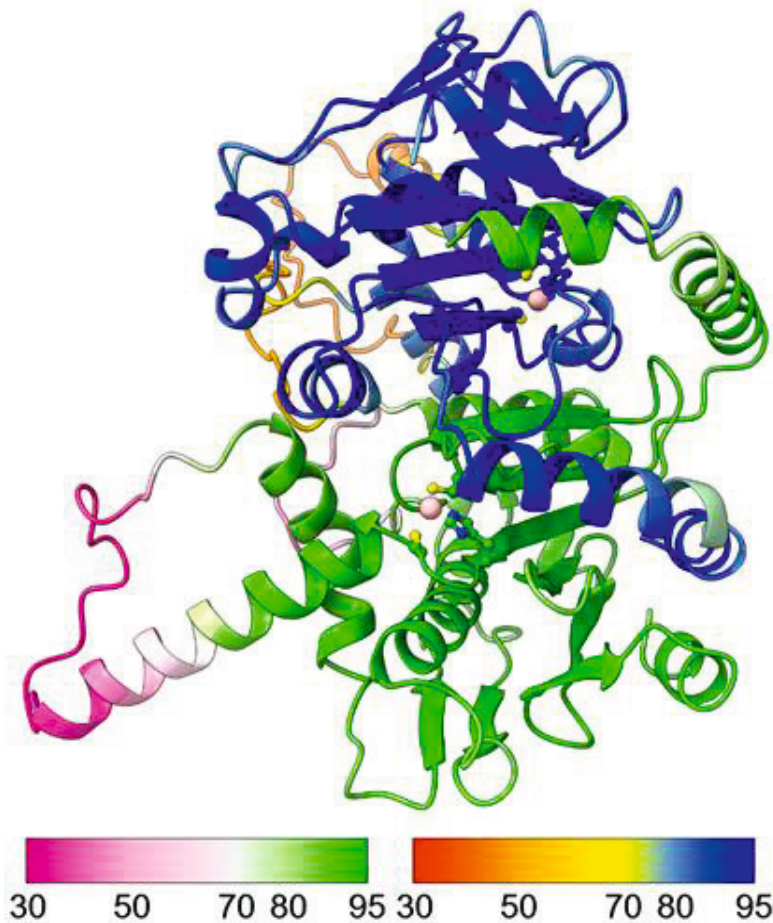


**Figure 18.** The 3D model of SmaBCA predicts the enzyme to be a dimer. The metal binding amino acids, Cys 38, His 103, and Cys 106, are shown with the coordinated Zinc<sup>2+</sup>-ion (pink sphere). Colors show the per-residue confidence score (pLDDT) for both monomers individually. The original figure is from publication III and reproduced here under a Creative Commons License.

#### 5.4.2 Sequence similarities of different protozoans

An MSA comparing the sequences of  $\beta$ -CAs of *Schistosoma* species is shown in Figure 19. The  $\beta$ -CAs are highly conserved among *Schistosoma* species, as 244 amino acids (91.7%) are at least 75% conserved and 175 amino acids (65.8%) are fully conserved. The MSA represents also the variability among different *Schistosoma* species in the N-terminus of the sequence, which was the site that our analysis revealed to be

incorrectly predicted earlier, which rendered the first attempts to produce recombinant SmaBCA unsuccessful.

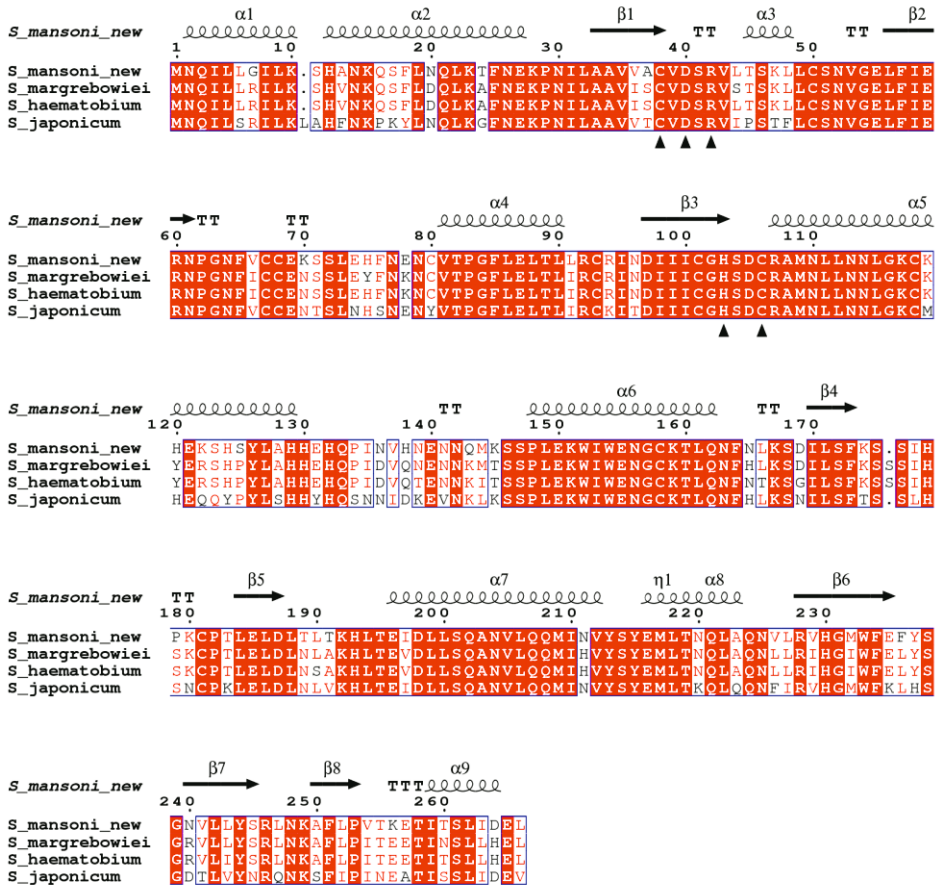


**Figure 19.** Multiple sequence alignment shows the similarities of the sequences of  $\beta$ -CAs of different *Schistosoma* species. Red areas represent fully conserved amino acids, and boxed areas represent at least 75% conserved residues. The active sites (CXDXR and HXXC) are fully conserved and are indicated with black triangles.  $\alpha$ -folds and  $\beta$ -sheets are indicated above the sequence rows. The original figure is from publication III and reproduced here under a Creative Commons License.

The sequence logo compares 162 metazoan sequences displaying 19 totally conserved areas and 26 almost conserved areas (Figure 20). This represents the high similarities among metazoans. Naturally, the totally conserved areas include the active site (CXDXR and HXXC).

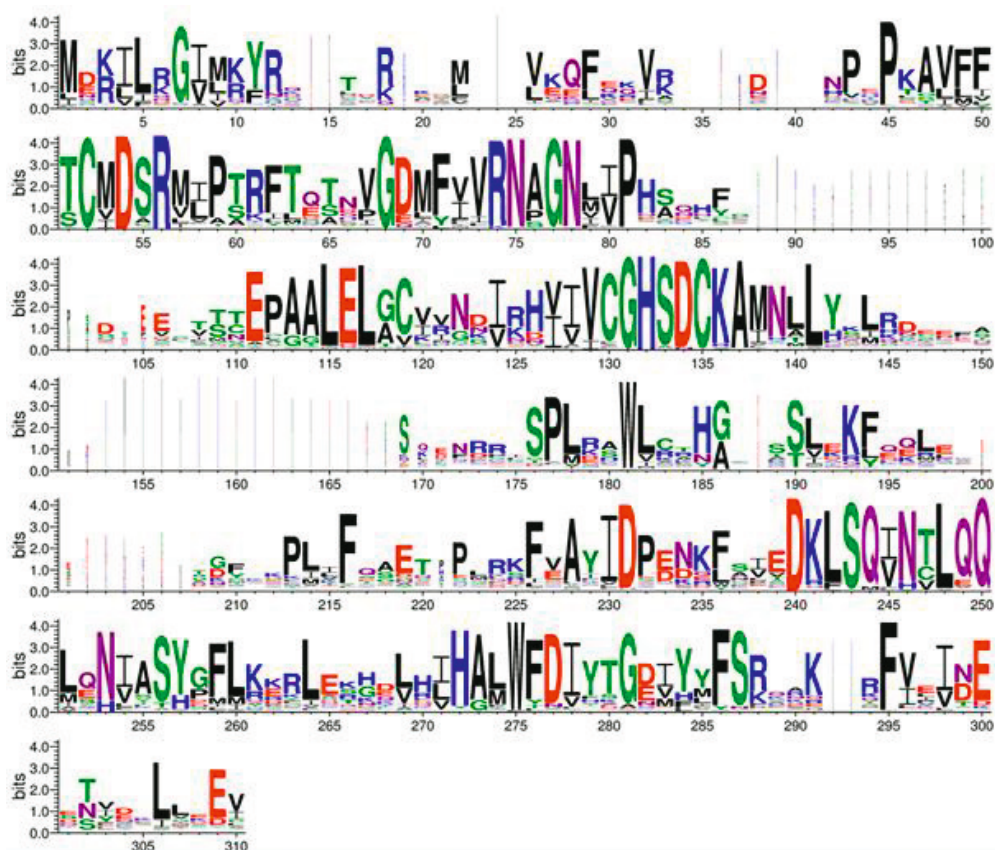


**Figure 20.** Sequence logo of 162 metazoan  $\beta$ -CA sequences. The active sites CXXR and HXXC are visualized on the second and third row respectively. The original figure is from publication III and reproduced here under a Creative Commons License.

### 5.4.3 Expression of CAs of *A. castellanii*

We analyzed the mRNA data of *A. castellanii* (König et al. 2017) to determine the expression levels of different CAs of *A. castellanii* to predict the possible effect of inhibitors on the organisms (Figure 21). It seems that at least four CAs show high or slightly higher expression levels compared to other genes. We found that one of the  $\gamma$ -CAs (ACA1\_260080) had high mRNA expression levels and all others, except one  $\alpha$ -CA (ACA1\_130470), had moderate expression compared to mRNA expression levels of all known genes of *A. castellanii*.

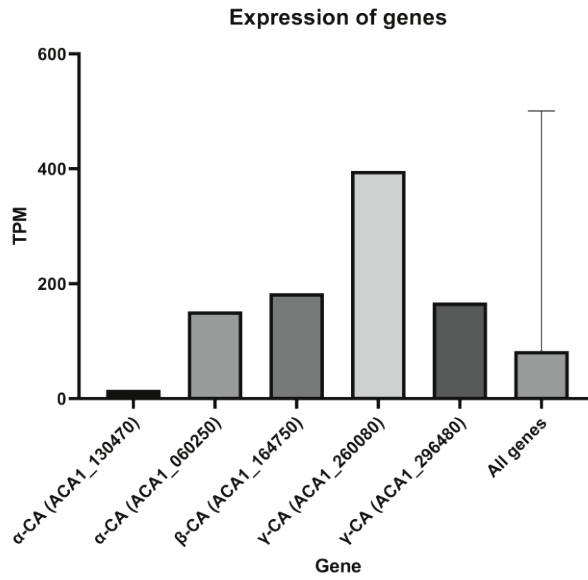


**Figure 21.** Expression of CAs of *A. castellanii* compared to the mean expression of all genes. TPM= transcripts per million

## 6 DISCUSSION

### 6.1 Fight against diarrhea

Diarrhea is the second leading cause of death in children under the age of five (Hart and Umar 2000; Centers for Disease Control and Prevention 2013). In 2015, it was a leading cause of death among all ages, with 1.31 million deaths globally (Troeger et al. 2017). Diarrhea can be caused by bacteria, viruses, fungi (Levine, Dykoski, and Janoff 1995), or parasites; approximately 5-10% of diarrhea in children under the age of five is caused by parasites (WHO). The severity of the symptoms may differ widely from mild intermittent abdominal pain to fever and dehydration. However, many parasites do not cause diarrhea. Diarrhea is a common symptom only in parasitic infections caused by *Entamoeba histolytica*, *Giardia lamblia*, *Cryptosporidium*, *Strongyloides*, *Trichuris trichiura*, *Schistosoma*, and occasionally *Ascaris* and *Ancylostoma* (Gendrel, Treluyer, and Richard-Lenoble 2003).

*S. mansoni* and *E. histolytica* are prevalent in the same areas of the world, which emphasizes the desire to have a single medication to treat both. Comparison of the inhibitors tested on SmaBCA and EhiCA revealed that there are compounds showing good inhibitory effects on both proteins. It may be a beneficial feature for the drug to be effective on both organisms as they are endemic in the same areas, thus leading to better compliance and adherence with the use of only one drug. It might also have economic benefits, as there would be a need for only one drug to treat two infections, even at the same time. Promising compounds inhibiting both recombinant enzyme proteins are 4-hydroxymethyl/ethyl-benzenesulfonamides (compounds 16 and 17), 4-(2-aminoethyl)benzenesulfonamide (compound 6), 4-((2-amino-4-pyrimidinyl)amino)benzenesulfonamide (compound 19) and acetazolamide with KIs of 36-798 nM for EhiCA and 44-600 nM for SmaBCA (Table 7). Currently, praziquantel is the only universal drug against infections caused by *Schistosoma* species; however, there are preliminary signs of rising resistance, which could cause major challenges in treatment and prevention if the resistance develops significantly (Doenhoff et al. 2002; Botros and Bennett 2007). The previously used drug, oxamniquine, is effective on *S. mansoni*, whereas it is inefficient against the other

species. The high similarity between sequences of  $\beta$ -CAs of different *Schistosoma* species offers insight into developing CAI-based universal drugs against them all.

## 6.2 Carbonic anhydrase inhibitors – the answer to antimicrobial resistance?

Antimicrobial resistance (AMR) is a global problem that the WHO has listed as one of the top 10 global public health threats (World Health Organization 17.11.2021, <https://www.who.int/news-room/fact-sheets/detail/antimicrobial-resistance>).

Antibiotics are originally chemical compounds produced by microbes to fight for living space in an ecosystem (Hutchings, Truman, and Wilkinson 2019). However, microbes have protected themselves against other microbes' attacks by developing resistance mechanisms, for example enzymes that degrade antibiotics. People learned to isolate and utilize antibiotics in the 20<sup>th</sup> century. Additionally, these were learned to synthesize on a large scale, which started the wide distribution revolution of the antibiotic era. Unfortunately, after the 1980s, there have been no new discoveries of mechanisms of action for antimicrobials (Hutchings, Truman, and Wilkinson 2019). Currently, the misuse and overuse of antimicrobials is a major global problem, which accelerates the development of microbes' resistance mechanisms, which worsens the AMR problem.

CAIs are a potential new class of antimicrobial agents that are under vigorous research (Nocentini, Capasso, and Supuran 2023). They are being investigated to fight tuberculosis (Aspatwar et al. 2018), *Helicobacter pylori* (Supuran and Capasso 2020; Flaherty, Seleem, and Supuran 2021) and vancomycin-resistant *Enterococcus* species (Supuran and Capasso 2020), for instance. Most of the studies have been performed *in vitro*, either investigating inhibitors against recombinant proteins or bacterial cell cultures (Nocentini, Capasso, and Supuran 2023). There have been promising results, but they require confirmation of action and efficiency in both animal and human testing. Unfortunately, no clinically approved CAIs are in use as antimicrobials. However, at least one clinical study has been conducted with volunteers with unsuccessful eradication of *Helicobacter pylori* with acetazolamide (Shahidzadeh et al. 2005), but the treatment time was too short to prove the CAI neither effective nor ineffective (Buzás 2005).

Inhibitor studies have been performed on, for example, the  $\beta$ -CAs of *Trichomonas vaginalis* (Urbanski et al. 2020), *Leishmania donovani chagasi* (Syrjänen et al. 2013) and

*Ascaris lumbricoides* (Emameh et al. 2015), but none of them have been investigated *in vivo*. The situation is now similar with *S. mansoni* and *E. histolytica*, as we conducted only *in vitro* studies on the inhibition of  $\beta$ -CAs. All of these inhibitor studies have introduced good candidates for antimicrobial agent development, but unfortunately, it will take years at a minimum to have CAI-based drugs in clinical use to fight against the infections caused by these parasites.

We selected a different approach for the purpose of investigating the possibilities of using CAIs against *A. castellanii*. First, we aimed to purify endogenous CAs of *A. castellanii* using a classical CA inhibitor affinity chromatography method. The purified enzymes would have been subjected for additional purification steps, such as ion exchange chromatography, and subsequent inhibition studies. However, the CA inhibitor affinity chromatography failed to produce any positive signal of CA in SDS-PAGE (data not shown). This can be explained by most *A. castellanii* CAs being membrane-bound or mitochondrial, which are challenging forms for isolation using the classical CA inhibitor affinity chromatography. Furthermore, it is possible that *A. castellanii* CAs do not bind efficiently enough to the p-aminomethylbenzene sulfonamide that is coupled to the chromatography matrix. Second, we also tried to produce the CAs as recombinant proteins in the *E. coli* expression system, but we were unsuccessful with the ligation of the insert to the plasmid. Since both prior attempts failed to produce desired proteins for inhibition studies, we decided to investigate the effects of selected CAIs directly in the amoeba culture. To reach this goal we first had to develop a new drug screening assay that could bypass the limitations of existing assays.

The most commonly used drug screening assay for *Acanthamoeba* is conducted with trypan blue and a hemocytometer to determine the cell count (Anwar, Numan, et al. 2019; Shahbaz et al. 2020). The problem in this method is the cell counting: as the analysis only takes a portion of the culture medium, the distribution of cells might be different in the whole medium than in the sample. Ortega-Rivas et al. created a new method for detecting the amoebicidal effects of a potential drug *in vitro* (Ortega-Rivas et al. 2016). They used a colorimetric assay based on sulforhodamine B (SRB) staining, which, unfortunately, generates a limitation to the method: SRB can bind only to trophozoites, whereas the cysts remain completely undetected. In the diagnostics of *A. castellanii*, detection of cysts is especially important, because they can serve as reservoirs for relapsing infections.

However, our method is not without limitations either. We found that propamidine and brinzolamide are prone to crystallization at high concentrations.

Chlorhexidine and polyhexamethylene biguanide hydrochloride crystallized even at low concentrations, which is why they were ruled out as controls. To avoid bias, we addressed this issue by inspecting the wells with a light microscope before the analysis. Nevertheless, a major benefit of our assay is that it enables us to test the inhibitors' effect on cysts and their ability to excystate different from the earlier method.

From various CAIs we selected acetazolamide, dorzolamide, brinzolamide and ethoxzolamide because they are or have been in clinical use for other indications. We also used Fc14-584B in the testing because it is a promising new CAI investigated as a new potential drug compound that is effective against mycobacterial beta-CAs. It has been tested on zebrafish and proven to have a minimal toxic effect at a concentration of 300  $\mu\text{M}$  and an LC<sub>50</sub> value of 498.1  $\mu\text{M}$  on five-day-old zebrafish larvae (Aspatwar et al. 2017). In our studies, it was effective against trophozoites at a concentration of 15.6  $\mu\text{M}$ .

Acetazolamide and dorzolamide are both used to treat glaucoma (Rosenberg et al. 1998; Scozzafava and Supuran 2014), and acetazolamide is also used in mountain sickness and epilepsy (Farzam and Abdullah 2022). Acetazolamide is administered orally or intravenously and, more rarely, intramuscularly, with doses of 250 mg to 1000 mg per day. Oral dose of 250 mg leads to a blood concentration of 72.0  $\mu\text{M}$  (Larsson and Alm 1998). There are no studies available on the concentration that is transmitted to aqueous humor from systemic circulation. Acetazolamide can cross the blood brain barrier (Sun et al. 2001; Provensi et al. 2019), which makes it a potential candidate for treating GAE and other invasive *A. castellanii* infections. Usually, invasive *A. castellanii* infections have high mortality; thus, this finding brings new possibilities to treat these devastating diseases. With intravenous administration of 250 mg, a concentration of 225  $\mu\text{M}$  can be achieved in blood, which would be more than enough considering the effective inhibitory concentration of 100  $\mu\text{M}$  against trophozoites.

We used commercially available dorzolamide to simulate the real effect of administering the drug topically in the eye. The concentration of the clinically used eye drops, Trusopt (Santen Oy), is 20 mg/ml which equals to approximately 55 mM. With this setting, dorzolamide was shown to have a good inhibitory effect against trophozoites at a concentration of 100 nM and against cysts at the concentration of 50 mM, which would be met with the already available eye drop. The result is especially promising as dorzolamide has been used in patient care for a long time



and its side effects are known. They are mainly mild, for example irritation of the eye, and severe or systemic side effects are rare.

### 6.3 Novel prospects for the diagnosis of *Acanthamoeba keratitis*

PCR is a basic research laboratory technique that was invented in the 1980s (Templeton 1992; Garcia and Ma 2005), and since then it has revolutionized not only research but also diagnostics of infections and genetic disorders, criminology, forensics, and archeology (Lenstra 1995). There have been many technological modifications, such as quantitative PCR, reverse transcription PCR and loop-mediated amplification.

Even though laboratory diagnostics of various diseases has tremendously developed during the past decades, old-fashioned tools and methods are still widely used in clinical laboratories worldwide. As such an example, culturing the cornea sample is still the gold standard for diagnosing AK. However, culturing is time-consuming and fairly inaccurate, while PCR would be faster, and most already existing qPCR methods can detect fewer than 10 amoebae (Rivière et al. 2006). The superiority of *in vivo* confocal microscopy and PCR methods is fortunately becoming recognized (Zhang et al. 2023). Many commercially available PCR-based detection methods for *A. castellanii* are available (publication IV), but for some reason, none of them dominate in the clinical laboratory diagnostics. One reason could be that they are stated to be for research purposes only, and they would need further validation and bureaucracy to be officially accepted as a medical device. However, El-Sayed et al. presented a method that can recognize *A. castellanii* directly from a smear sample, but they did not state how many amoebae they can recognize and whether cysts can be detected (El-Sayed et al. 2014). Although their method has been tested on patient samples, it has not yet reached widespread use. In addition, Qvarnstrom et al. presented a technique that identifies *A. castellanii*, *Balamuthia mandrillaris* and *Naegleria fowleri* (Qvarnstrom et al. 2006). It could be a good choice for the detection of invasive infections caused by these pathogens including brain abscesses.

qRT-PCR is considered more effective than traditional PCR in large diagnostic laboratories, as it is more automated and can analyze more samples at once. Traditional PCR can also be performed with limited budget as there is no special need for expensive equipment other than a normal thermal cycler. A new insight would be to develop a point-of-care device for rapid diagnostics, removing the need

for a sample transfer to the clinical laboratory, and thus, could also be performed in rural and distant areas without an easy access to the diagnostic laboratory.

## 7 SUMMARY AND CONCLUSIONS

The experiments and results of this thesis are part of the larger project of Seppo Parkkila's research group where we investigate protozoan CAs. This thesis aimed to extend the knowledge of three different parasites and the diseases they cause with biochemical and bioinformatic methods. The diseases caused by these parasites are poorly treated and have limited prevention options. We produced two novel recombinant proteins of *S. mansoni* and *E. histolytica*, found promising inhibitors against them *in vitro*, and developed a new rapid diagnostic method for AK diagnostics as well as a robust drug screening assay tool for discovering new potential medicines for infections caused by *A. castellanii*. We also presented auspicious CA inhibitors to treat the infections.

The achieved results were as follows:

- Successful production of recombinant  $\beta$ -CA of *S. mansoni*, and the most effective CAI against it is 4-(2-amino-pyrimidin-4-yl)-benzenesulfonamide (compound 19) with a  $K_i$  of 44 nM.
- Successful production of recombinant  $\beta$ -CA of *E. histolytica*, and the most effective CAI against it is 4-hydroxyethyl-benzenesulfonamide (compound 17) with a  $K_i$  of 36 nM.
- *S. mansoni* and *E. histolytica* have greatly overlapping endemic areas, and the most effective CAIs against  $\beta$ -CAs of *S. mansoni* and *E. histolytica* are 4-hydroxymethyl-benzenesulfonamide (compound 16,  $K_i$ s 600 nM and 89 nM, respectively), 4-hydroxyethyl-benzenesulfonamide (compound 17,  $K_i$ s 346 nM and 36 nM, respectively) and 4-(2-amino-pyrimidin-4-yl)-benzenesulfonamide (compound 19,  $K_i$ s 44 nM and 521 nM, respectively).
- Development of two novel diagnostic methods taking less than three hours for detecting *A. castellanii* from a biological sample. The detection protocol based on qRT-PCR can also be used as a foundation for other detection protocols for free-living amoebae.

- A novel drug screening method including assays for both trophozoites and cysts helps to investigate potential drugs to treat infections caused by *A. castellanii*.
- Acetazolamide and dorzolamide, already widely clinically used CAIs, are effective against both trophozoites and cysts of *A. castellanii* and offer new potential drug candidates to be investigated in managing the infections caused by *A. castellanii*.

## 8 REFERENCES

- Abreu Ferrari, Teresa Cristina De. 2004. "Involvement of Central Nervous System in the Schistosomiasis." In *Memorias Do Instituto Oswaldo Cruz*, 99:59–62. Instituto Oswaldo Cruz, Ministério da Saúde. <https://doi.org/10.1590/s0074-02762004000900010>.
- Adekiya, Tayo A., Pradeep Kumar, Pierre P.D. Kondiah, Viness Pillay, and Yahya E. Choonara. 2021. "Synthesis and Therapeutic Delivery Approaches for Praziquantel: A Patent Review (2010-Present)." *Expert Opinion on Therapeutic Patents* 31 (9): 851–65. <https://doi.org/10.1080/13543776.2021.1915292>.
- Adeva-Andany, María M., Carlos Fernández-Fernández, Rocío Sánchez-Bello, Cristóbal Donapetry-García, and Julia Martínez-Rodríguez. 2015. "The Role of Carbonic Anhydrase in the Pathogenesis of Vascular Calcification in Humans." *Atherosclerosis*. <https://doi.org/10.1016/j.atherosclerosis.2015.05.012>.
- Agarwal, Shalini, Pragyan Parimita Rath, Gaurav Anand, and Samudrala Gourinath. 2020. "Uncovering the Cyclic AMP Signaling Pathway of the Protozoan Parasite Entamoeba Histolytica and Understanding Its Role in Phagocytosis." *Frontiers in Cellular and Infection Microbiology* 10 (September): 566726. <https://doi.org/10.3389/fcimb.2020.566726>.
- Agatsuma, Takeshi. 2003. "Origin and Evolution of Schistosoma Japonicum." *Parasitology International*, 52:335–40. [https://doi.org/10.1016/S1383-5769\(03\)00049-7](https://doi.org/10.1016/S1383-5769(03)00049-7).
- Airenne, Kari J., Erik Peltomaa, Vesa P. Hytönen, Olli H. Laitinen, and Seppo Ylä-Herttua. 2003. "Improved Generation of Recombinant Baculovirus Genomes in Escherichia Coli." *Nucleic Acids Research* 31 (17): e101–e101. <https://doi.org/10.1093/nar/gng102>.
- Akhter, Md Habban, Irfan Ahmad, Mohammad Y. Alshahrani, Alhanouf I. Al-Harbi, Habibullah Khalilullah, Obaid Afzal, Abdulmalik S.A. Altamimi, Shehla Nasar Mir Najib Ullah, Abhijeet Ojha, and Shahid Karim. 2022. "Drug Delivery Challenges and Current Progress in Nanocarrier-Based Ocular Therapeutic System." *Gels*. <https://doi.org/10.3390/gels8020082>.
- Akocak, Suleyman, and Claudiu T. Supuran. 2019. "Activation of  $\alpha$ -,  $\beta$ -,  $\gamma$ -  $\delta$ -,  $\zeta$ - and  $\eta$ -Class of Carbonic Anhydrases with Amines and Amino Acids: A Review." *Journal of Enzyme Inhibition and Medicinal Chemistry*. <https://doi.org/10.1080/14756366.2019.1664501>.

- Alantary, Noor, Wayne Heaselgrave, and Scott Hau. 2022. "Correlation of Ex Vivo and in Vivo Confocal Microscopy Imaging of Acanthamoeba." *British Journal of Ophthalmology* (June): 1–6. <https://doi.org/10.1136/bjophthalmol-2022-321402>.
- Alterio, Vincenzo, Emma Langella, Giuseppina De Simone, and Simona Maria Monti. 2015. "Cadmium-Containing Carbonic Anhydrase CDCA1 in Marine Diatom *Thalassiosira weissflogii*." *Marine Drugs*. <https://doi.org/10.3390/md13041688>.
- Alterio, Vincenzo, Emma Langella, Francesca Viparelli, Daniela Vullo, Giuseppina Ascione, Nina A. Dathan, Francois M.M. Morel, Claudiu T. Supuran, Giuseppina De Simone, and Simona Maria Monti. 2012. "Structural and Inhibition Insights into Carbonic Anhydrase CDCA1 from the Marine Diatom *Thalassiosira weissflogii*." *Biochimie* 94 (5): 1232–41. <https://doi.org/10.1016/j.biochi.2012.02.013>.
- Amata, Orazio, Tiziana Marino, Nino Russo, and Marirosa Toscano. 2011. "Catalytic Activity of a  $\zeta$ -Class Zinc and Cadmium Containing Carbonic Anhydrase. Compared Work Mechanisms." *Physical Chemistry Chemical Physics* 13 (8): 3468–77. <https://doi.org/10.1039/c0cp01053g>.
- Anderson, Jackie, and Elizabeth Paterek. 2022. "Flea Bites." *Pests of Paradise*, September, 55–58. <https://doi.org/10.1515/9780824844035-013>.
- Angeli, Andrea, Marta Ferraroni, Fabrizio Carta, Cécile Häberli, Jennifer Keiser, Gabriele Costantino, and Claudiu T. Supuran. 2022. "Development of Praziquantel Sulphonamide Derivatives as Antischistosomal Drugs." *Journal of Enzyme Inhibition and Medicinal Chemistry* 37 (1): 1479–94. <https://doi.org/10.1080/14756366.2022.2078970>.
- Angeli, Andrea, Mariana Pinteala, Stelian S. Maier, Bogdan C. Simionescu, Akram A. Da'dara, Patrick J. Skelly, and Claudiu T. Supuran. 2020. "Sulfonamide Inhibition Studies of an  $\alpha$ -Carbonic Anhydrase from *Schistosoma mansoni*, a Platyhelminth Parasite Responsible for Schistosomiasis." *International Journal of Molecular Sciences* 21 (5). <https://doi.org/10.3390/ijms21051842>.
- Anwar, Ayaz, Arshid Numan, Ruqaiyyah Siddiqui, Mohammad Khalid, and Naveed Ahmed Khan. 2019. "Cobalt Nanoparticles as Novel Nanotherapeutics against *Acanthamoeba castellanii*." *Parasites and Vectors* 12 (1). <https://doi.org/10.1186/s13071-019-3528-2>.
- Anwar, Ayaz, Kavitha Rajendran, Ruqaiyyah Siddiqui, Muhammad Raza Shah, and Naveed Ahmed Khan. 2019. "Clinically Approved Drugs against CNS Diseases as Potential Therapeutic Agents to Target Brain-Eating Amoebae." *ACS Chemical Neuroscience* 10 (1): 658–66. <https://doi.org/10.1021/acscemneuro.8b00484>.
- Apweiler, Rolf, Amos Bairoch, Cathy H. Wu, Winona C. Barker, Brigitte Boeckmann, Serenella Ferro, Elisabeth Gasteiger, et al. 2004. "UniProt: The Universal Protein Knowledgebase." *Nucleic Acids Research* 32 (DATABASE ISS.): 2699–2699. <https://doi.org/10.1093/nar/gky092>.

- Arbabi, Amirmohsen, Xuan Bao, Wesam Shamseldin Shalaby, and Reza Razeghinejad. 2022. "Systemic Side Effects of Glaucoma Medications." *Clinical and Experimental Optometry*. <https://doi.org/10.1080/08164622.2021.1964331>.
- Aspatwar, Ashok, Milka Hammarén, Sanni Koskinen, Bruno Luukinen, Harlan Barker, Fabrizio Carta, Claudiu T. Supuran, Matalena Parikka, and Seppo Parkkila. 2017. "β-CA-Specific Inhibitor Dithiocarbamate Fc14–584B: A Novel Antimycobacterial Agent with Potential to Treat Drug-Resistant Tuberculosis." *Journal of Enzyme Inhibition and Medicinal Chemistry* 32 (1): 832–40. <https://doi.org/10.1080/14756366.2017.1332056>.
- Aspatwar, Ashok, Jean Yves Winum, Fabrizio Carta, Claudiu T. Supuran, Milka Hammaren, Matalena Parikka, and Seppo Parkkila. 2018. "Carbonic Anhydrase Inhibitors as Novel Drugs against Mycobacterial β-Carbonic Anhydrases: An Update on in Vitro and in Vivo Studies." *Molecules* 23 (11): 2911. <https://doi.org/10.3390/molecules23112911>.
- Aspatwar, Ashok, Milka Hammaren, Matalena Parikka, Seppo Parkkila, Fabrizio Carta, Murat Bozdog, Daniela Vullo, and Claudiu T. Supuran. 2020. "In Vitro Inhibition of Mycobacterium Tuberculosis β-Carbonic Anhydrase 3 with Mono- and Dithiocarbamates and Evaluation of Their Toxicity Using Zebrafish Developing Embryos." *Journal of Enzyme Inhibition and Medicinal Chemistry* 35 (1): 65–71. <https://doi.org/10.1080/14756366.2019.1683007>.
- Bacon, A. S., D. G. Frazer, J. K.G. Dart, A. S. Matheson, L. A. Ficker, and P. Wright. 1993. "A Review of 72 Consecutive Cases of Acanthamoeba Keratitis, 1984-1992." *Eye (Basingstoke)* 7 (6): 719–25. <https://doi.org/10.1038/eye.1993.168>.
- Bagga, Bhupesh, Savitri Sharma, Ruchi Pratap Singh Gour, Ashik Mohamed, Joveeta Joseph, Varsha M Rathi, and Prashant Garg. 2021. "A Randomized Masked Pilot Clinical Trial to Compare the Efficacy of Topical 1% Voriconazole Ophthalmic Solution as Monotherapy with Combination Therapy of Topical 0.02% Polyhexamethylene Biguanide and 0.02% Chlorhexidine in the Treatment of Acanthamoeba K." *Eye (London, England)* 35 (5): 1326–33. <https://doi.org/10.1038/s41433-020-1109-4>.
- Baig, Abdul M., R. Zohaib, S. Tariq, and H. R. Ahmad. 2018. "Evolution of PH Buffers and Water Homeostasis in Eukaryotes: Homology between Humans and Acanthamoeba Proteins." *Future Microbiology* 13 (2): 195–207. <https://doi.org/10.2217/fmb-2017-0116>.
- Baig, Abdul Mannan, Zohaib Rana, Nuzair Waliani, Saiqa Karim, and Mehdi Rajabali. 2019. "Evidence of Human-like Ca<sup>2+</sup> Channels and Effects of Ca<sup>2+</sup> Channel Blockers in Acanthamoeba Castellani." *Chemical Biology and Drug Design* 93 (3): 351–63. <https://doi.org/10.1111/cbdd.13421>.
- Baird Hastings, A., Harald A. Salvesen, Julius Sendroy, and Donald D. Van Slyke. 1927. "Studies of Gas and Electrolyte Equilibria in the Blood: IX. The Distribution of

- Electrolytes between Transudates and Sertrm.” *Journal of General Physiology* 8 (6): 701–11. <https://doi.org/10.1085/jgp.8.6.701>.
- Bamefleh, Hanaa, and Ghadah O Al-Hussain. 2021. “Secondary Spontaneous Pneumothorax Caused by Pulmonary Schistosomiasis.” *Cureus* 13 (10). <https://doi.org/10.7759/cureus.18709>.
- Barsoum, Rashad. 2004. “The Changing Face of Schistosomal Glomerulopathy.” *Kidney International* 66 (6): 2472–84. <https://doi.org/10.1111/j.1523-1755.2004.66042.x>.
- Berrino, Emanuela, Silvia Bua, Mattia Mori, Maurizio Botta, Vallabhaneni S. Murthy, Vijayaparthasarathi Vijayakumar, Yasinalli Tamboli, et al. 2017. “Novel Sulfamide-Containing Compounds as Selective Carbonic Anhydrase i Inhibitors.” *Molecules* 22 (7). <https://doi.org/10.3390/molecules22071049>.
- Botros, Sanaa S., and James L. Bennett. 2007. “Praziquantel Resistance.” *Expert Opinion on Drug Discovery* 2 (SUPPL. 1). <https://doi.org/10.1517/17460441.2.S1.S35>.
- Braun, Hans Peter, and Eduardo Zabaleta. 2007. “Carbonic Anhydrase Subunits of the Mitochondrial NADH Dehydrogenase Complex (Complex I) in Plants.” In *Physiologia Plantarum*, 129:114–22. <https://doi.org/10.1111/j.1399-3054.2006.00773.x>.
- Brondfield, Max N., Michael J.A. Reid, Rachel L. Rutishauser, Jennifer R. Cope, Jevon Tang, Jana M. Ritter, Almea Matanock, et al. 2017. “Disseminated Acanthamoeba Infection in a Heart Transplant Recipient Treated Successfully with a Miltefosine-Containing Regimen: Case Report and Review of the Literature.” *Transplant Infectious Disease* 19 (2). <https://doi.org/10.1111/tid.12661>.
- Buzás, György M. 2005. “Carbonic Anhydrase, Acetazolamide and Helicobacter Pylori Infection [2].” *Helicobacter*. <https://doi.org/10.1111/j.1523-5378.2005.00353.x>.
- Cainzos, Maximiliano, Fernanda Marchetti, Cecilia Popovich, Patricia Leonardi, Gabriela Pagnussat, and Eduardo Zabaleta. 2021. “Gamma Carbonic Anhydrases Are Subunits of the Mitochondrial Complex I of Diatoms.” *Molecular Microbiology* 116 (1): 109–25. <https://doi.org/10.1111/mmi.14694>.
- Campos, Najla Santos Pacheco de, Bruna Santos Souza, Giselle Correia Próspero da Silva, Victoria Alves Porto, Ghanbar Mahmoodi Chalbatani, Gabriela Lagrec, Bassam Janji, and Eloah Rabello Suarez. 2022. “Carbonic Anhydrase IX: A Renewed Target for Cancer Immunotherapy.” *Cancers*. <https://doi.org/10.3390/cancers14061392>.
- Cannon, Gordon C., Sabine Heinhorst, and Cheryl A. Kerfeld. 2010. “Carboxysomal Carbonic Anhydrases: Structure and Role in Microbial CO<sub>2</sub> Fixation.” *Biochimica et Biophysica Acta - Proteins and Proteomics*. <https://doi.org/10.1016/j.bbapap.2009.09.026>.
- Capasso, Clemente, and Claudiu T. Supuran. 2015. “An Overview of the Alpha-, Beta-



and Gamma-Carbonic Anhydrases from Bacteria: Can Bacterial Carbonic Anhydrases Shed New Light on Evolution of Bacteria?” *Journal of Enzyme Inhibition and Medicinal Chemistry*. <https://doi.org/10.3109/14756366.2014.910202>.

Capela, Rita, Rui Moreira, and Francisca Lopes. 2019. “An Overview of Drug Resistance in Protozoal Diseases.” *International Journal of Molecular Sciences*. <https://doi.org/10.3390/ijms20225748>.

Carrijo-Carvalho, Linda Christian, Viviane Peracini Sant’ana, Annette Silva Foronda, Denise de Freitas, and Fabio Ramos de Souza Carvalho. 2017. “Therapeutic Agents and Biocides for Ocular Infections by Free-Living Amoebae of *Acanthamoeba* Genus.” *Survey of Ophthalmology* 62 (2): 203–18. <https://doi.org/10.1016/j.survophthal.2016.10.009>.

Center for Discovery and Innovation in Parasitic Diseases. 2020. “Amebiasis: Global Impact.” *Chemistry and Industry (London)*. [https://doi.org/10.1002/cind.8410\\_2.x](https://doi.org/10.1002/cind.8410_2.x).

Centers for Disease Control and Prevention. 2013. “Global Diarrhea Burden Diarrhea: Common Illness, Global Killer.” *U.S. Department of Health and Human Services*, 1–4. <https://www.cdc.gov/healthywater/global/diarrhea-burden.html>.

Chasen, Nathan M., Beejan Asady, Leandro Lemgruber, Rossiane C. Vommaro, Jessica C. Kissinger, Isabelle Coppens, and Silvia N. J. Moreno. 2017. “A Glycosylphosphatidylinositol-Anchored Carbonic Anhydrase-Related Protein of *Toxoplasma Gondii* Is Important for Rhoptry Biogenesis and Virulence.” *MSphere* 2 (3). <https://doi.org/10.1128/msphere.00027-17>.

Chávez-Munguía, Bibiana, Maritza Omaña-Molina, Mónica González-Lázaro, Arturo González-Robles, Patricia Bonilla, and Adolfo Martínez-Palomo. 2005. “Ultrastructural Study of Encystation and Excystation in *Acanthamoeba Castellani*.” *Journal of Eukaryotic Microbiology* 52 (2): 153–58. <https://doi.org/10.1111/j.1550-7408.2005.04-3273.x>.

Chegwidden, W. R., and N. D. Carter. 2000. “Introduction to the Carbonic Anhydrases.” *EXS*. [https://doi.org/10.1007/978-3-0348-8446-4\\_2](https://doi.org/10.1007/978-3-0348-8446-4_2).

Chelkha, Nisrine, Anthony Levasseur, Pierre Pontarotti, Didier Raoult, Bernard La Scola, and Philippe Colson. 2018. “A Phylogenomic Study of *Acanthamoeba Polyphaga* Draft Genome Sequences Suggests Genetic Exchanges with Giant Viruses.” *Frontiers in Microbiology* 9 (SEP): 408228. <https://doi.org/10.3389/fmicb.2018.02098>.

Chew, Hall F., Elvin H. Yildiz, Kristin M. Hammersmith, Ralph C. Eagle, Christopher J. Rapuano, Peter R. Laibson, Brandon D. Ayres, Ya Ping Jin, and Elisabeth J. Cohen. 2011. “Clinical Outcomes and Prognostic Factors Associated with *Acanthamoeba* Keratitis.” *Cornea* 30 (4): 435–41. <https://doi.org/10.1097/ICO.0b013e3181ec905f>.

Cioli, Donato, Livia Pica-Mattoccia, and Sydney Archer. 1995. “Antischistosomal Drugs:

- Past, Present ... and Future?" *Pharmacology and Therapeutics*.  
[https://doi.org/10.1016/0163-7258\(95\)00026-7](https://doi.org/10.1016/0163-7258(95)00026-7).
- Cioli, Donato, Livia Pica-Mattocchia, Annalisa Basso, and Alessandra Guidi. 2014. "Schistosomiasis Control: Praziquantel Forever?" *Molecular and Biochemical Parasitology*. <https://doi.org/10.1016/j.molbiopara.2014.06.002>.
- Colley, Daniel G., Amaya L. Bustinduy, W. Evan Secor, and Charles H. King. 2014. "Human Schistosomiasis." *The Lancet*, 383:2253–64.  
[https://doi.org/10.1016/S0140-6736\(13\)61949-2](https://doi.org/10.1016/S0140-6736(13)61949-2).
- Cornick, Steve, and Kris Chadee. 2017. "Entamoeba Histolytica: Host Parasite Interactions at the Colonic Epithelium." *Tissue Barriers*.  
<https://doi.org/10.1080/21688370.2017.1283386>.
- Cox, E. H., G. L. McLendon, F. M.M. Morel, T. W. Lane, R. C. Prince, I. J. Pickering, and G. N. George. 2000. "The Active Site Structure of Thalassiosira Weissflogii Carbonic Anhydrase 1." *Biochemistry* 39 (40): 12128–30.  
<https://doi.org/10.1021/bi001416s>.
- Crooks, Gavin E., Gary Hon, John Marc Chandonia, and Steven E. Brenner. 2004. "WebLogo: A Sequence Logo Generator." *Genome Research* 14 (6): 1188–90.  
<https://doi.org/10.1101/gr.849004>.
- Davis, Christopher, and Peter Hackett. 2017. "Advances in the Prevention and Treatment of High Altitude Illness." *Emergency Medicine Clinics of North America*.  
<https://doi.org/10.1016/j.emc.2017.01.002>.
- Doenhoff, Michael J., John R. Kusel, Gerald C. Coles, and Donato Cioli. 2002. "Resistance of Schistosoma Mansoni to Praziquantel: Is There a Problem?" *Transactions of the Royal Society of Tropical Medicine and Hygiene*.  
[https://doi.org/10.1016/S0035-9203\(02\)90405-0](https://doi.org/10.1016/S0035-9203(02)90405-0).
- Duguid, I. G.M., J. K.G. Dart, N. Morlet, B. D.S. Allan, M. Matheson, L. Ficker, and S. Tuft. 1997. "Outcome of Acanthamoeba Keratitis Treated with Polyhexamethyl Biguanide and Propamidine." *Ophthalmology* 104 (10): 1587–92.  
[https://doi.org/10.1016/S0161-6420\(97\)30092-X](https://doi.org/10.1016/S0161-6420(97)30092-X).
- Eisenstein, Barry I. 1990. "The Polymerase Chain Reaction. A New Method of Using Molecular Genetics for Medical Diagnosis." *The New England Journal of Medicine* 322 (3): 178–83. <https://doi.org/10.1056/NEJM199001183220307>.
- El-Sayed, Nagwa M.ostafa, Mohamed S.aad Younis, Azza M.ohamed Elhamshary, Amina I.brahim Abd-Elmaboud, and Shereen M.agdy Kishik. 2014. "Acanthamoeba DNA Can Be Directly Amplified from Corneal Scrapings." *Parasitology Research* 113 (9): 3267–72. <https://doi.org/10.1007/s00436-014-3989-3>.
- Elbaz, Tamer, and Gamal Esmat. 2013. "Hepatic and Intestinal Schistosomiasis:

Review.” *Journal of Advanced Research* 4 (5): 445–52.  
<https://doi.org/10.1016/J.JARE.2012.12.001>.

- Emameh, Reza Zolfaghari, Marianne Kuuslahti, Daniela Vullo, Harlan R Barker, and Claudiu T Supuran. 2015. “Ascaris Lumbricoides  $\beta$  Carbonic Anhydrase: A Potential Target Enzyme for Treatment of Ascariasis.” *Parasites & Vectors*, 1–10.  
<https://doi.org/10.1186/s13071-015-1098-5>.
- Emameh, Reza Zolfaghari, Harlan R Barker, Martti E E Tolvanen, Seppo Parkkila, and Vesa P Hytönen. 2016. “Horizontal Transfer of  $\beta$ -Carbonic Anhydrase Genes from Prokaryotes to Protozoans, Insects, and Nematodes.”  
<https://doi.org/10.1186/s13071-016-1415-7>.
- Eyayu, Tahir, Ayalew Jewaw Zeleke, and Ligabaw Worku. 2020. “Current Status and Future Prospects of Protein Vaccine Candidates against Schistosoma Mansoni Infection.” *Parasite Epidemiology and Control*.  
<https://doi.org/10.1016/j.parepi.2020.e00176>.
- Farzam, Khashayar, and Muhammad Abdullah. 2022. “Acetazolamide.” *XPharm: The Comprehensive Pharmacology Reference*, December, 1–5.  
<https://doi.org/10.1016/B978-008055232-3.61158-4>.
- Feoktistova, Maria, Peter Geserick, and Martin Leverkus. 2016. “Crystal Violet Assay for Determining Viability of Cultured Cells.” *Cold Spring Harbor Protocols* 2016 (4): 343–46. <https://doi.org/10.1101/pdb.prot087379>.
- Fernley, Ross T., Roy D. Wright, John P. Coghlan. 1991. "Radioimmunoassay of carbonic anhydrase VI in saliva and sheep tissues." *Biochem J.* 274 (Pt 2):313-316. doi:10.1042/bj2740313
- Ferraroni, Marta, Sonia Del Prete, Daniela Vullo, Clemente Capasso, and Claudiu T. Supuran. 2015. “Crystal Structure and Kinetic Studies of a Tetrameric Type II  $\beta$ -Carbonic Anhydrase from the Pathogenic Bacterium Vibrio Cholerae.” *Acta Crystallographica Section D: Biological Crystallography* 71 (12): 2449–56.  
<https://doi.org/10.1107/S1399004715018635>.
- Ferry, James G. 2010. “The  $\gamma$  Class of Carbonic Anhydrases.” *Biochimica et Biophysica Acta - Proteins and Proteomics*. <https://doi.org/10.1016/j.bbapap.2009.08.026>.
- Flaherty, Daniel P., Mohamed N. Seleem, and Claudiu T. Supuran. 2021. “Bacterial Carbonic Anhydrases: Underexploited Antibacterial Therapeutic Targets.” *Future Medicinal Chemistry*. <https://doi.org/10.4155/fmc-2021-0207>.
- Freeman, Collin D., Neu E. Klutman, and Kenneth C. Lamp. 1997. “Metronidazole. A Therapeutic Review and Update.” *Drugs*. <https://doi.org/10.2165/00003495-199754050-00003>.
- Fu, Lanxing, F.R.C.Ophth., and Ahmed Gomaa. 2019. “Acanthamoeba Keratitis.” *The New England Journal of Medicine* 381 (3): 274–274.

<https://doi.org/10.1056/NEJMCM1817678>.

- Fuerst, Paul A. 2014. "Insights from the DNA Databases: Approaches to the Phylogenetic Structure of *Acanthamoeba*." *Experimental Parasitology* 145 (S): S39–45. <https://doi.org/10.1016/j.exppara.2014.06.020>.
- Fuerst, Paul A., Gregory C. Booton, and Monica Crary. 2015. "Phylogenetic Analysis and the Evolution of the 18S rRNA Gene Typing System of *Acanthamoeba*." *Journal of Eukaryotic Microbiology*. <https://doi.org/10.1111/jeu.12186>.
- Garcia, Joe G.N., and Shwu Fan Ma. 2005. "Polymerase Chain Reaction: A Landmark in the History of Gene Technology." *Critical Care Medicine* 33 (12 SUPPL.). <https://doi.org/10.1097/01.CCM.0000186782.93865.00>.
- Gasim, Gasim I., Abdelhaleem Bella, and Ishag Adam. 2015. "Schistosomiasis, Hepatitis B and Hepatitis C Co-Infection." *Virology Journal*. <https://doi.org/10.1186/s12985-015-0251-2>.
- Gawryluk, Ryan Mr, and Michael W. Gray. 2010. "Evidence for an Early Evolutionary Emergence of  $\gamma$ -Type Carbonic Anhydrases as Components of Mitochondrial Respiratory Complex I." *BMC Evolutionary Biology* 10 (1). <https://doi.org/10.1186/1471-2148-10-176>.
- Gawryluk, Ryan M.R., Kenneth A. Chisholm, Devanand M. Pinto, and Michael W. Gray. 2012. "Composition of the Mitochondrial Electron Transport Chain in *Acanthamoeba Castellani*: Structural and Evolutionary Insights." *Biochimica et Biophysica Acta - Bioenergetics* 1817 (11): 2027–37. <https://doi.org/10.1016/j.bbabi.2012.06.005>.
- Gendrel, D., J. M. Treluyer, and D. Richard-Lenoble. 2003. "Parasitic Diarrhea in Normal and Malnourished Children." *Fundamental and Clinical Pharmacology* 17 (2): 189–97. <https://doi.org/10.1046/j.1472-8206.2003.00169.x>.
- Gholizadeh, Shima, Ziqing Wang, Xi Chen, Reza Dana, and Nasim Annabi. 2021. "Advanced Nanodelivery Platforms for Topical Ophthalmic Drug Delivery." *Drug Discovery Today*. <https://doi.org/10.1016/j.drudis.2021.02.027>.
- Gilmour, K. M. 2010. "Perspectives on Carbonic Anhydrase." *Comparative Biochemistry and Physiology - A Molecular and Integrative Physiology*. <https://doi.org/10.1016/j.cbpa.2010.06.161>.
- Gryseels, Bruno, Katja Polman, Jan Clerinx, and Luc Kestens. 2006. "Human Schistosomiasis." *Lancet*. [https://doi.org/10.1016/S0140-6736\(06\)69440-3](https://doi.org/10.1016/S0140-6736(06)69440-3).
- Gryseels, Bruno. 2012. "Schistosomiasis." *Infectious Disease Clinics of North America*. <https://doi.org/10.1016/j.idc.2012.03.004>.
- Grzegorek, Katharina, Inge Kroidl, Clarissa Prazeres da Costa, and Camilla Rothe. 2023. "Spectrum of Helminth Infections in Migrants from Sub-Saharan Africa to Europe: A Literature Review." *The American Journal of Tropical Medicine and Hygiene*

108 (6): 1096–1104. <https://doi.org/10.4269/ajtmh.22-0354>.

- Gu, Xiaobin, Xiuhai Lu, Shudan Lin, Xinrui Shi, Yue Shen, Qingsong Lu, Yiyang Yang, et al. 2022. “A Comparative Genomic Approach to Determine the Virulence Factors and Horizontal Gene Transfer Events of Clinical *Acanthamoeba* Isolates.” *Microbiology Spectrum* 10 (2). <https://doi.org/10.1128/spectrum.00025-22>.
- Gundamaraju, Rohit. 2014. “Novel Antipathy for Schistosomiasis—the Most Lethal Ailment of the Tropical Region.” *Asian Pacific Journal of Tropical Biomedicine*. <https://doi.org/10.12980/APJTB.4.2014C831>.
- Hallgren, Jeppe, Konstantinos D. Tsirogos, Mads Damgaard Pedersen, José Juan Almagro Armenteros, Paolo Marcatili, Henrik Nielsen, Anders Krogh, Ole Winther. 2022. “DeepTMHMM predicts alpha and beta transmembrane proteins using deep neural networks” *bioRxiv* 04.08.487609 <https://doi.org/10.1101/2022.04.08.487609>
- Hambrook, Jacob R., and Patrick C. Hanington. 2021. “Immune Evasion Strategies of Schistosomes.” *Frontiers in Immunology*. <https://doi.org/10.3389/fimmu.2020.624178>.
- Haque, R., N. U. Mollah, I. K.M. Ali, K. Alam, A. Eubanks, D. Lyerly, and Jr Petri. 2000. “Diagnosis of Amebic Liver Abscess and Intestinal Infection with the TechLab Entamoeba Histolytica II Antigen Detection and Antibody Tests.” *Journal of Clinical Microbiology* 38 (9): 3235–39. <https://doi.org/10.1128/jcm.38.9.3235-3239.2000>.
- Haque, Rashidul, Christopher D. Huston, Molly Hughes, Eric Houpt, and William A. Jr. Petri. 2003. “Amebiasis.” *The New England Journal of Medicine* 348 (16): 1565–73. <https://doi.org/10.1056/NEJMRA022710>.
- Hart, C. A., and L. W. Umar. 2000. “Diarrhoeal Disease.” *Tropical Doctor* 30 (3): 170–72. <https://doi.org/10.1177/004947550003000321>.
- Hashmey, Rayhan, Robert M. Genta, and A. Clinton White. 1997. “Parasites and Diarrhea. I: Protozoans and Diarrhea.” *Journal of Travel Medicine*. <https://doi.org/10.1111/j.1708-8305.1997.tb00769.x>.
- Hasni, Issam, Julien Andréani, Philippe Colson, and Bernard La Scola. 2020. “Description of Virulent Factors and Horizontal Gene Transfers of Keratitis-Associated Amoeba *Acanthamoeba Triangularis* by Genome Analysis.” *Pathogens* 9 (3). <https://doi.org/10.3390/pathogens9030217>.
- Hennessey, Mathew, Louise Whatford, Sophie Payne-Gifford, Kate F. Johnson, Steven Van Winden, David Barling, and Barbara Häsler. 2020. “Antimicrobial & Antiparasitic Use and Resistance in British Sheep and Cattle: A Systematic Review.” *Preventive Veterinary Medicine*. <https://doi.org/10.1016/j.prevetmed.2020.105174>.

- Hirakawa, Yoshihisa, Miki Senda, Kodai Fukuda, Hong Yang Yu, Masaki Ishida, Masafumi Taira, Kazushi Kinbara, and Toshiya Senda. 2021. "Characterization of a Novel Type of Carbonic Anhydrase That Acts without Metal Cofactors." *BMC Biology* 19 (1). <https://doi.org/10.1186/s12915-021-01039-8>.
- Horn, Matthias, Michael Wagner, Karl Dieter Müller, Ernst N. Schmid, Thomas R. Fritsche, Karl Heinz Schleifer, and Rolf Michel. 2000. "Neochlamydia Hartmannellae Gen. Nov., Sp. Nov. (Parachlamydiaceae), an Endoparasite of the Amoeba Hartmannella Vermiformis." *Microbiology* 146 (5): 1231–39. <https://doi.org/10.1099/00221287-146-5-1231>.
- Horn, Matthias, and Michael Wagner. 2004. "Bacterial Endosymbionts of Free-Living Amoebae." In *Journal of Eukaryotic Microbiology*, 51:509–14. <https://doi.org/10.1111/j.1550-7408.2004.tb00278.x>.
- Huang, Fu Chin, Min Hsiu Shih, Kai Fei Chang, Jian Ming Huang, Jyh Wei Shin, and Wei Chen Lin. 2017. "Characterizing Clinical Isolates of Acanthamoeba Castellani with High Resistance to Polyhexamethylene Biguanide in Taiwan." *Journal of Microbiology, Immunology and Infection* 50 (5): 570–77. <https://doi.org/10.1016/j.jmii.2015.10.011>.
- Hutchings, Matt, Andrew Truman, and Barrie Wilkinson. 2019. "Antibiotics: Past, Present and Future." *Current Opinion in Microbiology*. <https://doi.org/10.1016/j.mib.2019.10.008>.
- Imray, Chris, Alex Wright, Andrew Subudhi, and Robert Roach. 2010. "Acute Mountain Sickness: Pathophysiology, Prevention, and Treatment." *Progress in Cardiovascular Diseases* 52 (6): 467–84. <https://doi.org/10.1016/j.pcad.2010.02.003>.
- Iovieno, Alfonso, Dolena R. Ledee, Darlene Miller, and Eduardo C. Alfonso. 2010. "Detection of Bacterial Endosymbionts in Clinical Acanthamoeba Isolates." *Ophthalmology* 117 (3): 445. <https://doi.org/10.1016/j.ophtha.2009.08.033>.
- Ishibashi, Yasuhisa. 1997. "Acanthamoeba Keratitis." *Ophthalmologica* 211 (Suppl. 1): 39–44. <https://doi.org/10.1159/000310885>.
- Jafari, Elham, Marzieh Rahmani Khajouei, Farshid Hassanzadeh, Gholam Hossein Hakimelahi, and Ghadam Ali Khodarahmi. 2016. "Quinazolinone and Quinazoline Derivatives: Recent Structures with Potent Antimicrobial and Cytotoxic Activities." *Research in Pharmaceutical Sciences*. [/pmc/articles/PMC4794932/](https://pmc/articles/PMC4794932/).
- Jensen, Erik L., Romain Clement, Artemis Kosta, Stephen C. Maberly, and Brigitte Gontero. 2019. "A New Widespread Subclass of Carbonic Anhydrase in Marine Phytoplankton." *ISME Journal* 13 (8): 2094–2106. <https://doi.org/10.1038/s41396-019-0426-8>.
- Kaitin, K. I. 2010. "Deconstructing the Drug Development Process: The New Face of Innovation." *Clinical Pharmacology and Therapeutics*.

<https://doi.org/10.1038/clpt.2009.293>.

- Kantor, Micaella, Anarella Abrantes, Andrea Estevez, Alan Schiller, Jose Torrent, Jose Gascon, Robert Hernandez, and Christopher Ochner. 2018. "Entamoeba Histolytica: Updates in Clinical Manifestation, Pathogenesis, and Vaccine Development." *Canadian Journal of Gastroenterology and Hepatology*. <https://doi.org/10.1155/2018/4601420>.
- Karhumaa Pepe, Jukka Leinonen, Seppo Parkkila, Kari Kaunisto, Juha Tapanainen, Hannu Rajaniemi. 2001. "The identification of secreted carbonic anhydrase VI as a constitutive glycoprotein of human and rat milk." *Proc Natl Acad Sci U S A*. 98(20):11604-11608. doi:10.1073/pnas.121172598
- Kehrenberg, Miriam C.A., and Hagen S. Bachmann. 2022. "Diuretics: A Contemporary Pharmacological Classification?" *Naunyn-Schmiedeberg's Archives of Pharmacology*. <https://doi.org/10.1007/s00210-022-02228-0>.
- Khalifah, R. G. 1971. "The Carbon Dioxide Hydration Activity of Carbonic Anhydrase. I. Stop-Flow Kinetic Studies on the Native Human Isoenzymes B and C." *Journal of Biological Chemistry* 246 (8): 2561–73. <https://pubmed-ncbi-nlm-nih-gov.libproxy.tuni.fi/4994926/>.
- Khan, Naveed Ahmed. 2006. "Acanthamoeba: Biology and Increasing Importance in Human Health." *FEMS Microbiology Reviews*. <https://doi.org/10.1111/j.1574-6976.2006.00023.x>.
- Khiani, Vijay, and Charles H. King. 2009. "Schistosomiasis." In *Medical Parasitology*, 129–35. CRC Press. <https://doi.org/10.1201/9781498713672-29>.
- Kikuchi, Tadashi, Michiko Koga, Shoichi Shimizu, Toshiyuki Miura, Haruhiko Maruyama, and Mikio Kimura. 2013. "Efficacy and Safety of Paromomycin for Treating Amebiasis in Japan." *Parasitology International* 62 (6): 497–501. <https://doi.org/10.1016/j.parint.2013.07.004>.
- Kikutani, Sae, Kensuke Nakajima, Chikako Nagasato, Yoshinori Tsuji, Ai Miyatake, and Yusuke Matsuda. 2016. "Thylakoid Luminal  $\Theta$ -Carbonic Anhydrase Critical for Growth and Photosynthesis in the Marine Diatom *Phaeodactylum Tricornutum*." *Proceedings of the National Academy of Sciences of the United States of America* 113 (35): 9828–33. <https://doi.org/10.1073/pnas.1603112113>.
- Kim, Subin, Jongmin Sung, Jungyoon Yeon, Seung Hun Choi, and Mi Sun Jin. 2019. "Crystal Structure of a Highly Thermostable  $\alpha$ -Carbonic Anhydrase from *Persephonella Marina* Ex-H1." *Molecules and Cells* 42 (6): 460–69. <https://doi.org/10.14348/MOLCELLS.2019.0029>.
- Kimber, M. S. 2000. "The Active Site Architecture of Pisum Sativum Beta -Carbonic Anhydrase Is a Mirror Image of That of Alpha -Carbonic Anhydrases." *The EMBO Journal* 19 (7): 1407–18. <https://doi.org/10.1093/emboj/19.7.1407>.

- Kleppe, K., E. Ohtsuka, R. Kleppe, I. Molineux, and H. G. Khorana. 1971. "Studies on Polynucleotides. XCVI. Repair Replication of Short Synthetic DNA's as Catalyzed by DNA Polymerases." *Journal of Molecular Biology* 56 (2): 341–61. [https://doi.org/10.1016/0022-2836\(71\)90469-4](https://doi.org/10.1016/0022-2836(71)90469-4).
- Köhler, Martina, David Leitsch, Norbert Müller, and Julia Walochnik. 2020. "Validation of Reference Genes for the Normalization of RT-QPCR Gene Expression in *Acanthamoeba* Spp." *Scientific Reports* 10 (1). <https://doi.org/10.1038/s41598-020-67035-0>.
- König, Lena, Alexander Siegl, Thomas Penz, Susanne Haider, Cecilia Wentrup, Julia Polzin, Evelynne Mann, Stephan Schmitz-Esser, Daryl Domman, and Matthias Horn. 2017. "Biphasic Metabolism and Host Interaction of a Chlamydial Symbiont." *MSystems* 2 (3). <https://doi.org/10.1128/mSystems.00202-16>.
- Kopp, Julian, Christoph Slouka, Sophia Ulonska, Julian Kager, Jens Fricke, Oliver Spadiut, and Christoph Herwig. 2018. "Impact of Glycerol as Carbon Source onto Specific Sugar and Inducer Uptake Rates and Inclusion Body Productivity in *E. Coli* BL21(DE3)." *Bioengineering* 5 (1). <https://doi.org/10.3390/bioengineering5010001>.
- Kumar, Amit, Kiran Siwach, Claudiu T. Supuran, and Pawan K. Sharma. 2022. "A Decade of Tail-Approach Based Design of Selective as Well as Potent Tumor Associated Carbonic Anhydrase Inhibitors." *Bioorganic Chemistry*. <https://doi.org/10.1016/j.bioorg.2022.105920>.
- Lacerda, Ana Gomes de, and Madalena Lira. 2021. "Acanthamoeba Keratitis: A Review of Biology, Pathophysiology and Epidemiology." *Ophthalmic and Physiological Optics*. <https://doi.org/10.1111/opo.12752>.
- Laitinen, Olli H., Kari J. Airene, Vesa P. Hytönen, Erik Peltomaa, Anssi J. Mähönen, Thomas Wirth, Miia M. Lind, et al. 2005. "A Multipurpose Vector System for the Screening of Libraries in Bacteria, Insect and Mammalian Cells and Expression in Vivo." *Nucleic Acids Research* 33 (4): 1–10. <https://doi.org/10.1093/nar/gni042>.
- Lakhundi, Sahreena, Naveed Ahmed Khan, and Ruqaiyyah Siddiqui. 2014. "The Effect of Environmental and Physiological Conditions on Excystation of *Acanthamoeba Castellani* Belonging to the T4 Genotype." *Parasitology Research* 113 (8): 2809–16. <https://doi.org/10.1007/s00436-014-3941-6>.
- Lane, Todd W., Mak A. Saito, Graham N. George, Ingrid J. Pickering, Roger C. Prince, and François M.M. Morell. 2005. "Biochemistry: A Cadmium Enzyme from a Marine Diatom." *Nature* 435 (7038): 42. <https://doi.org/10.1038/435042a>.
- Larsson, Lill Inger, and Albert Alm. 1998. "Aqueous Humor Flow in Human Eyes Treated with Dorzolamide and Different Doses of Acetazolamide." *Archives of Ophthalmology* 116 (1): 19–24. <https://doi.org/10.1001/archoph.116.1.19>.
- Lee, Andrew G., Randy Anderson, Randy H. Kardon, and Michael Wall. 2004.



- “Presumed ‘Sulfa Allergy’ in Patients with Intracranial Hypertension Treated with Acetazolamide or Furosemide: Cross-Reactivity, Myth or Reality?” *American Journal of Ophthalmology* 138 (1): 114–18. <https://doi.org/10.1016/j.ajo.2004.02.019>.
- Lemon, Nicole, Elisa Canepa, Marc A. Ilies, and Silvia Fossati. 2021. “Carbonic Anhydrases as Potential Targets Against Neurovascular Unit Dysfunction in Alzheimer’s Disease and Stroke.” *Frontiers in Aging Neuroscience*. <https://doi.org/10.3389/fnagi.2021.772278>.
- Lenstra, J. A. 1995. “The Applications of the Polymerase Chain Reaction in the Life Sciences.” *Cellular and Molecular Biology (Noisy-Le-Grand, France)*. <https://pubmed.ncbi.nlm.nih.gov/7580841/>.
- Levine, Jimmy, Richard K. Dykoski, and Edward N. Janoff. 1995. “Candida-Associated Diarrhea: A Syndrome in Search of Credibility.” *Clinical Infectious Diseases* 21 (4): 881–86. <https://doi.org/10.1093/CLINIDS/21.4.881>.
- Li, Yunhong, Yujing Zhang, and Ying Zhang. 2018. “Research Advances in Pathogenesis and Prophylactic Measures of Acute High Altitude Illness.” *Respiratory Medicine*. <https://doi.org/10.1016/j.rmed.2018.11.004>.
- Lieshout, Lisette Van, and Jaco J. Verweij. 2010. “Newer Diagnostic Approaches to Intestinal Protozoa.” *Current Opinion in Infectious Diseases*. <https://doi.org/10.1097/QCO.0b013e32833de0eb>.
- Liljas, A., and M. Laurberg. 2000. “A Wheel Invented Three Times. The Molecular Structures of the Three Carbonic Anhydrases.” *EMBO Reports* 1 (1): 16–17. <https://doi.org/10.1093/EMBO-REPORTS/KVD016>.
- Llanwarne, Felix, and Helena Helmbj. 2020. “Granuloma Formation and Tissue Pathology in *Schistosoma Japonicum* versus *Schistosoma Mansoni* Infections.” *Parasite Immunology* 43 (2): e12778. <https://doi.org/10.1111/pim.12778>.
- Loftsson, Thorsteinn, Phatsawee Jansook, and Einar Stefánsson. 2012. “Topical Drug Delivery to the Eye: Dorzolamide.” *Acta Ophthalmologica*. <https://doi.org/10.1111/j.1755-3768.2011.02299.x>.
- Lomelino, Carrie L., Jacob T. Andring, and Robert McKenna. 2018. “Crystallography and Its Impact on Carbonic Anhydrase Research.” *International Journal of Medicinal Chemistry* 2018 (September): 1–21. <https://doi.org/10.1155/2018/9419521>.
- Lorenzo-Morales, Jacob, Naveed A. Khan, and Julia Walochnik. 2015. “An Update on *Acanthamoeba Keratitis*: Diagnosis, Pathogenesis and Treatment.” *Parasite*. <https://doi.org/10.1051/parasite/2015010>.
- LoVerde, Philip T. 2019. “Schistosomiasis.” In *Advances in Experimental Medicine and Biology*, 1154:45–70. *Adv Exp Med Biol*. [https://doi.org/10.1007/978-3-030-18616-6\\_3](https://doi.org/10.1007/978-3-030-18616-6_3).
- Luther, Anatol, Matthias Urfer, Michael Zahn, Maik Müller, Shuang Yan Wang, Milon

- Mondal, Alessandra Vitale, et al. 2019. "Chimeric Peptidomimetic Antibiotics against Gram-Negative Bacteria." *Nature* 576 (7787): 452–58. <https://doi.org/10.1038/s41586-019-1665-6>.
- Määttä, Juha A.E., Yael Eisenberg-Domovich, Henri R. Nordlund, Ruchama Hayouka, Markku S. Kulomaa, Oded Livnah, and Vesa P. Hytönen. 2011. "Chimeric Avidin Shows Stability against Harsh Chemical Conditions-Biochemical Analysis and 3D Structure." *Biotechnology and Bioengineering* 108 (3): 481–90. <https://doi.org/10.1002/bit.22962>.
- Madeira, Fábio, Matt Pearce, Adrian R.N. Tivey, Prasad Basutkar, Joon Lee, Ossama Edbali, Nandana Madhusoodanan, Anton Kolesnikov, and Rodrigo Lopez. 2022. "Search and Sequence Analysis Tools Services from EMBL-EBI in 2022." *Nucleic Acids Research* 50 (W1): W276–79. <https://doi.org/10.1093/nar/gkac240>.
- Marbach, Anja, and Katja Bettenbrock. 2012. "Lac Operon Induction in Escherichia Coli: Systematic Comparison of IPTG and TMG Induction and Influence of the Transacetylase LacA." *Journal of Biotechnology* 157 (1): 82–88. <https://doi.org/10.1016/j.jbiotec.2011.10.009>.
- Marciano-Cabral, Francine, and Guy Cabral. 2003. "Acanthamoeba Spp. as Agents of Disease in Humans." *Clinical Microbiology Reviews*. <https://doi.org/10.1128/CMR.16.2.273-307.2003>.
- Mattar, Fathy E, and Thomas J Byers. 1971. "Morphological Changes and the Requirements for Macromolecule Synthesis during Excystment of Acanthamoeba Castellanii." *Journal of Cell Biology* 49 (2): 507–19. <https://doi.org/10.1083/jcb.49.2.507>.
- Maycock, Nicholas J.R., and Rakesh Jayaswal. 2016. "Update on Acanthamoeba Keratitis: Diagnosis, Treatment, and Outcomes." *Cornea* 35 (5): 713–20. <https://doi.org/10.1097/ICO.0000000000000804>.
- Mboge, Mam Y., Brian P. Mahon, Robert McKenna, and Susan C. Frost. 2018. "Carbonic Anhydrases: Role in PH Control and Cancer." *Metabolites*. <https://doi.org/10.3390/metabo8010019>.
- McBride, James, Paul R. Ingram, Fiona L. Henriquez, and Craig W. Roberts. 2005. "Development of Colorimetric Microtiter Plate Assay for Assessment of Antimicrobials against Acanthamoeba." *Journal of Clinical Microbiology* 43 (2): 629–34. <https://doi.org/10.1128/JCM.43.2.629-634.2005>.
- McKenna, Robert, and Claudiu T. Supuran. 2014. "Carbonic Anhydrase Inhibitors Drug Design." *Sub-Cellular Biochemistry* 75: 291–323. [https://doi.org/10.1007/978-94-007-7359-2\\_15](https://doi.org/10.1007/978-94-007-7359-2_15).
- McManus, Donald P., David W. Dunne, Moussa Sacko, Jürg Utzinger, Birgitte J. Vennervald, and Xiao Nong Zhou. 2018. "Schistosomiasis." *Nature Reviews Disease Primers* 4 (1). <https://doi.org/10.1038/s41572-018-0013-8>.

- Mechrgui, Monia, and Suleman Kanani. 2022. "The Ophthalmic Side Effects of Topiramate: A Review." *Cureus* 14 (8). <https://doi.org/10.7759/cureus.28513>.
- Meldrum, N. U., and F. J.W. Roughton. 1933a. "Carbonic Anhydrase and the State of Carbon Dioxide in Blood [6]." *Nature*. <https://doi.org/10.1038/131874b0>.
- Meldrum, N. U., and F. J.W. Roughton. 1933b. "Carbonic Anhydrase. Its Preparation and Properties." *The Journal of Physiology* 80 (2): 113–42. <https://doi.org/10.1113/jphysiol.1933.sp003077>.
- Mirabedini, Zahra, Naveed Ahmed Khan, Maryam Niyati, Ehsan Javanmard, Mohammad Hamedanipour, and Zahra Arab-Mazar. 2022. "Can Free Living Acanthamoeba Act as a Trojan Horse for SARS-Cov-2 on Viral Survival and Transmission in the Environment? A Narrative Review." *Iranian Journal of Parasitology*. Iran J Parasitol. <https://doi.org/10.18502/ijpa.v17i2.9529>.
- Mirahmadi, Hadi, Maryam Mansouri Nia, Adel Ebrahimzadeh, Ahmad Mehravaran, Reza Shafiei, Mohammad Taghi Rahimi, Reza Zolfaghari Emameh, and Harlan R. Barker. 2019. "Genotyping Determination of Acanthamoeba Strains: An Original Study and a Systematic Review in Iran." *Journal of Water and Health* 17 (5): 717–27. <https://doi.org/10.2166/wh.2019.048>.
- Moseley, S. L., I. Huq, A. R.M.A. Alim, M. So, M. Samadpour-Motalebi, and S. Falkow. 1980. "Detection of Enterotoxigenic Escherichia Coli by DNA Colony Hybridization." *Journal of Infectious Diseases* 142 (6): 892–98. <https://doi.org/10.1093/infdis/142.6.892>.
- Nagaraja, Shruti; Ankri, Serge. 2019. "Target Identification and Intervention Strategies against Amebiasis." *Drug Resistance Updates* 44 (May): 1–14. <https://doi.org/10.1016/j.drup.2019.04.003>.
- Naghavi, Mohsen, Haidong Wang, Rafael Lozano, Adrian Davis, Xiaofeng Liang, Maigeng Zhou, Stein Emil Vollset, et al. 2015. "Global, Regional, and National Age-Sex Specific All-Cause and Cause-Specific Mortality for 240 Causes of Death, 1990-2013: A Systematic Analysis for the Global Burden of Disease Study 2013." *Lancet* 385 (9963): 117. [https://doi.org/10.1016/S0140-6736\(14\)61682-2](https://doi.org/10.1016/S0140-6736(14)61682-2).
- Nation, Catherine S., Akram A. Da'dara, Jeffrey K. Marchant, and Patrick J. Skelly. 2020. "Schistosome Migration in the Definitive Host." *PLoS Neglected Tropical Diseases*. <https://doi.org/10.1371/journal.pntd.0007951>.
- Nayak, Kritika, Manisha Vinayak Choudhari, Swati Bagul, Tejas Avinash Chavan, and Manju Misra. 2020. "Ocular Drug Delivery Systems." In *Drug Delivery Devices and Therapeutic Systems*, 515–66. <https://doi.org/10.1016/B978-0-12-819838-4.00006-7>.
- Neish, Arthur Charles. 1939. "Studies on Chloroplasts." *Biochemical Journal* 33 (3): 300–308. <https://doi.org/10.1042/bj0330300>.

- Nelwan, Martin L. 2019. "Schistosomiasis: Life Cycle, Diagnosis, and Control." *Current Therapeutic Research - Clinical and Experimental*.  
<https://doi.org/10.1016/j.curtheres.2019.06.001>.
- Nesher, Ronit, and Uriel Ticho. 2003. "Switching from Systemic to the Topical Carbonic Anhydrase Inhibitor Dorzolamide: Effect on the Quality of Life of Glaucoma Patients with Drug-Related Side Effects." *Israel Medical Association Journal* 5 (4): 260–63. <https://pubmed.ncbi.nlm.nih.gov/14509130/>.
- Neves, Precil Diego Miranda de Menezes, Leticia Barbosa Jorge, Livia Barreira Cavalcante, Denise Malheiros, Viktoria Woronik, and Cristiane Bitencourt Dias. 2020. "Schistosomiasis-Associated Glomerulopathy: Clinical Aspects, Pathological Characteristics, and Renal Outcomes." *Clinical Nephrology* 93 (5): 251–61. <https://doi.org/10.5414/cn110013>.
- Niederkorn, Jerry Y. 2021. "The Biology of Acanthamoeba Keratitis." *Experimental Eye Research*. <https://doi.org/10.1016/j.exer.2020.108365>.
- Nocentini, Alessio, Clemente Capasso, and Claudiu T. Supuran. 2023. "Carbonic Anhydrase Inhibitors as Novel Antibacterials in the Era of Antibiotic Resistance: Where Are We Now?" *Antibiotics*. <https://doi.org/10.3390/antibiotics12010142>.
- Ogbera, Anthonia O., and Ehiaghe Anaba. 2000. *Protozoa and Endocrine Dysfunction. Endotext*. <https://www.ncbi.nlm.nih.gov/books/NBK568562/>.
- Ortega-Rivas, Antonio, José M. Padrón, Basilio Valladares, and Hany M. Elsheikha. 2016. "Acanthamoeba Castellanii: A New High-Throughput Method for Drug Screening in Vitro." *Acta Tropica* 164: 95–99. <https://doi.org/10.1016/j.actatropica.2016.09.006>.
- Park, Haewon, Bongkeun Song, and François M.M. Morel. 2007. "Diversity of the Cadmium-Containing Carbonic Anhydrase in Marine Diatoms and Natural Waters." *Environmental Microbiology* 9 (2): 403–13. <https://doi.org/10.1111/j.1462-2920.2006.01151.x>.
- Pastorekova, Silvia, Seppo Parkkila, Jaromir Pastorek, and Claudiu T. Supuran. 2004. "Carbonic Anhydrases: Current State of the Art, Therapeutic Applications and Future Prospects." *Journal of Enzyme Inhibition and Medicinal Chemistry*. <https://doi.org/10.1080/14756360410001689540>.
- Paulos, Silvia, José María Saugar, Aida De Lucio, Isabel Fuentes, María Mateo, and David Carmena. 2019. "Comparative Performance Evaluation of Four Commercial Multiplex Real-Time PCR Assays for the Detection of the Diarrhoea-Causing Protozoa Cryptosporidium Hominis/Parvum, Giardia Duodenalis and Entamoeba Histolytica." *PLoS ONE* 14 (4). <https://doi.org/10.1371/journal.pone.0215068>.
- Petreni, Andrea, Viviana De Luca, Andrea Scaloni, Alessio Nocentini, Clemente Capasso, and Claudiu T. Supuran. 2021. "Anion Inhibition Studies of the Zn(II)-

Bound  $\iota$ -Carbonic Anhydrase from the Gram-Negative Bacterium *Burkholderia Territorii*.” *Journal of Enzyme Inhibition and Medicinal Chemistry* 36 (1): 372–76. <https://doi.org/10.1080/14756366.2020.1867122>.

- Pinard, Melissa A., Shalaka R. Lotlikar, Christopher D. Boone, Daniela Vullo, Claudiu T. Supuran, Marianna A. Patrauchan, and Robert McKenna. 2015. “Structure and Inhibition Studies of a Type II Beta-Carbonic Anhydrase PsCA3 from *Pseudomonas Aeruginosa*.” *Bioorganic and Medicinal Chemistry* 23 (15): 4831–38. <https://doi.org/10.1016/j.bmc.2015.05.029>.
- Pinard, Melissa A., Brian Mahon, and Robert McKenna. 2015. “Probing the Surface of Human Carbonic Anhydrase for Clues towards the Design of Isoform Specific Inhibitors.” *BioMed Research International*. <https://doi.org/10.1155/2015/453543>.
- Powers, J. H. 2004. “Antimicrobial Drug Development - The Past, the Present, and the Future.” *Clinical Microbiology and Infection, Supplement* 10 (4): 23–31. <https://doi.org/10.1111/j.1465-0691.2004.1007.x>.
- Prete, Sonia Del, Daniela Vullo, Viviana De Luca, Claudiu T. Supuran, and Clemente Capasso. 2014. “Biochemical Characterization of the  $\delta$ -Carbonic Anhydrase from the Marine Diatom *Thalassiosira Weissflogii*, TweCA.” *Journal of Enzyme Inhibition and Medicinal Chemistry* 29 (6): 906–11. <https://doi.org/10.3109/14756366.2013.868599>.
- Prete, Sonia Del, Alessio Nocentini, Claudiu T. Supuran, and Clemente Capasso. 2020. “Bacterial  $\iota$ -Carbonic Anhydrase: A New Active Class of Carbonic Anhydrase Identified in the Genome of the Gram-Negative Bacterium *Burkholderia Territorii*.” *Journal of Enzyme Inhibition and Medicinal Chemistry* 35 (1): 1060–68. <https://doi.org/10.1080/14756366.2020.1755852>.
- Provensi, Gustavo, Fabrizio Carta, Alessio Nocentini, Claudiu T. Supuran, Fiorella Casamenti, M. Beatrice Passani, and Silvia Fossati. 2019. “A New Kid on the Block? Carbonic Anhydrases as Possible New Targets in Alzheimer’s Disease.” *International Journal of Molecular Sciences*. <https://doi.org/10.3390/ijms20194724>.
- Purcell, Andrew, Rachel Lau, and Andrea K. Boggild. 2017. “Azithromycin and Doxycycline Attenuation of *Acanthamoeba* Virulence in a Human Corneal Tissue Model.” *Journal of Infectious Diseases* 215 (8): 1303–11. <https://doi.org/10.1093/infdis/jiw410>.
- Putaporntip, Chaturong, Napaporn Kuamsab, Warisa Nuprasert, Rattanaporn Rojrung, Urassaya Pattanawong, Taweesak Tia, Surasuk Yanmanee, and Somchai Jongwutiwes. 2021. “Analysis of *Acanthamoeba* Genotypes from Public Freshwater Sources in Thailand Reveals a New Genotype, T23 *Acanthamoeba Bangkokensis* Sp. Nov.” *Scientific Reports* 11 (1): 17290. <https://doi.org/10.1038/s41598-021-96690-0>.
- Quach, Jeanie, Joëlle St-Pierre, and Kris Chadee. 2014. “The Future for Vaccine Development against *Entamoeba Histolytica*.” *Human Vaccines and*

*Immunotherapeutics*. <https://doi.org/10.4161/hv.27796>.

- Qvarnstrom, Yvonne, Govinda S. Visvesvara, Rama Sriram, and Alexandre J. Da Silva. 2006. "Multiplex Real-Time PCR Assay for Simultaneous Detection of *Acanthamoeba* Spp., *Balamuthia Mandrillaris*, and *Naegleria Fowleri*." *Journal of Clinical Microbiology* 44 (10): 3589–95. <https://doi.org/10.1128/JCM.00875-06>.
- Rahmani, Abolfazl, Masoud Baei, Maryam Rostamtabar, Ahmad Karkhah, Solmaz Alizadeh, Mehdi Tourani, and Hamid Reza Nouri. 2019. "Development of a Conserved Chimeric Vaccine Based on Helper T-Cell and CTL Epitopes for Induction of Strong Immune Response against *Schistosoma Mansoni* Using Immunoinformatics Approaches." *International Journal of Biological Macromolecules* 141 (December): 125–36. <https://doi.org/10.1016/j.ijbiomac.2019.08.259>.
- Rayamajhee, Binod, Dinesh Subedi, Hari Kumar Peguda, Mark Duncan Willcox, Fiona L. Henriquez, and Nicole Carnt. 2021. "A Systematic Review of Intracellular Microorganisms within *Acanthamoeba* to Understand Potential Impact for Infection." *Pathogens*. <https://doi.org/10.3390/pathogens10020225>.
- Rayamajhee, Binod, Mark D.P. Willcox, Fiona L. Henriquez, Constantinos Petsoglou, Dinesh Subedi, and Nicole Carnt. 2022. "Acanthamoeba, an Environmental Phagocyte Enhancing Survival and Transmission of Human Pathogens." *Trends in Parasitology*. <https://doi.org/10.1016/j.pt.2022.08.007>.
- Rice, Christopher A., Beatrice L. Colon, Emily Chen, Mitchell V. Hull, and Dennis E. Kyle. 2020. "Discovery of Repurposing Drug Candidates for the Treatment of Diseases Caused by Pathogenic Free-Living Amoebae." *PLoS Neglected Tropical Diseases* 14 (9): 1–21. <https://doi.org/10.1371/journal.pntd.0008353>.
- Rivière, Delphine, Florence Ménard Szczebara, Jean Marc Berjeaud, Jacques Frère, and Yann Héchard. 2006. "Development of a Real-Time PCR Assay for Quantification of *Acanthamoeba* Trophozoites and Cysts." *Journal of Microbiological Methods* 64 (1): 78–83. <https://doi.org/10.1016/j.mimet.2005.04.008>.
- Robert, Xavier, Patrice Gouet. 2014. "Deciphering key features in protein structures with the new ENDscript server." *Nucleic Acids Res.* doi:10.1093/nar/gku316
- Rong, Guoguang, Yuqiao Zheng, Yin Chen, Yanjun Zhang, Peixi Zhu, and Mohamad Sawan. 2022. "COVID-19 Diagnostic Methods and Detection Techniques." In *Encyclopedia of Sensors and Biosensors: Volume 1-4, First Edition*, 1–4:17–32. <https://doi.org/10.1016/B978-0-12-822548-6.00080-7>.
- Rosenberg, Lisa F., Theodore Krupin, Li Qi Tang, Pauline H. Hong, and Jon M. Ruderman. 1998. "Combination of Systemic Acetazolamide and Topical Dorzolamide in Reducing Intraocular Pressure and Aqueous Humor Formation." *Ophthalmology* 105 (1): 88–93. [https://doi.org/10.1016/S0161-6420\(98\)91421-X](https://doi.org/10.1016/S0161-6420(98)91421-X).
- Rowlett, Roger S. 2010. "Structure and Catalytic Mechanism of the  $\beta$ -Carbonic Anhydrases." *Biochimica et Biophysica Acta - Proteins and Proteomics*.

<https://doi.org/10.1016/j.bbapap.2009.08.002>.

- Rugel, Anastasia R., Meghan A. Guzman, Alexander B. Taylor, Frédéric D. Chevalier, Reid S. Tarpley, Stanton F. McHardy, Xiaohang Cao, et al. 2020. “Why Does Oxamniquine Kill *Schistosoma Mansoni* and Not *S. Haematobium* and *S. Japonicum*?” *International Journal for Parasitology: Drugs and Drug Resistance* 13 (August): 8–15. <https://doi.org/10.1016/j.ijpddr.2020.04.001>.
- Samarawickrema, Nirma A., David M. Brown, Jacqueline A. Upcroft, Nitaya Thammapalerd, and Peter Upcroft. 1997. “Involvement of Superoxide Dismutase and Pyruvate:ferredoxin Oxidoreductase in Mechanisms of Metronidazole Resistance in *Entamoeba Histolytica*.” *Journal of Antimicrobial Chemotherapy* 40 (6): 833–40. <https://doi.org/10.1093/jac/40.6.833>.
- Sangkanu, Suthinee, Watcharapong Mitsuwan, Wilawan Mahabusarakam, Tajudeen O. Jimoh, Polrat Wilairatana, Ana Paula Girol, Ajoy K. Verma, et al. 2021. “Anti-Acanthamoeba Synergistic Effect of Chlorhexidine and Garcinia Mangostana Extract or  $\alpha$ -Mangostin against *Acanthamoeba Triangularis* Trophozoite and Cyst Forms.” *Scientific Reports* 11 (1): 8053. <https://doi.org/10.1038/s41598-021-87381-x>.
- Sardar, Sanjib K., Seiki Kobayashi, Koushik Das, Yumiko Saito-Nakano, Shanta Dutta, Tomoyoshi Nozaki, and Sandipan Ganguly. 2023. “Development of a Simple PCR–RFLP Technique for Detection and Differentiation of *E. Histolytica*, *E. Dispar* and *E. Moshkovskii*.” *Parasitology Research* 122 (1): 139–44. <https://doi.org/10.1007/s00436-022-07706-1>.
- Schaumberg, Debra A., Kristin K. Snow, and M. Reza Dana. 1998. “The Epidemic of *Acanthamoeba Keratitis*: Where Do We Stand?” *Cornea*. <https://doi.org/10.1097/00003226-199801000-00001>.
- Scozzafava, Andrea, and Claudiu T. Supuran. 2014. “Glaucoma and the Applications of Carbonic Anhydrase Inhibitors.” *Sub-Cellular Biochemistry* 75: 349–59. [https://doi.org/10.1007/978-94-007-7359-2\\_17](https://doi.org/10.1007/978-94-007-7359-2_17).
- Sebastián-Pérez, Víctor, Ines Sifaoui, María Reyes-Batlle, Angélica Domínguez-De Barros, Atteneri López-Arencia, Nuria E. Campillo, José E. Piñero, Jacob Lorenzo-Morales, and Carmen Gil. 2021. “Discovery of Amoebicidal Compounds by Combining Computational and Experimental Approaches.” *Antimicrobial Agents and Chemotherapy* 65 (2). <https://doi.org/10.1128/AAC.01749-20>.
- Shahbaz, Muhammad Saquib, Ayaz Anwar, Syed Muhammad Saad, Kanwal, Areeba Anwar, Khalid Mohammed Khan, Ruqaiyyah Siddiqui, and Naveed Ahmed Khan. 2020. “Antiamoebic Activity of 3-Aryl-6,7-Dimethoxyquinazolin-4(3H)-One Library against *Acanthamoeba Castellani*.” *Parasitology Research* 119 (7): 2327–35. <https://doi.org/10.1007/s00436-020-06710-7>.
- Shahidzadeh, Rassa, Antone Opekun, Akiko Shiotani, and David Y. Graham. 2005. “Effect of the Carbonic Anhydrase Inhibitor, Acetazolamide, on *Helicobacter*

- Pylori Infection in Vivo: A Pilot Study.” *Helicobacter* 10 (2): 136–38. <https://doi.org/10.1111/j.1523-5378.2005.00306.x>.
- Shirley, Debbie Ann T., Laura Farr, Koji Watanabe, and Shannon Moonah. 2018. “A Review of the Global Burden, New Diagnostics, and Current Therapeutics for Amebiasis.” *Open Forum Infectious Diseases* 5 (7). <https://doi.org/10.1093/ofid/ofy161>.
- Showler, Adrienne J., and Andrea K. Boggild. 2013. “Entamoeba Histolytica.” *CMAJ: Canadian Medical Association Journal = Journal de l'Association Médicale Canadienne* 185 (12): 1064. <https://doi.org/10.1503/cmaj.121576>.
- Sievers, Fabian, Andreas Wilm, David Dineen, Toby J. Gibson, Kevin Karplus, Weizhong Li, Rodrigo Lopez, et al. 2011. “Fast, Scalable Generation of High-Quality Protein Multiple Sequence Alignments Using Clustal Omega.” *Molecular Systems Biology* 7. <https://doi.org/10.1038/msb.2011.75>.
- Silva, Vinícius Barros Ribeiro da, Bruna Rafaella Koresch Leiva Campos, Jamerson Ferreira de Oliveira, Jean Luc Decout, and Maria do Carmo Alves de Lima. 2017. “Medicinal Chemistry of Antischistosomal Drugs: Praziquantel and Oxamniquine.” *Bioorganic and Medicinal Chemistry*. <https://doi.org/10.1016/j.bmc.2017.04.031>.
- Simone, Giuseppina De, Anna Di Fiore, Clemente Capasso, and Claudiu T. Supuran. 2015. “The Zinc Coordination Pattern in the  $\eta$ -Carbonic Anhydrase from Plasmodium Falciparum Is Different from All Other Carbonic Anhydrase Genetic Families.” *Bioorganic and Medicinal Chemistry Letters* 25 (7): 1385–89. <https://doi.org/10.1016/j.bmcl.2015.02.046>.
- Singh, Srishti, Carrie L. Lomelino, Mam Y. Mboge, Susan C. Frost, and Robert McKenna. 2018. “Cancer Drug Development of Carbonic Anhydrase Inhibitors beyond the Active Site.” *Molecules*. <https://doi.org/10.3390/molecules23051045>.
- Siqueira, Lidiany da Paixão, Danilo Augusto Ferreira Fontes, Cindy Siqueira Britto Aguilera, Taysa Renata Ribeiro Timóteo, Matheus Alves Ângelos, Laysa Creusa Paes Barreto Barros Silva, Camila Gomes de Melo, Larissa Araújo Rolim, Rosali Maria Ferreira da Silva, and Pedro José Rolim Neto. 2017. “Schistosomiasis: Drugs Used and Treatment Strategies.” *Acta Tropica*. <https://doi.org/10.1016/j.actatropica.2017.08.002>.
- Spellberg, Brad, John H. Powers, Eric P. Brass, Loren G. Miller, and John E. Edwards. 2004. “Trends in Antimicrobial Drug Development: Implications for the Future.” *Clinical Infectious Diseases* 38 (9): 1279–86. <https://doi.org/10.1086/420937>.
- Stanley, Samuel L. 2003. “Amoebiasis.” *Lancet*, 361:1025–34. [https://doi.org/10.1016/S0140-6736\(03\)12830-9](https://doi.org/10.1016/S0140-6736(03)12830-9).
- Starkey, Lindsay A., and Byron L. Blagburn. 2022. “Antiparasitic Drugs.” *Greene's Infectious Diseases of the Dog and Cat, Fifth Edition*, 149–60.



<https://doi.org/10.1016/B978-0-323-50934-3.00013-6>.

- Stauffer, William; Ravdin, Jonathan I. 2003. "Entamoeba Histolytica: An Update." *Current Opinion in Infectious Diseases* 16 (5): 479–85. <https://doi.org/10.1097/00001432-200310000-00016>
- Stothard, Diane R., Jill M. Schroeder-Diedrich, Mohammad H. Awwad, Rebecca J. Gast, Dolena R. Ledee, Salvador Rodriguez-Zaragoza, Chantal L. Dean, Paul A. Fuerst, and Thomas J. Byers. 1998. "The Evolutionary History of the Genus *Acanthamoeba* and the Identification of Eight New 18S rRNA Gene Sequence Types." *Journal of Eukaryotic Microbiology*, 45:45–54. <https://doi.org/10.1111/j.1550-7408.1998.tb05068.x>.
- Sun, Miao Kun, Wei Qin Zhao, Thomas J. Nelson, and Daniel L. Alkon. 2001. "Theta Rhythm of Hippocampal CA1 Neuron Activity: Gating by GABAergic Synaptic Depolarization." *Journal of Neurophysiology* 85 (1): 269–79. <https://doi.org/10.1152/jn.2001.85.1.269>.
- Supuran, Claudiu T. 2018. "Carbonic Anhydrases and Metabolism." *Metabolites* 8 (2). <https://doi.org/10.3390/METABO8020025>.
- Supuran, Claudiu T., Abdulmalik Saleh Alfawaz Altamimi, and Fabrizio Carta. 2019. "Carbonic Anhydrase Inhibition and the Management of Glaucoma: A Literature and Patent Review 2013-2019." *Expert Opinion on Therapeutic Patents*. <https://doi.org/10.1080/13543776.2019.1679117>.
- Supuran, Claudiu T., and Clemente Capasso. 2020. "Antibacterial Carbonic Anhydrase Inhibitors: An Update on the Recent Literature." *Expert Opinion on Therapeutic Patents*. <https://doi.org/10.1080/13543776.2020.1811853>.
- Supuran, Claudiu T.. 2022. "Anti-Obesity Carbonic Anhydrase Inhibitors: Challenges and Opportunities." *Journal of Enzyme Inhibition and Medicinal Chemistry*. <https://doi.org/10.1080/14756366.2022.2121393>.
- Syrjänen, Leo, Alane Beatriz Vermelho, Igor De Almeida Rodrigues, Suzana Corte-Real, Terhi Salonen, Peiwen Pan, Daniela Vullo, Seppo Parkkila, Clemente Capasso, and Claudiu T. Supuran. 2013. "Cloning, Characterization, and Inhibition Studies of a  $\beta$ -Carbonic Anhydrase from *Leishmania Donovanii* Chagasi, the Protozoan Parasite Responsible for Leishmaniasis." *Journal of Medicinal Chemistry* 56 (18): 7372–81. <https://doi.org/10.1021/jm400939k>.
- Templeton, N. S. 1992. "The Polymerase Chain Reaction. History, Methods, and Applications." *Diagnostic Molecular Pathology: The American Journal of Surgical Pathology, Part B* 1 (1): 58–72. <https://doi.org/10.1097/00019606-199203000-00008>.
- Terreni, Marco, Marina Taccani, and Massimo Pregnolato. 2021. "New Antibiotics for Multidrug-Resistant Bacterial Strains: Latest Research Developments and Future Perspectives." *Molecules*. <https://doi.org/10.3390/molecules26092671>.

- Tonissen, Kathryn F., and Sally Ann Poulsen. 2021. "Carbonic Anhydrase XII Inhibition Overcomes P-Glycoprotein-Mediated Drug Resistance: A Potential New Combination Therapy in Cancer." *Cancer Drug Resistance*. <https://doi.org/10.20517/cdr.2020.110>.
- Troeger, Christopher, Mohammad Forouzanfar, Puja C. Rao, Ibrahim Khalil, Alexandria Brown, Robert C. Reiner, Nancy Fullman, et al. 2017. "Estimates of Global, Regional, and National Morbidity, Mortality, and Aetiologies of Diarrhoeal Diseases: A Systematic Analysis for the Global Burden of Disease Study 2015." *The Lancet Infectious Diseases* 17 (9): 909–48. [https://doi.org/10.1016/S1473-3099\(17\)30276-1](https://doi.org/10.1016/S1473-3099(17)30276-1).
- Urbanski, Linda J., Anna Di Fiore, Latifeh Azizi, Vesa P. Hytönen, Marianne Kuuslahti, Martina Buonanno, Simona M. Monti, et al. 2020. "Biochemical and Structural Characterisation of a Protozoan Beta-Carbonic Anhydrase from *Trichomonas Vaginalis*." *Journal of Enzyme Inhibition and Medicinal Chemistry* 35 (1): 1292–99. <https://doi.org/10.1080/14756366.2020.1774572>.
- Vale, Nuno, Maria João Gouveia, Gabriel Rinaldi, Paul J. Brindley, Fátima Gärtner, and José M. Correia Da Costa. 2017. "Praziquantel for Schistosomiasis: Single-Drug Metabolism Revisited, Mode of Action, and Resistance." *Antimicrobial Agents and Chemotherapy*. <https://doi.org/10.1128/AAC.02582-16>.
- Vasconcelos, Mariana Pinheiro Alves, Juan Camilo Sánchez-Arcila, Luciana Peres, Paulo Sérgio Fonseca de Sousa, Marcelo Augusto dos Santos Alvarenga, Júlio Castro-Alves, Maria de Fatima Ferreira-da-Cruz, Marilza Maia-Herzog, and Joseli Oliveira-Ferreira. 2023. "Malarial and Intestinal Parasitic Co-Infections in Indigenous Populations of the Brazilian Amazon Rainforest." *Journal of Infection and Public Health* 16 (4): 603–10. <https://doi.org/10.1016/j.jiph.2023.02.012>.
- Verweij, Jaco J., and C. Rune Stensvold. 2014. "Molecular Testing for Clinical Diagnosis and Epidemiological Investigations of Intestinal Parasitic Infections." *Clinical Microbiology Reviews* 27 (2): 371–418. <https://doi.org/10.1128/CMR.00122-13>.
- Wan, Yingfeng, Katherine G. Holste, Ya Hua, Richard F. Keep, and Guohua Xi. 2023. "Brain Edema Formation and Therapy after Intracerebral Hemorrhage." *Neurobiology of Disease* 176 (January): 105948. <https://doi.org/10.1016/j.nbd.2022.105948>.
- Wassmann, Claudia, Andrea Hellberg, Egbert Tannich, and Iris Bruchhaus. 1999. "Metronidazole Resistance in the Protozoan Parasite *Entamoeba Histolytica* Is Associated with Increased Expression of Iron-Containing Superoxide Dismutase and Peroxiredoxin and Decreased Expression of Ferredoxin 1 and Flavin Reductase." *Journal of Biological Chemistry* 274 (37): 26051–56. <https://doi.org/10.1074/jbc.274.37.26051>.
- Wong, Marisa L., and Juan F. Medrano. 2005. "Real-Time PCR for mRNA Quantitation." *BioTechniques*. <https://doi.org/10.2144/05391RV01>.

- Worms ; Thomson, Allen, F D R S Ivi, T Barker, and M D Herbert. 1856. "Parasites of the Human Body." *Journal of Public Health, and Sanitary Review* 2 (6): 113. <https://doi.org/10.1093/ajcp/43.3.375>.
- Xu, Yan, Liang Feng, Philip D. Jeffrey, Yigong Shi, and François M.M. Morel. 2008. "Structure and Metal Exchange in the Cadmium Carbonic Anhydrase of Marine Diatoms." *Nature* 452 (7183): 56–61. <https://doi.org/10.1038/nature06636>.
- Yang, Samuel, and Richard E. Rothman. 2004. "PCR-Based Diagnostics for Infectious Diseases: Uses, Limitations, and Future Applications in Acute-Care Settings." *Lancet Infectious Diseases*. [https://doi.org/10.1016/S1473-3099\(04\)01044-8](https://doi.org/10.1016/S1473-3099(04)01044-8).
- Yrjänäinen, Alma, Maarit S. Patrikainen, Latifeh Azizi, Martti E. E. Tolvanen, Mikko Laitaoja, Janne Jänis, Vesa P. Hytönen, Alessio Nocentini, Claudiu T. Supuran, & Seppo Parkkila. 2022. "Biochemical and Biophysical Characterization of Carbonic Anhydrase VI from Human Milk and Saliva." *The protein journal* 41(4-5), 489–503. <https://doi.org/10.1007/s10930-022-10070-9>
- Yu, Jun Jun, Ya Lin Hu, Cheng Zheng Liu, Shuai Bin Wu, Zi Jian Zheng, Ze Hua Cui, Li Chen, et al. 2023. "ARSCP: An Antimicrobial Residue Surveillance Cloud Platform for Animal-Derived Foods." *Science of the Total Environment* 858 (February): 159807. <https://doi.org/10.1016/j.scitotenv.2022.159807>.
- Yuan, Lin, Minghua Wang, Tianqi Liu, Yinsheng Lei, Qiang Miao, Quan Li, Hongxing Wang, Guoqing Zhang, Yinglong Hou, and Xiaotian Chang. 2019. "Carbonic Anhydrase 1-Mediated Calcification Is Associated With Atherosclerosis, and Methazolamide Alleviates Its Pathogenesis." *Frontiers in Pharmacology* 10 (July): 766. <https://doi.org/10.3389/fphar.2019.00766>.
- Zhang, Yuheng, Xizhan Xu, Zhenyu Wei, Kai Cao, Zijun Zhang, and Qingfeng Liang. 2023. "The Global Epidemiology and Clinical Diagnosis of Acanthamoeba Keratitis." *Journal of Infection and Public Health*. <https://doi.org/10.1016/j.jiph.2023.03.020>.
- Zhao, Shanrong, Zhan Ye, and Robert Stanton. 2020. "Misuse of RPKM or TPM Normalization When Comparing across Samples and Sequencing Protocols." *RNA* 26 (8): 903–9. <https://doi.org/10.1261/RNA.074922.120>.
- Zhao, Yongxi, Feng Chen, Qian Li, Lihua Wang, and Chunhai Fan. 2015. "Isothermal Amplification of Nucleic Acids." *Chemical Reviews*. <https://doi.org/10.1021/acs.chemrev.5b00428>.
- Zimmerman, Sabrina A., Jean Francois Tomb, and James G. Ferry. 2010. "Characterization of CamH from Methanosarcina Thermophila, Founding Member of a Subclass of the  $\gamma$  Class of Carbonic Anhydrases." *Journal of Bacteriology* 192 (5): 1353–60. <https://doi.org/10.1128/JB.01164-09>.
- Zolfaghari Emameh, Reza, Marianne Kuuslahti, Hassan Nosrati, Hannes Lohi, and Seppo Parkkila. 2020. "Assessment of Databases to Determine the Validity of  $\beta$ -

A Nd  $\gamma$ -Carbonic Anhydrase Sequences from Vertebrates.” *BMC Genomics* 21 (1).  
<https://doi.org/10.1186/s12864-020-6762-2>.

# ORIGINAL COMMUNICATIONS



# PUBLICATION

I

## **Cloning, characterization and anion inhibition of a $\beta$ -carbonic anhydrase from the pathogenic protozoan *Entamoeba histolytica***

Susanna Haapanen, Silvia Bua, Marianne Kuuslahti, Seppo Parkkila, Claudiu T. Supuran

Molecules. 2018;23(12):3112

<https://doi.org/10.3390/molecules23123112>

**Publication reprinted with the permission of the copyright holders.**







Article

# Cloning, Characterization and Anion Inhibition Studies of a $\beta$ -Carbonic Anhydrase from the Pathogenic Protozoan *Entamoeba histolytica*

Susanna Haapanen <sup>1</sup>, Silvia Bua <sup>2</sup>, Marianne Kuuslahti <sup>1</sup>, Seppo Parkkila <sup>1,3</sup> and Claudiu T. Supuran <sup>2,\*</sup>

<sup>1</sup> Faculty of Medicine and Health Technology, Tampere University, 33100 Tampere, Finland; Haapanen.Susanna.E@student.uta.fi (S.H.); Marianne.Kuuslahti@staff.uta.fi (M.K.); seppo.parkkila@staff.uta.fi (S.P.)

<sup>2</sup> Neurofarba Dept., Sezione di Scienze Farmaceutiche e Nutraceutiche, Università degli Studi di Firenze, Via U. Schiff 6, Sesto Fiorentino, 50019 Florence, Italy; silvia.bua@unifi.it

<sup>3</sup> Fimlab Ltd., Tampere University Hospital, 33100 Tampere, Finland

\* Correspondence: claudiu.supuran@unifi.it; Tel./Fax: +39-055-4573729

Received: 1 November 2018; Accepted: 27 November 2018; Published: 28 November 2018



**Abstract:** We report the cloning and catalytic activity of a  $\beta$ -carbonic anhydrase (CA, EC 4.2.1.1), isolated from the pathogenic protozoan *Entamoeba histolytica*, EhiCA. This enzyme has a high catalytic activity for the physiologic CO<sub>2</sub> hydration reaction, with a  $k_{\text{cat}}$  of  $6.7 \times 10^5 \text{ s}^{-1}$  and a  $k_{\text{cat}}/K_{\text{m}}$  of  $8.9 \times 10^7 \text{ M}^{-1} \times \text{s}^{-1}$ . An anion inhibition study of EhiCA with inorganic/organic anions and small molecules revealed that fluoride, chloride, cyanide, azide, pyrodiphosphate, perchlorate, tetrafluoroborate and sulfamic acid did not inhibit the enzyme activity, whereas pseudohalides (cyanate and thiocyanate), bicarbonate, nitrate, nitrite, diethyldithiocarbamate, and many complex inorganic anions showed inhibition in the millimolar range ( $K_{\text{I}}$ s of 0.51–8.4 mM). The best EhiCA inhibitors were fluorosulfonate, sulfamide, phenylboronic acid and phenylarsonic acid ( $K_{\text{I}}$ s in the range of 28–86  $\mu\text{M}$ ). Since  $\beta$ -CAs are not present in vertebrates, the present study may be useful for detecting lead compounds for the design of effective enzyme inhibitors, with potential to develop anti-infectives with alternative mechanisms of action.

**Keywords:** carbonic anhydrase; metalloenzymes; protozoan; *Entamoeba histolytica*; anions; inhibitor

## 1. Introduction

The carbonic anhydrases (CAs, EC 4.2.1.1) are enzymes that effectively catalyze the reaction between CO<sub>2</sub> and water, yielding bicarbonate (HCO<sub>3</sub><sup>−</sup>) and protons (H<sup>+</sup>). They are among the fastest catalysts known in nature [1–3]. CAs are multifunctional enzymes, which play a central role in different physiological, biochemical, and metabolic processes, such as acid-base homeostasis; respiratory gas exchange; electrolyte secretion; and biosynthesis of urea, glucose, fatty acids, and carbamoyl phosphate. They are also vital in ionic transport, muscular contraction (in vertebrates), and photosynthesis (in plants and algae). Seven distinct genetic families (i.e., the  $\alpha$ ,  $\beta$ ,  $\gamma$ ,  $\delta$ ,  $\zeta$ ,  $\eta$ , and  $\theta$  class CAs) are known to date, with a wide distribution in organisms throughout the tree of life [4–10]. The CA classes do not share any significant sequence and structural identity, being a paradigmatic example of convergent evolution at the molecular level [1–3].

The first  $\beta$ -CA was discovered in 1939, but it took several decades until it was recognized as evolutionarily and structurally distinct from the previously studied CAs, those belonging to the  $\alpha$ -class [11]. After the 1990s, many new  $\beta$ -CAs were discovered in the genomes of various

organisms [11]. Based on current knowledge, these enzymes are found in photosynthetic organisms, eubacteria, yeasts, and Archaea [11–13]. Later on, it was discovered that they are also present in the genomes of insects, nematodes, and protozoans, but not in mammals [14]. Therefore,  $\beta$ -CAs are considered promising target enzymes for antiparasitic drugs [15–17]. The physiological significance of  $\beta$ -CAs is somehow ambiguous in most organisms studied so far, because frequently there are more than one enzyme class present [1–3,14–18]. However,  $\beta$ -CAs were shown to have important roles (for instance, in providing bicarbonate/ $\text{CO}_2$  for the photosynthetic enzyme Rubisco in the chloroplasts of many plants/algae [11,17,18]). *Helicobacter pylori* contains only one  $\alpha$ - and one  $\beta$ -CA, whose inhibition with sulfonamides impairs the growth of the pathogen in vitro and in vivo [13,15]. The physiological relevance of  $\beta$ -CAs in many organisms, including protozoans belonging to the Amoebozoas, is yet to be discovered. However, in *Leishmania* spp., a  $\beta$ -class CA enzyme (LdcCA) was recently shown to be a potential drug target [19–21]. Indeed, the inhibition of protozoan  $\beta$ -CAs with sulfonamides, formulated as nanoemulsions, had a profound effect on the survival and growth of *L. amazonensis* and *L. infantum*, two species which provoke serious disease in the tropical and subtropical countries [21].

*Entamoeba histolytica* is a pathogenic protozoan human parasite causing amebiasis, which can be expressed as colitis or abscess of intestines or liver [22,23]. The common symptoms are diarrhea, colitis, and dysentery, but the majority of infections are asymptomatic [22,23]. *E. histolytica* is ingested with contaminated food or water as mature cysts, which excystate in the small intestine. The released trophozoites will then invade the large intestine [22]. *E. histolytica* is capable of lysing human tissues, killing immune effector cells by contact-dependent cytolysis [22,24]. The parasite has many virulence mechanisms, as it can adhere to host cells with multi-subunit GalGalNAc lectins, degrade the host extracellular matrix with cysteine proteases, and lyses target cells with amoebapores [25]. The invasive forms of the infection generally include cyst formation in the liver, which can lead to complications such as pleural effusion, due to the rupture of the cyst [22,26]. Rarely, they also disseminate through other extraintestinal organs (e.g., the brain or pericardium) [22,23]. Although there are effective medications for treating *E. histolytica*, therapies for the invasive forms produce many adverse side effects [22,23], and there are additional limitations to such therapies, among which is an increasing prevalence of resistance to commonly used drugs, which emphasizes the need for new drug targets against this protozoan [23,25]. Thus, we decided to clone and investigate in detail the  $\beta$ -CA present in this pathogenic protozoan. Here we report the cloning, purification, investigation of the catalytic activity, and the anion inhibition profile of the recombinant enzyme belonging to the  $\beta$ -class, identified in the genome of the pathogenic protozoan *E. histolytica*, denominated EhiCA.

## 2. Results and Discussion

We produced the  $\beta$ -CA of *E. histolytica*, EhiCA, in the *E. coli* production system (see Experimental for details) as reported earlier for other CAs, such as hCA VII [19]. As a result, we obtained a 21 kDa protein, which was confirmed to be the right  $\beta$ -CA with mass spectrometry (MS) and SDS-PAGE (Figure 1). Furthermore, atomic absorption spectroscopy allowed us to determine the presence of one zinc ion per polypeptide chain (data not shown), which confirmed the MS data.

We measured the catalytic activity of the recombinant EhiCA (for the  $\text{CO}_2$  hydration reaction) [27], comparing its kinetic parameters with those of other such enzymes, belonging to the  $\alpha$ -class, such as hCA I and II, (h stands for human isoform). Table 1 shows that EhiCA has a significant catalytic activity (for the physiologic reaction,  $\text{CO}_2$  hydration to bicarbonate and protons), with a  $k_{\text{cat}}$  of  $6.7 \times 10^5 \text{ s}^{-1}$  and a  $k_{\text{cat}}/K_m$  of  $8.9 \times 10^7 \text{ M}^{-1} \times \text{s}^{-1}$ , being thus 1.8 times more effective as a catalyst, compared to the slow human isoform hCA I (considering the  $k_{\text{cat}}/K_m$  values). Furthermore, like most enzymes belonging to the CA superfamily, EhiCA was inhibited by acetazolamide (AZA, 5-acetamido-1,3,4-thiadiazole-2-sulfonamide): A standard, clinically used sulfonamide CA inhibitor [1–3]. It can be observed that, similar to hCA I, EhiCA was inhibited in the high nanomolar range by this compound, with an inhibition constant  $K_i$ s of 509 nM (Table 1).

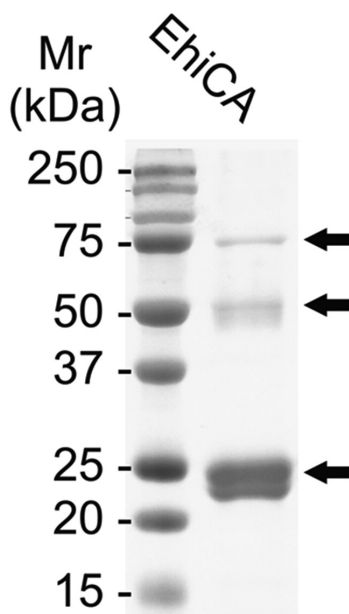


**Figure 1.** SDS PAGE of the  $\beta$ -CA from *E. histolytica* (EhiCA) showing a 21/25 kDa doublet polypeptide and additional polypeptides of about 50 and 75 kDa (arrows). Left lane: Standard Mw markers. The dimer and the trimer of EhiCA are also seen (arrows), as reported for other  $\beta$ -CAs cloned and purified earlier [11–15].

In order to rationalize the effective catalytic activity of EhiCA, we aligned the amino acid sequence of this protein with that of other  $\beta$ -CAs, such as those from the pathogenic bacteria *Haemophilus influenzae*, *Vibrio cholerae*, *Escherichia coli*, *Salmonella typhimurium*, two isoforms from *Mycobacterium tuberculosis* [11,27–29], and the cyanobacterium *Synechocystis* sp. PCC 6803 [30] (Figure 2).

**Table 1.** Kinetic parameters for the  $\text{CO}_2$  hydration reaction catalyzed by the human cytosolic isozymes hCA I and II ( $\alpha$ -class CAs) at 20 °C and pH 7.5 in 10 mM HEPES buffer and 20 mM  $\text{Na}_2\text{SO}_4$ , and the  $\beta$ -CA EhiCA from *E. histolytica* measured at 20 °C, pH 8.3 in 20 mM TRIS buffer and 20 mM  $\text{NaClO}_4$ . Inhibition data with the clinically used sulfonamide acetazolamide (5-acetamido-1,3,4-thiadiazole-2-sulfonamide) are also provided [31].

Enzyme	Activity Level	Class	$k_{\text{cat}}$ ( $\text{s}^{-1}$ )	$K_{\text{m}}$ (mM)	$k_{\text{cat}}/K_{\text{m}}$ ( $\text{M}^{-1} \times \text{s}^{-1}$ )	$K_{\text{I}}$ (Acetazolamide) (nM)
hCA I	moderate	$\alpha$	$2.0 \times 10^5$	4.0	$5.0 \times 10^7$	250
hCA II	very high	$\alpha$	$1.4 \times 10^6$	9.3	$1.5 \times 10^8$	2
EhiCA	high	$\beta$	$(6.7 \pm 0.2) \times 10^5$	$7.5 \pm 0.08$	$(8.9 \pm 0.1) \times 10^7$	509



structural elements connected to them, may explain the catalytic activity of EhiCA reported in this paper (Table 1).

We also investigated the inhibition of EhiCA with a set of inorganic simple and complex anions, as well as small organic molecules known [11–15,27–30] to interact with CAs, such as diethyl-dithiocarbamate, sulfamide, sulfamic acid, phenylboronic and phenylphosphonic acid, among others (Table 2).

**Table 2.** Inhibition constants of anionic inhibitors against the  $\alpha$ -CA isoforms hCA II and hCA I, as well as the  $\beta$ -class protozoan enzyme EhiCA, for the CO<sub>2</sub> hydration reaction at 20 °C [31].

Inhibitor <sup>§</sup>	K <sub>i</sub> [mM] <sup>#</sup>		
	hCA II	hCA I	EhiCA
F <sup>-</sup>	>300	>300	>100
Cl <sup>-</sup>	200	6.0	>100
Br <sup>-</sup>	63	4.1	36.8
I <sup>-</sup>	26	0.3	7.4
CNO <sup>-</sup>	0.03	0.0007	0.77
SCN <sup>-</sup>	1.6	0.2	7.9
CN <sup>-</sup>	0.02	0.0005	>100
N <sub>3</sub> <sup>-</sup>	1.51	0.0012	>100
HCO <sub>3</sub> <sup>-</sup>	85	12	0.28
CO <sub>3</sub> <sup>2-</sup>	73	15	2.4
NO <sub>3</sub> <sup>-</sup>	35	7.0	3.6
NO <sub>2</sub> <sup>-</sup>	63	8.4	1.7
HS <sup>-</sup>	0.04	0.0006	6.9
HSO <sub>3</sub> <sup>-</sup>	89	18	11.5
SO <sub>4</sub> <sup>2-</sup>	>200	63	21.6
SnO <sub>3</sub> <sup>2-</sup>	0.83	0.57	0.51
SeO <sub>4</sub> <sup>2-</sup>	112	118	6.0
TeO <sub>4</sub> <sup>2-</sup>	0.92	0.66	0.61
P <sub>2</sub> O <sub>7</sub> <sup>4-</sup>	48.50	25.8	>100
V <sub>2</sub> O <sub>7</sub> <sup>4-</sup>	0.57	0.54	>100
B <sub>4</sub> O <sub>7</sub> <sup>2-</sup>	0.95	0.64	0.29
ReO <sub>4</sub> <sup>-</sup>	0.75	0.11	7.1
RuO <sub>4</sub> <sup>-</sup>	0.69	0.10	7.0
S <sub>2</sub> O <sub>8</sub> <sup>2-</sup>	0.084	0.11	8.4
SeCN <sup>-</sup>	0.086	0.085	0.87
CS <sub>3</sub> <sup>2-</sup>	0.0088	0.0087	6.0
Et <sub>2</sub> NCS <sub>2</sub> <sup>-</sup>	3.1	0.00079	0.51
ClO <sub>4</sub> <sup>-</sup>	>200	>200	>100
BF <sub>4</sub> <sup>-</sup>	>200	>200	>100
FSO <sub>3</sub> <sup>-</sup>	0.46	0.79	0.086
PF <sub>6</sub> <sup>-</sup>	>200	>200	>100
CF <sub>3</sub> SO <sub>3</sub> <sup>-</sup>	>200	>200	>100
NH(SO <sub>3</sub> ) <sub>2</sub> <sup>2-</sup>	0.76	0.31	2.2
H <sub>2</sub> NSO <sub>2</sub> NH <sub>2</sub>	1.13	0.31	0.028
H <sub>2</sub> NSO <sub>3</sub> H	0.39	0.021	>100
Ph-B(OH) <sub>2</sub>	23.1	38.6	0.047
Ph-AsO <sub>3</sub> H <sub>2</sub>	49.2	31.7	0.038

<sup>§</sup> As sodium salt; <sup>#</sup> Errors were in the range of 3–5% of the reported values, from three different assays.

The following observations can be made from the inhibition data shown in Table 2:

(i) The anions which did not show inhibitory activity against EhiCA were fluoride, chloride, and, surprisingly, cyanide and azide, which are highly effective inhibitors of  $\alpha$ -CAs such as hCA I and II [32]; pyrodiphosphate and divanadate; perchlorate, tetrafluoroborate, hexafluorophosphate, and triflate (which usually do not significantly inhibit any CA [32]); and, again surprisingly, sulfamic

acid. All these compounds did not show significant inhibition up to a 100 mM concentration in the assay system.

(ii) The most effective EhiCA inhibitors were sulfamide (which is structurally highly similar to sulfamic acid, except that the pKa of the two compounds is highly different) [33,34] and fluorosulfonate, as well as phenylboronic acid and phenylarsonic acid, which showed  $K_{1s}$  in the range of 28–86  $\mu\text{M}$  (Table 2). As seen in Table 2, many of these small molecules/anions also act as inhibitors of hCA I and II, but with a rather different efficacy [33].

(iii) Several anions, such as cyanate, selenocyanate, bicarbonate, stannate, tellurate, tetraborate, and *N,N*-diethyl-dithiocarbamate were also sub-millimolar EhiCA inhibitors, with  $K_{1s}$  in the range of 0.28–0.87 mM. Some of these compounds are typical metal complexing agents (cyanate, selenocyanate, *N,N*-diethyl-dithiocarbamate), and their propensity to bind the zinc ion in this  $\beta$ -CA explains these inhibitory activities. However, others, (among which are bicarbonate, stannate, tellurate, and tetraborate) show less affinity to act as metal complexing anions [32]. The inhibitory action of bicarbonate, one of the reaction products/substrates of the CA, is particularly interesting, possibly indicating that the enzyme is not acting as a highly efficient bicarbonate dehydratase, but instead that the  $\text{CO}_2$  hydratase activity might be crucial during the life cycle of this protozoan. However, this speculation needs careful validation.

(iv) Many anions acted as low millimolar EhiCA inhibitors. They include iodide, thiocyanate, carbonate, nitrate, nitrite, hydrogensulfide, selenite, perrhenate, perruthenate, peroxydisulfate, trithiocarbonate, and imidosulfonate ( $K_{1s}$  in the range of 1.7–8.4 mM).

(v) Anions with a less effective inhibitory action against EhiCA were bromide, bisulfite, and sulfate, with  $K_{1s}$  in the range of 11.5–365.8 mM (Table 1).

### 3. Materials and Methods

#### 3.1. Vector Construction

We produced the EhiCA as a recombinant protein in *E. coli*. The DNA sequence was retrieved from UniProt, and modified for recombinant protein production. We provided the sequence of the insert, and the actual construction of the plasmid vector was performed by GeneArt (Invitrogen, Regensburg, Germany). The structure of the insert was specifically modified for production in *E. coli*. The insert was ligated into a modified plasmid vector, pBVboost.

#### 3.2. Production of the Protein

The freeze-dried plasmid was prepared, according to manufacturer's manual. Deep-frozen BL21 Star™ (DE3) cells (Invitrogen, Carlsbad, CA, USA) were slowly melted on ice. Once melted, 25  $\mu\text{L}$  of the cell suspension and 1  $\mu\text{L}$  of the plasmid solution were combined. The suspension was kept on ice for 30 min. Heat shock was performed by submerging the suspension-containing tube into 42 °C water for 30 s, and was then incubated on ice for 2 min. To the tube 125  $\mu\text{L}$  of S.O.C Medium (Invitrogen, Carlsbad, CA, USA) was added, and the tube was incubated for 1 h with constant shaking (200 rpm) at 37 °C. Growth plates (gentamycin-LB medium, ratio 1:1000) were prewarmed at 37 °C for 40 min. Then, 20  $\mu\text{L}$  and 50  $\mu\text{L}$  of suspension was spread on two plates which were incubated overnight at 37 °C. A volume of 5 mL preculture was prepared by inoculating single colonies from growth plates onto an LB medium with gentamycin (ratio 1:1000). It was then incubated overnight at 37 °C with constant shaking (200 rpm). The production was executed according to pO-stat fed batch protocol, which is essentially as described in Määttä et al. [35]. There were some alterations to the previously described protocol: The fermentation medium did not contain glycerol, as the cell line used did not require it. The induction of the culture was performed with 1 mM IPTG, 12 h after starting the fermentation. Temperature was decreased to 25 °C at the time of the induction. Culturing was stopped after 12 h of the induction with the OD 34 ( $A_{600}$ ). The cells were collected by centrifugation, and the wet weight of the cell pellet was 303 g. The fermentation was performed by the Tampere facility

of Protein Services (PS). The cell pellet (approximately 35 g) was suspended in 150 mL of binding buffer containing 50 mM Na<sub>2</sub>HPO<sub>4</sub>, 0.5 M NaCl, 50 mM imidazole, and 10% glycerol (pH 8.0), and the suspension was homogenized with an EmulsiFlex-C3 (AVESTIN, Ottawa, Canada) homogenizer. The lysate was centrifuged at 13,000× *g* for 15 min at 4 °C, and the clear supernatant was mixed with HisPur™ Ni-NTA Resin (Thermo Fisher Scientific, Waltham, MA, USA) and bound to the resin for 2 h at room temperature on the magnetic stirrer. Then resin was washed with the binding buffer and collected onto an empty column with an EMD Millipore™ vacuum filtering flask (Merck, Kenilworth, NJ, USA) and filter paper. The protein was eluted from the resin with 50 mM Na<sub>2</sub>HPO<sub>4</sub>, 0.5 M NaCl, 350 mM imidazole, and 10% glycerol (pH 7.0). The protein was re-purified with TALON® Superflow™ cobalt resin (GE Healthcare, Chicago, IL, USA). The eluted protein fractions were diluted with binding buffer (50 mM Na<sub>2</sub>HPO<sub>4</sub>, 0.5 M NaCl, and 10% glycerol pH 8.0), so that the imidazole concentration was under 10 mM. The protein binding and elution was performed as described above. The purity of the protein was determined with gel electrophoresis (SDS-PAGE), and visualized with PageBlue Protein staining solution (Thermo Fisher Scientific, Waltham, MA, USA). Protein fractions were pooled and concentrated with 10 kDa Vivaspin® Turbo 15 centrifugal concentrators (Sartorius™, Göttingen, Germany) at 4000× *g* at 4 °C. Buffer exchange in 50 mM TRIS (pH 7.5) was done using the same centrifugal concentrators. His-tag was cleaved from the purified protein by Thrombin CleanCleave Kit (Sigma-Aldrich, Saint Louis, MO, USA), according to manufacturer's manual.

### 3.3. CA Activity and Inhibition Measurements

An Sx.18Mv-R Applied Photophysics (Oxford, UK) stopped-flow instrument has been used to assay the catalytic activity of various CA isozymes for the CO<sub>2</sub> hydration reaction [31]. Phenol red (at a concentration of 0.2 mM) was used as indicator (working at the absorbance maximum of 557 nm). Following the CA-catalyzed CO<sub>2</sub> hydration reaction, 10 mM Hepes (pH 7.5, for α-CAs) or TRIS (pH 8.3, for β-CAs) as buffers, and 0.1 M NaClO<sub>4</sub> (for maintaining constant ionic strength), were used for a period of 10 s at 25 °C. The CO<sub>2</sub> concentrations ranged from 1.7 to 17 mM, for the determination of the kinetic parameters and inhibition constants. For each inhibitor, at least six traces of the initial 5–10% of the reaction were used for determining the initial velocity. The uncatalyzed rates were determined in the same manner, and subtracted from the total observed rates. Stock solutions of inhibitors (10 mM) were prepared in distilled and deionized water, and dilutions of up to 1 μM were done thereafter with the assay buffer. Enzyme and inhibitor solutions were pre-incubated together for 15 min (standard assay at room temperature) prior to assay, in order to allow for the formation of the enzyme–inhibitor complex. The inhibition constants were obtained by non-linear least-squares methods, using PRISM 3 and the Cheng–Prusoff equation [36–38].

## 4. Conclusions

In the search for alternative drug targets against anti-protozoan agents, we report the cloning and catalytic activity of a β-CA from *Entamoeba histolytica*, EhiCA, the etiological agent of diarrhea and amebic liver abscesses. This new enzyme has a high catalytic activity for the physiologic CO<sub>2</sub> hydration reaction, with a  $k_{cat}$  of  $6.7 \times 10^5 \text{ s}^{-1}$  and a  $k_{cat}/K_m$  of  $8.9 \times 10^7 \text{ M}^{-1} \times \text{s}^{-1}$ . An anion inhibition study of EhiCA with inorganic/organic anions and small molecules was performed, in order to detect interesting leads for effective inhibitors. Fluoride, chloride, cyanide, azide, pyrodiphosphate, perchlorate, tetrafluoroborate, and sulfamic acid did not inhibit the enzyme activity, whereas pseudohalides (cyanate and thiocyanate), bicarbonate, nitrate, nitrite, diethyldithiocarbamate, and many complex inorganic anions showed inhibition in the millimolar range ( $K_i$ s of 0.51–8.4 mM). The best EhiCA inhibitors were fluorosulfonate, sulfamide, phenylboronic acid, and phenylarsonic acid ( $K_i$ s in the range of 28–86 μM). Since β-CAs are not present in vertebrates, the present study may be useful for detecting lead compounds for the design of effective enzyme inhibitors, with potential to develop anti-infectives with alternative mechanisms of action.

**Author Contributions:** S.H., S.B. and M.K. performed the experiments. S.P. and C.T.S. supervised the experiments and wrote the article. All authors contributed to the final version of the paper.

**Funding:** The work has been supported by grants from the Academy of Finland, the Sigrid Juselius Foundation, and the Jane and Aatos Erkko Foundation.

**Acknowledgments:** The authors acknowledge the Tampere Facility of Protein Services (PS) for their service.

**Conflicts of Interest:** The authors do not declare conflict of interest.

## References

1. Supuran, C.T. Structure and function of carbonic anhydrases. *Biochem. J.* **2016**, *473*, 2023–2032. [CrossRef] [PubMed]
2. Supuran, C.T. Carbonic anhydrases: Novel therapeutic applications for inhibitors and activators. *Nat. Rev. Drug Discov.* **2008**, *7*, 168–181. [CrossRef] [PubMed]
3. Neri, D.; Supuran, C.T. Interfering with pH regulation in tumours as a therapeutic strategy. *Nat. Rev. Drug Discov.* **2011**, *10*, 767–777. [CrossRef] [PubMed]
4. Capasso, C.; Supuran, C.T. An overview of the alpha-, beta- and gamma-carbonic anhydrases from Bacteria: Can bacterial carbonic anhydrases shed new light on evolution of bacteria? *J. Enzyme Inhib. Med. Chem.* **2015**, *30*, 325–332. [CrossRef] [PubMed]
5. Vullo, D.; Del Prete, S.; Di Fonzo, P.; Carginale, V.; Donald, W.A.; Supuran, C.T.; Capasso, C. Comparison of the sulfonamide inhibition profiles of the  $\beta$ - and  $\gamma$ -carbonic anhydrases from the pathogenic bacterium *Burkholderia pseudomallei*. *Molecules* **2017**, *22*, 421. [CrossRef] [PubMed]
6. Berrino, E.; Bua, S.; Mori, M.; Botta, M.; Murthy, V.S.; Vijayakumar, V.; Tamboli, Y.; Bartolucci, G.; Mugelli, A.; Cerbai, E.; et al. Novel sulfamide-containing compounds as selective carbonic anhydrase i inhibitors. *Molecules* **2017**, *22*, 1049. [CrossRef] [PubMed]
7. Saad, A.E.; Ashour, D.S.; Abou Rayia, D.M.; Bedeer, A.E. Carbonic anhydrase enzyme as a potential therapeutic target for experimental trichinellosis. *Parasitol. Res.* **2016**, *115*, 2331–2339. [CrossRef] [PubMed]
8. Alterio, V.; Langella, E.; Viparelli, F.; Vullo, D.; Ascione, G.; Dathan, N.A.; Morel, F.M.; Supuran, C.T.; De Simone, G.; Monti, S.M. Structural and inhibition insights into carbonic anhydrase CDCA1 from the marine diatom *Thalassiosira weissflogii*. *Biochimie* **2012**, *94*, 1232–1241. [CrossRef] [PubMed]
9. Cau, Y.; Mori, M.; Supuran, C.T.; Botta, M. Mycobacterial carbonic anhydrase inhibition with phenolic acids and esters: Kinetic and computational investigations. *Org. Biomol. Chem.* **2016**, *14*, 8322–8330. [CrossRef] [PubMed]
10. Supuran, C.T. Advances in structure-based drug discovery of carbonic anhydrase inhibitors. *Expert Opin. Drug Discov.* **2017**, *12*, 61–88. [CrossRef] [PubMed]
11. Rowlett, R.S. Structure and catalytic mechanism of the  $\beta$ -carbonic anhydrases. *Biochim. Biophys. Acta Proteins Proteomics* **2010**, *1804*, 362–373. [CrossRef] [PubMed]
12. Zolfaghari Emameh, R.; Barker, H.; Hytönen, V.P.; Tolvanen, M.E.E.; Parkkila, S. Beta carbonic anhydrases: Novel targets for pesticides and anti-parasitic agents in agriculture and livestock husbandry. *Parasites Vect.* **2014**, *7*, 403. [CrossRef] [PubMed]
13. Nishimori, I.; Onishi, S.; Takeuchi, H.; Supuran, C.T. The  $\alpha$  and  $\beta$  classes carbonic anhydrases from *helicobacter pylori* as novel drug targets. *Curr. Pharm. Des.* **2008**, *14*, 622–630. [PubMed]
14. Syrjänen, L.; Parkkila, S.; Scozzafava, A.; Supuran, C.T. Sulfonamide inhibition studies of the  $\beta$  carbonic anhydrase from *Drosophila melanogaster*. *Bioorg. Med. Chem. Lett.* **2014**, *24*, 2797–2801. [CrossRef] [PubMed]
15. Supuran, C.T.; Capasso, C. An overview of the bacterial carbonic anhydrases. *Metabolites* **2017**, *7*, 56. [CrossRef] [PubMed]
16. Supuran, C.T.; Capasso, C. New light on bacterial carbonic anhydrases phylogeny based on the analysis of signal peptide sequences. *J. Enzym. Inhib. Med. Chem.* **2016**, *31*, 1254–1260. [CrossRef]
17. Supuran, C.T.; Capasso, C. Biomedical applications of prokaryotic carbonic anhydrases. *Expert Opin. Ther. Pat.* **2018**, *28*, 745–754. [CrossRef] [PubMed]
18. Del Prete, S.; De Luca, V.; Capasso, C.; Supuran, C.T.; Carginale, V. Recombinant thermoactive phosphoenolpyruvate carboxylase (PEPC) from *Thermosynechococcus elongatus* and its coupling with mesophilic/thermophilic bacterial carbonic anhydrases (CAs) for the conversion of CO<sub>2</sub> to oxaloacetate. *Bioorg. Med. Chem.* **2016**, *24*, 220–225. [CrossRef] [PubMed]



19. Bootorabi, F.; Jänis, J.; Smith, E.; Waheed, A.; Kukkurainen, S.; Hytönen, V.; Valjakka, J.; Supuran, C.T.; Vullo, D.; Sly, W.S.; et al. Analysis of a shortened form of human carbonic anhydrase VII expressed in vitro compared to the full-length enzyme. *Biochimie* **2010**, *92*, 1072–1080. [CrossRef] [PubMed]
20. Vermelho, A.B.; Capaci, G.R.; Rodrigues, I.A.; Cardoso, V.S.; Mazotto, A.M.; Supuran, C.T. Carbonic anhydrases from Trypanosoma and Leishmania as anti-protozoan drug targets. *Bioorg. Med. Chem.* **2017**, *25*, 1543–1555. [CrossRef] [PubMed]
21. Da Silva Cardoso, V.; Vermelho, A.B.; Ricci Junior, E.; Almeida Rodrigues, I.; Mazotto, A.M.; Supuran, C.T. Antileishmanial activity of sulphonamide nanoemulsions targeting the  $\beta$ -carbonic anhydrase from Leishmania species. *J. Enzym. Inhib. Med. Chem.* **2018**, *33*, 850–857. [CrossRef] [PubMed]
22. Hashmeh, N.; Genta, N.; White, N., Jr. Parasites and Diarrhea. I: Protozoans and Diarrhea. *J. Travel Med.* **1997**, *4*, 17–31. [CrossRef] [PubMed]
23. Meier, A.; Erler, H.; Beitz, E. Targeting Channels and Transporters in Protozoan Parasite Infections. *Front. Chem.* **2018**, *6*, 88. [CrossRef] [PubMed]
24. Quach, J.; St-Pierre, J.; Chadee, K. The future for vaccine development against Entamoeba histolytica. *Hum. Vaccin. Immunother.* **2014**, *10*, 1514–1521. [CrossRef] [PubMed]
25. Loftus, B.; Anderson, I.; Davies, R.; Alsmark, U.C.M.; Samuelson, J.; Amedeo, P.; Roncaglia, P.; Berriman, M.; Hirt, R.P.; Mann, B.J.; et al. The genome of the protist parasite *Entamoeba histolytica*. *Nature* **2005**, *433*, 865–868. [CrossRef] [PubMed]
26. Hoffner, R.J.; Kilagbhan, T.; Esekogwu, V.I.; Henderson, S.O. Common presentations of amebic liver abscess. *Ann. Emerg. Med.* **1999**, *34*, 351–355. [CrossRef]
27. Covarrubias, A.S.; Bergfors, T.; Jones, T.A.; Högbom, M. Structural mechanics of the pH-dependent activity of beta-carbonic anhydrase from Mycobacterium tuberculosis. *J. Biol. Chem.* **2006**, *281*, 4993–4999. [CrossRef] [PubMed]
28. Nishimori, I.; Minakuchi, T.; Vullo, D.; Scozzafava, A.; Innocenti, A.; Supuran, C.T. Carbonic anhydrase inhibitors. Cloning, characterization, and inhibition studies of a new beta-carbonic anhydrase from Mycobacterium tuberculosis. *J. Med. Chem.* **2009**, *52*, 3116–3120. [CrossRef] [PubMed]
29. Ferraroni, M.; Del Prete, S.; Vullo, D.; Capasso, C.; Supuran, C.T. Crystal structure and kinetic studies of a tetrameric type II  $\beta$ -carbonic anhydrase from the pathogenic bacterium *Vibrio cholerae*. *Acta Crystallogr. D Biol. Crystallogr.* **2015**, *71*, 2449–2456. [CrossRef] [PubMed]
30. McGurn, L.D.; Moazami-Goudarzi, M.; White, S.A.; Suwal, T.; Brar, B.; Tang, J.Q.; Espie, G.S.; Kimber, M.S. The structure, kinetics and interactions of the  $\beta$ -carboxysomal  $\beta$ -carbonic anhydrase, CcaA. *Biochem. J.* **2016**, *473*, 4559–4572. [CrossRef] [PubMed]
31. Khalifah, R.G. The carbon dioxide hydration activity of carbonic anhydrase. I. Stop-flow kinetic studies on the native human isoenzymes B and C. *J. Biol. Chem.* **1971**, *246*, 2561–2573. [PubMed]
32. De Simone, G.; Supuran, C.T. (In)organic anions as carbonic anhydrase inhibitors. *J. Inorg. Biochem.* **2012**, *111*, 117–129. [CrossRef] [PubMed]
33. Abbate, F.; Supuran, C.T.; Scozzafava, A.; Orioli, P.; Stubbs, M.T.; Klebe, G. Nonaromatic sulfonamide group as an ideal anchor for potent human carbonic anhydrase inhibitors: Role of hydrogen-bonding networks in ligand binding and drug design. *J. Med. Chem.* **2004**, *47*, 550–557. [CrossRef]
34. Murray, A.B.; Aggarwal, M.; Pinard, M.; Vullo, D.; Patrauchan, M.; Supuran, C.T.; McKenna, R. Structural Mapping of Anion Inhibitors to  $\beta$ -Carbonic Anhydrase psCA3 from *Pseudomonas aeruginosa*. *ChemMedChem* **2018**, *13*, 2024–2029. [CrossRef] [PubMed]
35. Määttä, J.A.E.; Eisenberg-Domovich, Y.; Nordlund, H.R.; Hayouka, R.; Kulomaa, M.S.; Livnah, O. Chimeric avidin shows stability against harsh chemical conditions—Biochemical analysis and 3D structure. *Biotechnol. Bioengin.* **2011**, *108*, 481–490. [CrossRef] [PubMed]
36. Borrás, J.; Scozzafava, A.; Menabuoni, L.; Mincione, F.; Briganti, F.; Mincione, G.; Supuran, C.T. Carbonic anhydrase inhibitors: Synthesis of water-soluble, topically effective intraocular pressure lowering aromatic/heterocyclic sulfonamides containing 8-quinoline-sulfonyl moieties: Is the tail more important than the ring? *Bioorg. Med. Chem.* **1999**, *7*, 2397–2406. [CrossRef]
37. Supuran, C.T.; Clare, B.W. Carbonic anhydrase inhibitors—Part 57: Quantum chemical QSAR of a group of 1,3,4-thiadiazole- and 1,3,4-thiadiazoline disulfonamides with carbonic anhydrase inhibitory properties. *Eur. J. Med. Chem.* **1999**, *34*, 41–50. [CrossRef]

38. Zimmerman, S.A.; Ferry, J.G.; Supuran, C.T. Inhibition of the archaeal beta-class (Cab) and gamma-class (Cam) carbonic anhydrases. *Curr. Top. Med. Chem.* **2007**, *7*, 901–908. [CrossRef] [PubMed]

**Sample availability:** Samples of the compounds described in the paper are available from the authors.



© 2018 by the authors. Licensee MDPI, Basel, Switzerland. This article is an open access article distributed under the terms and conditions of the Creative Commons Attribution (CC BY) license (<http://creativecommons.org/licenses/by/4.0/>).

PUBLICATION  
II

**Sulfonamide inhibition studies of a new  $\beta$ -carbonic anhydrase from the pathogenic protozoan *Entamoeba histolytica***

Silvia Bua, Susanna Haapanen, Marianne Kuuslahti, Seppo Parkkila, Claudiu T. Supuran

International journal of molecular sciences. 2018;19(12):3946  
<https://doi.org/10.3390/ijms19123946>

**Publication reprinted with the permission of the copyright holders.**





Article

# Sulfonamide Inhibition Studies of a New $\beta$ -Carbonic Anhydrase from the Pathogenic Protozoan *Entamoeba histolytica*

Silvia Bua <sup>1</sup>, Susanna Haapanen <sup>2</sup> , Marianne Kuuslahti <sup>2</sup>, Seppo Parkkila <sup>2,3</sup> and Claudiu T. Supuran <sup>1,\*</sup>

<sup>1</sup> Sezione di Scienze Farmaceutiche e Nutraceutiche, Neurofarba Dept., Università degli Studi di Firenze, Via U. Schiff 6, 50019 Sesto Fiorentino, Florence, Italy; silvia.bua@unifi.it

<sup>2</sup> Faculty of Medicine and Health Technology, Tampere University, 33100 Tampere, Finland; Haapanen.Susanna.E@student.uta.fi (S.H.); Marianne.Kuuslahti@staff.uta.fi (M.K.); seppo.parkkila@staff.uta.fi (S.P.)

<sup>3</sup> Fimlab Ltd., Tampere University Hospital, 33100 Tampere, Finland

\* Correspondence: claudiu.supuran@unifi.it; Tel./Fax: +39-055-4573729

Received: 9 November 2018; Accepted: 6 December 2018; Published: 8 December 2018



**Abstract:** A newly described  $\beta$ -carbonic anhydrase (CA, EC 4.2.1.1) from the pathogenic protozoan *Entamoeba histolytica*, EhiCA, was recently shown to possess a significant catalytic activity for the physiologic CO<sub>2</sub> hydration reaction ( $k_{\text{cat}}$  of  $6.7 \times 10^5 \text{ s}^{-1}$  and a  $k_{\text{cat}}/K_m$  of  $8.9 \times 10^7 \text{ M}^{-1} \text{ s}^{-1}$ ). A panel of sulfonamides and one sulfamate, some of which are clinically used drugs, were investigated for their inhibitory properties against EhiCA. The best inhibitors detected in the study were 4-hydroxymethyl/ethyl-benzenesulfonamide ( $K_i$ s of 36–89 nM), whereas some sulfanilyl-sulfonamides showed activities in the range of 285–331 nM. Acetazolamide, methazolamide, ethoxzolamide, and dichlorophenamide were less effective inhibitors ( $K_i$ s of 509–845 nM) compared to other sulfonamides investigated here. As  $\beta$ -CAs are not present in vertebrates, the present study may be useful for detecting lead compounds for the design of more effective inhibitors with potential to develop anti-infectives with alternative mechanisms of action.

**Keywords:** carbonic anhydrase; metalloenzymes; protozoan; *Entamoeba histolytica*; sulfonamides; sulfamates; inhibitor

## 1. Introduction

The pathogenic protozoan *Entamoeba histolytica* is the leading cause of diarrhea globally, producing a disease called amebiasis. Endemic in poor communities in developing countries, amebiasis emerged as an important infection among travelers returning from such countries as well as immigrants residing in the developed world [1–3]. The invasive forms of the *E. histolytica* infection may include liver cyst formation, which can produce complications such as pleural effusion due to the rupture of the cysts [4–6]. Rarely, the cysts may disseminate to other extra-intestinal organs, such as the brain or pericardium, with fatal consequences. Amebiasis causes around 70,000 deaths annually and is the third cause of death due to parasites worldwide [7–9]. The pharmacological treatment relies on the use of metronidazole and related compounds (e.g., tinidazole), which show multiple adverse side effects, being rather toxic, mutagenic and carcinogenic, and led to the emergence of resistance [4,9]. Unfortunately, better therapeutic alternatives are lacking, and the nitroimidazoles do not effectively eradicate the luminal cysts of the parasite life cycle. Therefore, it has become necessary to administer a luminal agent, such as nitazoxanide or the aminoglycoside paromomycin, which are expensive new drugs, which is difficult to use in developing countries [4,9]. Ultimately, the gold(I) derivative

Auranofin, used for the treatment of rheumatoid arthritis, has entered clinical drug development as an antiparasitic agent targeting amebiasis [4–9]. However, the treatment options are few, their effectiveness is not very high, and the presently available drugs have many side effects and led to the development of drug resistance. All these facts make the search for new anti-amoeba targets of great relevance [4–10].

In recent years, we have investigated the role of the metalloenzymes, carbonic anhydrases (CAs, EC 4.2.1.1), in various pathogenic organisms belonging to the bacteria, fungal or protozoan domains [11–13]. These enzymes effectively catalyze the reaction between CO<sub>2</sub> and water, with the formation of bicarbonate (HCO<sub>3</sub><sup>−</sup>) and protons (H<sup>+</sup>), being among the very fast catalysts known in nature [14–20]. CAs are multifunctional enzymes which play central roles in various physiological, biochemical, and metabolic processes, such as acid-base homeostasis, respiratory gas exchange, electrolytes secretion, biosynthesis of urea, glucose, fatty acids, and carbamoyl phosphate, and also in the ionic transport, muscular contraction (in vertebrates), and photosynthesis (in plants and algae). Seven distinct genetic families, i.e., the  $\alpha$ ,  $\beta$ ,  $\gamma$ ,  $\delta$ ,  $\zeta$ ,  $\eta$ , and  $\theta$  class CAs are known to date, with a wide distribution in organisms all over the tree of life [21–27]. The CA classes do not share any significant sequence and structural identity since they are a paradigmatic example of convergent evolution at the molecular level [11–13]. Recently, we have shown that the inhibition of the  $\alpha$ - or  $\beta$ -CAs from the pathogenic protozoans *Trypanosoma cruzi* [28] or *Leishmania* spp. [29] has a potent anti-protozoan effect, with the possibility to inhibit the growth of the pathogen. Considering that the genome of *E. histolytica* has been published [30], we decided to investigate in detail whether the  $\beta$ -CA present in this pathogenic protozoan may have a similar role to the enzymes investigated earlier in other pathogenic protozoans [28,29]. Here we report an investigation of the catalytic activity and the sulfonamide/sulfamate inhibition profile of the recombinant enzyme belonging to the  $\beta$ -class, identified in the genome of the pathogenic protozoan *E. histolytica*, denominated EhiCA.

## 2. Results and Discussion

We produced the  $\beta$ -CA of *E. histolytica*, EhiCA, in the *E. coli* expression system (see Experimental for details) and obtained 21/25 kDa doublet polypeptide and additional polypeptides of about 50 and 75 kDa detected by SDS-PAGE. These four polypeptide bands were subjected to mass spectrometric identification, which showed that they all represent EhiCA. This result suggests that EhiCA, similar to other  $\beta$ -CAs [31], can exist as dimers and higher oligomerization forms [32–34].

The catalytic activity of the recombinant EhiCA (for the CO<sub>2</sub> hydration reaction), has been measured by using a stopped-flow technique [35], comparing its kinetic parameters with those of other such enzymes, belonging to the  $\alpha$ - (e.g., hCA I and II, where h stays for human isoform) or  $\beta$ -class CAs (e.g., mtCA 1 and mtCA 2 from the pathogenic bacterium *Mycobacterium tuberculosis* [31,32]). Data in Table 1 show that EhiCA has a significant catalytic activity (for the physiologic CO<sub>2</sub> hydration reaction), with a  $k_{\text{cat}}$  of  $6.7 \times 10^5 \text{ s}^{-1}$  and a  $k_{\text{cat}}/K_{\text{m}}$  of  $8.9 \times 10^7 \text{ M}^{-1} \text{ s}^{-1}$ , being, thus, 1.8 times more effective as a catalyst compared to the slow human isoform hCA I (considering the  $k_{\text{cat}}/K_{\text{m}}$  values). Furthermore, like most enzymes belonging to the CA superfamily, EhiCA was inhibited by acetazolamide (AZA, 5-acetamido-1,3,4-thiadiazole-2-sulfonamide), a standard, clinically used sulfonamide CA inhibitor [1–3]. Thus, EhiCA shows a catalytic activity similar to that of mtCA 2 and hCA I, being a highly effective catalyst for the hydration of CO<sub>2</sub>, whereas its inhibition by acetazolamide is similar to the behavior of mtCA 1, which has a low affinity for this inhibitor, with a  $K_{\text{i}}$  of 480 nM, comparable to that of EhiCA, of 509 nM (Table 1).

To rationalize the effective catalytic activity of EhiCA, we aligned the amino acid sequence of this protein with that of other  $\beta$ -CAs, such as those from the pathogenic bacteria *Haemophilus influenza* [21], *Vibrio cholera* [33], *Escherichia coli* [21], *Salmonella typhimurium* [36], two isoforms from *Mycobacterium tuberculosis* [31,32], and the cyanobacterium *Synechocystis* sp. PCC 6803 [34] (Figure 1).

**Table 1.** Kinetic parameters for the CO<sub>2</sub> hydration reaction catalyzed by the human cytosolic isozymes hCA I and II ( $\alpha$ -class CAs) at 20 °C and pH 7.5 in 10 mM HEPES buffer and 20 mM Na<sub>2</sub>SO<sub>4</sub>, and the  $\beta$ -CA from *M. tuberculosis* (mtCA 1 and 2) and form *E. histolytica* EhiCA, measured at 20 °C, pH 8.3 in 20 mM TRIS buffer and 20 mM NaClO<sub>4</sub>. Inhibition data with the clinically used sulfonamide acetazolamide (5-acetamido-1,3,4-thiadiazole-2-sulfonamide) are also provided [35].

Enzyme	Activity Level	Class	k <sub>cat</sub> (s <sup>-1</sup> )	k <sub>cat</sub> /K <sub>m</sub> (M <sup>-1</sup> s <sup>-1</sup> )	K <sub>i</sub> (Acetazolamide) (nM)	Ref
hCA I	moderate	$\alpha$	2.0 × 10 <sup>5</sup>	5.0 × 10 <sup>7</sup>	250	[12]
hCA II	very high	$\alpha$	1.4 × 10 <sup>6</sup>	1.5 × 10 <sup>8</sup>	12	[12]
mtCA 1	moderate	$\beta$	3.9 × 10 <sup>5</sup>	3.7 × 10 <sup>7</sup>	480	[32]
mtCA 2	high	$\beta$	9.6 × 10 <sup>5</sup>	9.3 × 10 <sup>7</sup>	9.8	[32]
EhiCA	high	$\beta$	6.7 × 10 <sup>5</sup>	8.9 × 10 <sup>7</sup>	509	this work

CLUSTAL O(1.2.4) multiple sequence alignment

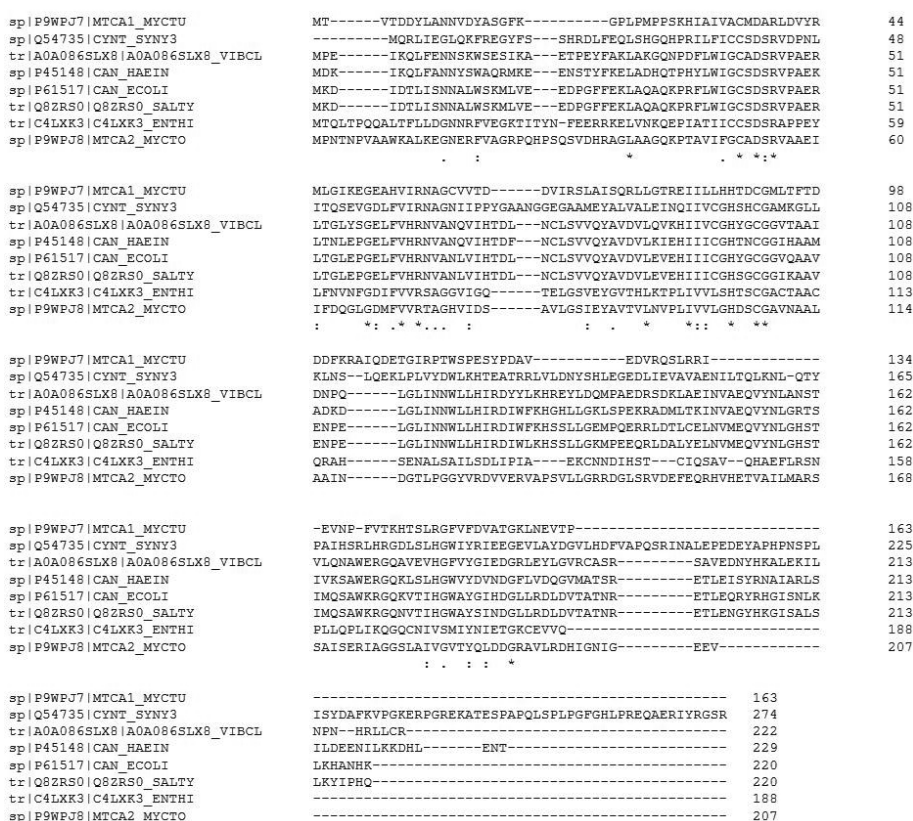


**Figure 1.** Multi-alignment of the amino acid sequences of the  $\beta$ -CAs from *M. tuberculosis* (isoform MTCA1\_MYCTU), *Synechocystis* sp. (SYNY3), *V. cholerae* (VIBCL), *H. influenzae* (HA EIN), *E. coli* (ECOLI), *S. typhimurium* (SALTY), *E. histolytica* (ENTHI), and *M. tuberculosis* (isoform MTCA2\_MYCTO) [21,30–36]. Conserved amino acids depicted by an asterisk (\*), semiconserved ones by (.) or (:).

As seen from data in Figure 1, similar to all  $\beta$ -CAs investigated to date, EhiCA has the conserved three zinc(II) ligands, Cys50, His103, and Cys106 (the fourth ligand is presumably a water molecule/hydroxide ion) as well as the catalytic dyad constituted by the pair Asp52-Arg54 (conserved in all enzymes belonging to this class) [21,31–34,36], which contributes to the enhancement of the

nucleophilicity of the water coordinated to the metal ion. The presence of these conserved amino acids and all the structural elements connected to them may explain the good catalytic activity of EhiCA reported in this paper (Table 1), although the X-ray crystal structure of this enzyme is not yet resolved.

Considering that the sulfonamides are the main class of CA inhibitors (CAIs) [11–13], we investigated the inhibition of EhiCA with a panel of such derivatives, some of which are clinically used drugs like diuretics, antiglaucoma, antiepileptics, antiobesity or antitumor agents [37–40] (Figure 2 and Table 2). The structures of the sulphonamides/sulfamates included in our study are shown in Figure 2. They include acetazolamide **AZ**, methazolamide **MZA**, ethoxzolamide **EZA** and dichlorophenamide **DCP** (the classical, systemically acting antiglaucoma CA inhibitors) [11,12], dorzolamide **DZA** and brinzolamide **BRZ**, topically-acting antiglaucoma drugs, benzolamide **BZA**, topiramate **TPM**, zonisamide **ZNS**, and sulthiame **SLT** [11–13,37–40]. Sulpiride **SLP**, indisulam **IND**, celecoxib **CLX**, and valdecoxib **VLX**, as well as saccharin and the diuretic hydrochlorothiazide **HCT** were also included in the assay [11–13]. The simpler sulfonamides **1–24** are known to possess CA inhibitory properties against many mammalian and prokaryotic such enzymes [25] and are also the building blocks for obtaining more complex CAIs [41–43].

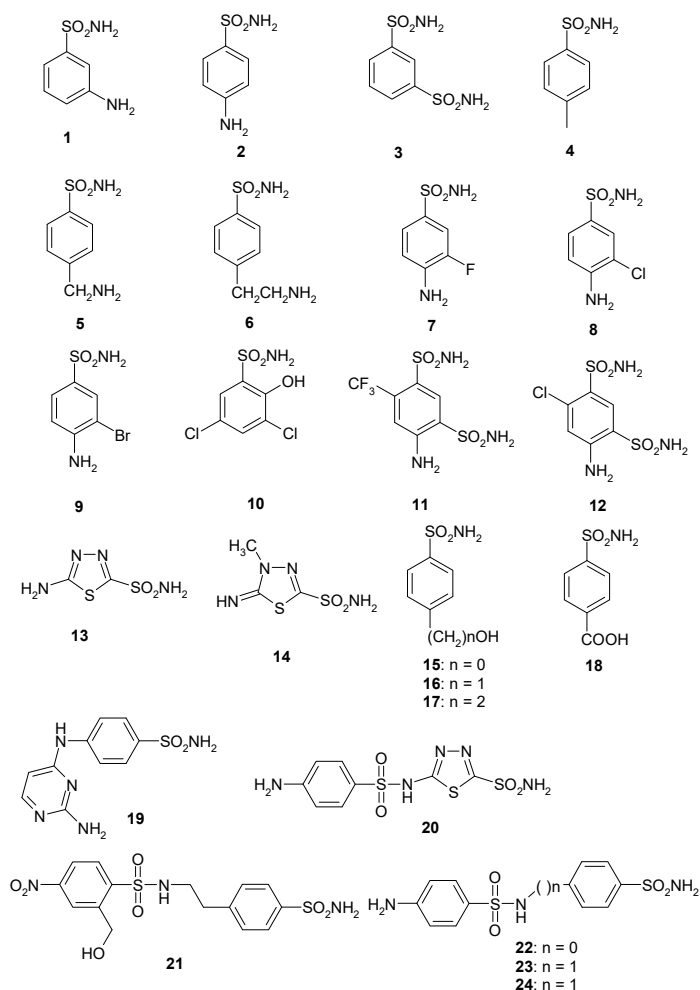
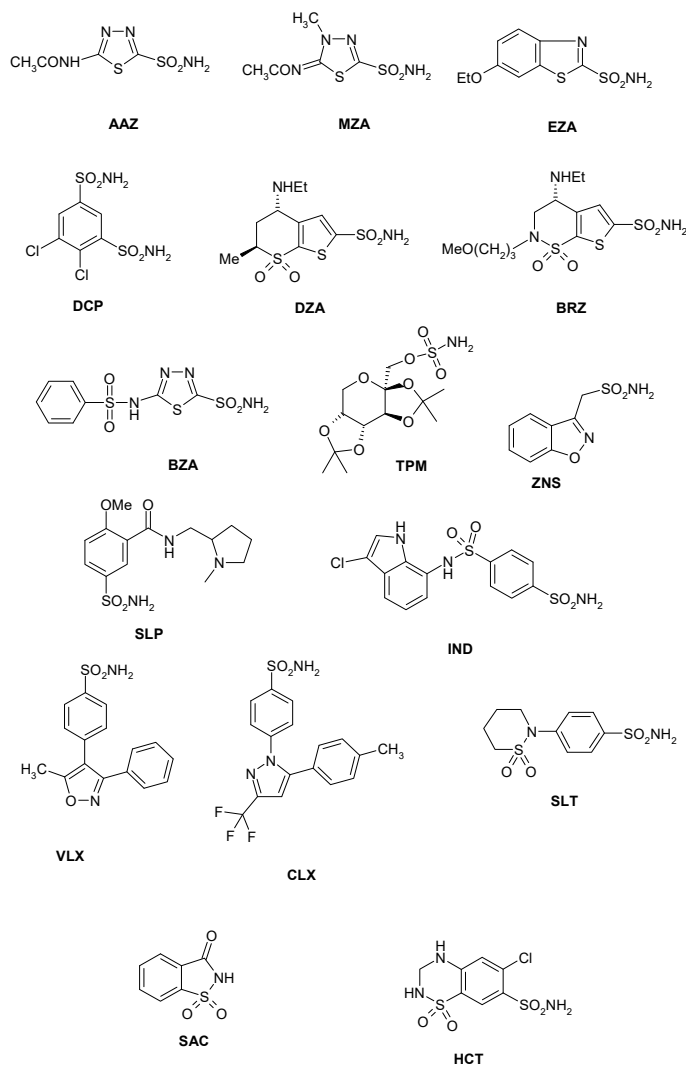


Figure 2. Cont.





**Figure 2.** Sulfonamide (1–24) and sulfonamide/sulfamate derivatives (**AAZ–HCT**) investigated as *Entamoeba histolytica* (EhiCA) inhibitors in the present study.

The following structure-activity relationship (SAR) can be drawn from the data of Table 2:

- (i) The most effective EhiCA inhibitors were the two simple compounds **16** and **17**, 4-hydroxymethyl/ethyl-benzenesulfonamides, which showed  $K_{I1}$ s ranging between 36 and 89 nM, with the longer linker derivative (**17**) being a more effective CAI compared to the hydroxymethyl one **16**. It should also be noted that **17** is a weaker hCA II inhibitor ( $K_I$  of 125 nM) and a quite ineffective hCA I inhibitor ( $K_I$  of 21  $\mu$ M), making it a slightly ameba-CA—selective compound.
- (ii) Several sulfonamides were slightly less effective as EhiCA inhibitors, with  $K_{I1}$ s ranging between 285 and 521 nM. They include **18–24** and acetazolamide **AAZ** (Table 2). Apart from **18** (4-carboxy-benzenesulfonamide) and **19** (a pyrimidinylamino-benzenesulfonamide), the remaining derivatives **20–24** belong to the sulfanilyl-sulfonamide class of CAIs, which possess an elongated molecule, shown to interact favorably with many other CAs belonging to the  $\beta$ -class [15,20,21] and, thus, leading to effective inhibitors. For the homologous series of **22–24**,

the efficacy as EhiCA inhibitors increases with the increase of the linker between the two aromatic rings. **AAZ** and **20** contain the 1,3,4-thiadiazole-2-sulfonamide motif present in many potent CAIs. In this case, aminobenzolamide **20** is a more effective EhiCA inhibitor compared to **AAZ**. It is interesting to note that **BZA**, lacking the amino moiety present in **20**, but with an identical scaffold, is a very weak CAI, with a  $K_I$  of 2471 nM (whereas it is a very potent hCA I and II inhibitor). Thus, minor structural changes in the molecule of the inhibitor lead to drastic effects on their inhibitory profiles against various CAs, including the one from the parasitic protozoan investigated here.

**Table 2.** Inhibition of the human isoforms hCA I and hCA II, and *Entamoeba histolytica* (EhiCA) from *Entamoeba histolytica* with sulfonamides **1–24** and the clinically used drugs **AAZ–HCT**, by a stopped-flow, CO<sub>2</sub> hydrase assay [35].

Inhibitor/Enzyme Class	$K_I$ * (nM)		
	hCA I <sup>a</sup> $\alpha$	hCA II <sup>a</sup> $\alpha$	EhiCA $\beta$
<b>1</b>	28,000	300	2363
<b>2</b>	25,000	240	6011
<b>3</b>	79	8	951
<b>4</b>	78,500	320	833
<b>5</b>	25,000	170	567
<b>6</b>	21,000	160	798
<b>7</b>	8300	60	>10,000
<b>8</b>	9800	110	>10,000
<b>9</b>	6500	40	>10,000
<b>10</b>	7300	54	4656
<b>11</b>	5800	63	742
<b>12</b>	8400	75	1911
<b>13</b>	8600	60	821
<b>14</b>	9300	19	579
<b>15</b>	5500	80	772
<b>16</b>	9500	94	89
<b>17</b>	21,000	125	36
<b>18</b>	164	46	383
<b>19</b>	109	33	521
<b>20</b>	6	2	385
<b>21</b>	69	11	368
<b>22</b>	164	46	331
<b>23</b>	109	33	290
<b>24</b>	95	30	285
<b>AAZ</b>	250	12	509
<b>MZA</b>	50	14	845
<b>EZA</b>	25	8	746
<b>DCP</b>	1200	38	790
<b>DZA</b>	50,000	9	6444
<b>BRZ</b>	45,000	3	3051
<b>BZA</b>	15	9	2471
<b>TPM</b>	250	10	3100
<b>ZNS</b>	56	35	9595
<b>SLP</b>	1200	40	>10,000
<b>IND</b>	31	15	822
<b>VLX</b>	54,000	43	>10,000
<b>CLX</b>	50,000	21	>10,000
<b>SLT</b>	374	9	6727
<b>SAC</b>	18,540	5959	>10,000
<b>HCT</b>	328	290	3402

\* Errors in the range of 5–10% of the reported data, from 3 different assays (data not shown). <sup>a</sup> Human recombinant isozymes, stopped flow CO<sub>2</sub> hydrase assay method, from References [11–15].

- (iii) The following compounds showed modest EhiCA inhibitory properties: **3–6, 11, 13–15, MZA, EZA, DCP, and IND**, with  $K_{IS}$  ranging between 567 and 951 nM. They belong to heterogeneous classes of sulfonamides, most of them being benzenesulfonamides (apart **13** and **14** which are the deacetylated precursors of **AAZ** and **MZA**, thus, heterocyclic derivatives). A special mention regards **15**, which is structurally related to the most effective EhiCA inhibitors detected here, compounds **16** and **17**. Indeed, **15** is 9–20 times a weaker EhiCA inhibitor compared to **16** and **17**, although they differ only by one or two  $\text{CH}_2$  functionalities. From these data, it is again obvious that SAR is very sensitive to small changes in the molecule of the inhibitor and that the 4-hydroxyalkyl-substituted-benzenesulfonamides may lead to highly effective and isoform-selective CAIs targeting the enzyme from this parasite.
- (iv) Weak, micromolar inhibition against EhiCA was observed with **1, 2, 10, 12, DZA, BRZ, BZA, TPM, ZNZ, SLT, and HCT** ( $K_{IS}$  ranging between 1.91–9.59  $\mu\text{M}$ ) as discussed earlier. In addition, these derivatives belong to heterogeneous classes of derivatives, but overall one may observe that they possess a bulkier scaffold and more substituents on the aromatic/heterocyclic ring compared to the effective EhiCA inhibitors described above.
- (v) The ineffective compounds as EhiCA inhibitors ( $K_I > 10 \mu\text{M}$ ) detected here were **7–9** (halogenated sulfanilamide derivatives), sulpiride **SLP**, the COX-2 inhibitors **CLX** and **VLX** (possessing a bulky, Y-shaped molecule), and saccharin **SAC**, the only acylated, secondary sulfonamide included in the study.
- (vi) The inhibition profile of EhiCA with sulfonamides/sulfamates is very different from those of the human isoforms hCA I and II, but only two compounds, **16** and **17** showed selectivity for the protozoan over the human isoforms (Table 2).

### 3. Experimental

#### 3.1. Vector Construction

We produced the EhiCA as a recombinant protein in *E. coli*. The DNA sequence was retrieved from UniProt and modified for recombinant protein production and purification to include N-terminal polyhistidine tag. We provided the sequence of the insert, and the actual construction of the plasmid vector was performed by GeneArt (Invitrogen, Regensburg, Germany). The structure of the insert was specifically modified for production in *E. coli*. The insert was ligated into a modified plasmid vector, pBVboost [44].

#### 3.2. Production of the Protein

The freeze-dried plasmid was prepared according to the manufacturer's manual. Deep-frozen BL21 Star<sup>TM</sup> (DE3) cells (Invitrogen, Carlsbad, CA, USA) were slowly melted on ice. 25  $\mu\text{L}$  of the melted cell suspension and 1  $\mu\text{L}$  of the plasmid solution were combined. The suspension was kept on ice for 30 min. Then the heat shock was performed by submerging the suspension containing tube into +42 °C water for 30 s and after that, incubated on ice for 2 min. 125  $\mu\text{L}$  of S.O.C. Medium (Invitrogen, Carlsbad, CA, USA) was added to the tube, and the tube was incubated for 1 h with constant shaking (200 rpm) at +37 °C. Growth plates (gentamycin-LB medium ratio 1:1000) were prewarmed at +37 °C for 40 min. Twenty microliters and 50  $\mu\text{L}$  of the suspension were spread on two plates, which were incubated overnight at +37 °C. A volume of 5 mL preculture was prepared by inoculating single colonies from growth plates to LB medium with gentamycin (ratio 1:1000). It was then incubated overnight at +37 °C with constant shaking of 200 rpm. Then the production was executed according to pO-stat fed batch protocol, which is essentially as described in Määttä et al. [45]. There were some alterations to the previously described protocol: The fermentation medium did not contain glycerol as the cell line used did not require it. The induction of the culture was performed with 1 mM IPTG 12 h after starting the fermentation. The temperature was decreased to 25 °C at the time of the induction. Culturing was stopped after 12 h of the induction with the OD 34 ( $A_{600}$ ). The cells were collected

by centrifugation, and the wet weight of cell pellet was 303 g. The fermentation was performed by Tampere facility of Protein Services (PS). The cell pellet (approximately 35 g) was suspended in 150 mL of binding buffer containing 50 mM Na<sub>2</sub>HPO<sub>4</sub>, 0.5 M NaCl, 50 mM imidazole, and 10% glycerol (pH 8.0) and the suspension was homogenized with EmulsiFlex-C3 (AVESTIN, Ottawa, ON, Canada) homogenizer. The lysate was centrifuged at 13,000 × *g* for 15 min at 4 °C, and the clear supernatant was mixed with HisPur™ Ni-NTA Resin (Thermo Fisher Scientific, Waltham, MA, USA) and incubated for 2 h at room temperature on a magnetic stirrer. Then, the resin was washed with the binding buffer and collected onto an empty column with EMD Millipore™ vacuum filtering flask (Merck, Kenilworth, NJ, USA) and a filter paper. The protein was eluted from the resin with 50 mM Na<sub>2</sub>HPO<sub>4</sub>, 0.5 M NaCl, 350 mM imidazole and 10% glycerol (pH 7.0). The protein was re-purified with TALON® Superflow™ cobalt resin (GE Healthcare, Chicago, IL, USA). The eluted protein fractions were diluted to binding buffer (50 mM Na<sub>2</sub>HPO<sub>4</sub>, 0.5 M NaCl, and 10% glycerol pH 8.0) so that the imidazole concentration was under 10 mM. The protein binding and elution were performed as described above. The purity of the protein was determined with gel electrophoresis (SDS-PAGE) and visualized with PageBlue Protein staining solution (Thermo Fisher Scientific, Waltham, MA, USA). Mass spectrometric identification of the obtained polypeptide bands was performed in the Tampere University Facility of Protein Services. Protein fractions were pooled and concentrated with 10 kDa Vivaspin® Turbo 15 centrifugal concentrators (Sartorius™, Göttingen, Germany) at 4000 × *g* at 4 °C. Buffer exchange in 50 mM TRIS (pH 7.5) was done with the same centrifugal concentrators. His-tag was cleaved from the purified protein by Thrombin CleanCleave Kit (Sigma-Aldrich, Saint Louis, MO, USA) according to manufacturer's manual.

### 3.3. CA Activity and Inhibition Measurements

An Sx.18Mv-R Applied Photophysics (Oxford, UK) stopped-flow instrument has been used to assay the catalytic activity of various CA isozymes for CO<sub>2</sub> hydration reaction [35]. Phenol red (at a concentration of 0.2 mM) was used as indicator, working at the absorbance maximum of 557 nm, with 10 mM HEPES (pH 7.5, for α-CAs) or TRIS (pH 8.3, for β-CAs) as buffers, 0.1 M NaClO<sub>4</sub> (for maintaining constant ionic strength), following the CA-catalyzed CO<sub>2</sub> hydration reaction for a period of 10 s at 25 °C. The CO<sub>2</sub> concentrations ranged from 1.7 to 17 mM for the determination of the kinetic parameters and inhibition constants. For each inhibitor at least six traces of the initial 5–10% of the reaction have been used for determining the initial velocity. The uncatalyzed rates were determined in the same manner and subtracted from the total observed rates. Stock solutions of inhibitors (0.1 mM) were prepared in distilled-deionized water, and dilutions up to 1 nM were done thereafter with the assay buffer. Enzyme and inhibitor solutions were pre-incubated together for 15 min before assay, to allow for the formation of the enzyme–inhibitor complex. The inhibition constants were obtained by non-linear least-squares methods using PRISM 3 and the Cheng–Prusoff equation, as reported earlier [46–48].

## 4. Conclusions

In the search for alternative drug targets for anti-protozoan agents, we report the first sulphonamide/sulfamate inhibition study of EhiCA, a β-class CA from the parasitic protozoan *Entamoeba histolytica*. The strong enzyme inhibitors identified in the study were 4-hydroxymethyl/ethyl-benzenesulfonamide (*K*<sub>i</sub>s of 36–89 nM), which were also selective for inhibiting the protozoan over the human CA isoforms. Some sulfanilyl-sulfonamides also showed good activities, with inhibition constants in the range of 285–331 nM. Acetazolamide, methazolamide, ethoxzolamide and dichlorophenamide, clinically used agents, were less effective EhiCA inhibitors (*K*<sub>i</sub>s of 509–845 nM) compared to other sulfonamides investigated here. As β-CAs are not present in vertebrates, the present study may be useful for detecting lead compounds for the design of more effective inhibitors with the potential to develop anti-infectives with alternative mechanisms of action. Compounds, such as the strong enzyme inhibitors detected

here, 4-hydroxymethyl/ethyl-benzenesulfonamide, may also be used as pharmacologic tools for understanding the role played by this enzyme in the life cycle of the protozoan.

**Author Contributions:** S.B., S.H. and M.K. performed the experiments. S.P. and C.T.S. supervised the experiments and wrote the manuscript. All authors were involved in the final writing of the work.

**Funding:** The work has been supported by grants from the Academy of Finland, Sigrid Juselius Foundation and Jane & Aatos Erkkö Foundation.

**Acknowledgments:** The authors acknowledge the Tampere University Facility of Protein Services for their service. We thank Ms. Linda Urbanski for the help in the design of the gene construct.

**Conflicts of Interest:** The authors do not declare conflict of interest.

## References

1. Sánchez, C.; López, M.C.; Galeano, L.A.; Qvarnstrom, Y.; Houghton, K.; Ramírez, J.D. Molecular detection and genotyping of pathogenic protozoan parasites in raw and treated water samples from southwest Colombia. *Parasit. Vectors* **2018**, *11*, 563. [CrossRef] [PubMed]
2. Domazetovska, A.; Lee, R.; Adhikari, C.; Watts, M.; Gilroy, N.; Stark, D.; Sivagnanam, S. A 12-Year Retrospective Study of Invasive Amoebiasis in Western Sydney: Evidence of Local Acquisition. *Trop. Med. Infect. Dis.* **2018**, *3*, 73. [CrossRef]
3. Costa, J.O.; Resende, J.A.; Gil, F.F.; Santos, J.F.G.; Gomes, M.A. Prevalence of Entamoeba histolytica and other enteral parasitic diseases in the metropolitan region of Belo Horizonte, Brazil. A cross-sectional study. *Sao Paulo Med. J.* **2018**, *136*, 319–323. [CrossRef] [PubMed]
4. Shirley, D.T.; Farr, L.; Watanabe, K.; Moonah, S. A Review of the Global Burden, New Diagnostics, and Current Therapeutics for Amebiasis. *Open Forum Infect. Dis.* **2018**, *5*, ofy161. [CrossRef] [PubMed]
5. Hashmey, N.; Genta, N.; White, N., Jr. Parasites and Diarrhea. I: Protozoans and Diarrhea. *J. Travel. Med.* **1997**, *4*, 17–31. [CrossRef] [PubMed]
6. Quach, J.; St-Pierre, J.; Chadee, K. The future for vaccine development against Entamoeba histolytica. *Hum. Vaccin. Immunother.* **2014**, *10*, 1514–1521. [CrossRef] [PubMed]
7. Capparelli, E.V.; Bricker-Ford, R.; Rogers, M.J.; McKerrow, J.H.; Reed, S.L. Phase I Clinical Trial Results of Aurano-fin, a Novel Antiparasitic Agent. *Antimicrob. Agents Chemother.* **2016**, *61*, e01947-16. [CrossRef]
8. Gonzales, M.L.; Dans, L.F.; Martinez, E.G. Antiamoebic drugs for treating amoebic colitis. *Cochrane Database Syst. Rev.* **2009**, *2*, CD006085. [CrossRef]
9. Andrade, R.M.; Reed, S.L. New drug target in protozoan parasites: The role of thioredoxin reductase. *Front. Microbiol.* **2015**, *6*, 975. [CrossRef]
10. Leitsch, D.; Williams, C.F.; Hrdý, I. Redox Pathways as Drug Targets in Microaerophilic Parasites. *Trends Parasitol.* **2018**, *34*, 576–589. [CrossRef]
11. Supuran, C.T. Structure and function of carbonic anhydrases. *Biochem. J.* **2016**, *473*, 2023–2032. [CrossRef] [PubMed]
12. Supuran, C.T. Carbonic anhydrases: Novel therapeutic applications for inhibitors and activators. *Nat. Rev. Drug Discov.* **2008**, *7*, 168–181. [CrossRef] [PubMed]
13. Neri, D.; Supuran, C.T. Interfering with pH regulation in tumours as a therapeutic strategy. *Nat. Rev. Drug Discov.* **2011**, *10*, 767–777. [CrossRef] [PubMed]
14. Capasso, C.; Supuran, C.T. An overview of the alpha-, beta- and gamma-carbonic anhydrases from Bacteria: Can bacterial carbonic anhydrases shed new light on evolution of bacteria? *J. Enzym. Inhib. Med. Chem.* **2015**, *30*, 325–332. [CrossRef] [PubMed]
15. Vullo, D.; Del Prete, S.; Di Fonzo, P.; Carginale, V.; Donald, W.A.; Supuran, C.T.; Capasso, C. Comparison of the Sulfonamide Inhibition Profiles of the  $\beta$ - and  $\gamma$ -Carbonic Anhydrases from the Pathogenic Bacterium *Burkholderia Pseudomallei*. *Molecules* **2017**, *22*, 421. [CrossRef] [PubMed]
16. Berrino, E.; Bua, S.; Mori, M.; Botta, M.; Murthy, V.S.; Vijayakumar, V.; Tamboli, Y.; Bartolucci, G.; Mugelli, A.; Cerbai, E.; et al. Novel Sulfamide-Containing. *Molecules* **2017**, *22*, 1049. [CrossRef] [PubMed]
17. Cau, Y.; Mori, M.; Supuran, C.T.; Botta, M. Mycobacterial carbonic anhydrase inhibition with phenolic acids and esters: Kinetic and computational investigations. *Org. Biomol. Chem.* **2016**, *14*, 8322–8330. [CrossRef] [PubMed]

18. Supuran, C.T. Advances in structure-based drug discovery of carbonic anhydrase inhibitors. *Expert Opin. Drug Discov.* **2017**, *12*, 61–88. [CrossRef]
19. Nishimori, I.; Onishi, S.; Takeuchi, H.; Supuran, C.T. The  $\alpha$  and  $\beta$  Classes Carbonic Anhydrases from *Helicobacter pylori* as Novel Drug Targets. *Curr. Pharm. Des.* **2008**, *14*, 622–630.
20. Supuran, C.T.; Capasso, C. An Overview of the Bacterial Carbonic Anhydrases. *Metab.* **2017**, *7*, 56. [CrossRef]
21. Rowlett, R.S. Structure and catalytic mechanism of the  $\beta$ -carbonic anhydrases. *Biochim. Biophys. Acta—Prot. Proteom.* **2010**, *1804*, 362–373. [CrossRef]
22. Zolfaghari Emameh, R.; Barker, H.; Hytönen, V.P.; Tolvanen, M.E.E.; Parkkila, S. Beta carbonic anhydrases: Novel targets for pesticides and anti-parasitic agents in agriculture and livestock husbandry. *Parasites Vect.* **2014**, *7*, 403. [CrossRef] [PubMed]
23. Syrjänen, L.; Parkkila, S.; Scozzafava, A.; Supuran, C.T. Sulfonamide inhibition studies of the  $\beta$  carbonic anhydrase from *Drosophila melanogaster*. *Bioorg. Med. Chem. Lett.* **2014**, *24*, 2797–2801. [CrossRef] [PubMed]
24. Supuran, C.T.; Capasso, C. New light on bacterial carbonic anhydrases phylogeny based on the analysis of signal peptide sequences. *J. Enzym. Inhib. Med. Chem.* **2016**, *2016*, 31, 1254–1260. [CrossRef]
25. Supuran, C.T.; Capasso, C. Biomedical applications of prokaryotic carbonic anhydrases. *Expert Opin. Ther. Pat.* **2018**, *28*, 745–754. [CrossRef] [PubMed]
26. Del Prete, S.; De Luca, V.; Capasso, C.; Supuran, C.T.; Carginale, V. Recombinant thermoactive phosphoenolpyruvate carboxylase (PEPC) from *Thermosynechococcus elongatus* and its coupling with mesophilic/thermophilic bacterial carbonic anhydrases (CAs) for the conversion of CO<sub>2</sub> to oxaloacetate. *Bioorg. Med. Chem.* **2016**, *24*, 220–225. [CrossRef] [PubMed]
27. Bootorabi, F.; Jänis, J.; Smith, E.; Waheed, A.; Kukkurainen, S.; Hytönen, V.; Valjakka, J.; Supuran, C.T.; Vullo, D.; Sly, W.S.; Parkkila, S. Analysis of a shortened form of human carbonic anhydrase VII expressed in vitro compared to the full-length enzyme. *Biochimie* **2010**, *92*, 1072–1080. [CrossRef]
28. Vermelho, A.B.; Capaci, G.R.; Rodrigues, I.A.; Cardoso, V.S.; Mazotto, A.M.; Supuran, C.T. Carbonic anhydrases from *Trypanosoma* and *Leishmania* as anti-protozoan drug targets. *Bioorg. Med. Chem.* **2017**, *25*, 1543–1555. [CrossRef] [PubMed]
29. da Silva Cardoso, V.; Vermelho, A.B.; Ricci Junior, E.; Almeida Rodrigues, I.; Mazotto, A.M.; Supuran, C.T. Antileishmanial activity of sulphonamide nanoemulsions targeting the  $\beta$ -carbonic anhydrase from *Leishmania* species. *J. Enzym. Inhib. Med. Chem.* **2018**, *33*, 850–857. [CrossRef] [PubMed]
30. Loftus, B.; Anderson, I.; Davies, R.; Alsmark, U.C.; Samuelson, J.; Amedeo, P.; Roncaglia, P.; Berriman, M.; Hirt, R.P.; Mann, B.J.; et al. The genome of the protist parasite *Entamoeba Histolytica*. *Nature* **2005**, *433*, 865–868. [CrossRef] [PubMed]
31. Covarrubias, A.S.; Bergfors, T.; Jones, T.A.; Högbom, M. Structural mechanics of the pH-dependent activity of beta-carbonic anhydrase from *Mycobacterium tuberculosis*. *J. Biol. Chem.* **2006**, *281*, 4993–4999. [CrossRef] [PubMed]
32. Nishimori, I.; Minakuchi, T.; Vullo, D.; Scozzafava, A.; Innocenti, A.; Supuran, C.T. Carbonic anhydrase inhibitors. Cloning, characterization, and inhibition studies of a new beta-carbonic anhydrase from *Mycobacterium tuberculosis*. *J. Med. Chem.* **2009**, *52*, 3116–3120. [CrossRef] [PubMed]
33. Ferraroni, M.; Del Prete, S.; Vullo, D.; Capasso, C.; Supuran, C.T. Crystal structure and kinetic studies of a tetrameric type II  $\beta$ -carbonic anhydrase from the pathogenic bacterium *Vibrio cholerae*. *Acta Crystallogr. D Biol. Crystallogr.* **2015**, *71*, 2449–2456. [CrossRef] [PubMed]
34. McGurn, L.D.; Moazzami-Goudarzi, M.; White, S.A.; Suwal, T.; Brar, B.; Tang, J.Q.; Espie, G.S.; Kimber, M.S. The structure, kinetics and interactions of the  $\beta$ -carboxysomal  $\beta$ -carbonic anhydrase, CcaA. *Biochem. J.* **2016**, *473*, 4559–4572. [CrossRef] [PubMed]
35. Khalifah, R.G. The carbon dioxide hydration activity of carbonic anhydrase. I. Stop-flow kinetic studies on the native human isoenzymes B and C. *J. Biol. Chem.* **1971**, *246*, 2561–2573. [PubMed]
36. Nishimori, I.; Minakuchi, T.; Vullo, D.; Scozzafava, A.; Supuran, C.T. Inhibition studies of the  $\beta$ -carbonic anhydrases from the bacterial pathogen *Salmonella enterica* serovar Typhimurium with sulfonamides and sulfamates. *Bioorg. Med. Chem.* **2011**, *19*, 5023–5030. [CrossRef] [PubMed]
37. Supuran, C.T. Carbonic anhydrase inhibitors and their potential in a range of therapeutic areas. *Expert Opin. Ther. Pat.* **2018**, *28*, 709–712. [CrossRef] [PubMed]
38. Supuran, C.T. Applications of carbonic anhydrases inhibitors in renal and central nervous system diseases. *Expert Opin Ther Pat.* **2018**, *28*, 713–721. [CrossRef] [PubMed]

39. Nocentini, A.; Supuran, C.T. Carbonic anhydrase inhibitors as antitumor/antimetastatic agents: A patent review (2008–2018). *Expert Opin Ther Pat.* **2018**, *28*, 729–740. [CrossRef]
40. Muñoz, W.; Lamm, A.; Poppers, D.; Lamm, S. Acetazolamide promotes decreased consumption of carbonated drinks and weight loss. *Oxf. Med. Case Rep.* **2018**, *2018*, Omy081. [CrossRef]
41. Abbate, F.; Supuran, C.T.; Scozzafava, A.; Orioli, P.; Stubbs, M.T.; Klebe, G. Nonaromatic sulfonamide group as an ideal anchor for potent human carbonic anhydrase inhibitors: Role of hydrogen-bonding networks in ligand binding and drug design. *J. Med. Chem.* **2004**, *47*, 550–557. [CrossRef]
42. Borrás, J.; Scozzafava, A.; Menabuoni, L.; Mincione, F.; Briganti, F.; Mincione, G.; Supuran, C.T. Carbonic anhydrase inhibitors: Synthesis of water-soluble, topically effective intraocular pressure lowering aromatic/heterocyclic sulfonamides containing 8-quinoline-sulfonyl moieties: Is the tail more important than the ring? *Bioorg. Med. Chem.* **1999**, *7*, 2397–2406. [CrossRef]
43. Supuran, C.T.; Clare, B.W. Carbonic anhydrase inhibitors—Part 57: Quantum chemical QSAR of a group of 1,3,4-thiadiazole- and 1,3,4-thiadiazoline disulfonamides with carbonic anhydrase inhibitory properties. *Eur. J. Med. Chem.* **1999**, *34*, 41–50. [CrossRef]
44. Laitinen, O.H.; Airene, K.J.; Hytönen, V.P.; Peltomaa, E.; Mähönen, A.J.; Wirth, T.; Lind, M.M.; Mäkelä, K.A.; Toivanen, P.I.; Schenkwein, D.; et al. A multipurpose vector system for the screening of libraries in bacteria, insect and mammalian cells and expression in vivo. *Nucleic Acids Res.* **2005**, *33*, e42. [CrossRef] [PubMed]
45. Määttä, J.A.E.; Eisenberg-Domovich, Y.; Nordlund, H.R.; Hayouka, R.; Kulomaa, M.S.; Livnah, O. Chimeric avidin shows stability against harsh chemical conditions—Biochemical analysis and 3D structure. *Biotechnol. Bioengin.* **2011**, *108*, 481–490. [CrossRef]
46. De Simone, G.; Supuran, C.T. (In)organic anions as carbonic anhydrase inhibitors. *J. Inorg. Biochem.* **2012**, *111*, 117–129. [CrossRef] [PubMed]
47. Murray, A.B.; Aggarwal, M.; Pinard, M.; Vullo, D.; Patrauchan, M.; Supuran, C.T.; McKenna, R. Structural Mapping of Anion Inhibitors to  $\beta$ -Carbonic Anhydrase psCA3 from *Pseudomonas aeruginosa*. *ChemMedChem.* **2018**, *13*, 2024–2029. [CrossRef] [PubMed]
48. Zimmerman, S.A.; Ferry, J.G.; Supuran, C.T. Inhibition of the archaeal beta-class (Cab) and gamma-class (Cam) carbonic anhydrases. *Curr. Top. Med. Chem.* **2007**, *7*, 901–908. [CrossRef]



© 2018 by the authors. Licensee MDPI, Basel, Switzerland. This article is an open access article distributed under the terms and conditions of the Creative Commons Attribution (CC BY) license (<http://creativecommons.org/licenses/by/4.0/>).





# PUBLICATION

## III

**Cloning, characterization and inhibition of the novel  $\beta$ -carbonic anhydrase from the parasitic blood fluke *Schistosoma mansoni***

Susanna Haapanen, Andrea Angeli, Martti Tolvanen, Reza Zolfaghari Emameh, Claudiu T. Supuran, Seppo Parkkila

Journal of enzyme inhibition and medicinal chemistry. 2023; 38(1):2184299

<https://doi.org/10.1080/14756366.2023.2184299>

**Publication reprinted with the permission of the copyright holders.**



RESEARCH PAPER



## Cloning, characterization, and inhibition of the novel $\beta$ -carbonic anhydrase from parasitic blood fluke, *Schistosoma mansoni*

Susanna Haapanen<sup>a\*</sup>, Andrea Angeli<sup>b\*</sup>, Martti Tolvanen<sup>c</sup>, Reza Zolfaghari Emameh<sup>d</sup>, Claudiu T. Supuran<sup>b\*</sup> and Seppo Parkkila<sup>a,e\*</sup>

<sup>a</sup>Faculty of Medicine and Health Technology, Tampere University, Tampere, Finland; <sup>b</sup>Neurofarba Department, Sezione di Chimica Farmaceutica e Nutraceutica, Università degli Studi di Firenze, Sesto Fiorentino, Italy; <sup>c</sup>Department of Computing, University of Turku, Turku, Finland;

<sup>d</sup>Department of Energy and Environmental Biotechnology, National Institute of Genetic Engineering and Biotechnology (NIGEB), Tehran, Iran;

<sup>e</sup>Fimlab Ltd, Tampere University Hospital, Tampere, Finland

### ABSTRACT

*Schistosoma mansoni* is an intestinal parasite with one  $\beta$ -class carbonic anhydrase, SmaBCA. We report the sequence enhancing, production, catalytic activity, and inhibition results of the recombinant SmaBCA. It showed significant catalytic activity on CO<sub>2</sub> hydration *in vitro* with  $k_{cat}$   $1.38 \times 10^5 s^{-1}$  and  $k_{cat}/K_m$   $2.33 \times 10^7 M^{-1} s^{-1}$ . Several sulphonamide inhibitors, from which many are clinically used, showed submicromolar or nanomolar inhibitory effects on SmaBCA. The most efficient inhibitor with a  $K_i$  of 43.8 nM was 4-(2-amino-pyrimidine-4-yl)-benzenesulfonamide. Other effective inhibitors with  $K_i$ s in the range of 79.4–95.9 nM were benzolamide, brinzolamide, topiramate, dorzolamide, saccharin, epacadostat, celecoxib, and famotidine. The other tested compounds showed at least micromolar range inhibition against SmaBCA. Our results introduce SmaBCA as a novel target for drug development against schistosomiasis, a highly prevalent parasitic disease.

### ARTICLE HISTORY

Received 16 January 2023  
Revised 13 February 2023  
Accepted 14 February 2023

### KEYWORDS

Carbonic anhydrase; anti-parasitic agents; inhibitor; sulphonamide; *Schistosoma mansoni*

### Introduction

*Schistosoma mansoni* is a parasitic blood fluke affecting ~200 million people worldwide.<sup>1,2</sup> It causes schistosomiasis and has been rated as the second most harmful parasite in the world; only malaria has been stated to cause more mortality.<sup>3,4</sup> *Schistosoma mansoni* is endemic in Africa, South America, the Caribbean, and the Middle East.<sup>5</sup> Schistosomiasis is an intestinal infection that produces acute symptoms of diarrhoea,<sup>6</sup> abdominal pain,<sup>6</sup> and fever.<sup>7</sup>

Patients are afflicted with *S. mansoni* as the larvae living in freshwater penetrate through healthy skin and travel via the bloodstream to the recipient's liver.<sup>8</sup> The larvae grow up and reach mesenteric veins to lay eggs.<sup>9</sup> Some of the larvae reside in the liver arteries<sup>10</sup> and can live for decades, causing granulomatous infection to the wall of the intestines as the eggs invade the gut wall.<sup>2,5</sup> Chronic granulomatous infection occurs in the liver, serving as an incubator for developing larvae and trapping some of the eggs,<sup>1</sup> and can lead to irreversible hepatic cirrhosis, especially if the affected person has chronic viral hepatitis, relatively common in the endemic areas of *S. mansoni*.<sup>11</sup> The chronic infection can be cured only via medical intervention as the host's immune system is unable to overcome the parasite.<sup>10</sup>

There is no vaccine against schistosomiasis<sup>12,13</sup> and the only currently known effective treatment against species of *Schistosoma*-genus parasites<sup>14</sup> is executed with praziquantel.<sup>10</sup> It is used as a preventive medicine and for treating patients,<sup>15</sup> but millions of people still get infected yearly.<sup>1</sup> Currently, the need for

preventive chemotherapy is over two times higher than the number of individuals receiving the required medication (Figure 1). The pervasive use of praziquantel for schistosomiasis has led to rising resistance against the drug.<sup>16,17</sup> Therefore, potential medicines with novel modes of action are urgently needed to fight this devastating disease.

In developing new drugs against parasitic diseases, carbonic anhydrases (CAs, EC 4.2.1.1) have recently emerged as potential targets.<sup>18–20</sup> CAs catalyse the reversible hydration of CO<sub>2</sub>, maintaining homeostasis in tissues and fluids of the body. Eight distinct families of CAs have been presented in classifications based on protein structures and the active site. Some of the families have evolved as a result of long divergent evolution, but there are at least four independent ancestors.<sup>21–23</sup> The  $\alpha$ - and  $\eta$ -CAs share a common protein fold but they contain different catalytic residues in the active sites.<sup>22</sup> The group of  $\beta$ -like-CAs includes  $\varepsilon$ -,  $\theta$ -, and  $\zeta$ -CAs (M. Tolvanen, unpublished observations). For  $\gamma$ -CAs and  $\iota$ -CAs, no structural or evolutionary relatedness to other classes has been reported. On the contrary,  $\delta$ -CAs show structural resemblance to  $\alpha$ -CAs, although they are considered a family of their own.<sup>24,25</sup> The earliest discovered enzyme forms are  $\alpha$ -CAs found in humans, other animals, and many other pro- and eukaryotic cells.<sup>26</sup>  $\beta$ -CAs are not found in vertebrates but are present in most prokaryotes, archaea, plants, fungi, and non-chordate metazoa.<sup>26,27</sup>  $\gamma$ -CAs have been identified in some prokaryotes, fungi, plants, and single-cell eukaryotic organisms, such as amoebas.<sup>27,28</sup>  $\delta$ -CAs are widely distributed in marine phytoplankton.<sup>29</sup>  $\zeta$ -CAs are mainly

**CONTACT** Susanna Haapanen  [susanna.haapanen@tuni.fi](mailto:susanna.haapanen@tuni.fi)  Faculty of Medicine and Health Technology, Tampere University, Tampere, 33520, Finland

\*These authors contributed equally to this work.

 Supplemental data for this article is available online at <https://doi.org/10.1080/14756366.2023.2184299>

© 2023 The Author(s). Published by Informa UK Limited, trading as Taylor & Francis Group.

This is an Open Access article distributed under the terms of the Creative Commons Attribution License (<http://creativecommons.org/licenses/by/4.0/>), which permits unrestricted use, distribution, and reproduction in any medium, provided the original work is properly cited.

## Preventive chemotherapy requirements vs. received

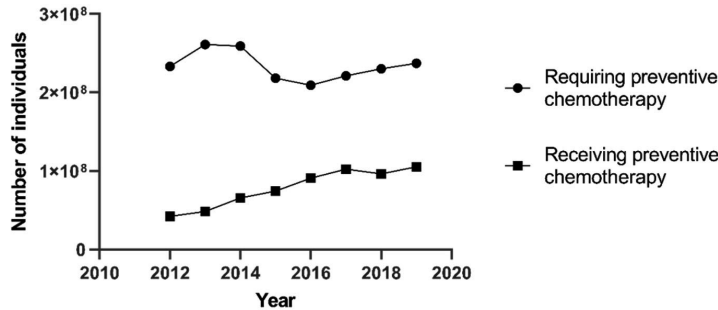


Figure 1. The worldwide requirement of preventive medication compared to the realised medication according to WHO [https://apps.who.int/neglected\_diseases/ntddata/sch/sch.html, figure visualisation made by Susanna Haapanen using GraphPad Prism (1992–2020 GraphPad Software, LLC, version 9.0.0)].

present in diatoms,<sup>30</sup> and  $\eta$ -CAs have been discovered in *Plasmodium*-parasites and in *Toxoplasma gondii*, thus far.<sup>22,31</sup>  $\theta$ -CAs have been found in marine diatoms, green algae, and bacteria,<sup>32</sup> and the most recently found  $\iota$ -CAs are widely found in bacteria, diatoms, green algae, and cyanobacteria.<sup>23,33</sup> *S. mansoni* has only one  $\beta$ -CA but six  $\alpha$ -CAs,<sup>34</sup> one of which has been previously produced as a recombinant protein and tested for inhibition properties using various sulphonamide and anion class inhibitors.<sup>35</sup> For instance, clorsulon, an antiparasitic sulphonamide, has a good inhibitory activity *in vitro*.<sup>36</sup> This study is focussed on the *S. mansoni*  $\beta$ -CA, for which we use the abbreviation SmaBCA.

CA inhibitors of the sulphonamide class are already in use as drugs to treat clinical conditions, such as glaucoma,<sup>37,38</sup> brain oedema,<sup>39</sup> and mountain sickness.<sup>40,41</sup> Ongoing research of new drug candidates for targeting different CA families aims at novel treatment of various diseases, such as cancer,<sup>38,42</sup> neuropathic pain,<sup>43</sup> migraine<sup>43</sup> as well as infectious diseases.<sup>42,44</sup> The clinically used inhibitors affect more than one CA isoform<sup>45</sup> and can contribute to significant adverse side effects.<sup>46</sup> The human genome has only  $\alpha$ -CAs, and the absence of  $\beta$ -CAs provides an excellent opportunity to design and generate more specific anti-parasitic drugs, explicitly targeting the  $\beta$ -CAs. This study aimed to produce and characterise recombinant SmaBCA and to test the efficacy of selected sulphonamide- and anion-type CA inhibitors against this enzyme. The results could help to determine the best inhibitor candidates for further development as lead compounds of antiparasitic drugs.

## Materials and methods

### Sequence retrieval

At the start of this study, we identified *S. mansoni*  $\beta$ -CA sequences by Blast searches at NCBI (https://blast.ncbi.nlm.nih.gov/Blast.cgi) and UniProt (https://www.uniprot.org/blast), using  $\beta$ -CA from *Drosophila melanogaster*<sup>47</sup> as a query sequence, finding XP\_018647616.1 at NCBI and G4V6B2 at UniProt, identical sequences of 241 aa. When a DNA sequence coding for this sequence could not be produced, we looked at the original sequence more carefully.

Further BlastP searches were carried out against NCBI RefSeq proteins with the *S. mansoni*  $\beta$ -CA XP\_018647616.1 as the query sequence, limiting the search to Platyhelminthes on May 14th, 2018. Selected hits were aligned using Clustal Omega (https://www.ebi.ac.uk/Tools/msa/clustalo/).<sup>48,49</sup> An N-terminally

incomplete *S. haematobium* protein XP\_012795040.1 matched well with *S. mansoni* XP\_018647616.1 but had a longer C-terminus, which resembles the C-termini of  $\beta$ -CA sequences of other parasites. This prompted us to revisit the gene model of XP\_018647616.1 to see if a sequence coding for a similar C-terminal extension could also be found in the *S. mansoni* genome. Using the *S. haematobium*  $\beta$ -CA protein as a query sequence in a Blast search at metazoa.ensembl.org, we identified a sequence coding for a full-length SmaBCA, which was used in the successful production of an active enzyme.

### Multiple sequence alignments (MSA)

In order to visualise sequence conservation in metazoan  $\beta$ -CAs for this article, we collected a new sequence set on 30 March 2022. *S. japonicum* KAH8855123.1 was used as a query sequence in BLAST at NCBI, with substitution matrix BLOSUM45, result list size of 5000, and taxonomy filter set to Metazoa. This resulted in 643 hits, filtered (with NCBI Blast result tools) for 85 % query coverage, leaving 520 sequences (https://github.com/MartiIT/S.-mansoni-BCA/blob/main/SmaBCA520%20blast%20hits%20Descriptions.xlsx). Incidentally, at this point, the RefSeq version of *S. mansoni*  $\beta$ -CA (XP\_018647616.1) was too short to pass the coverage filter. The longest 35 sequences (of 998–2153 aa, all from rotifers) were removed. The remaining 485 sequences were aligned preliminarily using the Clustal Omega<sup>48,49</sup> within SeaView 5.0.4,<sup>50</sup> and sequences with unique insertions or clearly mismatching sequences within conserved regions were manually deleted (using SeaView). The remaining 390 sequences were realigned with SeaView, and the resulting MSA (https://github.com/MartiIT/S.-mansoni-BCA/blob/main/SeaView%20MSA%20390.aln) was filtered for sequences with more than 90 % identity against any other sequence in the set. The Decrease redundancy tool at https://web.expasy.org/decrease\_redundancy/ was used for this purpose (Cédric Notredame, unpublished), and a final realignment was performed on the obtained set of 162 protein sequences with Clustal Omega at EBI (https://www.ebi.ac.uk/Tools/msa/clustalo/)<sup>49</sup> (Supplementary File 1).

A sequence logo was constructed to visualise this MSA using Berkeley WebLogo version 3.7.12 (https://weblogo.threeplusone.com/)<sup>51</sup> with the parameters of 1st pos –112, logo from 1 to 310, no adjustment for composition, no error bars, colour scheme chemistry (Figure 6).

To compare schistosomal  $\beta$ -CA sequences (Figure 2), we prepared a Clustal Omega alignment of the SmaBCA sequence of this study with *S. margrebowiei* VDO63334.1, *S. haematobium*

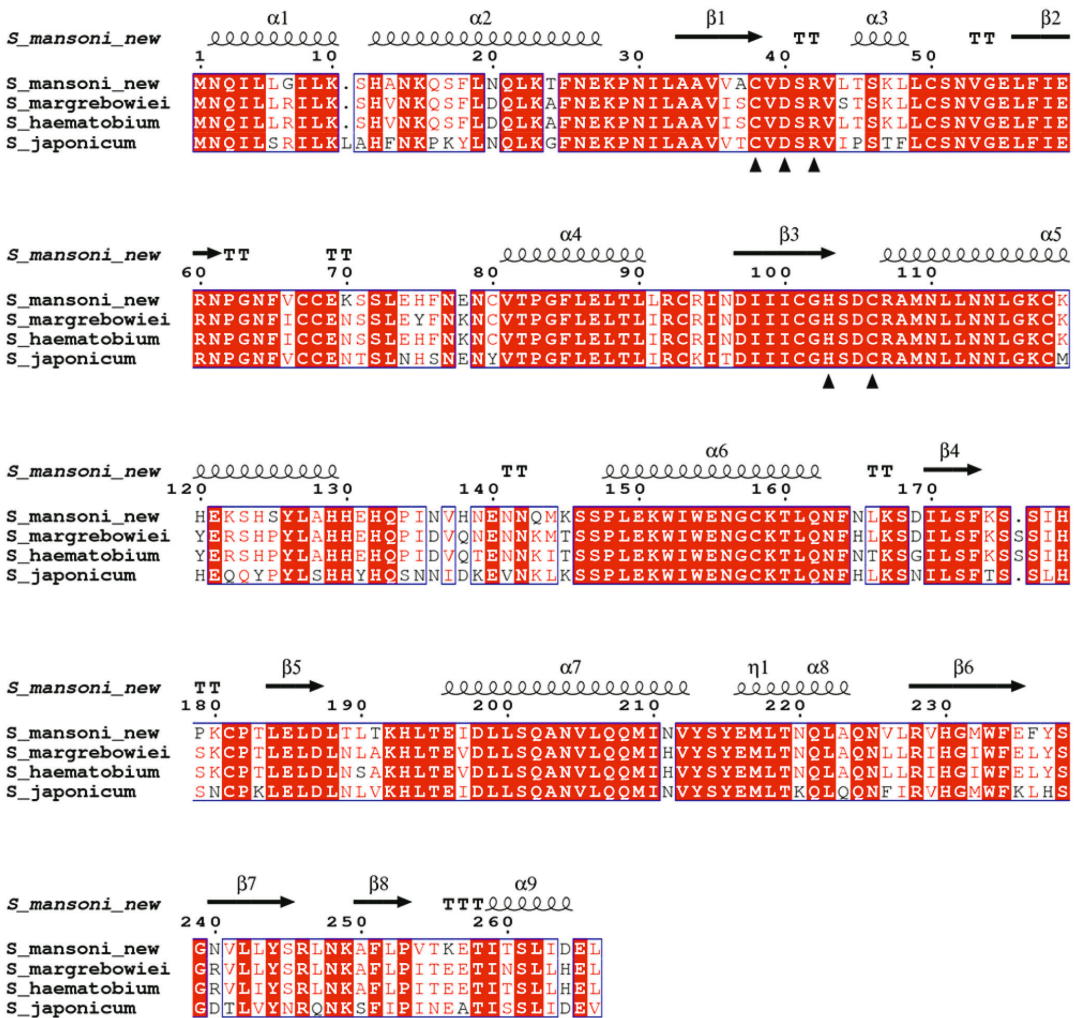


**Figure 2.** Comparison of the β-CA protein sequence of this study (*S\_mansoni\_new*) by sequence alignment to homologs from three other *Schistosoma* species. The conserved residues of the catalytic-site motifs, CXDXR and HXXC, are indicated with black triangles (C: Cys, D: Asp, H: His, R: Arg, X: any residue). Columns with fully conserved residues are shown as red with white letters. Boxed columns denote positions in which at least 75 % of residues are of a similar type, consisting of a total of 244 aa (91.7 %), of which 175 aa are totally conserved (65.8 %). The top line indicates the secondary structures of the AlphaFold model for *S. mansoni* β-CA. α: α-helices; β: β-strands; η: 3<sub>10</sub>-helices; T: turns.

KAH9593836.1, and *S. japonicum* TNN15731.1. This alignment was visualised using ESPript 3.0 at <https://esprict.ibcp.fr/ESPript/cgi-bin/ESPript.cgi>.<sup>52</sup> A global score cut-off of 0.75 used for colouring the blocks and secondary structure assignments for the top line were taken from the *S. mansoni* β-CA model retrieved from the AlphaFold protein structure database, <https://alphafold.ebi.ac.uk/entry/A0A3Q0KBP5>.<sup>53,54</sup>

### Dimer modelling

The monomer model retrieved from the AlphaFold protein structure database has a visual resemblance to the pea β-CA model (PDB 1ekj) in that the N-terminal alpha helices are detached from

the catalytic domain of the monomer structure. In the full octamer model of 1ekj, we can see that these alpha helices wrap around another monomer to create the basic dimer unit, which is repeated as four copies. This inspired us to create a 3D dimer model for *SmaBCA* using ChimeraX (daily build 1.4.dev202202030703), developed by the UCSF Resource for Biocomputing, Visualisation, and Informatics (San Francisco, California, USA), supported in part by the National Institutes of Health. The AlphaFold multimer modelling interface<sup>55</sup> was used to submit the prediction to run at Google Colab, giving two copies of our *SmaBCA* sequence as input, on 6 April 2022. The dimer model is available at <https://github.com/MarttiT/S.-mansoni-BCA/blob/main/SmaBCA%20dimer.pdb>.

### Vector construction, protein production, and purification

The same production procedure was followed both for the unsuccessful production of the protein corresponding to UniProt G4V6B2 and our amended sequence with a full-length last exon. The amended sequence contains the modifications to C-terminus as described above as well as the silent mutations to prevent Rho-independent termination site forming, on the contrary, to the unsuccessful production of the protein to which the sequence was unmodified.

Since some coding genes may contain termination codes in the middle of mRNA coding sequences and lead to early transcription termination and the consequent production of immature mRNA, a prediction approach was performed using ARNold (<http://rssf.i2bc.paris-saclay.fr/toolbox/arnold/>) web tool<sup>56</sup> to find Rho-independent transcription termination sites on the *SmaBCA* gene (NCBI gene ID: 8342150). To prevent the formation of immature mRNA for *SmaBCA*, five silent mutations were introduced to change the nucleotides of Rho-independent termination sites to other nucleotides.

The finalised sequence of the insert was sent to GeneArt (Invitrogen, Regensburg, Germany), where a modified plasmid vector, pBVboost, was constructed.<sup>57</sup>

The plasmid vector was prepared according to the manufacturer's instructions and then transformed with heat shock into BL21 Star™ (DE3) cells (Invitrogen, Carlsbad, USA), as described previously.<sup>58</sup> The production of recombinant protein was executed manually in LB broth (Sigma-Aldrich, St. Louis, MO, USA) with 1:1000 gentamicin (Sigma-Aldrich) and 1:100 glycerol (VWR International, Radnor, PA, USA)/glucose (Sigma-Aldrich) as proposed in Kopp et al.<sup>59</sup> at +37 degrees and shaking with 200 rpm. Both glycerol and glucose proved to be equally effective additives in the growth medium to reduce the number of impurities. The OD (Fisher Scientific Colorimeter Model 45 (WA12173), Fisherbrand, Thermo Fisher Scientific, Waltham, MA, USA) was measured and at the OD 0.4–0.5 1 M isopropyl- $\beta$ -D-thiogalactopyranoside (IPTG, Thermo Fisher Scientific) was added in relation of 1:1000 to LB medium. Growth continued overnight and was terminated the next day by pelleting the cells by centrifugation at 5000  $\times$  g for 20 min resulting in a total incubation and production time of 24 h.

A few alterations were made to the purification protocol compared to Haapanen et al.<sup>58</sup> We used 50 mM Na<sub>2</sub>HPO<sub>4</sub> (Sigma-Aldrich), 0.5 M NaCl (VWR International), and 50 mM imidazole (Sigma-Aldrich) (pH 8.0) as a binding buffer and washed the nickel resin (HisPur™ Ni-NTA Resin, Thermo Fisher Scientific) with 15  $\times$  25 ml of 50 mM Na<sub>2</sub>HPO<sub>4</sub>, 0.5 M NaCl, 50 mM imidazole, and 20 % glycerol (pH 8.0) with EMD Millipore™ vacuum filtering flask (Merck, Kenilworth, NJ, USA) and filter paper (pore size 2  $\mu$ m, Whatman™, Maidstone, UK). The glycerol was washed off with 10  $\times$  25 ml of binding buffer with the same vacuum filtering flask. Subsequently, the resin was collected into an empty column (Maxi Columns, G-Biosciences, St. Louis, MO, USA). The protein was eluted from the resin with elution buffer (50 mM Na<sub>2</sub>HPO<sub>4</sub>, 0.5 M NaCl, and 350 mM imidazole, pH 8.5). Re-purification was performed twice, similarly to the initial purification, except using 50 mM Na<sub>2</sub>HPO<sub>4</sub>, 0.5 M NaCl (pH 8.0) as a binding buffer to make the imidazole concentration under 20 mM. The purity of the collected fractions was verified with 12 % SDS-PAGE (sodium dodecyl sulfate-polyacrylamide gel electrophoresis) under reducing conditions using Precision Plus Protein™ Standards Dual Colour (Bio-Rad Laboratories, Inc., Hercules, CA, USA) as a standard molecular weight (MW) marker. The MW marker and bands were visualised with PageBlue™ Protein Staining Solution (Thermo Fisher

Scientific) on the gel by letting the gel stain for 30 min and then washing with distilled water. The bands were confirmed to be *SmaBCA* with mass spectrometry (data not shown).

### CA enzyme activity and inhibition

Before activity measurements, the buffer was changed into 50 mM TRIS (VWR International) (pH 8.5) with 10 kDa Vivaspin® Turbo 15 centrifugal concentrators (Sartorius™, Göttingen, Germany) at 4000  $\times$  g at +4°C. The CA-catalysed CO<sub>2</sub> hydration activity was measured using an Applied Photophysics stopped-flow instrument.<sup>60</sup> The measurement protocol was identical to the previously described in Berrino et al.<sup>61</sup>

### Results

To produce the recombinant protein of *SmaBCA*, an insert sequence was retrieved from the National Centre of Biotechnology Information (NCBI Reference Sequence: XM\_018793067.1). It was included in our construct because it was the only  $\beta$ -CA of *S. mansoni* available in sequence databases in 2018 (also represented in UniProt protein entry G4V6B2). We did not obtain any protein from recombinant production using this original sequence. Upon closer inspection, the sequence seemed to have an incorrectly predicted splice site in the actual last exon, joined to a superfluous exon, coding only for three residues instead of extending the last exon up to a stop codon. The full-length sequence for the last exon was discovered in the *S. mansoni* genome by searching with other schistosomal  $\beta$ -CA sequences. The amended last exon coded for 28 additional amino acids (aa), highly similar to the search query sequences. This sequence also led to the successful production of the active enzyme described in this study. A full-length sequence of *SmaBCA* was added in UniProt after we had already produced our protein (A0A3Q0KBP5, 13 February 2019). This sequence is probably derived from a later genome version than ours (which came from *S. mansoni* genome assembly ASM23792v2 as of 14 May 2018 at metazoa.ensembl.org), and it differs by one amino acid substitution (N264D) from our sequence. This is a variable site even within *Schistosoma* species (Figure 2).

Our analysis also revealed that the *SmaBCA* gene sequence contains a Rho-independent transcription termination site, a GC-rich area in the sequence causing loop formation and detachment of RNA polymerase, which introduces an early termination of transcription in bacteria and consequently a non-functional messenger RNA (mRNA) (Figure 3). To enable the recombinant production in *Escherichia coli*, we chose to create single nucleotide mutations in the coding sequence to disrupt base pairs in the stem (blue in Figure 3) without any effect on the translated amino acid sequence.

As a result of recombinant protein production, we obtained six protein bands of ~13, 22, 25, 29, 38, and 75 kDa in size (Figure 4). All these bands represented different forms of *SmaBCA* as confirmed by mass spectrometry (data not shown). The calculated molecular weight of the translated coding sequence is 30.4 kDa, not accounting for any post-translational modifications.

Kinetic analysis of *SmaBCA* showed that the enzyme (with Histag) is moderately active with  $k_{cat}$   $1.38 \times 10^5$  s<sup>-1</sup>,  $K_m$  5.92 mM, and  $k_{cat}/K_m$   $2.33 \times 10^7$  M<sup>-1</sup> s<sup>-1</sup>. Several sulphonamide and anion inhibitors<sup>46,62,63</sup> were tested to evaluate their inhibitory properties against *SmaBCA*. The most efficient inhibitors showed submicromolar or nanomolar inhibitory effects on *SmaBCA* (Table 1 and Figure 5). The most efficient inhibitor with a  $K_i$  of 43.8 nM was



**Figure 3.** The coding sequence of the  $\beta$ -CA gene from *S. mansoni*. The predicted Rho-independent transcription termination site is marked in underlined blue and red text in the sequence, and the corresponding Rho-independent stem-loop is shown on the right.

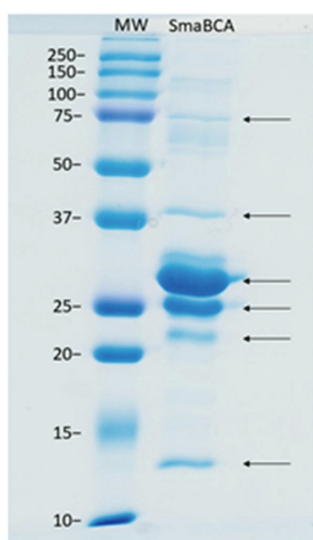


**Figure 4.** SDS-PAGE of  $\beta$ -CA of *S. mansoni* (SmaBCA) showing six polypeptide bands confirmed to represent SmaBCA by mass-spectrometry (data not shown). Right lane: The most intense bands of 25 and 29 kDa are the main forms of the expressed protein, and the additional polypeptides either are degraded forms (13 and 22 kDa) or oligomers (38 and 75 kDa). Left lane: Standard molecular weight (MW) markers in kDa.

4-(2-amino-pyrimidine-4-yl)-benzenesulfonamide (compound 19). Other effective inhibitors included several clinically used drugs. Benzolamide (BZA), brinzolamide (BRZ), topiramate (TPM), dorzolamide (DZA), saccharin (SAC), epacacostat (EPT), celecoxib (CLX), and famotidine (FAM) showed  $K_i$ s in the range of 79.4–95.9 nM. The other tested compounds inhibited SmaBCA at micromolar or millimolar concentrations.

Our protein sequence was aligned with  $\beta$ -CA sequences of other *Schistosoma* species, as shown in Figure 2. All these sequences are highly similar, with identities to the protein of this study ranging from 75.6 to 86.8%. The identity percentages are even higher in the protein core and in the active site, which suggests that any drugs developed to inhibit SmaBCA would also be inhibitory for  $\beta$ -CAs of other *Schistosoma* species.

**Table 1.** Inhibition data for SmaBCA with sulphonamide analogs 1–24, clinically used compounds, and anions.

Compound	SmaBCA $K_i$ ( $\mu$ M)*	Compound	SmaBCA $K_i$ ( $\mu$ M)*
1	1.830	BRZ	0.083
2	2.516	BZA	0.079
3	1.556	TPM	0.083
4	0.776	NO <sub>3</sub> <sup>-</sup>	>10 000
5	0.788	NO <sub>3</sub> <sup>-</sup>	2270
6	0.327	HCO <sub>3</sub> <sup>-</sup>	7840
7	0.872	CO <sub>3</sub> <sup>2-</sup>	740
8	0.372	HCO <sub>3</sub> <sup>-</sup>	4260
9	0.960	SO <sub>4</sub> <sup>2-</sup>	3720
10	0.935	F <sup>-</sup>	6280
11	2.040	Cl <sup>-</sup>	2850
12	0.417	Br <sup>-</sup>	2840
13	0.314	I <sup>-</sup>	840
14	0.375	CNO <sup>-</sup>	890
15	0.982	SCN <sup>-</sup>	930
16	0.600	HS <sup>-</sup>	820
17	0.346	CN <sup>-</sup>	930
18	1.043	N <sub>3</sub> <sup>-</sup>	800
19	0.044	Sulfamide	8
20	0.316	Sulfamic acid	40
21	0.255	Phenylarsonic acid	20
22	0.378	Phenylboronic acid	520
23	0.241	SnO <sub>3</sub> <sup>2-</sup>	960
24	0.750	SeO <sub>4</sub> <sup>2-</sup>	3490
SLP	0.254	TeO <sub>4</sub> <sup>2-</sup>	4900
IND	0.812	OsO <sub>3</sub> <sup>2-</sup>	580
ZNS	0.521	P <sub>2</sub> O <sub>7</sub> <sup>2-</sup>	>10 000
CLX	0.092	V <sub>2</sub> O <sub>7</sub> <sup>2-</sup>	>10 000
VLX	0.474	B <sub>4</sub> O <sub>7</sub> <sup>2-</sup>	4300
SLT	0.758	ReO <sub>4</sub> <sup>-</sup>	9090
SAC	0.091	RuO <sub>4</sub> <sup>-</sup>	3650
HCT	0.918	S <sub>2</sub> O <sub>8</sub> <sup>2-</sup>	>10 000
FAM	0.096	SeCN <sup>-</sup>	220
DCP	0.545	NH(SO <sub>3</sub> ) <sub>2</sub> <sup>-</sup>	>10 000
EPT	0.092	FSO <sub>3</sub> <sup>-</sup>	>10 000
AAZ	0.286	CS <sub>3</sub> <sup>2-</sup>	3330
MZA	0.210	Et <sub>3</sub> NCS <sub>2</sub> <sup>-</sup>	420
EZA	0.246	PF <sub>6</sub> <sup>-</sup>	>10 000
DZA	0.090	Triflate	>10 000

\*Mean from three different assays, by a stopped-flow technique (errors were in the range of  $\pm$ 5–10% of the reported values).

The sequence logo of Figure 6 extracts information from a multiple sequence alignment (MSA) of 162 metazoan  $\beta$ -CA sequences showing 19 perfectly conserved aa sites and 26 almost conserved sites. Of course, we find highly conserved areas at the motifs, which are part of the active site (CXDXR and HXXC), and

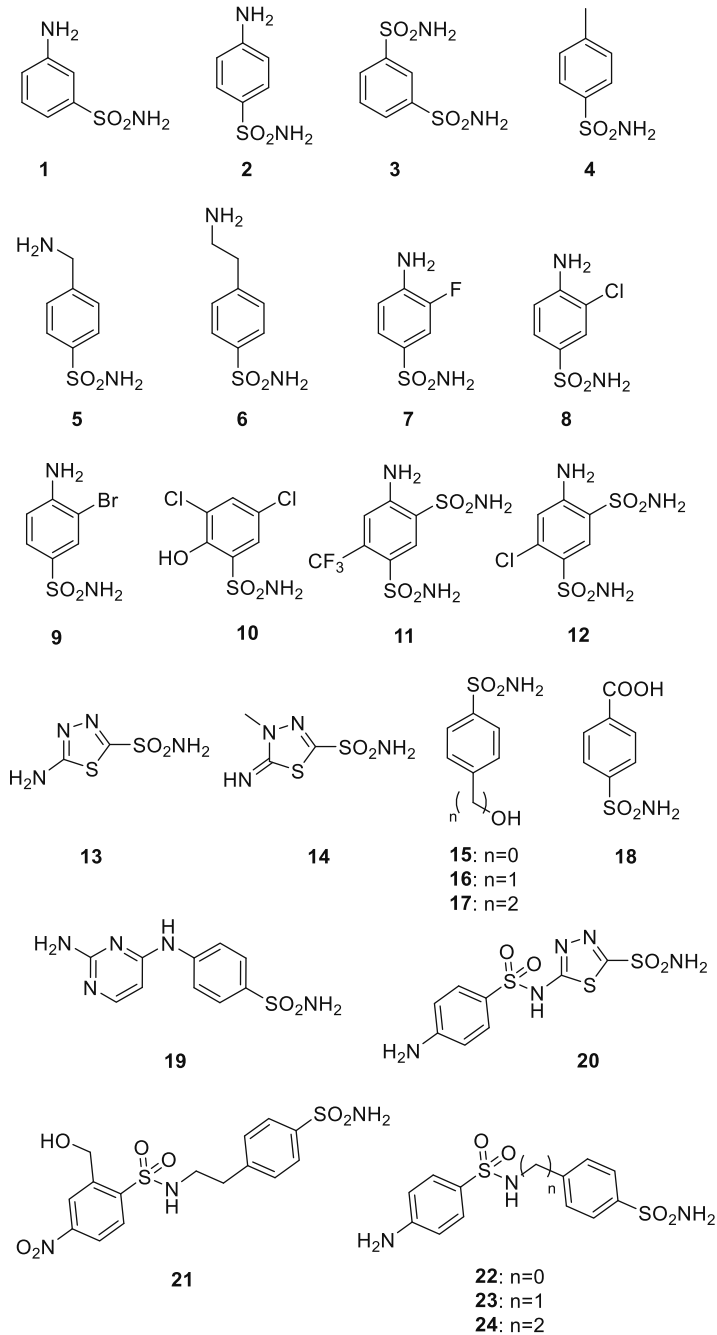


Figure 5. Chemical structures of sulphonamide (1–24) and sulphonamide/sulfamate derivatives (AAZ-EPT) tested as inhibitors against  $\beta$ -CA of *Schistosoma mansoni* (SmaBCA) in this study.



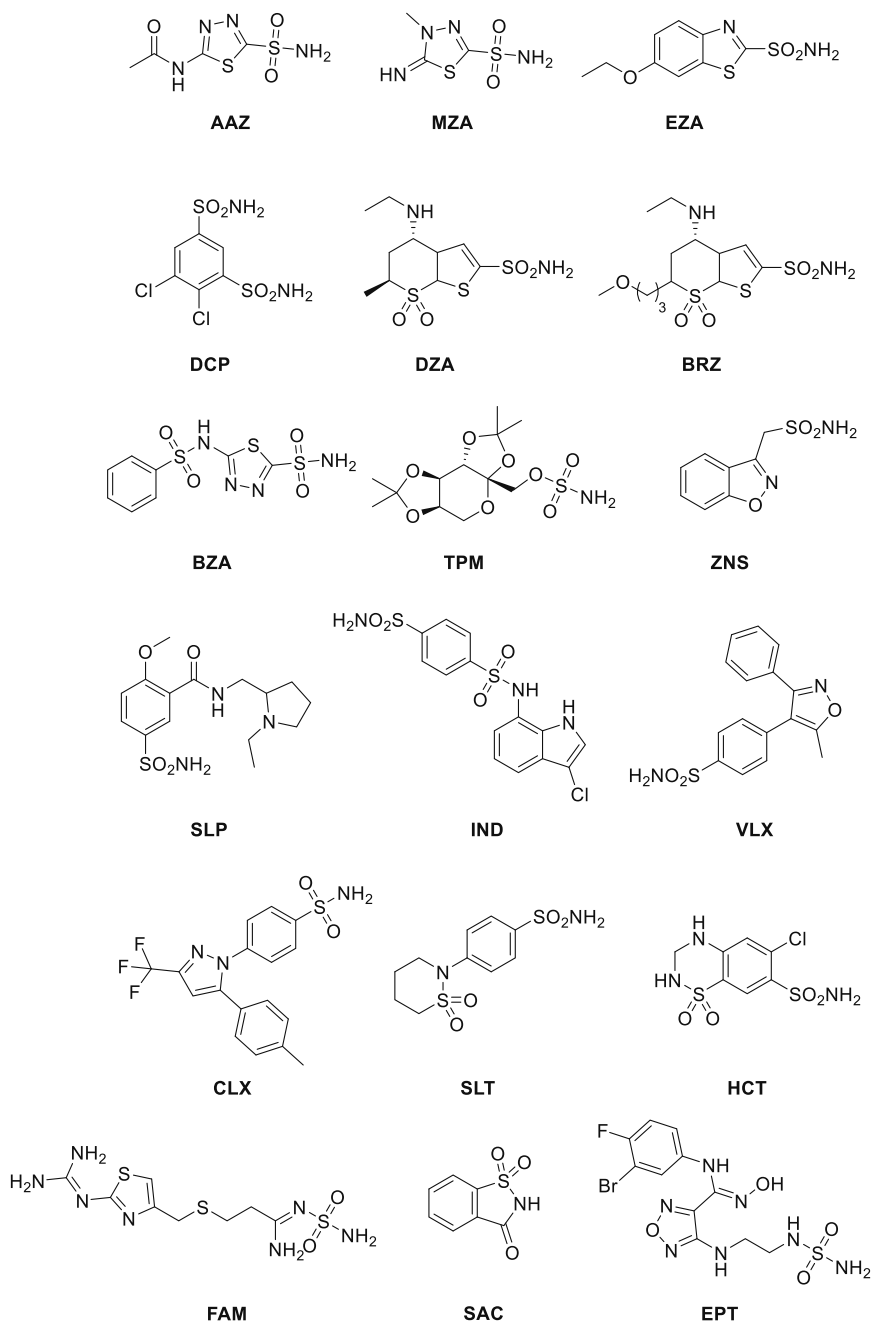
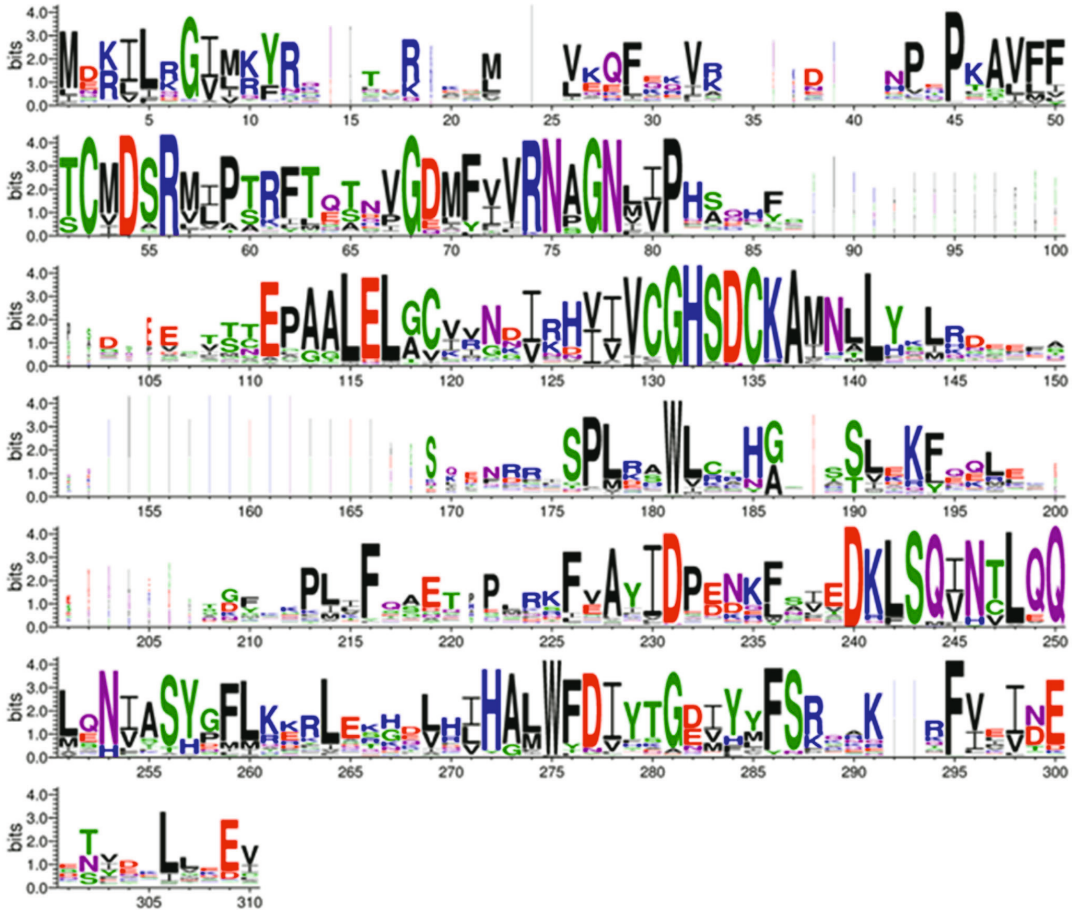


Figure 5. Continued.



**Figure 6.** Comparison of metazoan  $\beta$ -CA proteins. This sequence logo represents an MSA of 162 sequences, cropped at both ends to show only the extent of the SmaBCA sequence. The height of each stack of letters represents the conservation (information content) of each column in the alignment. The width of the letters represents the number of non-gap characters in each column (i.e. very narrow letters indicate positions in which only few of the aligned proteins have any sequence).

additionally, at columns 68–81 and 240–250. The gap region at columns 151–168 in the MSA (Figure 6) is due to an insertion seen only in *Schistosoma* sequences of our sequence set. The entire MSA is provided as Supplementary File S1. More data is available as noted in the Experimental procedures.

We built a computational 3D model of the SmaBCA dimer using AlphaFold multimer. In this model, the alpha-helical segments in the N-terminus are positioned along the side of the other monomer, similar to the dimers of *Pisum sativum* (pea)  $\beta$ -CA (PDB 1ekj).<sup>64</sup> These segments are also present in the AlphaFold monomer model (<https://alphafold.ebi.ac.uk/entry/A0A3Q0KBP5>), in which their position away from the core of the protein looks odd, but in the dimer model (Figure 7) it makes perfect sense. The orientation between the monomers in our model is nearly identical to pea  $\beta$ -CA dimers (1ekj, e.g. chains C and D, data not shown).

AlphaFold gives a confidence score (predicted local distance difference test, pLDDT) to the position of each residue in the model, pLDDT >90 indicating “very high confidence” and pLDDT >70 “confident”. In our model, two regions (69–79 and 119–145) have pLDDT values <70. They correspond to regions of low

conservation and insertions of variable lengths in our MSA of metazoan  $\beta$ -CA sequences (columns 83–108 and 148–174 in Figure 6). These two regions are also slightly different between the AlphaFold database monomer model and our dimer model (data not shown).

## Discussion

Schistosomiasis causes high morbidity in tropical and subtropical countries, and despite the treatment with praziquantel,<sup>65</sup> the infection remains a significant health problem.<sup>66</sup> Unfortunately, there are already initial signs of developing resistance against praziquantel<sup>67</sup> which emphasises the need for novel medication. In this study, we cloned the SmaBCA and found many already clinically used CA inhibitors with significant inhibitory effects against SmaBCA.

SmaBCA has a similar distribution of bands in SDS-PAGE as  $\beta$ -CAs from *Entamoeba histolytica* (EhICA)<sup>58</sup> and *Trichomonas vaginalis*<sup>57</sup> before His-tag removal: they all contain the major dual-band at a size which is predicted according to the aa chain composition. However, the dual-band formation disappears from

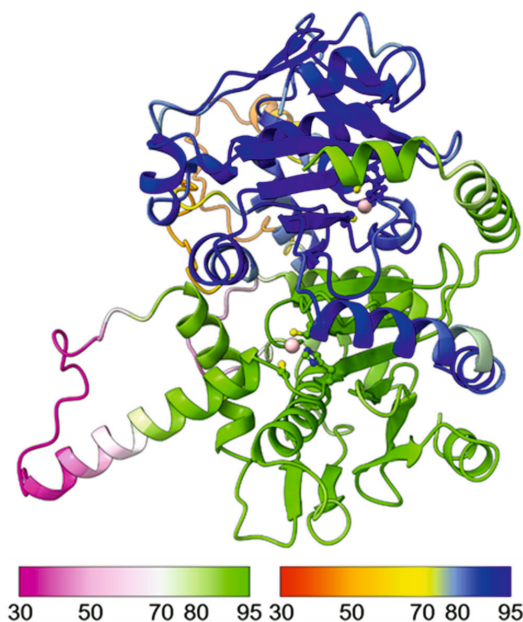


**Figure 7.** Molecular model of a hypothetical SmBCA dimer, constructed using AlphaFold multimer. Colouring is shown based on the per-residue confidence score (pLDDT), with two different palettes, as shown in the colour keys at the bottom left and right, for the bottom and top monomer, respectively. Metal-binding residues at the catalytic site (Cys 38, His 103, and Cys 106) are shown in balls-and-sticks style. The zinc ion at the catalytic site is displayed in pink.

$\beta$ -CAs of *T. vaginalis* as the His-tag is removed, contrary to EhiCA, which retains the double band appearance after the cleavage of His-tag.

SmaBCA shows enzyme activity with  $k_{\text{cat}}$   $1.38 \times 10^5 \text{ s}^{-1}$  and  $k_{\text{cat}}/K_m$   $2.33 \times 10^7 \text{ M}^{-1} \text{ s}^{-1}$ , within a similar range compared with the  $\beta$ -CAs from *T. vaginalis* ( $k_{\text{cat}}$   $4.9 \times 10^5$  and  $k_{\text{cat}}/K_m$   $8.0 \times 10^7$ ).<sup>57</sup> *Leishmania donovani chagasi* ( $k_{\text{cat}}$   $9.35 \times 10^5 \text{ s}^{-1}$  and  $k_{\text{cat}}/K_m$   $5.9 \times 10^7 \text{ M}^{-1} \text{ s}^{-1}$ ),<sup>68</sup> *Ascaris lumbricoides* ( $k_{\text{cat}}$   $6.0 \times 10^5 \text{ s}^{-1}$ ,  $k_{\text{cat}}/K_m$   $4.3 \times 10^7 \text{ M}^{-1} \text{ s}^{-1}$ ),<sup>69</sup> and EhiCA ( $k_{\text{cat}}$  of  $6.7 \times 10^5 \text{ s}^{-1}$  and a  $k_{\text{cat}}/K_m$  of  $8.9 \times 10^7 \text{ M}^{-1} \times \text{s}^{-1}$ ),<sup>58</sup> demonstrating the possibly crucial role in the metabolism of the organisms, as the magnitude of activity is considered from moderate (SmaBCA) to high ( $\beta$ -CAs from *T. vaginalis*, *Leishmania donovani chagasi*, *Ascaris lumbricoides*, and EhiCA) compared to human CA I (moderate,  $k_{\text{cat}}$   $2.0 \times 10^5$  and  $k_{\text{cat}}/K_m$   $5.0 \times 10^7$ ), for instance.

Schistosomiasis and amoebiasis (intestinal infection caused by *E. histolytica*) are endemic in the same areas of the world<sup>70</sup> and coinfections are not unusual<sup>71,72</sup> leading to the conclusion of achievable benefits from treating the infections with only one drug: less adverse side effects for the patient, better treatment compliance, and lower costs for the society. SmaBCA and EhiCA are both well-inhibited with many anion and sulphonamide derivatives. The most effective ones for EhiCA are 4-hydroxymethyl-ethyl-benzenesulfonamides (compounds 16 and 17) with  $K_i$  values of 89 and 36 nM, respectively,<sup>63</sup> with good inhibition activity against SmaBCA with  $K_i$ s of 600 and 346 nM, respectively. They are weak in inhibiting human CA II ( $K_i$  of 125 nM) and almost inefficient inhibitors of human CA I ( $K_i$  of 21  $\mu\text{M}$ ),<sup>63</sup> indicating a slight parasite selectivity. This kind of inhibitors could potentially have minimal side effects on humans. Other nanomolar range inhibitors are 4-(2-aminoethyl)benzenesulfonamide (compound 6), 4-(2-

amino-4-pyrimidinyl)amino)benzenesulfonamide (compound 19), and acetazolamide (AAZ) with  $K_i$ s of 509–798 nM for EhiCA and  $K_i$ s of 44–286 nM for SmaBCA, from which acetazolamide is already in clinical use.<sup>73–76</sup> With low micromolar range are sulfamide and phenylarsonic acid with  $K_i$ s of 28–38 and 8–20  $\mu\text{M}$ , for EhiCA and SmaBCA, respectively. The many agents with good inhibitory activity demonstrate the possibilities for developing CA inhibitors as anti-parasitic drugs against both enzymes of these parasites.

AA sequences of SmaBCA and  $\beta$ -CAs of other *Schistosoma* species are highly similar, as shown by MSA (Figure 2). In particular, the essential parts (the protein core and the active site) of the  $\beta$ -CA sequences are highly conserved, hence, opening an exciting opportunity to find functioning CA inhibitor-based drugs effective against all the species as praziquantel nowadays is. To our knowledge, only one other *Schistosoma* species, *S. japonicum*, has had its only  $\beta$ -CA produced as a recombinant protein previously.<sup>77</sup> Cong-Hui *et al.* produced 38 kDa recombinant protein with CA activity, but they did not make any comparison to  $\beta$ -CAs of other *Schistosoma* species. *S. mansoni* and *S. japonicum* are genetically distinct as they were separated as their own phylogenetic branches  $\sim 14$  million years ago,<sup>78</sup> and they are endemic in different parts of the world: *S. japonicum* in South-East Asia and *S. mansoni* mainly in Africa, South America, the Caribbean, and Middle East, both causing similar intestinal infections.<sup>1,5</sup> A new universal anti-schistosomal agent could have clinical value in very large areas covering most of the globe.

The  $\beta$ -CA of *S. mansoni* is a promising target for the development of new anti-schistosomal drugs. In this study, we produced a novel SmaBCA recombinant protein, tested it against different CA inhibitors, leading to the discovery of several well-inhibiting compounds, from which some are already used in treating other conditions. Based on structural and sequence analyses, we also propose that it is feasible to develop one universally functional anti-parasitic drug against several *Schistosoma* species which could also be effective against other parasites, such as *Entamoeba histolytica*.

## Acknowledgements

We thank Marianne Kuuslahti and Sanna Kavén for their skillful technical assistance; Juha Määttä, PhD, and Niklas Kähkönen for the help with protein purification and Maarit Patrikainen, PhD, for the help with refining the article text. We acknowledge the Tampere Facility of Protein Services (PS) for their service.

## Author contributions

SH, AA, SP, and CTS designed the experiments. SH and AA performed the experiments in the laboratory. MT and RZE planned the modifications to the sequence. MT planned and prepared the bioinformatic analyses. SH drafted this manuscript. SP, MT, and CTS reviewed the drafts and modified the manuscript. All authors read and approved the final manuscript.

## Disclosure statement



No potential conflict of interest was reported by all authors except Claudiu T. Supuran. C. T. Supuran is Editor-in-Chief of the Journal of Enzyme Inhibition and Medicinal Chemistry. He was not involved in the assessment, peer review, or decision-making process of this paper. The authors have no relevant affiliations of financial involvement with any organisation or entity with a

financial interest in or financial conflict with the subject matter or materials discussed in the manuscript. This includes employment, consultancies, honoraria, stock ownership or options, expert testimony, grants or patents received or pending, or royalties.

## Funding

This work was supported by the Finnish Medical Foundation under Grant number 5299; and the Academy of Finland under Grant number 348972. The funders had no role in study design, data collection and analysis, publication decision, or manuscript preparation.

## ORCID

Susanna Haapanen  <http://orcid.org/0000-0003-3833-6629>  
 Andrea Angeli  <http://orcid.org/0000-0002-1470-7192>  
 Reza Zolfaghari Emameh  <http://orcid.org/0000-0002-3253-7844>  
 Claudiu T. Supuran  <http://orcid.org/0000-0003-4262-0323>  
 Seppo Parkkila  <http://orcid.org/0000-0001-7323-8536>

## Data availability statement

The data that support the findings of this study are openly available in MarttiT/S.-mansonii-BCA at <https://github.com/MarttiT/S.-mansonii-BCA>.

## References

- Gryseels B, Polman K, Clerinx J, Kestens L. Human schistosomiasis. *Lancet*. 2006;368(9541):1106–1118.
- McManus DP, Dunne DW, Sacko M, Utzinger J, Vennervald BJ, Zhou XN. Schistosomiasis. *Nat Rev Dis Prim*. 2018;4(1).
- Kamau E, Yates A, Maisiba R, Singoei V, Opot B, Adeny R, Arima CO, Otieno V, Sumbi CS, Okoth RO, et al. Epidemiological and clinical implications of asymptomatic malaria and schistosomiasis co-infections in a rural community in western Kenya. *BMC Infect Dis*. 2021;21(1).
- Wilson S, Vennervald BJ, Dunne DW. Chronic hepatosplenomegaly in African school children: a common but neglected morbidity associated with schistosomiasis and malaria. *PLOS Negl Trop Dis*. 2011;5(8):e1149.
- Gryseels B. Schistosomiasis. *Infect Dis Clin North Am*. 2012;26(2):383–397.
- Elbaz T, Esmat G. Hepatic and intestinal schistosomiasis: review. *J Adv Res*. 2013;4(5):445–452.
- Nelwan ML. Schistosomiasis: life cycle, diagnosis, and control. *Curr Ther Res Clin Exp*. 2019;91:5–9.
- Colley DG, Bustinduy AL, Secor WE, King CH. Human schistosomiasis. *Lancet*. 2014;383(9936):2253–2264.
- Costain AH, MacDonald AS, Smits HH. Schistosome egg migration: mechanisms, pathogenesis and host immune responses. *Front Immunol*. 2018;9.
- Siqueira L. d P, Fontes DAF, Aguilera CSB, Timóteo TRR, Ângelos MA, Silva LCPBB, de Melo CG, Rolim LA, da Silva RMF, Neto PJR, et al. Schistosomiasis: drugs used and treatment strategies. *Acta Trop*. 2017;176:179–187.
- Gasim GI, Bella A, Adam I. Schistosomiasis, hepatitis B and hepatitis C co-infection. *Virology*. 2015;12(1).
- Rahmani A, Bae M, Rostamtabar M, Karkhah A, Alizadeh S, Tourani M, Nouri HR. Development of a conserved chimeric vaccine based on helper T-cell and CTL epitopes for induction of strong immune response against *Schistosoma mansoni* using immunoinformatics approaches. *Int J Biol Macromol*. 2019;141:125–136.
- Eyayu T, Zeleke AJ, Worku L. Current status and future prospects of protein vaccine candidates against *Schistosoma mansoni* infection. *Parasite Epidemiol Control*. 2020;11:e00176.
- LoVerde PT. Schistosomiasis. *Adv Exp Med Biol*. 2019;1154:45–70.
- Cioli D, Pica-Mattoccia L, Basso A, Guidi A. Schistosomiasis control: praziquantel forever? *Mol Biochem Parasitol*. 2014;195(1):23–29.
- Doenhoff MJ, Kusel JR, Coles GC, Cioli D. Resistance of *Schistosoma mansoni* to praziquantel: is there a problem? *Trans R Soc Trop Med Hyg*. 2002;96(5):465–469.
- Botros SS, Bennett JL. Praziquantel resistance. *Expert Opin Drug Discov*. 2007;2(sup1):S35–S40.
- Capasso C, Supuran CT. Anti-infective carbonic anhydrase inhibitors: a patent and literature review. *Expert Opin Ther Pat*. 2013;23(6):693–704.
- Bonardi A, Vermelho AB, da Silva Cardoso V, de Souza Pereira MC, da Silva Lara L, Selli S, Gratteri P, Supuran CT, Nocentini A. *N*-nitrosulfonamides as carbonic anhydrase inhibitors: a promising chemotype for targeting Chagas disease and Leishmaniasis. *ACS Med Chem Lett*. 2019;10(4):413–418.
- D'Ambrosio K, Supuran CT, De Simone G. Are carbonic anhydrases suitable targets to fight protozoan parasitic diseases? *Curr Med Chem*. 2018;25(39):5266–5278.
- Liljas A, Laurberg M. A wheel invented three times. The molecular structures of the three carbonic anhydrases. *EMBO Rep*. 2000;1(1):16–17.
- De Simone G, Di Fiore A, Capasso C, Supuran CT. The zinc coordination pattern in the  $\eta$ -carbonic anhydrase from *Plasmodium falciparum* is different from all other carbonic anhydrase genetic families. *Bioorg Med Chem Lett*. 2015;25(7):1385–1389.
- Jensen EL, Clement R, Kosta A, Maberly SC, Gontero B. A new widespread subclass of carbonic anhydrase in marine phytoplankton. *ISME J*. 2019;13(8):2094–2106.
- Cox EH, McLendon GL, Morel FM, Lane TW, Prince RC, Pickering IJ, George GN. The active site structure of *Thalassiosira weissflogii* carbonic anhydrase 1. *Biochemistry*. 2000;39(40):12128–12130.
- Del Prete S, Vullo D, De Luca V, Supuran CT, Capasso C. Biochemical characterization of the  $\delta$ -carbonic anhydrase from the marine diatom *Thalassiosira weissflogii*, TweCA. *J Enzyme Inhib Med Chem*. 2014;29(6):906–911.
- Capasso C, Supuran CT. An overview of the alpha-, beta- and gamma- carbonic anhydrases from bacteria: can bacterial carbonic anhydrases shed new light on evolution of bacteria? *J Enzyme Inhib Med Chem*. 2015;30(2):325–332.
- Zolfaghari Emameh R, Kuuslahti M, Nosrati H, Lohi H, Parkkila S. Assessment of databases to determine the validity of  $\beta$ -A and  $\gamma$ -carbonic anhydrase sequences from vertebrates. *BMC Genomics*. 2020;21(1):352.
- Ferry JG. The  $\gamma$  class of carbonic anhydrases. *Biochim Biophys Acta Proteins Proteomics*. 2010;1804(2):374–381.
- Alterio V, Langella E, Viparelli F, Vullo D, Ascione G, Dathan NA, Morel FMM, Supuran CT, De Simone G, Monti SM. Structural and inhibition insights into carbonic anhydrase CDCA1 from the marine diatom *Thalassiosira weissflogii*. *Biochimie*. 2012;94(5):1232–1241.

30. Park H, Song B, Morel FMM. Diversity of the cadmium-containing carbonic anhydrase in marine diatoms and natural waters. *Environ Microbiol.* 2007;9(2):403–413.
31. Chasen NM, Asady B, Lemgruber L, Vommaro RC, Kissinger JC, Coppens I, Moreno SNJ. A glycosylphosphatidylinositol-anchored carbonic anhydrase-related protein of *Toxoplasma gondii* is important for rhoptry biogenesis and virulence. *mSphere.* 2017;2(3).
32. Kikutani S, Nakajima K, Nagasato C, Tsuji Y, Miyatake A, Matsuda Y. Thylakoid luminal  $\Theta$ -carbonic anhydrase critical for growth and photosynthesis in the marine diatom *Phaeodactylum tricornutum*. *Proc Natl Acad Sci USA.* 2016; 113(35):9828–9833.
33. Angeli A, Berrino E, Carradori S, Supuran CT, Cirri M, Carta F, Costantino G. Amine- and amino acid-based compounds as carbonic anhydrase activators. *Molecules.* 2021;26(23):7331.
34. Berriman M, Haas BJ, LoVerde PT, Wilson RA, Dillon GP, Cerqueira GC, Mashiyama ST, Al-Lazikani B, Andrade LF, Ashton PD, et al. The genome of the blood fluke *Schistosoma mansoni*. *Nature.* 2009;460(7253):352–358.
35. Da'dara AA, Angeli A, Ferraroni M, Supuran CT, Skelly PJ. Crystal structure and chemical inhibition of essential schistosome host-interactive virulence factor carbonic anhydrase SmCA. *Commun Biol.* 2019;2(1).
36. Ferraroni M, Angeli A, Carradori S, Supuran CT. Inhibition of *Schistosoma mansoni* carbonic anhydrase by the antiparasitic drug clorsulon: X-ray crystallographic and *in vitro* studies. *Acta Crystallogr D Struct Biol.* 2022;78(Pt 3):321–327.
37. Supuran CT, Altamimi ASA, Carta F. Carbonic anhydrase inhibition and the management of glaucoma: a literature and patent review 2013–2019. *Expert Opin Ther Pat.* 2019; 29(10):781–792.
38. Lomelino C, McKenna R. Carbonic anhydrase inhibitors: a review on the progress of patent literature (2011–2016). *Expert Opin Ther Pat.* 2016;26(8):947–956.
39. Li Y, Zhang Y, Zhang Y. Research advances in pathogenesis and prophylactic measures of acute high altitude illness. *Respir Med.* 2018;145:145–152.
40. Imray C, Wright A, Subudhi A, Roach R. Acute mountain sickness: pathophysiology, prevention, and treatment. *Prog Cardiovasc Dis.* 2010;52(6):467–484.
41. Davis C, Hackett P. Advances in the prevention and treatment of high altitude illness. *Emerg Med Clin North Am.* 2017;35(2):241–260.
42. Supuran CT. Advances in structure-based drug discovery of carbonic anhydrase inhibitors. *Expert Opin Drug Discov.* 2017;12(1):61–88.
43. Supuran CT. Carbonic anhydrase inhibitors and their potential in a range of therapeutic areas. *Expert Opin Ther Pat.* 2018;28(10):709–712.
44. McKenna R, Supuran CT. Carbonic anhydrase inhibitors drug design. *Subcell Biochem.* 2014;75:291–323.
45. Supuran CT. Novel carbonic anhydrase inhibitors. *Future Med Chem.* 2021;13(22):1935–1937.
46. Supuran CT. Carbonic anhydroses: novel therapeutic applications for inhibitors and activators. *Nat Rev Drug Discov.* 2008;7(2):168–181.
47. Enameh RZ, Sylanen L, Barker H, Supuran CT, Parkkila S. *Drosophila melanogaster*: a model organism for controlling Dipteran vectors and pests. *J Enzyme Inhib Med Chem.* 2015;30(3):505–513.
48. Sievers F, Wilm A, Dineen D, Gibson TJ, Karplus K, Li W, Lopez R, McWilliam H, Remmert M, Söding J, et al. Fast, scalable generation of high-quality protein multiple sequence alignments using clustal omega. *Mol Syst Biol.* 2011;7(1):539.
49. Madeira F, Pearce M, Tivey ARN, Basutkar P, Lee J, Edbali O, Madhusoodanan N, Kolesnikov A, Lopez R. Search and sequence analysis tools services from EMBL-EBI in 2022. *Nucleic Acids Res.* 2022;50(W1):W276–W279.
50. Gouy M, Guindon S, Gascuel O. Sea view version 4: a multi-platform graphical user interface for sequence alignment and phylogenetic tree building. *Mol Biol Evol.* 2010;27(2): 221–224.
51. Crooks GE, Hon G, Chandonia JM, Brenner SE. WebLogo: a sequence logo generator. *Genome Res.* 2004;14(6):1188–1190.
52. Robert X, Gouet P. Deciphering key features in protein structures with the new ENDscript server. *Nucleic Acids Res.* 2014;42(W1):W320–W324.
53. Varadi M, Anyango S, Deshpande M, Nair S, Natassia C, Yordanova G, Yuan D, Stroe O, Wood G, Laydon A, et al. AlphaFold protein structure database: massively expanding the structural coverage of protein-sequence space with high-accuracy models. *Nucleic Acids Res.* 2022;50(D1):D439–D444.
54. Jumper J, Evans R, Pritzel A, Green T, Figurnov M, Ronneberger O, Tunyasuvunakool K, Bates R, Židek A, Potapenko A, et al. Highly accurate protein structure prediction with AlphaFold. *Nature.* 2021;596(7873):583–589.
55. Evans R, O'Neill M, Pritzel A, et al. Protein complex prediction with AlphaFold-Multimer. *bioRxiv.* 2021: 2021.10.04.463034.
56. Naville M, Ghuillot-Gaudeffroy A, Marchais A, Gautheret D. ARNold: a web tool for the prediction of rho-independent transcription terminators. *RNA Biol.* 2011;8(1):11–13.
57. Urbański LJ, Di Fiore A, Azizi L, Hytönen VP, Kuuslahti M, Buonanno M, Monti SM, Angeli A, Zolfaghari Enameh R, Supuran CT, et al. Biochemical and structural characterisation of a protozoan beta-carbonic anhydrase from *Trichomonas vaginalis*. *J Enzyme Inhib Med Chem.* 2020; 35(1):1292–1299.
58. Haapanen S, Bua S, Kuuslahti M, Parkkila S, Supuran CT. Cloning, characterization and anion inhibition studies of a  $\beta$ -carbonic anhydrase from the pathogenic protozoan *Entamoeba histolytica*. *Molecules.* 2018;23(12):3112.
59. Kopp J, Slouka C, Ulonska S, Kager J, Fricke J, Spadiut O, Herwig C. Impact of glycerol as carbon source onto specific sugar and inducer uptake rates and inclusion body productivity in *E. coli* BL21(DE3). *Bioengineering.* 2017;5(1):1.
60. Khalifah RG. The carbon dioxide hydration activity of carbonic anhydrase. I. Stop-flow kinetic studies on the native human isoenzymes B and C. *J Biol Chem.* 1971;246(8):2561–2573.
61. Berrino E, Bua S, Mori M, Botta M, Murthy VS, Vijayakumar V, Tamboli Y, Bartolucci G, Mugelli A, Cerbai E, et al. Novel sulfamide-containing compounds as selective carbonic anhydrase I inhibitors. *Molecules.* 2017;22(7):1049.
62. Urbanski LJ, Bua S, Angeli A, Kuuslahti M, Hytönen VP, Supuran CT, Parkkila S. Sulphonamide inhibition profile of *Staphylococcus aureus*  $\beta$ -carbonic anhydrase. *J Enzyme Inhib Med Chem.* 2020;35(1):1834–1839.
63. Bua S, Haapanen S, Kuuslahti M, Parkkila S, Supuran CT. Sulfonamide inhibition studies of a new  $\beta$ -carbonic anhydrase from the pathogenic protozoan *Entamoeba histolytica*. *Int J Mol Sci.* 2018;19(12):3946.

64. Kimber MS, Pai EF. The active site architecture of *Pisum sativum* beta-carbonic anhydrase is a mirror image of that of alpha-carbonic anhydrases. *EMBO J.* 2000;19(7):1407–1418.
65. Vale N, Gouveia MJ, Rinaldi G, Brindley PJ, Gärtner F, Da Costa JMC. Praziquantel for schistosomiasis: single-drug metabolism revisited, mode of action, and resistance. *Antimicrob Agents Chemother.* 2017;61(5).
66. Li EY, Gurarie D, Lo NC, Zhu X, King CH. Improving public health control of schistosomiasis with a modified WHO strategy: a model-based comparison study. *Lancet Glob Health.* 2019;7(10):e1414–e1422.
67. Wang W, Wang L, Liang YS. Susceptibility or resistance of praziquantel in human schistosomiasis: a review. *Parasitol Res.* 2012;111(5):1871–1877.
68. Syrjänen L, Vermelho AB, Rodrigues I. d A, Corte-Real S, Salonen T, Pan P, Vullo D, Parkkila S, Capasso C, Supuran CT. Cloning, characterization, and inhibition studies of a  $\beta$ -carbonic anhydrase from *Leishmania donovani chagasi*, the protozoan parasite responsible for leishmaniasis. *J Med Chem.* 2013;56(18):7372–7381.
69. Zolfaghari Emameh R, Kuuslahti M, Vullo D, Barker HR, Supuran CT, Parkkila S. *Ascaris lumbricoides*  $\beta$  carbonic anhydrase: a potential target enzyme for treatment of ascariasis. *Parasites Vectors.* 2015;8(1).
70. Khubchandani IT, Bub DS. Parasitic infections. *Clin Colon Rectal Surg.* 2019;32(5):364–371.
71. Mansour NS, Youssef FG, Mikhail EM, Mohareb EW. Amebiasis in schistosomiasis endemic and non-endemic areas in Egypt. *J Egypt Soc Parasitol.* 1997;27(3):617–628.
72. Dolabella SS, Coelho PMZ, Borçari IT, Mello NAST, Andrade ZDA, Silva EF. Morbidity due to *Schistosoma mansoni* – *Entamoeba histolytica* coinfection in hamsters (*Mesocricetus auratus*). *Rev Soc Bras Med Trop.* 2007;40(2):170–174.
73. Gulati S, Aref AA. Oral acetazolamide for intraocular pressure lowering: balancing efficacy and safety in ophthalmic practice. *Expert Rev Clin Pharmacol.* 2021;14(8):955–961.
74. Leaf DE, Goldfarb DS. Mechanisms of action of acetazolamide in the prophylaxis and treatment of acute mountain sickness. *J Appl Physiol.* 2007;102(4):1313–1322.
75. Adamson R, Swenson ER. Acetazolamide use in severe chronic obstructive pulmonary disease pros and cons. *Ann Am Thorac Soc.* 2017;14(7):1086–1093.
76. Van Berkel MA, Elefritz JL. Evaluating off-label uses of acetazolamide. *Am J Health Syst Pharm.* 2018;75(8):524–531.
77. Cong-Hui Z, Huai-Min Z. Cloning and characterization of  $\beta$ -carbonic anhydrase, a potential drug target of *Schistosoma japonicum*. *Zhongguo Xue Xi Chong Bing Fang Zhi Za Zhi.* 2016;28(2):161–166.
78. Llanwarne F, Helmsby H. Granuloma formation and tissue pathology in *Schistosoma japonicum* versus *Schistosoma mansoni* infections. *Parasite Immunol.* 2021;43(2):e12778.

# PUBLICATION IV

## **Ultrasensitive and rapid diagnostic tool for detection of *Acanthamoeba castellanii***

Susanna Haapanen, Maarit S. Patrikainen, Seppo Parkkila

Diagnostic microbiology and infectious disease. 2023; 107(2):116014  
<https://doi.org/10.1016/j.diagmicrobio.2023.116014>

**Publication reprinted with the permission of the copyright holders.**







## Original Article

# Ultrasensitive and rapid diagnostic tool for detection of *Acanthamoeba castellanii*



Susanna Haapanen<sup>a,\*</sup>, Maarit S. Patrikainen<sup>a</sup>, Seppo Parkkila<sup>a,b</sup>

<sup>a</sup> Faculty of Medicine and Health Technology, Tampere University, Tampere, Finland

<sup>b</sup> Fimlab Ltd, Tampere University Hospital, Tampere, Finland

## ARTICLE INFO

## Article history:

Received 13 April 2023

Accepted 29 June 2023

Available online 6 July 2023

## Keywords:

*Acanthamoeba keratitis*

Diagnostic method

Polymerase chain reaction

## ABSTRACT

*Acanthamoeba keratitis* is a devastating infectious disease of the cornea caused by an opportunistic amoeba, *Acanthamoeba castellanii*. It is poorly recognized, and diagnostic delays can lead to irreversible damage to the vision. The gold standard for diagnosis has been a sample culture that lasts approximately 2 weeks. Nevertheless, the essence of time has led to the need for an accurate and fast technique to detect *A. castellanii* from a sample. We developed both traditional and quantitative real-time-PCR-based methods to detect *A. castellanii* in less than 3 hours and with the sensitivity of one amoeba. Diagnostic laboratories can select the best-suited method for their purposes from 2 comparable methods. The correct treatment can be initiated from the emergency room when the diagnosis has been made quickly within a few hours, hence saving the patient from long-term complications.

© 2023 The Author(s). Published by Elsevier Inc. This is an open access article under the CC BY license (<http://creativecommons.org/licenses/by/4.0/>)

## 1. Introduction

Corneal opacity causes 1.5 to 2 million cases of new monocular blindness per year (WHO). The leading cause of opacity is infectious keratitis (bacterial, viral, fungal, amoebae), with an incidence of 2.5 to 799 infections per 100,000 [1,2]. Different bacteria are the most common cause of infectious keratitis in general; however, *Acanthamoeba* infections are responsible for 1.96% to 12.5% of infectious keratitis in contact lens wearers [3].

*Acanthamoeba castellanii* is an opportunistic pathogenic amoeba found in soil and water worldwide. It commonly causes keratitis and, in rare cases, can cause invasive infections, such as granulomatous amoebic encephalitis (GAE). *Acanthamoeba keratitis* (AK) is a sight-threatening and poorly recognized condition with only moderately effective treatment options [4,5]. In particular, wearing contact lenses when swimming in natural waters is considered a high-risk activity. Other risk factors for catching AK are negligence in hygiene when handling eye contact lenses, usage of ophthalmic corticosteroids [6], and perioperative period of ophthalmic operations [4]. There are over 150 million contact lens wearers globally [7], and the yearly sale of contact lenses is approximately 10.1 billion USD emphasizing the vast part of the population belonging to the risk group [8].

In clinical examination, AK resembles viral, bacterial, and fungal keratitis [9–11]. The gold standard for diagnosing AK is culturing the

corneal swab sample for approximately 2 weeks [9]. Specialized centers use confocal microscopy, which, when in capable hands, has good sensitivity and specificity; nonetheless, the need for experienced microscopists and equipment limits the usefulness of the method [12]. New approaches based on gene multiplication and detection has been developed, but they have yet to reach widespread use in clinical diagnostics [4,13].

*A. castellanii* has 8 carbonic anhydrases (CAs, EC 4.2.1.1) belonging to 3 different evolutionary families: 3  $\alpha$ -, 3  $\beta$ - and 2  $\gamma$ -CAs [14,15]. To date, 8 different families of CAs have been recognized in different organisms [16,17], yet the human genome only contains enzymes belonging to 1 family,  $\alpha$ -CAs [17]. CAs are metalloproteases with various roles in fundamental physiological processes in almost all living organisms. CAs catalyze the reversible hydration of carbon dioxide and, for instance, participate in maintaining acid-base homeostasis [18,19]. Recognition of CA-genes of parasites from a sample is arising as a tool to detect different parasites, for example, finding the trichinosis-causing parasite *Trichinella spiralis* from meat samples [20].

Due to the diagnostic challenges, the diagnosis of AK is often delayed, and up to two-thirds of the patients are initially treated with antibacterial eyedrops and the same number with antiviral medication [21]. The approximate delay of the correct diagnosis is 39 days [21]. This emphasizes the need for a sensitive and rapid diagnostic method to optimally provide the result during the patient's visit to the emergency room. In this article, we describe a novel rapid and sensitive PCR-based method and a quantitative real-time PCR (qRT-PCR) method for detecting the  $\beta$ - and  $\gamma$ -CA genes of *A.*

\* Corresponding author. Tel.: +358400156493

E-mail address: [susanna.haapanen@tuni.fi](mailto:susanna.haapanen@tuni.fi) (S. Haapanen).

*castellanii*. We consider these methods promising tools for clinical diagnostics of AK from biological samples containing amoebas with no unspecific signal from the human genome.

## 2. Materials and methods

### 2.1. Culture initiation and maintenance

The axenic *A. castellanii* (ATCC® 30010™) culture was initiated and maintained in T 25 tissue culture flasks (Thermo Fischer Scientific, Waltham, MA, USA) in ATCC Medium 712: PYG (protease peptone, yeast and glucose) with additives (Sigma-Aldrich, St. Louis, MO, USA) according to the recommendation of the cell provider. The cells were cultured at +25°C with constant temperature monitoring to ensure stable growth conditions. To maintain the culture, the medium was changed twice a week.

### 2.2. Collecting and lysing the samples

Initially, genomic DNA was isolated from amoeba culture with a NucleoSpin Tissue Kit (Macherey-Nagel, Düren, Germany) according to the manufacturer's instructions. Consequently, the isolated DNA, concentration measured with Thermo Scientific™ NanoDrop™ One Microvolume UV-Vis Spectrophotometer (Thermo Fisher Scientific), was used in testing the primers and optimizing the PCR protocol.

Specific numbers of amoebae were collected in vision control with a light microscope. A borosilicate needle was used to collect the desired number of trophozoites and/or cysts from a petri dish with amoebae in the medium. Approximately 1.2 to 3.5 µL of culture media was contained in 1 amoeba sample. The collected sample was transferred to 100 µL DirectPCR Lysis Reagent (Tail) (Nordic BioSite, Täby, Sverige). Three microliters of proteinase K (20 mg/mL, Macherey-Nagel) were added to the reaction, and the tube was placed in an incubator at +55°C and shook at 200 rpm for 30 minutes. The lysis reaction was terminated by transferring the tube to a heating block at +85°C for 50 minutes.

Human cell samples were collected from buccal mucosa swab samples. They were compiled with sterile loops, which were subsequently

dipped in 100 µL DirectPCR Lysis Reagent (Tail) (Nordic BioSite, Täby, Sverige) and thawed. Loops were removed and discarded. As described above, the desired numbers of amoebae were added to the tubes with 3 µL Proteinase K (20 mg/mL, Macherey-Nagel). The lysis reaction was performed similarly to the samples with amoebae only.

### 2.3. Primer design

Primers for traditional and qRT-PCR were designed using the NCBI Primer-BLAST tool (<http://www.ncbi.nlm.nih.gov/tools/primer-blast/>). The most promising primers were selected, manually inspected, and modified to improve their performance. As a result, we obtained 21 and 5 primer pairs for traditional and qRT-PCR, respectively (Table 1).

### 2.4. Traditional PCR method

The study involved 2 consecutive phases of PCR. First, the crude exclusion of nonworking primers was performed with PCR 1 according to the manufacturer's manual of the master mix 2 x Phusion Flash High Fidelity (Thermo Fischer Scientific, Waltham, MA, USA) with 46.7 ng of isolated genomic DNA per reaction. The non-working primers were excluded, and the functioning primers were chosen for further processes. The amount of genomic DNA was reduced to 2.3 ng per reaction, and again, the nonfunctional primers were excluded. PCR assay 1 was performed with a thermocycler according to the manufacturer's protocol except for 35 cycles and an annealing temperature of +65°C.

In the second phase, we used lysis samples as the template. PCR mix 2 had the same composition as PCR mix 1 apart from 2 µL of a lysed sample as template DNA. There were 6 lysis samples: 1 trophozoite, 1 cyst, 10 amoebae (5 cysts and 5 trophozoites), buccal mucosa, buccal mucosa, and amoebae combined, and hundreds of amoebae. A reaction mix with 2 µL of H<sub>2</sub>O as a sample was used as a negative control. The PCR assay 2 was optimized from the basis of PCR assay 1 as a result of the functioning method in a thermocycler with 38 cycles and an annealing temperature of +67°C. The PCR product was visualized in 1.6% agarose gel (Meridian Bioscience Inc., Cincinnati, OH, USA)

**Table 1**

21 and 5 primer pairs for traditional PCR and qRT-PCR, respectively, constructed for the development of the diagnostic tool. The final primer pairs used in the diagnostic tool are underlined. The primer pair for the reference gene (RG) used in qRT-PCR is also shown.

Primer pair	Forward (5' - 3')	Reverse (5' - 3')	Target gene (Entry ID)	Product length (bp)
<b>bCA_1</b>	<u>AAACATTGCCAACCGCTCC</u>	<u>GGTCAGAGATCGTACGCCAG</u>	<i>mitBCA (L8GR38)</i>	326
<b>bCA_2</b>	<u>CTGGCGTACGATCTCTGACC</u>	<u>AAGGGTCTCTACTCCGGAC</u>	<i>mitBCA (L8GR38)</i>	332
<b>bCA_3</b>	<u>TTCTAATGACCGGGACAGG</u>	<u>GCAAAGGGTCTCTACTCCG</u>	<i>mitBCA (L8GR38)</i>	249
<b>bCA_4</b>	<u>AAAGCTGTACTCACTGCC</u>	<u>AGGTAGTACTCGCCGTCTAT</u>	<i>cpBCA (L8GLS7)</i>	476
<b>bCA_5</b>	<u>ATCTTTGACGAGGGCATGGG</u>	<u>AGAAGGAGGTGTACGGACCT</u>	<i>cpBCA (L8GLS7)</i>	623
<b>bCA_6</b>	<u>TAATCTGGTCCGGTCTCGTC</u>	<u>TGGGAGAAGGAGGTGTACGG</u>	<i>cpBCA (L8GLS7)</i>	418
<b>bCA_7</b>	<u>CCGGAGCTCATCTTTGACGA</u>	<u>GAGAAGGAGGTGTACGGACC</u>	<i>cpBCA (L8GLS7)</i>	633
<b>bCA_8</b>	<u>CGAACCACTGTATGGGCTGT</u>	<u>GAGCGAAAGCGATGAGGGAT</u>	<i>tmBCA (L8H861)</i>	310
<b>bCA_9</b>	<u>CCTCCCTGGTTGATTTCTCGG</u>	<u>CCGTCTGTATGAGCCACTTC</u>	<i>tmBCA (L8H861)</i>	499
<b>bCA_10</b>	<u>CGGTACCCTACATCCCCGA</u>	<u>CACCAGAGCTGAGGCAGTAG</u>	<i>tmBCA (L8H861)</i>	352
<b>bCA_11</b>	<u>CGTCAGGTACTCCATCAGGG</u>	<u>CGCAGGATCTTAGCCACGAG</u>	<i>tmBCA (L8H861)</i>	358
<b>bCA_12</b>	<u>GTGTGACCTGGAACTTGCTG</u>	<u>CGCAAGAGATGAGGGATAGA</u>	<i>tmBCA (L8H861)</i>	395
<b>bCA_13</b>	<u>CAGTGTGACGTGGAACTTGC</u>	<u>GAGCGAAAGCGATGAGGGATA</u>	<i>tmBCA (L8H861)</i>	399
<b>aCA_1</b>	<u>CTGATACCACGCAACGCATC</u>	<u>CAAACCAACACACACACGAC</u>	<i>aCA (L8GFJ9)</i>	472
<b>aCA_2</b>	<u>TTGCAAGTTATACAGCACCC</u>	<u>TCTTTGGGTAGGAAAGCCCC</u>	<i>aCA (L8H518)</i>	476
<b>aCA_3</b>	<u>CACACCTCAAGAAGCAGCTG</u>	<u>GAAAGGGTGGGTACCGTCC</u>	<i>aCA (L8GXK3)</i>	440
<b>aCA_4</b>	<u>CGGTACCCACCCCTTCTCTC</u>	<u>CCACGAGATCCAGCTTAGC</u>	<i>aCA (L8GXK3)</i>	326
<b>gCA_1</b>	<u>TGCGACATGTAGGACGGAAAC</u>	<u>TGGCGCATGAAAGATGGACG</u>	<i>gCA (L8HK20)</i>	671
<b>gCA_2</b>	<u>GATCGTTGGCACTGGGTTA</u>	<u>TGACAAAAGCTCGGTGTGG</u>	<i>gCA (L8HK20)</i>	645
<b>gCA_3</b>	<u>GCCTGTACGATAAGCAGCCT</u>	<u>GAACGATAACAACGGCGGG</u>	<i>gCA (L8GFM8)</i>	579
<b>gCA_4</b>	<u>GTGGGAAGAAGACTCCAT</u>	<u>GCACAGCTCAGCCACTGTAT</u>	<i>gCA (L8GFM8)</i>	419
<b>qgCA_1</b>	<u>CAACAAGCACACTACGCTGG</u>	<u>GTCATACCAGACGGAGGCAC</u>	<i>gCA (L8HK20)</i>	130
<b>qgCA_2</b>	<u>CCACTGGCTTACCATCGGTC</u>	<u>CACCAAGGATGGATCGCAT</u>	<i>gCA (L8HK20)</i>	125
<b>qbCA_1</b>	<u>GCAGGAACCTCAAGACGAA</u>	<u>GCTTACGGCAGCAGTGTITT</u>	<i>mitBCA (L8GR38)</i>	128
<b>qbCA_2</b>	<u>GCTTGCTTCTCCATCTCC</u>	<u>GTGCTGTGAAGGGGTGAAGA</u>	<i>mitBCA (L8GR38)</i>	96
<b>qbCA_3</b>	<u>TTCTAATGACCGGGACAGG</u>	<u>GAAAACGTTCCGGCTCTTCC</u>	<i>mitBCA (L8GR38)</i>	125
<b>18S900 (RG)</b>	<u>GCCAGATCGTTTACCCTGA</u>	<u>CATTACCTAGTCTCCGGC</u>	<i>18s rRNA (L8GCJ8)</i>	148

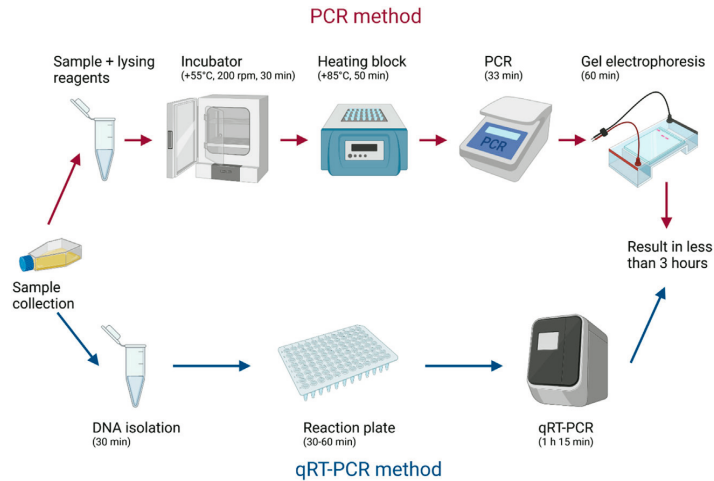


Fig. 1. The workflow for performing PCR (above) and qRT-PCR (below).

with 0.5  $\mu\text{L}$  of Midori Green (Nippon Genetics Europe GmbH, Düren, Germany) at 105 V for 60 minutes. The picture of the gel was taken with Image Lab™ Software (version 6.0, 2017, Bio-Rad Laboratories Inc., Hercules, CA, USA) with GelGreen protocol and otherwise default settings but inverted colors. The obtained gel bands were confirmed using Sanger sequencing by the Tampere Genomics Facility.

### 2.5. qRT-PCR method

We designed qRT-PCR primers with the NCBI Primer-BLAST tool, as described above. As a reference gene, we used primer pair 18S900 from the 18S rRNA gene, as recommended in Köhler et al. [22] (Table 1). qRT-PCR was performed in a MicroAmp™ Optical 96-Well Reaction Plate with Barcode (Applied Biosystems™, Thermo Fischer Scientific) with the reaction mix recommended by the manufacturer of PowerUp™ SYBR™ Green Master Mix (Applied Biosystems™, Thermo Fischer Scientific). The isolated genomic DNA had varying concentrations between 0.001 ng/ $\mu\text{L}$  and 100 ng/ $\mu\text{L}$  per well. Instead of a DNA sample, we used 1  $\mu\text{L}$  of H<sub>2</sub>O for the no template control and 1  $\mu\text{L}$  of the isolated human genome from buccal mucosa (8.4 ng/ $\mu\text{L}$ ) for the negative control. The assay was run with a QuantStudio 12K Flex Real-Time PCR System (Applied Biosystems™, Thermo Fischer Scientific) with the program recommended by the manufacturer of the master mix with an annealing and extension temperature of +62°C. Due to the lack of clinical samples, we only generated a standard curve.

## 3. Results and discussion

We aimed to improve the time-consuming and challenging diagnosis of AK by developing ultrasensitive and rapid diagnostic methods based on both traditional PCR and qRT-PCR (Fig. 1).

For traditional PCR, we identified three equally rapid, sensitive, and accurate primer pairs with the same PCR protocol, hence providing three alternative pairs to use (Table 1). All three primer pairs can detect amoebae from a sample ranging from only one cyst or trophozoite to many thousands without unspecific amplification of human genes (Fig. 2). They can also be used in parallel PCR to verify the achieved result. The protocol includes only five simple steps (Fig. 1) and gives the result in less than three hours. The protocol in traditional PCR can be performed in any diagnostic laboratory without requiring special laboratory equipment. Two primer pairs detected mitochondrial  $\beta$ -CA (Entry ID L8GR38) and one  $\gamma$ -CA (Entry ID L8HK20).

In qRT-PCR, both primer pairs (Table 1) were found to detect *A. castellanii* from a sample with only 0.01 ng of the genome. The whole genome of *A. castellanii* is 42.02 Mb [23] equivalent to 1.9 ng, indicating that the method can recognize only 1 amoeba from a sample. DNA isolation takes approximately 30 minutes, and qRT-PCR takes 1.25 hours. Depending on the pipetting method, the duration from

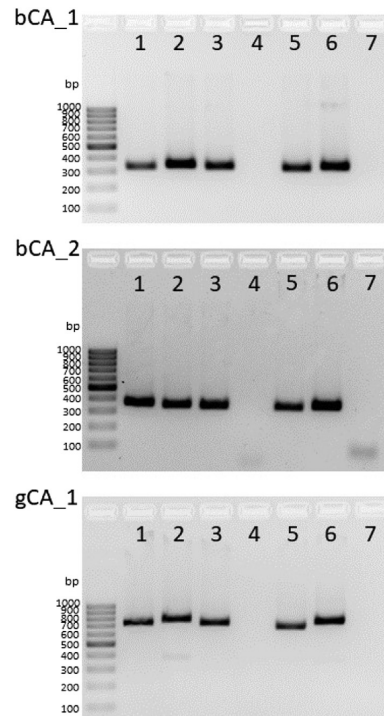


Fig. 2. Traditional PCR results of all three primer pairs used in the diagnostic method visualized in agarose gel (figure cropped with Image Lab™ Software [version 6.0]). A 1 kbp ladder was used as a standard marker. The lines were assigned as follows: 1) one cyst; 2) one trophozoite; 3) 10 amoebae; 4) buccal mucosa; 5) buccal mucosa and amoebae; 6) hundreds of amoebae; 7) negative control

sample collection to result is approximately 2.5 to 3 hours: the same range as the traditional PCR method.

Several diagnostic methods based on PCR have been developed; however, they have limitations, for instance, time-consuming procedures, the need for DNA isolation before PCR, and a limited ability to detect no less than 10 amoebae in a sample [24–26]. Previously presented most commonly used PCR methods are qRT-PCR or isothermal loop-mediated amplification [27,28] and were designed to detect the 18S ribosomal RNA gene [28]. Previously presented DNA amplification directly from a smear sample was at least as fast as our method and has no requirement for DNA isolation, yet, they do not state the lowest number of amoebae detected or whether they can recognize cysts [13].

At least six commercially available diagnostic kits for detecting AK are all intended for research purposes only. “*Acanthamoeba\_spp* 18S ribosomal RNA (18S) gene” (Genesig, Primerdesign, Chandler’s Ford, UK), “*Acanthamoeba castellanii* Real-time PCR Kit” (Nzytech, Lisbon, Portugal), “ParoReal Kit *Acanthamoeba*” (Ingenetix, Wien, Austria) and “HumPCR™ *Acanthamoeba* Detection Kit and HumqPCR-real-time™ *Acanthamoeba* Real-Time PCR Kit” (Bioingentech Ltd., Concepción, Bio Bio, Chile) provide 18S ribosomal RNA gene -detection based kits; “Techne™ PrimePRO QPCR DNA detection Kit, All *Acanthamoeba* species” (Thermo Fisher Scientific) does not provide further information on the target gene. They require DNA isolation, and none of the kits provide instructions for performing isolation. They are also more time-consuming than either of our methods; the fastest one promises results in five hours at the minimum. Five are based on quantitative real-time PCR, and the sixth, “HumPCR™ *Acanthamoeba* Detection Kit”, uses traditional PCR as our first PCR method. Our qRT-PCR method also requires DNA isolation before the reaction, for which we recommend a commercially available kit. In contrast, our traditional PCR method does not require DNA isolation, removing one error-sensitive step from the protocol.

To summarize, we developed 2 PCR-based methods to detect *A. castellanii* parasites in less than 3 hours, enabling faster diagnosis and initiation of treatment from the emergency room visit. More rapid diagnosis also hinders unnecessary treatment starting with a suspicion of AK, and thus, treatment-related harmful side effects can be avoided. We only had samples from cultured parasites, and the negative control sample was a buccal mucosa sample from a healthy volunteer; thus, our method needs further testing with clinical samples.

## Declaration of Competing Interest

The authors declare no conflicts of interest.

## Acknowledgment

The authors acknowledge the Biocenter Finland (BF) and Tampere Genomics Facility for the sequencing service. We also thank Marianne Kuuslahti for her expertise in setting up and maintaining amoeba culture. Figure 1 was created with BioRender.com.

## Funding

The work was supported by grants from the Finnish Medical Foundation (SH, grant number 5299) and the Academy of Finland (SP, grant number 348972).

## Author contributions

SP, MSP and SH designed the experiments; SH conducted the PCR laboratory work; SH and MSP conducted the qRT-PCR laboratory work; SH prepared the first manuscript draft; all authors wrote and finalized the article.

## References

- [1] Ung L, Bispo PJM, Shanbhag SS, Gilmore MS, Chodosh J. The persistent dilemma of microbial keratitis: global burden, diagnosis, and antimicrobial resistance. *Survey Ophthalmol* 2019;64(3):255–71 NIH Public Access.
- [2] Ting DSJ, Ho CS, Deshmukh R, Said DG, Dua HS. Infectious keratitis: an update on epidemiology, causative microorganisms, risk factors, and antimicrobial resistance. *Eye (Basingstoke)*, 35. Nottingham, UK: Nature Publishing Group; 2021. p. 1084–101.
- [3] Waghmare SV, Jeria S. A review of contact lens-related risk factors and complications. *Cureus* 2022;14(10).
- [4] Maycock NJR, Jayaswal R. Update on acanthamoeba keratitis: diagnosis, treatment, and outcomes. *Cornea* 2016;35(5):713–20.
- [5] Niederhorn JY. The biology of *Acanthamoeba* keratitis. *Exp Eye Res* 2021; 202:108365 NIH Public Access.
- [6] Nakagawa H, et al. Corticosteroid eye drop instillation aggravates the development of *Acanthamoeba* keratitis in rabbit corneas inoculated with *Acanthamoeba* and bacteria. *Sci. Rep.* 2019;9(1):1–7.
- [7] Moreddu R, Vigolo D, Yetisen AK. Contact lens technology: from fundamentals to applications. *Adv Healthc Mater* 2019;8(15):1–24.
- [8] “Contact Lenses Market Size and Share Estimation 2022–2028 [CAGR of 4.60%] | Regional Overview, Growth Opportunity, Business Prospect and New Challenges - Digital Journal.” [Online]. Available: <https://www.digitaljournal.com/pr/contact-lenses-market-size-and-share-estimation-2022-2028-cagr-of-4-60-regional-overview-growth-opportunity-business-prospect-and-new-challenges>. [Accessed: 30-Mar-2023].
- [9] Cabrera-Aguas M, Khoo P, Watson SL. Infectious keratitis: a review. *Clin Exp Ophthalmol* 2022;50(5):543–62 Wiley-Blackwell.
- [10] Hudson J, Al-Kharsan H, Carletti P, Miller D, Dubovy SR, Amescua G. Role of corneal biopsy in the management of infectious keratitis. *Curr Opin Ophthalmol* 2022;33(4):290–5 Lippincott Williams and Wilkins.
- [11] Kowalski RP, et al. The prevalence of bacteria, fungi, viruses, and *Acanthamoeba* from 3,004 cases of Keratitis, Endophthalmitis, and Conjunctivitis. *Eye Contact Lens* 2020;46(5):265–8.
- [12] Alantary N, Heaselgrave W, Hau S. Correlation of ex vivo and in vivo confocal microscopy imaging of *Acanthamoeba*. *Br. J. Ophthalmol.* 2022;1–6.0.
- [13] El-Sayed NM, Younis MS, Elhamsary AM, Abd-Elmaboud AI, Kishik SM. *Acanthamoeba* DNA can be directly amplified from corneal scrapings. *Parasitol. Res.* 2014;113(9):3267–72.
- [14] Baig AM, Rana Z, Waliyani N, Karim S, Rajabali M. Evidence of human-like Ca 2+ channels and effects of Ca 2+ channel blockers in *Acanthamoeba castellanii*. *Chem. Biol. Drug Des.* 2019;93(3):351–63.
- [15] Baig AM, Zohaib R, Tariq S, Ahmad HR. Evolution of pH buffers and water homeostasis in eukaryotes: Homology between humans and *Acanthamoeba* proteins. *Future Microbiol* 2018;13(2):195–207.
- [16] Akocak S, Supuran CT. Activation of  $\alpha$ -,  $\beta$ -,  $\gamma$ -  $\delta$ -  $\zeta$ - and  $\eta$ - class of carbonic anhydrases with amines and amino acids: a review. *J Enzyme Inhib Med Chem* 2019;34(1):1652–9.
- [17] Capasso C, Supuran CT, Capasso C, Supuran CT. An overview of the alpha-, beta- and gamma- carbonic anhydrases from Bacteria : can bacterial carbonic anhydrases shed new light on evolution of bacteria? *J Enzyme Inhib Med Chem* 2014;30(2):325–32.
- [18] Keilin D, Mann T. Carbonic anhydrase. Purification and nature of the enzyme. *Biochem J* 1940;34(8-9):1163–76.
- [19] Krishnamurthy VM, Kaufman GK, Urbach AR, Gitlin I, Gudiksen KL, Weibel DB, et al. Carbonic anhydrase as a model for biophysical and physical-organic studies of proteins and protein-ligand binding. *Chem Rev* 2008;108(3):946–1051.
- [20] Zolfaghari Emameh R, Kuuslahti M, Näreaho A, Sukura A, Parkkila S. Innovative molecular diagnosis of *Trichinella* species based on  $\beta$ -carbonic anhydrase genomic sequence. *Microb. Biotechnol.* 2016;9(2):172–9.
- [21] Chew HF, et al. Clinical outcomes and prognostic factors associated with acanthamoeba keratitis. *Cornea* 2011;30(4):435–41.
- [22] Köhler M, Leitsch D, Müller N, Walochnik J. Validation of reference genes for the normalization of RT-qPCR gene expression in *Acanthamoeba* spp. *Sci Rep.* 2020;10(1):1–12.
- [23] Hasni I, Andréani J, Colson P, Scola Bla. Description of virulent factors and horizontal gene transfers of keratitis-associated amoeba *acanthamoeba triangularis* by genome analysis. *Pathogens* 2020;9(3):2–4.
- [24] Mewara A, et al. Evaluation of loop-mediated isothermal amplification assay for rapid diagnosis of *Acanthamoeba* keratitis. *Indian J. Med. Microbiol.* 2017;35(1):90–4.
- [25] Lehmann OJ. Polymerase chain reaction analysis of corneal epithelial and tear samples in diagnosis of acanthamoeba keratitis. *Investig. Ophthalmol. Vis. Sci.* 1997;38(4):1261–5.
- [26] Ge Z, Qing Y, Zicheng S, Shiyang S. Rapid and sensitive diagnosis of *Acanthamoeba* keratitis by loop-mediated isothermal amplification. *Clin. Microbiol. Infect.* 2013;19(11):1042–8.
- [27] Lek-Uthai U, Passara R, Roongruangchai K, Buddhirakul P, Thammapalerd N. Rapid identification of *Acanthamoeba* from contact lens case using loop-mediated isothermal amplification method. *Exp. Parasitol.* 2009;121(4):342–5.
- [28] Yang HW, et al. Loop-mediated isothermal amplification targeting 18S ribosomal DNA for rapid detection of *Acanthamoeba*. *Korean J. Parasitol.* 2013;51(3):269–77.

PUBLICATION  
V

**A novel drug screening assay for *Acanthamoeba castellanii* and the anti-amoebic effect of carbonic anhydrase inhibitors**

Susanna Haapanen, Harlan Barker, Fabrizio Carta, Claudiu T. Supuran, Seppo Parkkila

Submitted manuscript

**Publication reprinted with the permission of the copyright holders.**



